SOUTH FLORIDA WATER MANAGEMENT DISTRICT

FINAL
Assessment of the Responses of the Caloosahatchee River Estuary to Low Freshwater Inflow in the Dry Season

March 2017

Prepared by:
Christopher Buzzelli, Peter Doering, Yongshan Wan, Teresa Coley, Detong Sun, Zhiquiang Chen, Cassondra Thomas, Don Medellin, and Toni Edwards

Coastal Ecosystems Section
South Florida Water Management District
3301 Gun Club Rd.
West Palm Beach, FL 33406

ACKNOWLEDGEMENTS

This document resulted from significant efforts by personnel in the Coastal Ecosystem Section at the South Florida Water Management District. R. Chamberlain at the St. Johns River Water Management District deserves special recognition for his contributions to studies of freshwater inflows and the ecological attributes of the Caloosahatchee River Estuary. We acknowledge the considerable efforts of S.G. Tolley et al. at Florida Gulf Coast University for their study of zooplankton and ichthyoplankton, and P. Montagna and T. Palmer at Texas A&M University-Corpus Christi for their analyses of historical macrobenthic data. The document greatly benefitted from constructive reviews provided by S. Gray, J. Brown, and S. Memberg at the South Florida Water Management District.

EXECUTIVE SUMMARY

The Caloosahatchee River minimum flows and minimum water levels (MFL) was established in 2001, reviewed in 2003, and is being reevaluated for 2017. MFL criteria define the point at which additional withdrawals of water will result in significant harm to the water resources (Sections 373.042 and 373.0421, Florida Statutes). The purpose of this study was to provide a comprehensive assessment of the effects of dry season (November–April) freshwater inflow on the Caloosahatchee River Estuary (CRE). This effort was composed of 11 component studies focused on hydrodynamics, water column and benthic habitats, and faunal indicators. The different indicators respond to inflow on different scales (days to years) and are located along the salinity gradient between the upstream water control structure (S-79) and the estuary mouth (~42 kilometers). The component studies emphasized the relationships between the indicators and inflows through the S-79 structure in the dry season. The indicator inflow (Q_I) was defined as the inflow rates below which there would be negative impacts, not significant harm.

The CRE has been structurally altered including the installation of the S-79 structure and the Sanibel Causeway, removal of oyster reefs around Shell Point, and channelization. These irreversible modifications have enhanced upstream salt transport throughout the estuary. Inflow-salinity relationships are influenced by the Tidal Basin downstream of S-79, which provides an estimated 18% of the total freshwater input over the period of record from 1966 through 2014. There were wide inter-annual variations in S-79 inflows (445 ± 218 cubic feet per second [cfs]) associated with a salinity of 10 at Fort Myers. Total dry season inflows less than 500 cfs appeared to promote bottom water hypoxia in the upper CRE as the chlorophyll *a* maximum migrated upstream over the deeper channel. Inflows less than 412 ± 165 cfs could lead to impingement of zooplankton assemblages on S-79, compressing their habitat. Flows less than 238 ± 256 could result in loss of preferred salinity habitat (<10) for juvenile fish in the upper estuary. Inflows of 501 ± 525 cfs and 296 ± 410 cfs supported stationary habitats in the upper (benthic macrofauna) and lower (oyster bed) CRE. Average inflows greater than 545 ± 774 cfs in the dry season from 1993 to 1999 promoted low salinity conditions for the survival of *Vallisneria americana* (tape grass). Conversely, the vegetated habitat declined as the average salinity at Fort Myers exceeded 10 from 2007 to 2013. Lee County blue crab harvest (1984–2013) was reduced when the average dry season inflows were less than 400 ± 57 cfs. The area of sawfish habitat area between S-79 and Shell Point was maximized when inflow from S-79 was 270 cfs in the 2007 dry season using a salinity range of 12 to 27. A different optimum salinity range from 18 to 30 was evaluated for juvenile sawfish in the CRE after receiving public comment. Habitat area was recalculated based on the same hydrodynamic modeling results and bathymetric data. The result of this analysis showed that as discharge increases habitat area and volume decreased.

There were three important results:

1. The magnitude of minimum indicator inflows (Q_I) from S-79 ranged from 237 cfs to 545 cfs among the 11 estimates.
2. Seasonally averaged S-79 inflows less than the respective Q_I for each indicator could result in phytoplankton blooms in the upper CRE (less than 10 kilometers from S-79), compress the water column habitat for

zooplankton and icthyoplankton against the structure, alter the composition of the macrobenthic community in the upper estuary, prevent the survival of *Vallisneria*, shrink the available habitat for the endangered sawfish, and lead to reduced harvest of blue crabs the following year.

3. Flow through S-79 accounts for 82% of the total inflow. The Tidal Basin inflows account for the remaining 18%. Assuming a median Q_I at S-79 of 400 cfs, the Tidal Basin flows are estimated at 88 cfs for a total inflow of 488 cfs.

A two-day public science symposium was held on September 14–15, 2016 in the Fort Myers area to communicate all of the science contained in this document. This public meeting allowed for a robust dialogue regarding the science and research conducted by District staff and the science symposium provided the public with an opportunity to ask questions and receive technical feedback. After the two-day science symposium, there was a public commenting period that allowed the public to provide written comments/feedback. An agenda of the science symposium with a table summarizing all of the public comments with responses are incorporated into this science document as **Appendix A**.

TABLE OF CONTENTS

LIST OF FIGURES

This page left blank intentionally.

LIST OF TABLES

This page left blank intentionally.

ACRONYMS AND ABBREVIATIONS

°C	degrees Celsius
# m^{-2}	number per square meter
# m^{-3}	number per cubic meter
#/m^3	number per cubic meter
$\%I_0$	percentage of surface irradiance at the bottom (model parameter)
η	variable water level
µg L^{-1}	micrograms per liter
µmoles m^{-2} s^{-1}	micromoles per square meter per second
ac-ft	acre-feet
a_{CHL}	attenuation factor for chlorophyll *a* (model parameter)
a_{color}	constant for salinity-color relationship (model parameter)
AM2	amplitude at the water level tide (M_2) determined for the Ft. Myers monitoring station (model parameter)
ANCOVA	analysis of covariance
ANOVA	analysis of variance
a_{NTU}	attenuation factor for turbidity (model parameter)
APRS	Adaptive Protocol Release Study
A_{saw}	area of sawfish habitat
b_{color}	constant for salinity-color relationship (model parameter)
C&SF Project	Central and Southern Florida Flood Control Project
CERP	Comprehensive Everglades Restoration Plan
cfs	cubic feet per second
CH3D	Curvilinear Hydrodynamic Three Dimensional Model
CHL	chlorophyll *a* concentration
CHL_{max}	chlorophyll *a* maximum concentration
C_{init}	initial *Vallisneria* biomass values (model parameter)
C_{max}	maximum *Vallisneria* biomass (model parameter)
COA	center of abundance
CPUE	catch per unit effort
CRE	Caloosahatchee River Estuary
C_{shoot}	changes in aboveground biomass of *Vallisneria* (model parameter)

DBHYDRO	South Florida Water Management District's corporate environmental database
DO	dissolved oxygen
FDEP	Florida Department of Environmental Protection
fS_{gross}	gross production of *Vallisneria* (model parameter)
fS_{loss}	mortality of *Vallisneria* (model parameter)
fT_{shoot}	photosynthesis-irradiance relationship (model parameter)
G	gross production of *Vallisneria* (model parameter)
gdw m^{-2}	grams dry weight per square meter
GPS	global positioning system
G_{shoot}	gross production of *Vallisneria* (model parameter)
Gz	grazing on *Vallisneria* (model parameter)
Gz_{shoot}	herbivorous grazing on *Vallisneria* (model parameter)
h	depth (model parameter)
I_0	irradiance at the water surface (model parameter)
IDR	inter-decile range
I_k	half-saturation irradiance value (model parameter)
I_z	irradiance at the sediment (model parameter)
k_{color}	attenuation coefficient for color (model parameter)
kg	kilogram
kGz	basal grazing rate for *Vallisneria* (model parameter)
km	kilometer
kM	basal rate of mortality for *Vallisneria* (model parameter)
km^2	square kilometers
kR	basal rate of respiration for *Vallisneria* (model parameter)
kS_{loss}	salinity-specific loss rate (model parameter)
k_t	total attenuation coefficient for submarine light (model parameter)
KT1	*Vallisneria* temperature constant for photosynthesis (model parameter)
KT2	*Vallisneria* temperature constant for photosynthesis (model parameter)
k_w	total attenuation coefficient for pure water (model parameter)
lb	pound

lbs/trap	pounds per trap
lbs/trap/inch	pounds per trap per inch
LORS2008	Lake Okeechobee Regulation Schedule 2008
LOSA	Lake Okeechobee Service Area
m	meter
M	shoot mortality of *Vallisneria* (model parameter)
m^{-1}	per meter
m^2	square meter
m^2 gdw^{-1}	square meter per grams dry weight
m^{-2}	per square meter
M_2	tidal water level
m^3	cubic meter
MDS	multi-dimensional scaling
MFL	minimum flows and minimum water levels
mg L^{-1}	milligrams per liter
M_{shoot}	salinity-based mortality of *Vallisneria* (model parameter)
n	sample size
NEEPP	Northern Everglades and Estuaries Protection Program
NOAA	National Oceanic and Atmospheric Administration
NTU	nephelometric turbidity unit; turbidity (model parameter)
PhM2	phase angle of the water level tide (M2) determined for the Ft. Myers monitoring station (model parameter)
P_m	maximum rate of photosynthesis (model parameter)
POR	period of record
P_{photo}	photoperiod (model parameter)
Q_{calc}	inflow rate associated with a salinity of 10 at the Ft. Myers monitoring station
Q_I	indictor inflow
Q_{inflow}	inflow rate
Q_{S79}	inflow at S-79
Q_{TB}	inflow at the Tidal Basin
r	root mean square correlation coefficient
R	respiration of *Vallisneria* (model parameter)

r^2	degree of fit
rkm	distance of a station from Shell Point
rkm_U	density-weighted center of abundance for each sampling event
RMS	root mean square
R_{shoot}	respiration for *Vallisneria* (model parameter)
S	salinity
S10	salinity of 10
S_{12}	position of salinity of 12
S_{27}	position of salinity of 27
SAV	submersed aquatic vegetation
S_{FtM}	average monthly salinity at the Ft. Myers monitoring station
SFWMD	South Florida Water Management District
S_{val1}	daily salinity at SAV monitoring Site 1 (model parameter)
Tfx	temperature effect (model parameter)
TM2	period of the water level tide (M2) determined for the Ft. Myers monitoring station (model parameter)
T_{opt}	optimum temperature (model parameter)
T_w	water temperature (model parameter)
USACE	United States Army Corps of Engineers
V_{saw}	habitat volume for sawfish
WY	Water Year; the time from May 1 to April 30 of the subsequent year, named for the year in which it ends
z	sediment elevation (model parameter)

SCIENCE SUMMARY

Purpose of Study

The purpose of this study was to provide a comprehensive and quantitative assessment of the effects of freshwater inflow on the hydrology and ecology of the Caloosahatchee River Estuary (CRE) in the dry season (November–April). The dry season was chosen for this study because these are the times when freshwater inflows are diminished and negative responses from various ecological indicators are most likely to occur. It also coincides with the times when the minimum flows and minimum water levels (MFL) criteria are most likely to be exceeded. The objectives were (1) to compile and document information about freshwater inflows into and salinity distributions within the CRE, and (2) to examine the responses of a suite of ecological indicators to dry season freshwater inflows. This effort was conducted in support of the 2017 update to the MFL (Sections 373.042 and 373.0421, Florida Statutes) for the Caloosahatchee River [Rule 40E-8.221(2), Florida Administrative Code]. Specifically, this study explored new data collected since adoption of the MFL, analyzed older data using updated statistical approaches, and applied recently developed ecological models.

Freshwater discharge, tides and wind drive the estuarine salinity gradients, which influence all ecological processes in the water column and sediments. Organisms ranging in size and complexity from plankton to fish respond to fluctuations in inflow and salinity over a range of time scales. This study relied on multiple research components to examine inflow-salinity response patterns for phytoplankton, zooplankton, benthic communities, submersed aquatic vegetation (SAV), oyster beds, blue crabs (*Callinectes sapidus*), and sawfish (*Pristis pectinata*).

The Franklin Lock and Dam (S-79) located near Olga, Florida, serves as the upstream boundary for the CRE (**Figure 1**). Freshwater inflow has been measured at this location since its completion in 1966. Although a majority of the total freshwater inflow is through the S-79 structure, there is ungauged input of fresh water from tributaries and groundwater in the Tidal Basin downstream of the structure. Recent estimates of the Tidal Basin's contribution have improved with data availability and advancements in modeling. However, all analyses of indicator responses were conducted relative to measured inflow at the S-79 water control structure. The contribution of the Tidal Basin was incorporated into the final assessment of the magnitude of total inflows to the estuary (total inflows = S-79 + Tidal Basin).

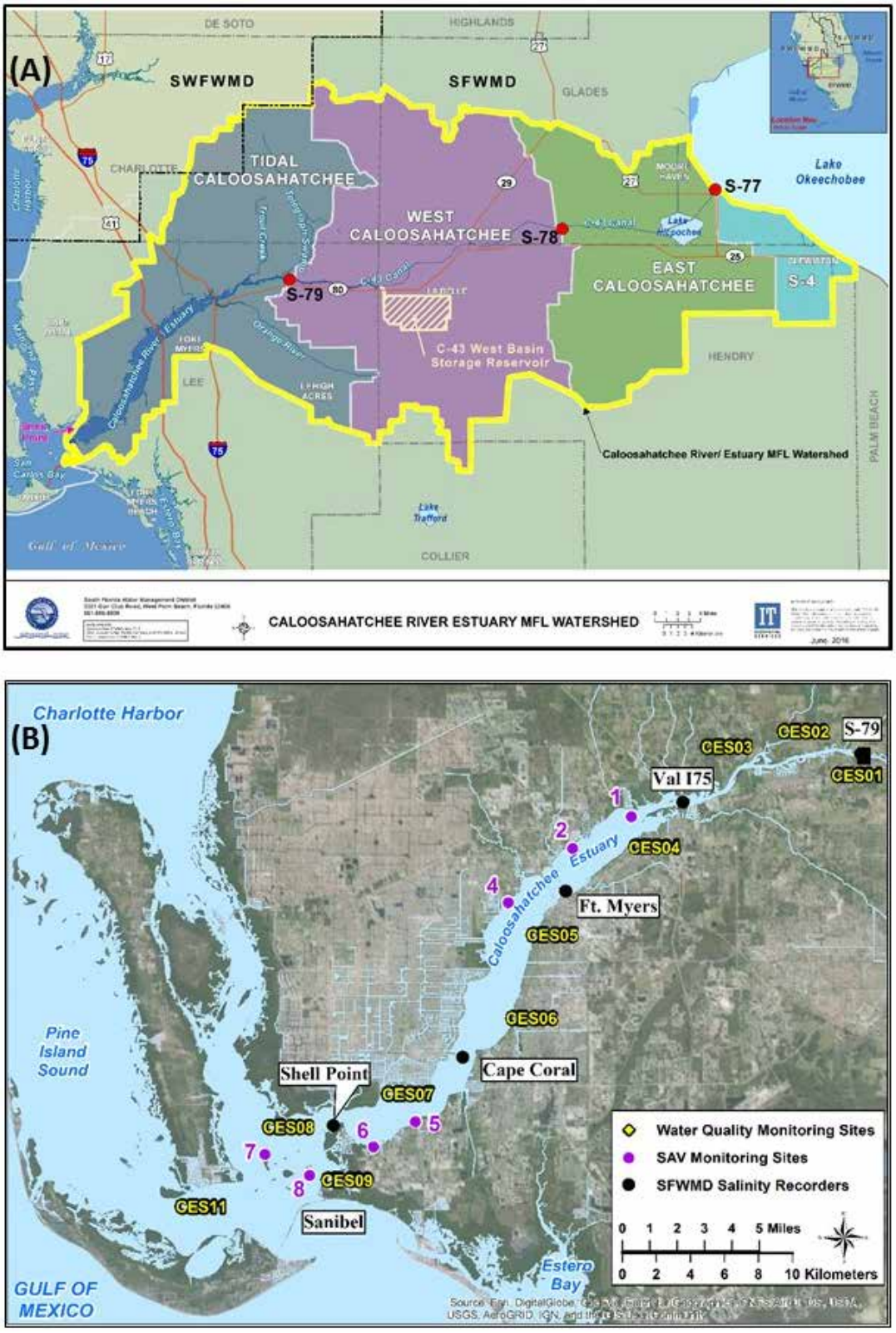

Figure 1. (**A**) The CRE MFL Watershed with its subwatersheds and major water control structures and (**B**) locations for the monitoring of water quality, SAV, and salinity recorders for the CRE.

Background Information

Alterations of the South Florida Landscape and CRE MFL Watershed

The CRE and the C-43 canal were connected to Lake Okeechobee through the evolution of the Central and Southern Florida Flood Control Project (C&SF Project). The C&SF Project is a complete system of canals, storage areas, and water control structures spanning the area from Lake Okeechobee to both the east and west coasts, and from Orlando south to the Everglades. It was designed and constructed during the 1950s and 1960s by the United States Army Corps of Engineers (USACE) to provide flood control and improve navigation and recreation. Most of the water bodies within the C&SF Project have specific regulation schedules that are federally mandated by USACE.

The South Florida Water Management District (SFWMD) is the local sponsor of the C&SF Project. In its capacity as local sponsor, SFWMD operates and maintains the C&SF Project. The operations require water to be moved out of certain water bodies when stages are above the regulation schedule to provide flood protection.

As a result of the C&SF Project, the modern South Florida aquatic landscape is highly engineered featuring ~3,380 kilometers (km) of canals, ~1,225 water control structures, more than 70 pumping stations, heavily managed wetlands, densely populated coastal watersheds, and highly impacted estuaries (Ogden et al. 2005, Obeysekera et al. 2011). This includes the region between Lake Okeechobee and the Gulf of Mexico encompassing the CRE MFL Watershed and CRE (**Figure 1A**; Buzzelli et al. 2015a). The portion of the watershed located upstream of the S-79 structure is referred to as the C-43 Watershed or C-43 Basin. The portion of the watershed located downstream of the S-79 structure is referred to as the Tidal Caloosahatchee subwatershed or Tidal Basin. Flows from the S-79 structure to the CRE are part of the C&SF Project. Water management must balance resource needs by protecting the natural system while simultaneously providing water supply, flood control, and recreation opportunities. As a result of these structural alterations, the availability of water that can be delivered to the CRE from the regional system to meet these needs is constrained.

In addition to the alterations described above, a multitude of other structural and physical alterations have occurred to the CRE MFL Watershed, historic Caloosahatchee River (now the C-43 canal), and CRE. These alterations changed the historical hydrologic conditions of the CRE MFL Watershed and downstream water bodies. A network of secondary and tertiary canals in the CRE MFL Watershed is connected to the C-43 canal and CRE. These canals provide navigational access or convey water for both drainage and irrigation to accommodate agricultural, urban, and other land uses in the watershed. Based on the 2012 land use land cover data, the primary land use type within the CRE MFL Watershed today is agricultural, which comprises 41.5%. Urban and built up land use comprises 18% and wetlands comprise approximately 15.1%.

Historically, the Caloosahatchee River was sinuous as it originated near Lake Flirt ~2 miles (3.2 km) east of La Belle at Fort Thompson. Beginning in the 1880s, the river channel was straightened, deepened, and connected to Lake Okeechobee. This resulted in a loss of 76 river bends and 8.2 miles (13.2 km) of river length (Antonini et al. 2002). Dredging alterations continued and, by 1918, three combination lock and spillway structures had been constructed at Moore Haven, Citrus Center, and Fort Thompson

(USACE 1957, Section 6.B.6). Flows within the historic Caloosahatchee River (now the C-43 canal) are controlled through the operation of multiple water control structures (S-77, S-78, and S-79) as these structures regulate downstream freshwater transport. The final lock and dam structure (S-79) was completed in 1966 at Olga to assure freshwater supply and prevent upstream saltwater intrusion. Discharges from Lake Okeechobee and the C-43 canal (between the S-77 and S-79 structures) are regulated by USACE.

Early descriptions of the CRE characterize it as barely navigable due to extensive shoals and oyster bars (Sackett 1888). Some of the alterations that have occurred include dredging a large navigational channel (Intracoastal Waterway) and secondary navigational channels, removing oyster bars upstream of Shell Point for roadway construction, removing the gulf bar at the mouth of the CRE, and the creation of two islands for construction of the Sanibel Causeway across the mouth of San Carlos Bay. Seven automobile bridges and one railroad bridge now connect the north and south shores of the estuary.

There are other more recent significant changes that affect water availability including the Lake Okeechobee Regulation Schedule that went into effect in 2008 (LORS2008), adaptive protocols for Lake Okeechobee, and establishment of a restricted allocation area for the Lake Okeechobee Service Area (LOSA). The restricted allocation area rule for LOSA that was adopted in 2008 limits allocations from Lake Okeechobee and integrated conveyance canal systems that are hydraulically connected to and receive surface water from Lake Okeechobee (Balci and Bertolotti 2012). This includes the C-43 and C-44 canals. The current regulation schedule (LORS2008) regulates the stage in Lake Okeechobee approximately one foot lower than the previous Water Supply and Environment Regulation Schedule. The adaptive protocols for Lake Okeechobee are intended to provide operational flexibility to facilitate environmental benefits without impacting other lake uses. The adaptive protocols were modified for use with the LORS2008 in the *Final Adaptive Protocols for Lake Okeechobee Operations* (SFWMD 2010), which was finalized on September 16, 2010.

The potential for removing the existing structural and physical alterations affecting the C-43 canal and the CRE may not be economically or technically feasible. Much of the existing development within the downstream water bodies is dependent upon the modern functions of these alterations (e.g. flood protection, navigation, water supply, and transportation). For this reason, SFWMD has been strategically focused on making improvements within the watershed rather than the downstream estuary. Programs and projects to improve water regimes and ecosystem health, or both, include the Dispersed Water Management Program; Caloosahatchee Storage/Treatment Project; Comprehensive Everglades Restoration Plan (CERP), including the CERP Caloosahatchee River (C-43) West Basin Storage Reservoir; Northern Everglades and Estuaries Protection Program (NEEPP); and other smaller projects (SFWMD 2012).

Freshwater Inflow and Estuaries

Small estuaries and embayments with subtropical climates and managed inflow are particularly susceptible to reduced freshwater input on scales of days (event-scale) to years (Schlacher et al. 2008, Buzzelli 2011, Azevedo et al. 2014). Inflows are managed because many estuarine rivers have dams at the upstream boundary (Montagna et al. 2002a) similar to the CRE. Low inflow increases hydrodynamic residence time as the upstream

encroachment of saltier water can establish a cascade of low inflow-related ecological responses (Sheldon and Alber 2006, Wan et al. 2013).

Submarine light often increases throughout the estuary with the reduced input of colored dissolved organic matter that freshwater inflow provides (Bowers and Brett 2008, Chen et al. 2015). Reduced flushing coupled with enhanced light in the surface layer can stimulate the rapid proliferation of phytoplankton in the upper estuary on scales of days to weeks (Murrell et al. 2007, Lancelot and Muylaert 2011, Cloern et al. 2014). Zooplankton and ichthyoplankton assemblages often shift upstream with their food resources (phytoplankton) while remaining within favorable salinity zones (Flannery et al. 2002). However, there is the possibility of habitat impingement and/or compression if upstream movement of planktonic assemblages is bounded by a water control structure (Crowder 1986, Tolley et al. 2010). The overall biological productivity in estuaries is proportional to freshwater inflow (Livingston et al. 1997, Gillson 2011).

Saltwater encroachment can alter the composition and density of the macrobenthic community upon which many estuarine fish and crustaceans are dependent (Palmer et al. 2011, Montagna et al. 2013). The freshwater macrophyte *Vallisneria americana* (tape grass) provides essential habitat in the oligohaline portion of many estuaries. However, it is very sensitive to increases in the frequency and duration of elevated salinity (Doering et al. 2002, French and Moore 2003, Rozas and Minello 2006). Increased salinity also can impact the survival of the eastern oyster (*Crassostrea virginica*) through the introduction of marine parasites and predators (Livingston et al. 2000, Petes et al. 2012). The life histories of many coastal fish populations rely on favorable salinity gradients as they utilize estuaries as nursery and feeding areas (Whitfield et al. 2012, Stevens et al. 2013, Sheaves et al. 2015). Finally, long-term reductions in freshwater inflow can be associated with declining harvests of important fishery species (Wilber 1994, Gillson 2011).

Fluctuations in freshwater inflows over time scales ranging from weeks to years have altered salinity regimes and impacted the ecology of the CRE (Chamberlain and Doering 1998a, Barnes 2005). Changes in freshwater inflows and salinity have been shown to affect the distribution and dynamics of many taxa and communities including phytoplankton and zooplankton (Tolley et al. 2010, Radabaugh and Peebles 2012), SAV (Doering et al. 2001, 2002, Lauer et al. 2011), oysters and pathogens (La Peyre et al. 2003, Barnes et al. 2007, Volety et al. 2009), fauna inhabiting oyster reefs (Tolley et al. 2005, 2006), and fishes (Collins et al. 2008, Heupel and Simpfendorfer 2008, Simpfendorfer et al. 2011, Poulakis et al. 2013, Stevens et al. 2013).

Freshwater Inflow and the CRE

South Florida has a subtropical climate featuring dry (November–April) and wet (May–October) seasons (Childers et al. 2006, Moses et al. 2013, Buzzelli et al. 2015a). Event-scale weather, extreme intra-annual seasonal variations in precipitation, and longer-term climatic fluctuations (3 to 6 years) are incorporated into water management (Obeysekera et al. 2007). In order to include both a wet and a dry season, a water year (WY) is defined as the time from May 1 to April 30 of the subsequent year. A WY is named for the year in which it ends.

The long-term annual average (WY1997–WY2014) rainfall within the CRE MFL Watershed was 51.5 inches with 21.9% in the dry season and 78.1% in the wet season

(**Figure 2A**). Freshwater discharge at the S-79 structure represents the combined contribution of rainfall-driven runoff from the CRE MFL Watershed as well as releases from Lake Okeechobee. The average annual total inflow (WY1997–WY2014) was 1.8 x 10^6 acre-feet (ac-ft) (2,220 x 10^6 cubic meters [m^3]). Over this time period, the relative contributions from Lake Okeechobee, the C-43 Watershed upstream of S-79, and the Tidal Basin downstream of S-79 averaged 31.6%, 47.6% and 20.8%, respectively (**Figure 2B**).

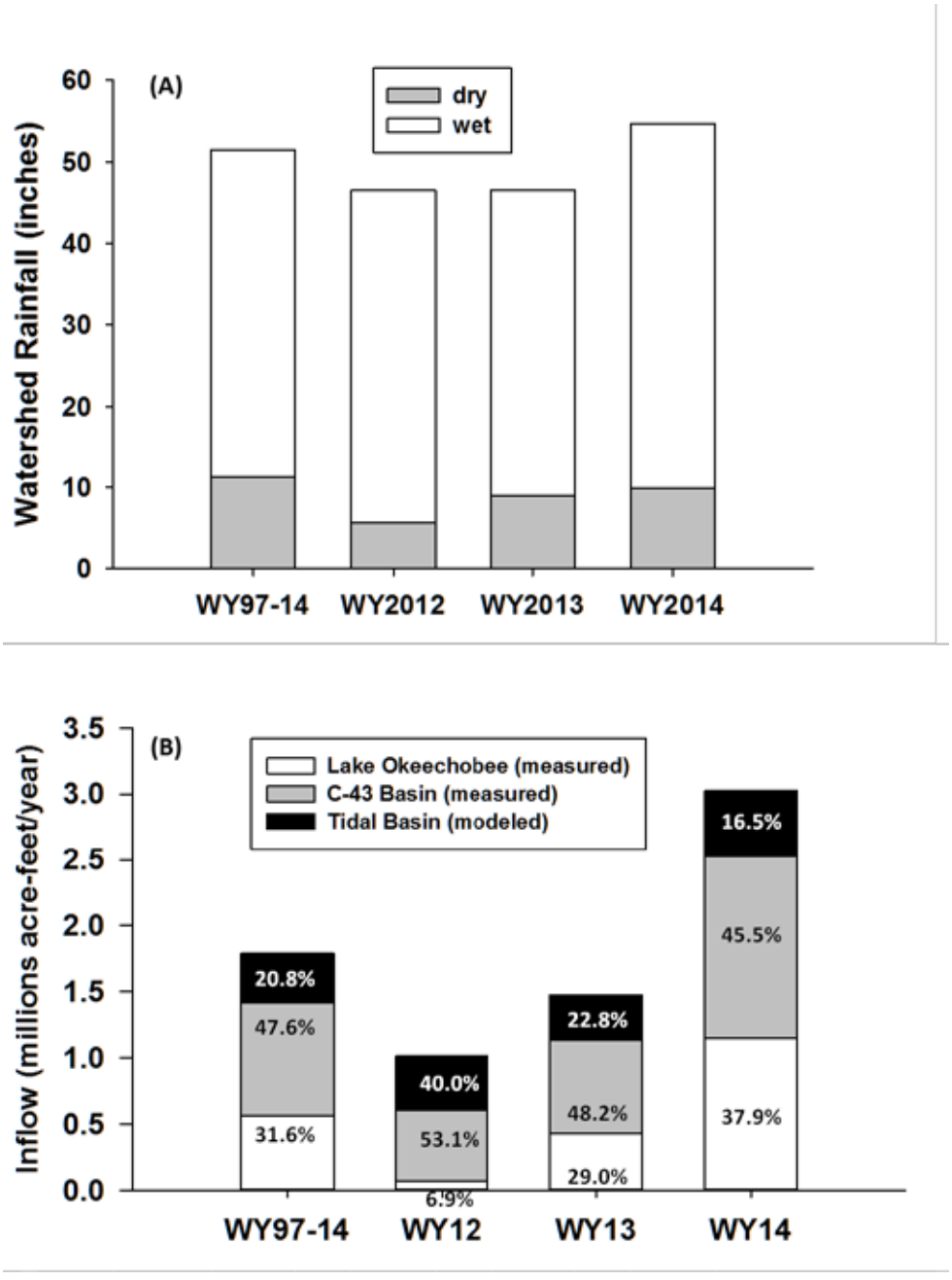

Figure 2. (**A**) Total rainfall to the Caloosahatchee River Estuary MFL Watershed by water year and season and (**B**) stacked bar chart for the total freshwater inflow (millions of ac-ft per year). Included are the long-term averages from WY1997–WY2014, WY2012, WY2013, and WY2014.

The CRE is bounded upstream by the S-79 structure and downstream by San Carlos Bay at the mouth (**Figure 1A**). The surface area of the CRE is 67.6 square kilometers (km^2) (6,764 hectares = 16,715 acres) with an average depth of 2.7 meters (Buzzelli et al. 2013b). Average flushing time ranges from 5 to 60 days (Wan et al. 2013, Buzzelli et al. 2013c). A variety of physical, chemical and biological variables are regularly monitored by SFWMD and other organizations (**Figure 1B**). Freshwater inflow has been measured at S-79 since 1966 and is reported as daily average cubic feet per second (cfs). Surface and bottom salinity have been monitored at multiple locations (S-79, Val I75, Ft. Myers, Cape Coral, Shell Point, and Sanibel) since the 1990s and is reported as average daily values. Salinity is derived from a dimensionless ratio and therefore has no units in reporting (Millero 2010). The distribution and density of SAV have been determined at the upper stations (1, 2, and 4) since 1998 and the in the lower estuary (5, 6, 7, and 8) bi-monthly since 2004. Oyster population attributes have been monitored seasonally at multiple locations in the lower estuary near Shell Point since 2000.

The term "ecohydrology" was coined to describe the integrative management of coastal basins based on the linkages among inflows, circulation, environmental conditions, habitat attributes, and biological integrity (Peterson 2003, Wolanski et al. 2004). Essential to this conceptualization are resource-based approaches to quantify minimum freshwater inflows (Chamberlain and Doering 1998b, Alber 2002). This approach seeks to identify the historical inflow regime, the biological resources to be protected, and the environmental conditions required to sustain them and determine inflow regimes needed to maintain the desired conditions (Palmer et al. 2011). Choosing an indicator resource that responds to freshwater inflow in a timeframe appropriate for management can be problematic (Dale and Beyeler 2001, Alber 2002). In many cases, there are limited data for, or changes in, the indicator resource that preclude extraction of useful information from the existing data.

The Caloosahatchee River MFL criteria were based on the salinity tolerance of *Vallisneria americana* (Doering et al. 1999, Doering et al. 2001, Doering et al. 2002, SFWMD 2003). *Vallisneria* was selected as an indicator because of its location in the estuary, its sensitivity to enhanced salinity, and its important habitat functions (sediment stabilization, nursery area, and food web support for invertebrate and vertebrate fauna). An independent peer review in 2000 of the SFWMD MFL document (SFWMD 2000) emphasized four problematic research areas: (1) lack of a hydrodynamic/salinity model; (2) lack of a numerical population model for *Vallisneria americana*; (3) no quantification of the habitat value of *Vallisneria* beds; and (4) lack of documentation of the effects of MFL flows on downstream estuarine biota (SFWMD 2003). A research program was initiated in 2001 to address some of these concerns and a review of the MFL criteria was conducted (SFWMD 2003).

There has been much effort towards addressing the problematic areas identified in the peer review. Salinity data collected at 15-minute intervals at multiple locations between S-79 and Shell Point have been central to the development and calibration of a three-dimensional hydrodynamic model (Qiu 2002, 2006, Qiu and Wan 2013, Wan et al. 2013). Additionally, the long-term time series of salinity at the Ft. Myers station (1992–present) and other locations are essential to a wide range of water quality and ecological studies supporting water management (Balci and Bertolotti 2012, Buzzelli et al. 2015a). The Florida Department of Environmental Protection (FDEP), SFWMD, and United States Geological Survey jointly conducted a flow monitoring program from October 2008 to

March 2013 to measure stage and flow at several locations in the Tidal Basin of the CRE (Telegraph Creek, Orange River, Popash Creek, Billy's Creek, Hancock Creek, Marker 52, and Shell Point). Lee County has monitored Whiskey Creek since April 1994. These data were collected to support further development and calibration of the Tidal Basin Model (Wan and Konyha 2015).

The distribution and abundance of *Vallisneria* have been documented since 1997 (Buzzelli et al. 2015a). Additionally, studies of the responses of *Vallisneria* to variable salinity and temperature (Doering et al. 2001, 2002, Bartleson et al. 2014) provided an information base for both empirical assessments and the development of a simulation model (this document). Site-specific assessment of *Vallisneria* habitat value has been impeded by the greatly reduced distribution and density of *Vallisneria* since droughts in 2001 and 2007–2008. Oyster beds were identified as stationary indicators of salinity and freshwater inflow in the lower estuary (Volety et al. 2009, Buzzelli et al. 2013a). Oyster population attributes have been monitored in the lower CRE as part of CERP since 2005 (RECOVER 2014).

The Conservancy of Southwest Florida filed a petition on September 3, 2010, requesting immediate initiation of rulemaking to revise the Caloosahatchee River MFL Rule. The SFWMD Governing Board denied this petition. However, SFWMD committed to review and update the Caloosahatchee River MFL Rule after conducting the appropriate scientific analyses based on the best available information.

Methods

Description of Component Studies

This effort was composed of 11 component studies to evaluate the effects of reduced freshwater inflow on the CRE in the dry season (**Table 1**). While the estimation of estuarine inflow requirements using multiple indicators offers a system of checks and balances, the quantitative assessment of the responses of a particular resource to variable levels of inflow can be very difficult (Adams et al. 2002).

Table 1. List of component studies and the basic description of research methods. Studies 2 through 11 resulted in estimates of indicator inflow magnitudes.

	Study	Method
1	Hydrodynamics	Influence of alterations on hydrodynamics
2	Inflow versus Salinity	Monthly freshwater-salinity relationships at Ft. Myers
3	Water Quality	Fine-scale relationships between water quality and inflow
4	Zooplankton	Inflow, zooplankton impingement, and habitat compression
5	Ichthyoplankton	Relationships between ichthyoplankton and inflow
6	Benthic Fauna	Macrofauna-salinity patterns relative to inflow
7	*Vallisneria* Data	Empirical relationships between *Vallisneria*, salinity, and inflow
8	*Vallisneria* Model	Model exploration of *Vallisneria*, salinity, light, and inflow
9	Oyster Habitat	Assess conditions for oyster survival in the lower CRE
10	Blue Crabs	Relationships between blue crab landings, rainfall, and inflow
11	Sawfish	Area and volume of sawfish habitat with variable dry season inflow

Implications of Uncertainty

Uncertainty is a fundamental property that can propagate through computational schemes and contribute to interpretative errors (Regan et al. 2002, Lehrter and Cebrian 2010). It is important that the uncertainty associated with proposed environmental actions be evaluated, quantified, and properly explained so that all stakeholders can better connect changes in ecological systems to effective scientific inquiry and improved management (Lamon et al. 1996, Halpern et al. 2006). Limits in data quantity, data quality, and an understanding of dynamic processes increase uncertainty in predictive models (Reckhow 1994). Although assessments of environmental risk using models can be inherently uncertain, the information contained in uncertainty can be applied to benefit environmental decision making (Reckhow 1994). For example, data gaps and missing information can be identified by evaluating uncertainty and variability (Ahn and James 2001).

Unlike environmental management of rivers or lakes, salinity serves as the connection between biotic resources in the receiving basin and the rate of freshwater inflow in estuaries (Alber 2002). Spatial and temporal salinity variations are complicated by wind and atmospheric frontal passages, tidal exchange, and vertical mixing. Thus, it is very difficult to directly relate freshwater inflows, hydrodynamic processes, and biological responses in coastal basins. Difficulties arise from a combination of scalar mismatches, complexity and uncertainty, temporal and spatial lags, and an overall lack of data.

This study included estimations of freshwater inflow associated with observed or simulated responses of selected estuarine indicators. These estimations were based on data, information, assumptions, discussions, and calculations, which carry varying amounts of inherent and systematic uncertainty. Despite inevitable uncertainty, this document provides the best available information through which to better understand the potential responses of selected indicators to salinity regimes within the CRE in the dry season.

Quantification of Indicator Freshwater Inflows in the Dry Season

This study applied elements of a resource-based approach to the quantification of freshwater inflows that might be limiting to the ecological functioning of the CRE in the dry season. The component studies emphasized the relationships between the indicators and inflows through the S-79 structure. The term "indicator inflow" or Q_I was defined as the S-79 inflow threshold below which there might be detrimental effects. There were 11 different approaches to estimate Q_I (Study Components 2 through 11).

1. Component Study 1 utilized hydrodynamic modeling as a tool to explore changes in circulation and salinity caused by structural alterations at the estuary scale but did not provide estimates of inflows relative to estuarine response variables.
2. Component Study 2 used the relationship between average monthly inflow at S-79 and average monthly salinity at the Ft. Myers station to estimate the quantity of fresh water associated with a salinity value of 10 from WY1993 to WY2013.
3. Component Study 3 emphasized the relationship between low inflow and elevated chlorophyll *a* concentrations (CHL) to estimate Q_I when CHL in the upper CRE was greater than the impaired estuarine waters target of 11 micrograms per liter ($\mu g\ L^{-1}$) (FDEP 2009). This approach was applied independently to both empirical and model-derived CHL values.
4. Component Study 4 estimated Q_I as the inflow threshold below which the upstream movement of the zooplankton community would be impinged against the S-79 structure.
5. Component Study 5 utilized salinity tolerances of ichthyoplankton to estimate the habitat area with reduced inflow.
6. Component Study 6 estimated Q_I from inflows on the days when the salinity in the upper CRE was greater than the tolerance range associated with the characteristic benthic macrofauna community.
7. Component Study 7 extracted dry season days where the salinity at the Ft. Myers station ranged from 9 to 10 from WY1993 to WY1999 when *Vallisneria* was abundant to calculate Q_I.
8. Component Study 8 applied a *Vallisneria* simulation model to identify the salinity and inflows where *Vallisneria* experienced net mortality.
9. Component Study 9 extracted days where the salinity at Cape Coral was 20 to 25 from WY2005 to WY2014 concurrent with oyster monitoring to calculate Q_I.
10. Component Study 10 examined the relationships between rainfall and Lee County blue crab catch data.
11. Component Study 11 assessed the impact of inflows on the area of favorable habitat for the endangered sawfish in the dry season.

Results

Summaries of Component Studies

Component 1: Three-dimensional Model Evaluation of Physical and Structural Alterations of the Caloosahatchee River and Estuary: Impact on Salt Transport

Hydrodynamic modeling of estuaries provides a platform to assess the effects of physical alterations on hydrodynamics, transport, and mixing. This study component utilized a three-dimensional hydrodynamic model (Curvilinear Hydrodynamic Three Dimensional Model or CH3D) of the CRE to compare simulated salinities between the existing condition and the reversal of five historical physical alterations to the estuary. The alterations evaluated were the (1) removal of the S-79 water control structure; (2) removal of the downstream causeway (Sanibel); (3) backfill of the oyster bar near the estuary mouth; (4) backfill of the navigation channel; and (5) reestablishment of predevelopment bathymetry. Model results indicated that refilling the navigation channel had profound effects with a 20% reduction in dry season salinity. The reduced salt transport was more pronounced with the predevelopment bathymetry because the estuary was much shallower. Increased estuary depth and cross-sectional area significantly increase salt transport to the upper estuary. Increased salt transport can push biologically relevant isohalines further upstream depending upon freshwater inflow conditions.

Component 2: Analysis of the Relationship between Freshwater Inflow at S-79 and Salinity in the CRE 1993–2013

The upstream migration of salt with reduced freshwater inflow alters the composition and productivity of oligohaline habitats in estuaries. This process can be problematic in subtropical estuaries with regulated freshwater inflow such as the CRE in southwestern Florida. This study component examined relationships between average monthly inflow (Q) and mid-estuary salinity (S) from 1993 to 2013. An exponential decay equation was fit to the inflow-salinity (Q-S) relationship for each water year (May 1 to April 30). Annual equations were used to estimate the inflow rate associated with salinity equaling 10 at the Ft. Myers monitoring station (Q_{calc}). Inflows varied both intra- and inter-annually. Q_{calc} ranged from 70 to 773 cfs with an average of 445 ± 218 cfs. At the estuary and annual scales, the quantity of fresh water to support a particular salinity target varied greatly. This variance was related to the variations in freshwater inputs from both the C-43 Watershed located upstream of the S-79 structure and the downstream Tidal Basin.

Component 3: Relationships between Freshwater Inflows and Water Quality Attributes during the Dry Season in the CRE

Decreased flushing with reduced inflow can lead to the deposition of phytoplankton biomass and bottom water hypoxia in estuaries. This study component utilized event-scale water quality data, long-term monitoring of CHL, and simulation modeling of phytoplankton dynamics to evaluate low freshwater inflows that could contribute to water quality problems in the upper CRE. The highest CHL and lowest dissolved oxygen (DO) concentrations occur in the upper CRE under low inflows. Although more research is needed, it is hypothesized that dry season inflows of less than approximately 500 to 600 fs may promote bottom water hypoxia in the deeper channel of the upper CRE. Field and model results indicated that CHL concentrations greater than the water quality standard of

11 µg L^{-1} were associated with inflows of 469 ± 689 cfs and 269 ± 493 cfs, respectively. Low level inflows (<500 cfs) need to be further studied to better quantify the discharge required to mitigate the potential for hypoxia in the upper CRE.

Component 4: Zooplankton Response to Freshwater Inflow in the CRE

Freshwater inflow to some estuaries, including the CRE, is regulated through control structures. Zooplankton assemblages provide an essential food web link whose position in the estuary fluctuates with inflow. Unfortunately, zooplankton habitat can be both impinged and compressed due to the presence of a water control structure as inflow is reduced in the dry season. This study assessed impingement and habitat compression for zooplankton under reduced inflow. Data used were from a CRE study conducted by Florida Gulf Coast University from 2008 to 2010. Zooplankton samples were collected monthly at each sampling site at night during a flood tide. The centers of abundance (COA) for the 13 taxa investigated migrated downstream and upstream as freshwater inflow increased and decreased, respectively. Both habitat compression and impingement were potentially harmful for zooplankton assemblages in the estuary. Impingement was possible if inflow from the S-79 structure ranged from 98 to 566 cfs and averaged 412 ± 165 cfs. Almost all taxa investigated (except *Menidia*) experienced habitat compression if the COA was < 12 km downstream of S-79.

Component 5: Ichthyoplankton Response to Freshwater Inflow in the CRE

Ichthyoplankton communities are key components of food webs in the upper, oligohaline reaches of most estuaries. This study analyzed historical (1986–1989) data to evaluate effects of salinity and freshwater inflow on ichthyoplankton communities in the CRE. Abundance of ichthyoplankton was greatest when the 30-day inflows at S-79 averaged between 151 and 600 cfs. Juvenile fish appeared to prefer salinities < 10 and their abundance was centered just downstream of Station 2 near Beautiful Island. Flows at S-79 associated with a salinity of 10 near Beautiful Island averaged 237.5 ± 255.5 cfs. Flows less than this could result in loss of favorable habitat.

Component 6: Summary and Interpretation of Macrobenthic Community Properties Relative to Salinity and Inflow in the CRE

The composition, distribution, and density of benthic invertebrate communities (macrofauna) can be used as indicators of salinity and inflow for estuaries. The goal of this study component was to explore the relationships between inflow, salinity, and benthic macrofauna in the CRE. Benthic samples were collected every 2 to 4 months at seven stations during two periods (February 1986–April 1989 and October 1994–December 1995). The abundance, diversity, and composition of the macrofaunal community were determined relative to observed fluctuations in salinity. Four distinct zones emerged based on salinity ranges and the composition of the macrobenthic community. Conditions conducive to maintain the characteristic community observed during the sampling periods in the most upstream zone (salinity = 0 to 4, 0 to 7 km from S-79) occurred on 54% of dry season days from 1993 to 2012. The indicator inflows (Q_I) ranged from 0 to 3,720 cfs and averaged 501 ± 525 cfs for the days where salinity was 3 to 4 (sample size [n] = 181).

Component 7: Relationships between Salinity and the Survival of Vallisneria americana *in the CRE*

Vallisneria americana is sensitive to increased salinity in many estuaries, including the CRE. Much of the *Vallisneria* observed from 1993 to 1999 in the CRE has been lost since droughts in 2001 and 2007–2008. This study examined relationships between *Vallisneria* and salinity through change-point analysis, assessment of long-term patterns of abundance, and exploration of the effects of salinity exposure time. Change-point analysis revealed salinity thresholds of 4, 9, and 15. Dry season average daily salinity was ~5 and rarely exceeded 10 when *Vallisneria* was abundant from 1993 to 1999. Indicator inflows (Q_I) ranging from 0 to 3,160 cfs and averaging 545 ± 774 cfs, were associated with dry season salinity values of 9 to 10 (n = 63) at the Ft. Myers station from 1993 to 1999. In contrast, *Vallisneria* was virtually absent from 2007 to 2013 as dry season average daily salinity exceeded 10. Negative changes in shoot density can be rapid as ~50 to 60% of the aboveground material was lost if salinity was > 10 for two to three weeks. These results highlight the effects of both the magnitude and duration of environmental conditions that can inhibit *Vallisneria* survival in the CRE.

Component 8: Development and Application of a Simulation Model for Vallisneria americana *in the CRE*

Monitoring of *Vallisneria americana* densities in the upper CRE from 1998 to 2007 was accompanied by mesocosm experiments to determine relationships between salinity and growth. This study built upon these efforts by developing a simulation model to examine the effects of temperature, salinity, and light on *Vallisneria* survival and biomass in the upper CRE from 1998 to 2014. The effects of salinity on *Vallisneria* mortality were explored using an eight-year experimental model based on favorable conditions from 1998 to 1999. Using the experimental model, the dry season salinity was systematically increased in 5% increments until the net annual biomass accumulation of *Vallisneria* was negative. A five-fold increase in grazing was required to stabilize model biomass under optimal conditions. A 55% salinity increase to 12 promoted shoot mortality in the experimental model. Annual inflow-salinity relationships for the Ft. Myers station were used to estimate that dry season inflows ranging from 15.2 to 629.0 cfs and averaging 342 ± 180 cfs were associated with a salinity of 12 at the Ft. Myers station. Model results suggested that an estimated 85.4% and 86.7% of the shoots were lost in the dry seasons of 2001 and 2007, respectively.

Component 9: Assessment of Dry Season Salinity and Freshwater Inflow Relevant for Oyster Habitat in the CRE

Short- and long-term alteration of salinity distributions in estuaries with variable freshwater inflow affects the survival, abundance, and extent of oyster habitat. The objective of this study was to evaluate salinity conditions at two locations, Cape Coral and Shell Point, in the CRE. Salinity data from the 2006 through 2014 dry seasons (November–April) were categorized relative to oyster habitat criteria and related to freshwater inflow. Daily salinity was within the appropriate range for oysters (10–25) on 70.1% of the observations. Daily inflow ranged from 0 to 2,000 cfs and averaged 296 ± 410 cfs when salinity ranged from 20 to 25 at Cape Coral in the dry season. The influence of the marine parasite *Perkinsus marinus* (Dermo) is limited due to the subtropical climate where temperature is low when salinity is high (dry season) and temperature is high when salinity

is low (wet season). Overall salinity patterns were favorable for oyster survival at the upstream extent of oyster habitat in the CRE.

Component 10: Ecohydrological Controls on Blue Crab Landings and Minimum Freshwater Inflow to the CRE

A long-term record (28 years) was used for blue crab landings in the CRE to establish relationships between (1) changes in hydrology and changes in water resource function and (2) the magnitude of the functional loss and time to recover. Annual catch per unit effort (CPUE), computed from monthly landings of crabs and measures of fishing effort, represented the resource function. Annual landings expressed as both unadjusted and de-trended CPUE were found to be significantly correlated with hydrologic variables, rainfall, and freshwater inflow during the previous year's dry season. Increases in CPUE from one year to the next were also positively related to dry season rainfall in the first of the two years. Geometric mean functional regressions and Monte Carlo simulations were used to identify the dry season rainfall associated with losses of water resource function (CPUE) that required 1, 2, or 3 years of average dry season rainfall to recover. A spectral analysis indicated that time series of both dry season rainfall and blue crab catch had periodicities of 5.6 years. A Monte Carlo analysis revealed that the rainfall associated with two- and three-year recoveries had return intervals of 5.8 and 8.2 years, respectively.

*Component 11: Relationships between Freshwater Inflow, Salinity, and Potential Habitat for Sawfish (***Pristis pectinata***) in the CRE*

The smalltooth sawfish is an endangered species that historically ranged from Texas to North Carolina. The distribution and abundance of sawfish have declined due to over-fishing and habitat loss. Presently, the CRE is an important sawfish nursery. Juvenile sawfish habitat can be characterized as nearshore environments < 1 meter in depth, where salinities range from 12 to 27. This study quantified sawfish habitat with variable inflow to the CRE in the dry season using a combination of bathymetric analyses and hydrodynamic modeling. Inflows of 150 to 300 cfs positioned the 12 and 27 salinities in the shallowest part of the estuary (10 to 30 km downstream). Specifically, the area of sawfish habitat was greatest (5.7 km^2) when inflow through the S-79 structure was 270 cfs in the dry season. Under reduced inflow, the habitat migrated into the channel above Beautiful Island where it was compressed against S-79. Higher inflows pushed S_{27} out of the estuary.

Quantification of Indicator Freshwater Inflows in the Dry Season

While there were 10 separate component studies that generated values for Q_I, the water quality component provided both empirically-based and modeled estimates using the same selection criteria (**Table 2** and **Figure 3**). Among 11 different calculations, the estimated magnitude of Q_I was least from the phytoplankton model (269 ± 493 cfs), the sawfish habitat assessment (270 cfs), analysis of ichthyoplankton data (237 ± 255 cfs), and evaluation of conditions relative to oyster tolerances (296 ± 410 cfs). While an inflow rate of 545 ± 774 cfs was estimated to inhibit *Vallisneria* survival, the modeling exercise predicted that inflow rates less than 342 ± 180 cfs could lead to *Vallisneria* mortality. There was a wide range of sample sizes (n) used to estimate Q_I among the calculations (2 to 422). For example, 16 annual values were used in Component 2 (S-79 inflow versus salinity at the Ft. Myers station) compared to 181 daily values derived in Component 6 (benthic

fauna). Four of the approaches used the salinity requirements of an indicator resource as a guide to select corresponding dry season inflows (benthic fauna, *Vallisneria* data, oysters, and sawfish). Each of these four estimates generally resulted in a wide range of possible inflows and therefore, large standard deviations that were greater than the average values. On the other hand, estimates among the customized approaches from the other five component studies (S-79 inflow versus salinity, zooplankton, icthyoplankton, *Vallisneria* model, and blue crabs) had narrower ranges and less variance (**Table 2**). For example, Q_I estimated for zooplankton and ichthyoplankton assemblages averaged 412 ± 165 cfs and 237 ± 255 cfs, respectively. As a result of the method, a single value for Q_I was estimated from assessment of sawfish habitat (270 cfs). A different optimum salinity range from 18 to 30 was evaluated for juvenile sawfish in the CRE after receiving public comment. Habitat area was recalculated based on the same hydrodynamic modeling results and bathymetric data. The result of this analysis showed that as discharge increases habitat area and volume decreased (see Addendum to Component 11).

Table 2. Summary of component studies, the method used to estimate the indicator inflow (Q_I), and the range and average + standard deviation (Avg + SD) values for Q_I (cfs). The median value for Q_I over all estimates is provided (362 cfs).

	Component	Method	Q_I (cfs)	
			Range	Avg + SD
1	Hydrodynamics	Hydrodynamic model used to evaluate long-term structural modifications to the CRE	Not applicable (NA)	NA
2	Inflow versus Salinity	Based on calculated inflow at S-79 associated with S-10 at the Ft. Myers station from monthly average long-term data (WY1993–WY2013; n = 16)	70–720	445 ± 218
3	Water Quality - Data	Estimated using monthly average dry season CHL > 11 µg L^{-1} observed at CES03 linked to daily freshwater inflow (n = 8).	0–2,270	469 ± 689
	Water Quality – Model	Estimated using daily average dry season CHL > 11 µg L^{-1} predicted in the upper CRE linked to daily freshwater inflow (n = 58).	0–2,450	269 ± 493
4	Zooplankton	Estimated using monthly zooplankton center of abundance (2008–2010) and lagged inflows with conditional regression (n = 7).	98–566	412 ± 165
5	Ichthyoplankton	Estimated using monthly icthyoplankton center of abundance (2008–2010) and 30-day average salinity at the Ft. Myers station (n = 11).	62–1191	237 ± 255
6	Benthic Fauna	Benthic fauna data used to establish optimal salinity in the upper reaches of the CRE (optimum salinity = 3–4). Long-term (WY1993–WY2012) inflow at S-79 and salinity at BR31 were used to calculate inflow on dry seasons days meeting optimal salinity criteria (n = 181).	0–3,720	501 ± 525
7	*Vallisneria* Data	Estimated using maximum salinity tolerance (salinity = 9–10) and dry season Ft. Myers station salinity data from the period when *Vallisneria* was abundant (WY1993–WY1999; n = 63).	0–3,160	545 ± 774
8	*Vallisneria* Model	Simulation series where dry season daily salinity was proportionally increased until *Vallisneria* biomass stabilized in optimized 8 year-model version. Estimated inflows from dry season days in 1998–1999 where salinity at Val Site 1 ranged from 6.3 to 6.5 (n = 32).	0–526	342 ± 180
9	Oyster Habitat	Estimated from maximum salinity tolerance (salinity = 20–25) and dry season daily salinity at Cape Coral from WY2005 to WY2014 (n = 422).	0–2,000	296 ± 410
10	Blue Crabs	Estimated using rainfall/discharge associated with significant harm to Lee County blue crab fishery from WY1981 to WY2013 (n= 2).		400 ± 57[a]
11	Sawfish	Estimated using hydrodynamic model to quantify relationship between the area that was < 1 meter and favorable salinity range (12–27 or 18–30) and inflow.		270[b]

a. Average from two estimates.

b. Only one value estimated for sawfish using the 12–27 salinity range.

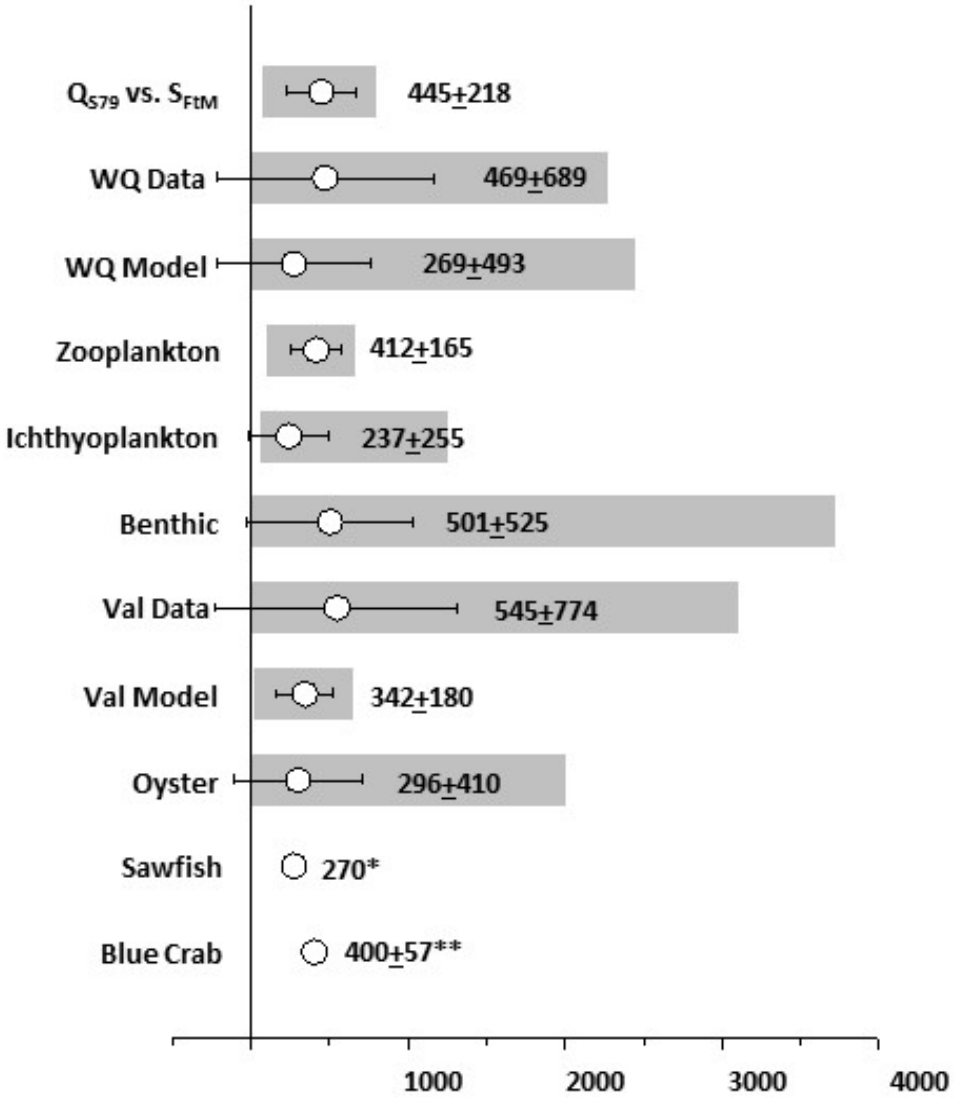

Figure 3. Graphical results showing the range (bar) and average + standard deviation (point + error bar and text) of the estimated indicator inflows (QI) for each of the component studies. See **Table 2** and text for calculation details related to each estimate.
*Only one value was estimated for sawfish using the 12–27 salinity range.
**Average from two estimates.

Discussion

The purpose of this study was to provide a comprehensive and quantitative assessment of the effects of freshwater inflow during the dry season on the hydrology and ecology of the CRE in the dry season (November–April). It is unique in its scope to incorporate multiple indicators along the length of the estuary that respond to fluctuations in discharge or salinity on time scales ranging from days (water quality) to decades (blue crab catch data).

There were three important findings from this study:

1. The magnitude of minimum indicator inflows (Q_I) from the S-79 structure ranged from 237 cfs to 545 cfs among the 11 estimates.
2. Seasonally averaged S-79 inflows less than the Q_I for each indicator could result in phytoplankton blooms in the upper CRE (< 10 km from S-79), compress the water column habitat for zooplankton and icthyoplankton against the structure, alter the composition of the macrobenthic community in the upper estuary, prevent the survival of *Vallisneria*, shrink the available habitat for the endangered sawfish, and lead to reduced harvest of blue crabs the following year.
3. Flow through S-79 accounts for 82% of the total inflow. The Tidal Basin inflows account for the remaining 18%. Assuming a median Q_I at S-79 of 400 cfs, the Tidal Basin flows are estimated at 88 cfs for a total inflow of 488 cfs.

Increased salinity through combinations of seawater encroachment and reduced freshwater input influences species composition, physiological processes and trophic dynamics (Gonzalez-Ortegon and Drake 2012). For example, long-term reductions in discharge to Apalachicola Bay in the northern Gulf of Mexico altered the food web leading to decreased biological productivity over time (Livingston et al. 1997). Therefore, it is important to describe the freshwater dry season inflows necessary to establish estuarine salinity gradients in both dynamic (water column) and static (benthic) habitats (Wolanski et al. 2004, Palmer et al. 2011).

Salinity varies over many time scales through complex hydrodynamic processes that integrate rainfall, surface inflows, submarine groundwater discharge, wind events, and tidal exchanges (Zheng and Weisberg 2004). Thus, simple correlations between inflow and salinity may be influenced by ungauged freshwater inputs. The diffuse inputs through submarine groundwater discharge is particularly difficult to quantify and model (Langevin 2003, Burnett et al. 2006). Recent efforts to measure and model the contribution of the Tidal Basin to total freshwater inflow to the CRE provided an estimate of ~18% over all dry seasons from 1966 to 2014 (Wan and Konyha 2015; this study). The relative contribution of the Tidal Basin ranged from 5 to 90% with values < 10% in very wet dry seasons (1995, 2005, and 2006) and values > 70% in the driest times (1982, 1990, 2001, and 2008). This potentially important source of fresh water must be incorporated into hydrodynamic models to account for changes in salinity that affect estuarine processes.

The balance between downstream transport of fresh water and the upstream encroachment of salinity creates gradients that influence all biogeochemical processes and patterns. The gradient can be represented by lines of equal salinity (e.g. isohalines) whose

positions fluctuate up and down the estuary with freshwater inflow(s), tidal cycles, and meteorological phenomena (e.g. fronts, winds, and storms). Particular isohalines provide useful indications of desirable (or undesirable) salinity conditions for sentinel organisms or communities (Jassby et al. 1995). For example, low salinity conditions indicative of a functional oligohaline benthic community served as the most upstream biological indicator. Salinity at this upstream location is extremely sensitive to fine scale changes in freshwater inflow. This sensitivity combined with the complexity and dynamism of macrobenthic assemblages accounted for the variability of the estimated Q_I (501 ± 525 cfs)—a range associated with salinity zones for characteristic macrobenthic communities in the dry season (Palmer et al. 2015).

Estimated mean daily dry season inflows of 300 to 550 cfs were associated with suitable dynamic and stationary habitats (water column and *Vallisneria*, respectively) located in the upper estuary around Beautiful Island (~10–15 km from S-79). Dry season inflows within this range should serve to maintain the area of maximum phytoplankton production and biomass from 9 to 16 km downstream. Maintaining the area of maximum CHL ³ 12 km downstream should diminish the potential for the accumulation of phyto-detritus and hypoxia in the upstream bottom water. Overall, the relationships between dry season inflow (< 500 cfs), the magnitude and position of the CHL maximum concentrations, and bottom water hypoxia in the upper CRE are complex and poorly understood.

Vallisneria was historically observed from 1993 to 1999 from Beautiful Island to the Ft. Myers station (Hoffaker 1994, Bortone and Turpin 2000). The acute sensitivity of this organism to increased salinity makes it an excellent candidate for the resource-based approach of prescribing freshwater inflows (Chamberlain and Doering 1998a, 1998b, Doering et al. 2002). Dry season freshwater inflows of 545 ± 774 cfs from 1993 to 1999 promoted the maximum tolerable salinity (9 to 10) for the survival of *Vallisneria*. Conversely, the *Vallisneria* habitat disappeared as the average salinity at the Ft. Myers station exceeded 10 from 2007 to 2013. *Vallisneria* habitat in the CRE has not recovered from drought-induced stress in 2001 and 2007–2008 when salinity was > 10 for 4 to 5 months. Loss of mature shoots greatly inhibits the potential for habitat reestablishment. There were signs of recovery on a scale of 3 to 6 years as salinity declined from 2003 to 2006. However, increased salinity in the upper CRE from 2007 to 2009 and again in 2012 severely limited the potential for *Vallisneria* survival.

There were three different indicator inflow estimates from analyses centered near the Ft. Myers station (~20 km downstream of S-79). Ft. Myers represents a location in the middle of the CRE just downstream of the *Vallisneria* beds where variations in basinwide total freshwater inflow are the main drivers for salinity (Wan et al. 2013, Buzzelli et al. 2015a). This study estimated that S-79 inflows averaging 445 ± 218 cfs were related to a salinity of 10 at this location. While a coarse-scale assessment, there are wide variations in the inflow from S-79 that accounts for a target salinity at Ft. Myers (e.g. 10). For example, more inflow is required from S-79 to maintain the magnitude and position of indicator isohalines when Tidal Basin inputs are diminished due to extended periods of drought.

Inflows from S-79 ranging from ~225 to 425 cfs maintain zooplankton and ichthyoplankton assemblages in downstream locations (~10–20 km and 10–30 km, respectively). Peak zooplankton abundance is often located downstream of the maximum CHL but can migrate far upstream under severely reduced inflow. It is under these

circumstances the water column biota could experience habitat impingement and compression against S-79. As with water quality, there should be further study of the effects of low inflow on planktonic dynamics in the upper estuary.

Oyster habitat located from Cape Coral to the mouth of the CRE served as the most seaward indicator of freshwater inflows. While oysters are excellent indicators to detect changes in and responses to environmental conditions, salinity in the lower estuary is highly influenced by oceanic processes. Assessment of the time series of inflows based on oyster salinity criteria (salinity of 20–25) resulted in reasonable but variable estimates of Q_I (296 ± 409 cfs). The relatively high variability was because a wide salinity range was applied (20–25) at a downstream location (Cape Coral ~30 km from S-79).

Estimates of the indicator inflows for the two mobile fauna species (blue crabs and sawfish) resulted from widely different approaches. Salinity gradients must be adequate for these two populations to most effectively utilize the estuary as a nursery (Wilbur 1994, Poulakis et al. 2013). The blue crab CPUE being proportional to freshwater inputs in the previous dry season demonstrates both the connectivity and lags between rainfall, inflows, salinity, and biotic responses. At the seasonal time scale, dry season mean monthly inflows of ~270 cfs would position the 12 to 27 salinity range ~10 to 30 km downstream of S-79, thus maximizing the potential sawfish habitat area. Dry season mean monthly inflows < 270 cfs could confine the sawfish habitat to the deeper, upper CRE where there is much less shoal area and lead to habitat compression against the structure. Upstream migration into a bathymetrically compressed habitat potentially places juvenile sawfish in closer proximity to larger predators such as bull sharks (*Carcharhinus leucas*) (Poulakis et al.2011).

COMPONENT STUDIES

Component Study 1: Three-Dimensional Model Evaluation of Physical and Structural Alterations of the Caloosahatchee River and Estuary: Impact on Salt Transport

Detong Sun and Yongshan Wan

Abstract

Hydrodynamic modeling of estuaries provides a platform to assess the effects of physical alterations on hydrodynamics, transport, and mixing. This study component utilized a three dimensional hydrodynamic model (Curvilinear Hydrodynamic Three Dimensional Model or CH3D) of the CRE to compare simulated salinities between the existing condition and the reversal of five historical physical alterations to the estuary. The alterations evaluated were the: (1) removal of the S-79 water control structure; (2) removal of the downstream causeway (Sanibel); (3) backfill of the oyster bar near the estuary mouth; (4) backfill of the navigation channel; and (5) the reestablishment of predevelopment bathymetry. Model results indicated that refilling the navigation channel had profound effects with a 20% reduction in dry season salinity. The reduced salt transport was more pronounced with the predevelopment bathymetry because the estuary was much shallower. Increased estuary depth and cross-sectional area significantly increase salt transport to the upper estuary. Increased salt transport can push biologically relevant isohalines further upstream depending upon freshwater inflow conditions.

Introduction

Hydrodynamic processes integrate freshwater inputs, wind events, and tidal exchanges to establish salinity conditions and modulate biodiversity and biological productivity. Estuaries are very sensitive to anthropogenic changes including urbanization, physical alterations of the estuarine systems, nutrient enrichment, and climate change (Alber 2002). Physical alterations such as dredging and dams change natural inflows, impact hydrodynamics and mixing with the coastal ocean, and dramatically affect salinity and water quality gradients in the estuary (Day et al. 1989). Anthropogenic changes to tributary rivers can have pronounced influence on both the quality and quantity of freshwater inputs to estuaries. Additionally, deep navigational channels can alter circulation, increase the upstream encroachment of saltwater, and promote hypoxia and anoxia.

The impacts of physical alterations on estuarine systems are noted worldwide. The Wadden Sea in the Netherlands and the Mississippi Delta in the United States serve as two examples of how physical alterations have changed coastal systems. In the Wadden Sea, coastal land reclamation was designed to protect natural resources while allowing for urban and agricultural development (Saundry and Cleveland 2011). In the Mississippi Delta, changes following the construction of dikes that cut the sources of riverine sediment, and dredging of canals led to significant hydrologic changes (Deegan et al. 1984, Barras et al. 2004, Day et al. 2005). In both cases, large areas of coastal ecosystem have been altered or destroyed.

Such changes are also evident in South Florida where river channels were dredged and widened for navigational purposes and water control structures were constructed near the

heads of the estuaries (Kimes and Crocker 1999, Antonini et al. 2002, Ogden et al. 2005). The modern landscape is highly engineered featuring ~3,380 km of canals, ~1,225 water control structures, more than 70 pumping stations, heavily managed wetlands, densely populated coastal watersheds, and highly impacted estuaries (Ogden et al. 2005, Obeysekera et al. 2011). These structural alterations have dramatically changed the watershed hydrological conditions as well as the geomorphology of the rivers and estuaries. In addition, agricultural and municipal demands for fresh water have increased. All these modifications have altered freshwater discharges to the estuaries (Balci and Bertolotti 2012).

Physical alterations at the landscape scale may have possibly irreversible impacts on estuarine ecosystems (Dyer and Orth 1994). Quantitative evaluation of these alterations remains a difficult task. Previous estuarine studies used hydrodynamic models to investigate saltwater intrusion in dredged navigational channels. Liu et al. (2001) utilized a vertical (laterally integrated) two-dimensional numerical model to study the hydrodynamic characteristics and extended saltwater intrusion in the Tanshui River estuarine system (Taiwan). The UnTRIM San Francisco Bay-Delta model, an unstructured grid hydrodynamic model, was used to study saltwater intrusion associated with deepening the Sacramento Deep Water Ship Channel (MacWilliams et al. 2009). In Louisiana, a semi-implicit version of Estuary and Coastal Model was used to study saltwater intrusion in navigation channels in Lake Pontchartrain (Georgiou 1999). In Florida, the Environmental Fluid Dynamics Code hydrodynamic model of the St. John's River was used to study the impact from dredging Jacksonville Harbor (USACE 2008). A more recent study applied the Finite Volume Coastal Ocean Model to explore the effects of changes to the navigational channel on circulation in Tampa Bay (Zhu et al. 2015).

The CRE has a watershed characterized by extensive agriculture and urbanization, is influenced by both unregulated and regulated freshwater inflow, and contains valuable biological resources (Chamberlain and Doering 1998a, Doering et al. 2006, Balci and Bertolotti 2012). Through climatic variations, landscape modification, flood protection, and managed operations, the CRE can experience reduced freshwater inflow during the dry season. In many estuaries, reduced freshwater inflow over time can result in the landward encroachment of salinity (Cloern and Jassby 2012). In the case of the CRE, upstream saltwater intrusion can reduce the extent of vegetated freshwater habitat (i.e., *Vallisneria americana*), impact community composition in the water column and benthos, and compress the oligohaline area of the estuary that is essential to a variety of faunal populations (Doering et al. 2002, Simpfendorfer et al. 2011, Stevens et al. 2013).

The objective of this study was to use a hydrodynamic model to evaluate the effects of physical alterations on salinity distribution in the CRE. CH3D was applied to the CRE. This study intended to quantify and rank the effects of different physical and structural alterations over the past century on modern day estuarine salinity patterns.

Methods

Study Site

The Caloosahatchee River and Estuary are located in Southwest Florida (**Figure 4**). The modern day C-43 canal runs 67 km from Lake Okeechobee to the Franklin Lock and Dam (S-79 structure), which marks the upstream boundary of the estuary that extends

42 km downstream to Shell Point. The system has been modified to provide for navigation, water supply, salinity control, and flood protection on both a local and regional scale (Chamberlain and Doering 1998a, Doering et al. 2006). The CRE is a funnel-shaped estuary whose width ranges from ~0.2 km in the upper portion to ~2.5 km near the mouth. The total surface area of the estuary is about 65 km^2 (Buzzelli et al. 2013b). The narrow section between the S-79 structure and Beautiful Island (~15 km downstream) was physically altered by channelization with an average depth of ~6 meters (m) while the downstream estuary has an average depth of 1.5 m.

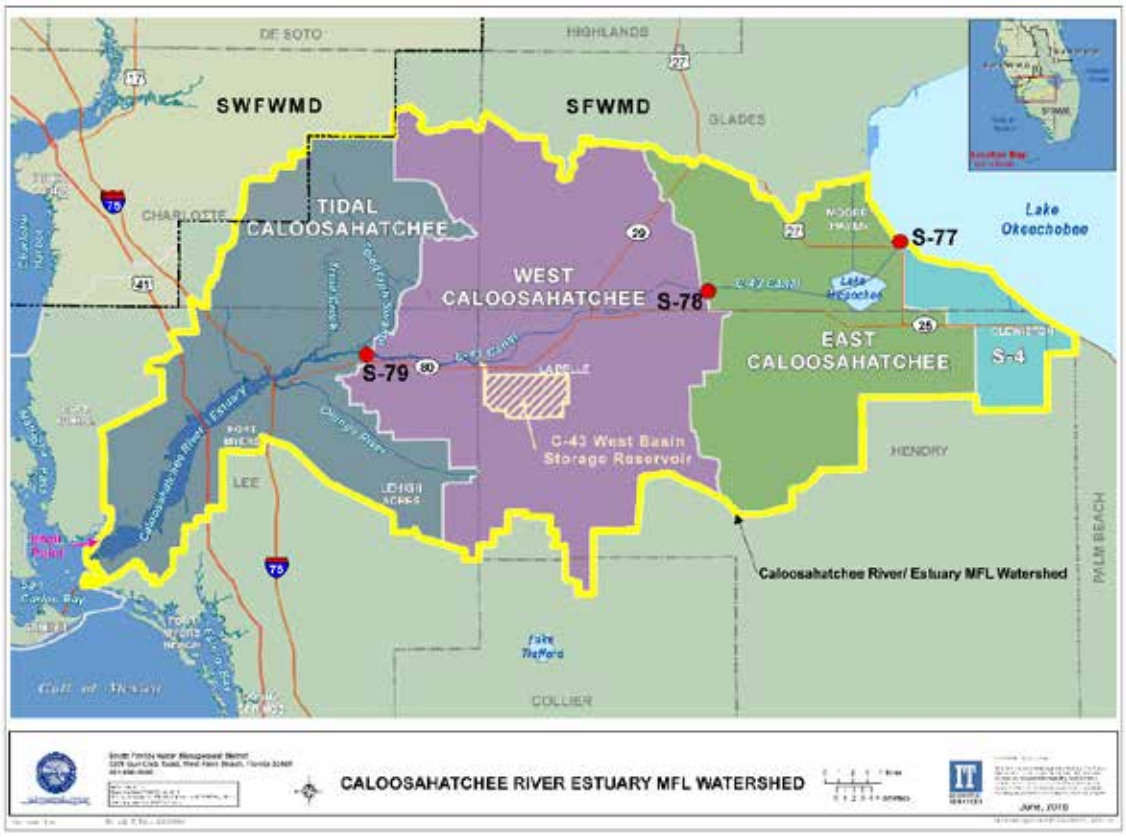

Figure 4. The CRE MFL Watershed with its subwatersheds and major water control structures. The future location of the Caloosahatchee River (C-43) West Basin Storage Reservoir is also shown.

Alterations within the CRE MFL Watershed

The CRE and the C-43 canal were connected to Lake Okeechobee through the evolution of the C&SF Project. The C&SF Project is a complete system of canals, storage areas, and water control structures spanning the area from Lake Okeechobee to both the east and west coasts, and from Orlando south to the Everglades. It was designed and constructed during the 1950s by USACE to provide flood control and improve navigation and recreation. In its role as a local sponsor, SFWMD is subject to balancing the water resource needs by providing flood control, water supply, recreation and protection for the natural system. As a result of structural alterations to the watershed, the existing C&SF Project has constraints on the availability of water that can be delivered to the CRE from the regional system.

In addition to the alterations described above, a multitude of other structural and physical alterations have occurred to the CRE MFL Watershed, historic Caloosahatchee River, and the CRE. These alterations changed the historical hydrologic conditions of the CRE MFL Watershed and its receiving water bodies. The CRE MFL Watershed is a system that has been highly altered from its natural state by human intervention to meet multiple objectives. Various land uses in a watershed dictate water demands and runoff volumes to estuarine receiving waters located downstream of S-79. A network of secondary and tertiary canals exists in the CRE MFL Watershed that is hydrologically connected to the C-43 canal and the CRE. These canals are used for navigational access or to convey water for both drainage and irrigation to accommodate existing agriculture, urban development and other land uses in the watershed.

The primary land use type within the CRE MFL Watershed today is agricultural, which comprises 41.5% of the total area. Urban and built up land uses occupy the next largest group (18%), followed by wetlands (15.1%) and upland forest (14%).

Historically, the Caloosahatchee River, present day C-43 canal, was a sinuous river, originating near Lake Flirt, ~2 miles (3.2 km) east of La Belle at Fort Thompson. Beginning in the 1880s, the river channel was straightened, deepened, and connected to Lake Okeechobee. This resulted in a loss of 76 river bends and 8.2 miles (13.2 km) of river length (Antonini et al. 2002). Dredging alterations continued and, by 1918, three combination lock and spillway structures had been constructed at Moore Haven, Citrus Center, and Fort Thompson (USACE 1957, Section 6.B.6). Flows within the historic Caloosahatchee River (now the C-43 canal) are controlled through operation of multiple water control structures (S-77, S-78, and S-79), and these structures regulate freshwater inflows to the downstream estuary. The final lock and dam structure (S-79) was completed in 1966 at Olga to assure freshwater supply and prevent upstream saltwater intrusion. Discharges from Lake Okeechobee and the C-43 Watershed or Basin (between the S-77 and S-79 structures) are regulated by USACE for various purposes, including flood control, water supply, and navigation. The modern C-43 canal spans 70 km from the S-77 structure at Lake Okeechobee to the S-79 structure (**Figure 4**).

The total effect of these alterations has been the loss of surface water storage in the CRE MFL Watershed, which has altered the magnitude, timing, and distribution of freshwater inflows to the estuary at the S-79 structure. As is typical of a watershed characterized by extensive drainage features (Hopkinson and Vallino 1995), runoff is more variable with higher wet season discharges and lower dry season discharges. Large volumes of fresh water during the wet season can flush all salt water from the tidally influenced sections of the water body. By contrast, inflow at S-79 can stop entirely during the dry season. Salt water intrudes to S-79, sometimes reaching a salinity of 20 (Chamberlain and Doering 1998a, 1998b). Fluctuations of this magnitude at the head and mouth of the system cause mortality of organisms at both ends of the salinity gradient (Doering et al. 2002).

The first recorded survey of the water bodies (CRE and historic Caloosahatchee River) within the watershed was conducted by Captain W.M. Black of the United States Army Engineers in 1887 (Black 1887). This survey indicated that the estuary was much shallower than today. An extensive shoal (< 1.6-m depth) spanned the mouth where the estuarine river discharged to San Carlos Bay. This shoal was part of an extensive tidal delta that bordered the eastern portion of the bay. Navigation was inhibited along the entire length

by the shoal and oyster bars, which extended ~27 km upstream to Fort Myers. The historical river channel from Fort Myers to LaBelle was shallow (~1 m), long (~70 km), and crooked. Early descriptions of the estuary characterize it as barely navigable due to extensive shoals and oyster bars (Sackett 1888). Some of the alterations that have occurred include dredging a large navigational channel (Intracoastal Waterway) and secondary navigational channels, removing oyster bars upstream of Shell Point for roadway construction, removing the gulf bar at the mouth of the CRE, and the creation of two islands for construction of the Sanibel Causeway across the mouth of San Carlos Bay. Seven automobile bridges and one railroad bridge now connect the north and south shores of the estuary.

The potential for removing the existing structural and physical alterations affecting the historic Caloosahatchee River (C-43 canal) and the CRE may not be feasible. Much of the existing development within these downstream water bodies is dependent upon the conditions these alterations currently provide (e.g. flood protection, navigation, water supply, transportation, etc.).

Hydrodynamic Model of the CRE

The CH3D model, originally developed by Sheng (1986), is a non-orthogonal curvilinear grid model capable of simulating complicated hydrodynamic processes including wind driven, density driven, and tidal circulation. The model has a robust turbulence closure scheme for accurate simulation of stratified flows in estuaries and coastal waters (Sheng 1986, 1987, Sheng and Villaret 1989). The non-orthogonal nature of the model enables it to represent the complex geometry of a tidal estuary such as the CRE. The model includes a circulation model to simulate three-dimensional hydrodynamics and a salinity model to simulate salt transport. The model is driven by external forcing prescribed at the boundaries including tidal forcing at the ocean boundary, freshwater inflow from the watershed, and meteorological forcing including wind and rainfall. The CH3D model has been successfully applied to many water bodies including east coast Florida estuaries such as the Indian River Lagoon, St. Lucie Estuary (Sun 2009), and Loxahatchee River Estuary (Sun 2004).

The Caloosahatchee Estuary CH3D model was developed from the Charlotte Harbor CH3D model (Sheng 2002). The original Charlotte Harbor model was calibrated using two months of hydrodynamic and salinity data collected during summer at six stations located in and around Pine Island Sound and the Peace River. SFWMD extended the model to the CRE using 16 months of continuous monitoring data (Qiu 2002, SFWMD 2003). The Caloosahatchee Estuary CH3D model was further calibrated with three years of salinity observations (October 2001–December 2004) at five stations in the estuary for the evaluation of various alternative plans of the Southwest Florida Feasibility Study and the Caloosahatchee River (C-43) West Basin Storage Reservoir Project (Sheng and Zhang 2006, Qiu 2006, USACE and SFWMD 2010). An external peer review of the model was conducted in 2006 for this application (Qiu 2006). The latest calibration of the model was conducted with data collected up to 2010 at seven locations in the estuary to support the development of the Lake Okeechobee Adaptive Protocols (SFWMD 2010).

The Caloosahatchee Estuary CH3D model domain covers the entire estuarine system, including Caloosahatchee Estuary, Charlotte Harbor, Pine Island Sound, San Carlos Bay, Estero Bay, and the major tributaries, as well as about 30 km offshore in the Gulf of Mexico

(**Figure 5**). The horizontal grid has 166 x 128 elements with 5,266 water cells allowing fine enough resolution to represent the numerous islands, including the two islands constructed as part of the Sanibel Causeway. The higher resolution within the CRE and San Carlos Bay (50–100 m) provides a more detailed representation of the complex shoreline and the navigation channel. Five vertical layers evenly spaced over the water column enable simulation of density stratification within the estuary.

Hydrodynamic Model Experiments

The effects of physical alterations on saltwater intrusion were quantified by comparing the results of altered scenarios with the existing condition under the same boundary forcing. This modeling strategy allowed for isolation of the effects of each physical alteration on salinity patterns. The existing condition was based on bathymetric survey data collected in 2003. Five model experiments were designed to simulate reversals of the historical alterations: (1) removal of S-79 water control structure at the upstream boundary, (2) removal of the Sanibel Causeway at the downstream boundary, (3) backfilling of the oyster bar near Shell Point, (4) filling the navigational channel throughout the estuary, (5) reestablishing the predevelopment bathymetry from the Captain Black's survey.

The first model experiment investigated the potential effects of removing the S-79 lock and dam on the distribution of salinity in the estuary. To simulate this effect, the model grid was extended from S-79 to S-78. Discharge at S-79 is a combination of discharge at S-78 and runoff from the intervening West Caloosahatchee subwatershed (**Figure 4**). Runoff from the watershed was calculated as the difference between discharges at S-79 versus S-78. This simulation applied measured flow at S-78 with the difference between the two discharges redistributed along the C-43 canal west of S-78.

In the second experiment, the CH3D model grid was modified to eliminate the causeway with its two man-made islands. Estuarine circulation and salinity patterns are heavily influenced by the input of salt water at the downstream boundary. Thus, this scenario simulated the influence of the causeway on salinity within the estuary. Removal of the Sanibel Causeway was implemented by activating the "island" cells of the causeway and assigning them an elevation equal to the average of the submerged neighboring cells (i.e., removal of the two islands).

The effects of the removal of the historical oyster bar were modeled by increasing the elevation of selected areas near Shell Point where historical oyster bars were dredged. This was accomplished by increasing the bottom elevation 0.6 m near the mouth of the CRE. Similarly, the effect of dredging the navigation channel was simulated by changing the elevation of the exiting navigation channel to that of the neighboring cells. The lower CRE and the majority of San Carlos Bay and Pine Island Sound were significantly shallower historically, mostly < 1.5 m in depth, compared to ~2 to 5 m deep in the present existing condition (**Figure 5**). The increase in depth was apparently due to the dredging of navigational channels including the Intracoastal Waterway. This was done by changing the channel depths in the CH3D model grid from the mouth to S-79 to a maximum of 1.5 m.

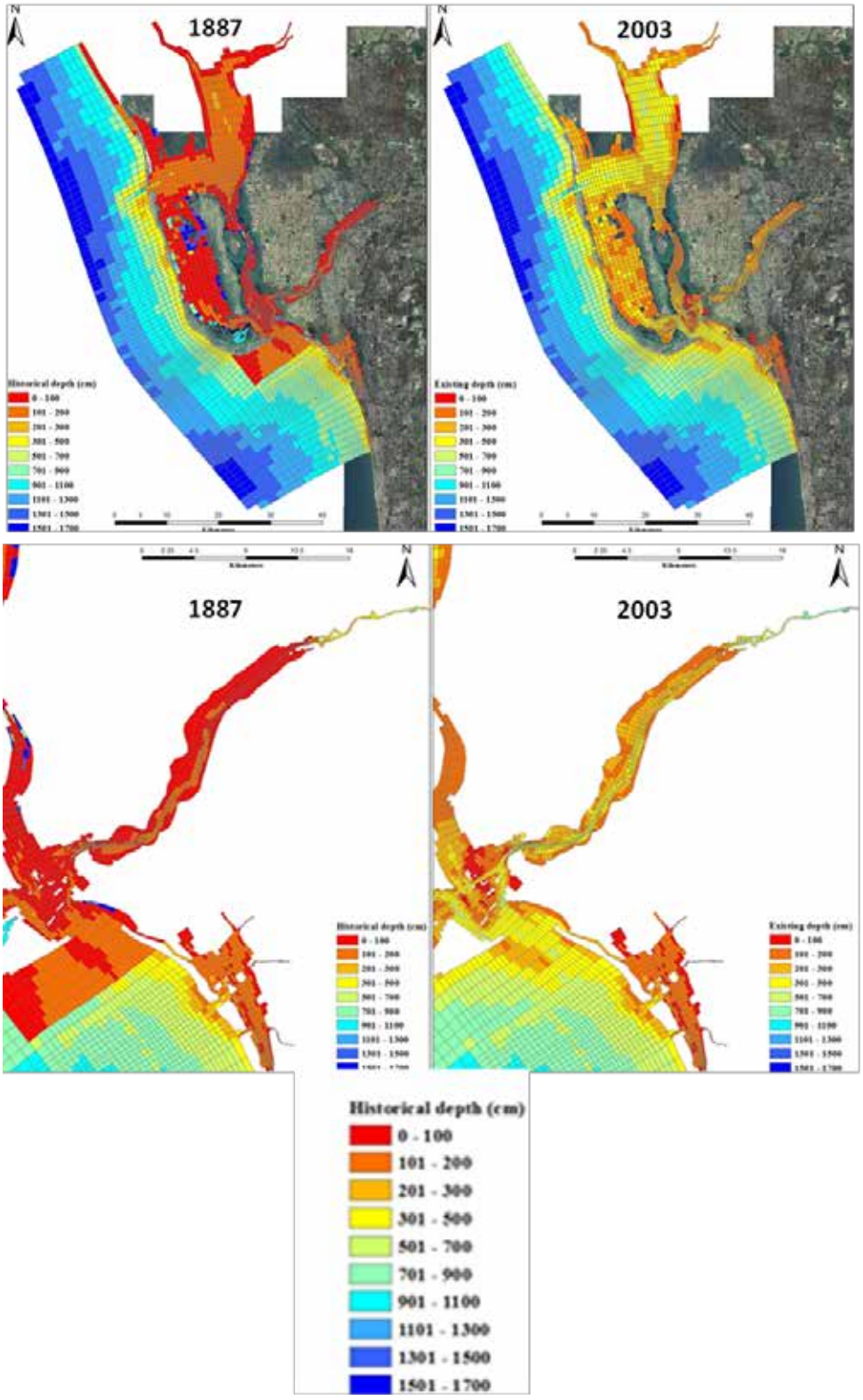

Figure 5. Comparison of bathymetry of the model domain for the CRE: (top left) the 1887 bathymetry for the entire domain, (bottom left) the 1887 bathymetry focused on the CRE, (top right) the 2003 bathymetry for the entire domain, and (bottom right) the 2003 bathymetry focused on the CRE.

The final hydrodynamic model experiment incorporated the bathymetric survey data generated by Captain Black into the existing model grid to represent the predevelopment condition. Historical bathymetry from Captain Black's 1887 survey was interpolated to the modified model grid, which was extended to the S-78 structure (**Figure 5**). Similar to the S-79 removal scenario, freshwater inflow was applied at the location of S-78 and distributed along the river between S-79 and S-78 with the same total freshwater inflow as the existing condition.

The model was calibrated using data from October 1, 2001, to December 31, 2011 (11 years or 3,744 days). For each run, predicted salinities at the Ft. Myers station and I-75 were compared to those from the existing condition to examine the impact from the change. These two locations were selected for their proximity to the existing MFL compliance monitoring point and monitoring associated with the implementation of the most recent operational schedule.

The existing boundary conditions including tidal water levels, freshwater inflow, and meteorological forcing remained the same for all model scenarios. Tidal data collected at a National Oceanic and Atmospheric Administration (NOAA) station located in Naples, Florida were used as the ocean boundary condition. The upstream boundary condition resulted from measured freshwater inflow at the S-79 structure available from the SFWMD's corporate environmental database, DBHYDRO (access the database using http://my.sfwmd.gov/dbhydroplsql/show_dbkey_info.main_menu) and predicted inflow from tributaries in the Tidal Basin downstream of S-79 (Konya and Wan 2011).

Freshwater inflow through the S-79 structure and the Tidal Basin exhibited significant inter-annual, seasonal, and daily variations during the simulation period. The surface boundary condition was driven by wind and rainfall/evaporation data available from DBHYDRO. Incoming fresh water at the upstream boundary was assigned a salinity of 0.0 while salinity at the downstream boundary was set at constant value of 35.0. Salinity time series observed at the monitoring stations located along the length of the estuary were interpolated over the model domain to serve as the initial condition. Three years of tidal discharge data (October 2007–September 2010) measured at the two transects at Shell Point and Marker 52 (**Figure 6**) provided a validation of the sum of tidal flow and freshwater discharge (**Figure 7**). Water levels were recorded at some of these stations. During the simulation, the Manning's bottom friction coefficient was held constant at 0.025 (Qiu 2006).

Validation of the existing condition involved long-term data for water level and salinity along with more recent tidal discharge data determined along two transects in the estuary. Seven continuous salinity monitoring stations maintained by SFWMD, including S-79, BR-31, I-75, Ft. Myers, Cape Coral, Shell Point, and Sanibel, provided hourly and daily data for salinity validation (**Figure 76**). Salinity is measured at two depths: surface (defined at 20% of the total depth below surface) and bottom (defined as 20% of the total depth above the bottom). Hourly salinity data and model results for the same five-year period were compared at five stations: S-79, BR-31, I-75, Ft. Myers, and Shell Point.

Figure 6. Salinity and inflow monitoring stations in the CRE used for model validation. Both freshwater inflow and salinity are monitored at the S-79 structure.

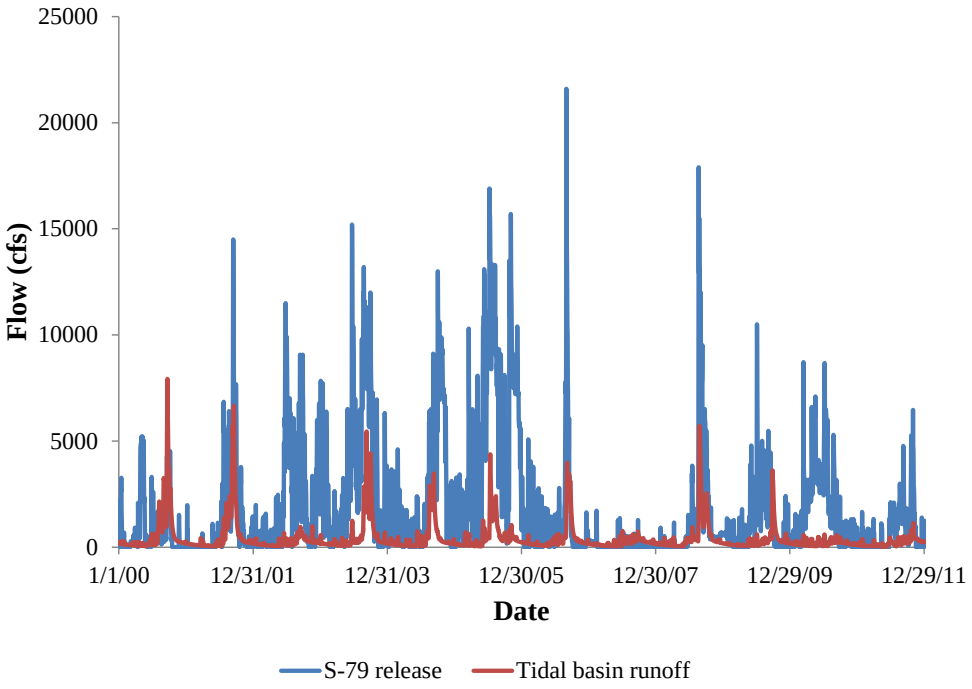

Figure 7. Freshwater inflow (cfs) from S-79 (blue) and the tidal basin downstream of S-79 (red).

Results

Validation of the Existing Condition

The modeled tidal water surface elevation was compared to measured water elevations at four locations: S-79, I-75, Shell Point, and Sanibel Causeway (**Figure 8**). Only two months (March and April, 2010) were presented. Overall, predicted water levels agreed with the measurement at all the four sites in terms of tidal range, tidal phase, and subtidal movement. The root mean square (RMS) error and correlation coefficient (r) along with the relative error defined by the RMS error divided by the average tidal range were calculated from the model results and the field observations over a five-year period (2007 to 2011; **Table 3**). Despite the relatively larger RMS error at Shell Point due to a small datum offset observed at that location, the RMS errors were within 15% of average tidal range. One possible source of error is the long open tidal boundary in the Gulf of Mexico where only tidal information at Naples was provided. Tidal range in the upper estuary (S-79 and BR-31) was slightly over-predicted possibly due to inadequate representation of the shoreline, floodplain, and bathymetry in this part of the estuary.

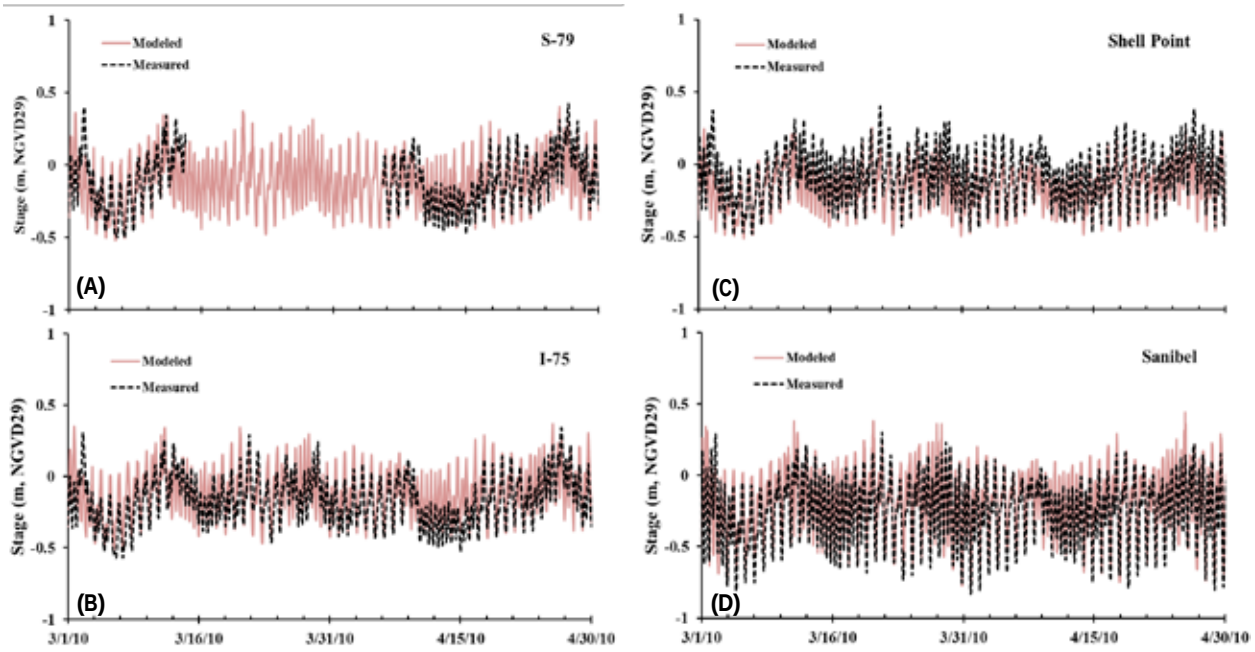

Figure 8. Modeled (red line) and measured (black dash) tidal elevations at (**A**) S-79, (**B**) I-75, (**C**) Shell Point, and (**D**) Sanibel Island from March to April 2011.

Table 3. Model performance statistics for hourly tidal elevation calculated over the period 2007 to 2011.

Station	r	RMS Error (m)	Relative Error
S-79	0.86	0.11	12.3%
I-75	0.88	0.12	12.5%
Shell Point	0.91	0.15	15%
Sanibel	0.94	0.10	10%

The discharge at Shell Point is due to the combined contribution determined along three subtransects, which in sum account for the total discharge at the mouth of the estuary (**Figure 9**). This total discharge was much larger than that at Marker 52 located about 20 km upstream near Fort Myers. The tidal component was dominant relative to the freshwater inflow at the two downstream transects. Model representation of tidal transport agreed with the empirical observations (**Table 4**).

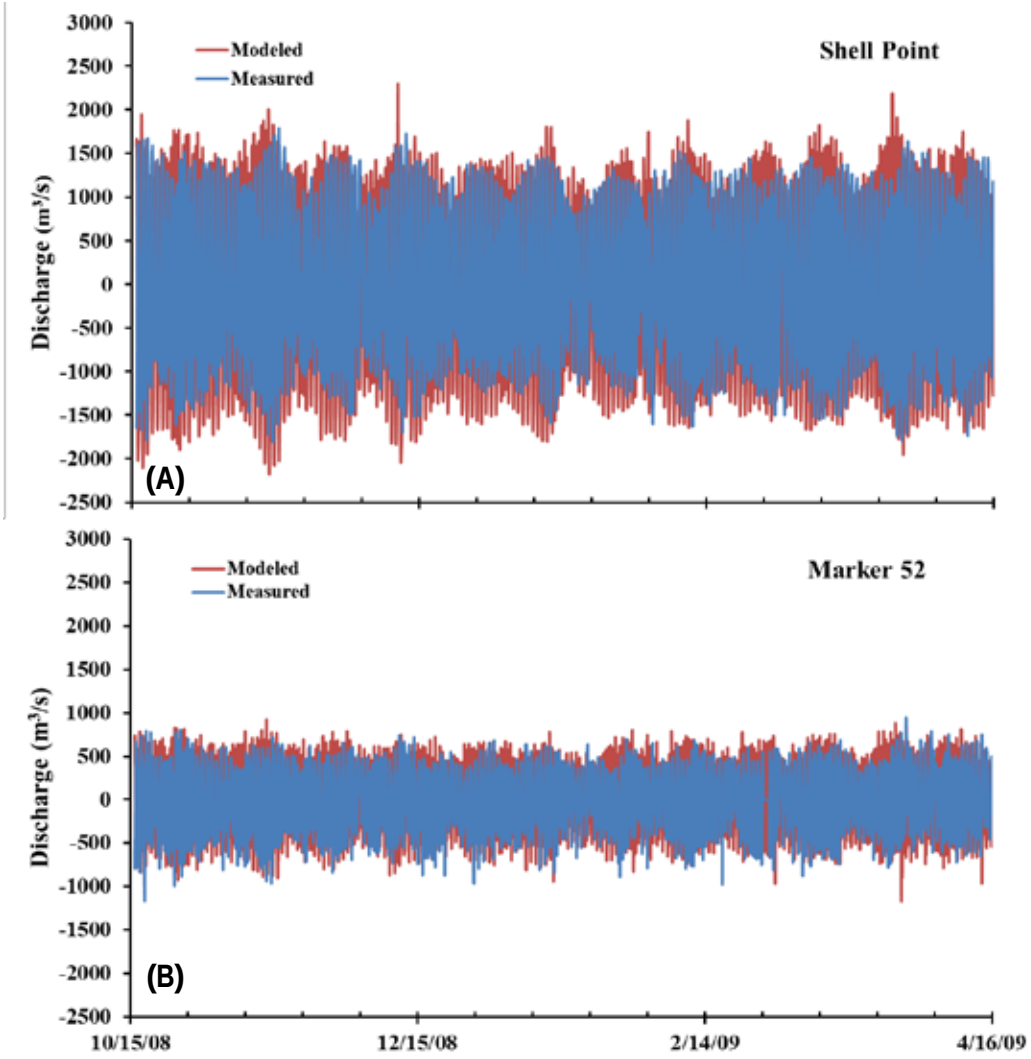

Figure 9. Modeled (red line) and measured (blue line) tidal discharge at (**A**) Shell Point, and (**B**) Marker 52 from October 15, 2008, to April 15, 2009.

Table 4. Model performance statistics for hourly and daily salinity calculated over the period from 2007 to 2011 and from 2001 to 2011, respectively. (Note $m^3 s^{-1}$ – cubic meters per second.)

Station	r	RMS Error ($m^3 s^{-1}$)	Relative Error
Shell point	0.82	446	17.3%
Marker 52	0.85	221	18.1%

Salinities predicted using the model agreed to the hourly data from 2010 (I-75, Ft. Myers, and Shell Point; **Figure 10**), and, the daily data for the entire period (S-79 and Ft. Myers; **Figure 11**). This included good representation of fine-scale variations (e.g. stratification), daily variability, and seasonal patterns. Simulation of short-term (daily or in the order of a few days) salinity fluctuations was more reliable at downstream sites (Shell Point and Ft. Myers) than at upstream sites (S-79 and BR-31). This was possibly due to a damping effect inherent in the modeling transport scheme. There was little difference (r = 0.9; RMS 2.5–3.5) between hourly salinities predicted by the model and those measured from 2007 to 2011 (**Table 5**). The reliability of the salinity prediction was greater at the daily time scale at all locations. These results suggest that the model is a reliable tool for salinity prediction to support decision making regarding water management operations for the CRE.

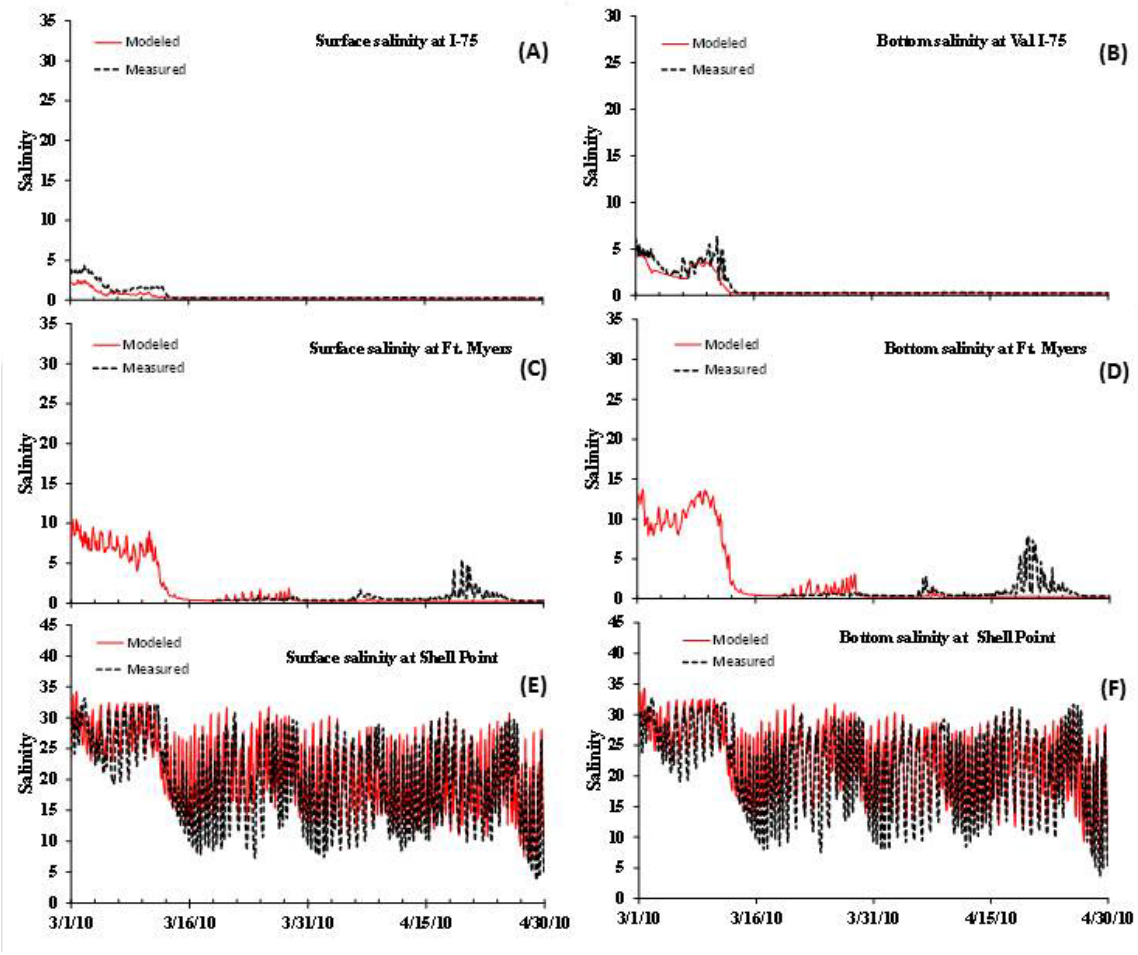

Figure 10. Modeled (red line) and measured (black dash) hourly surface and bottom salinity at I-75 (**A** and **B**), Ft. Myers (**C** and **D**), and Shell Point (**E** and **F**) from March to April 2010.

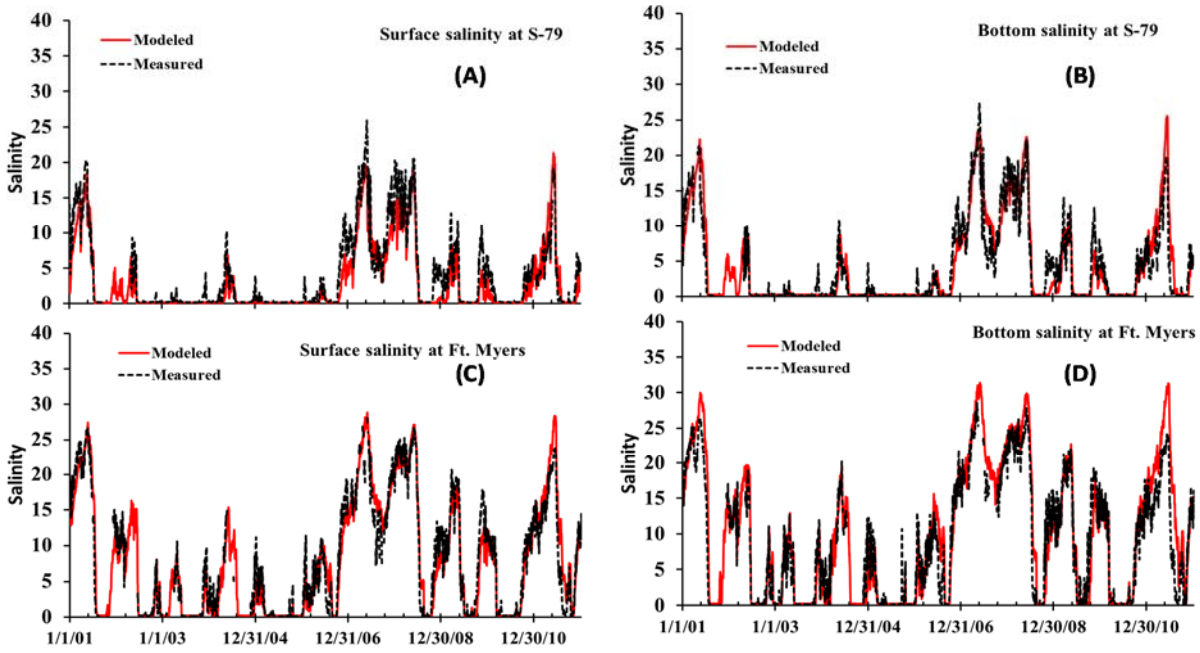

Figure 11. Modeled (red line) and measured (black dash) daily surface and bottom salinity at S-79 (**A** and **B**) and Ft. Myers (**C** and **D**) from 2001 to 2010.

Table 5. Model performance statistics for hourly and daily salinity calculated over the period from 2007 to 2011 and from 2001 to 2011, respectively.

Station	Hourly (2007 to 2011)				Daily (2001 to 2011)			
	Surface		Bottom		Surface		Bottom	
	r	RMS	r	RMS	r	RMS	r	RMS
S-79	0.92	2.68	0.92	3.27	0.94	2.17	0.93	2.25
BR-31	0.94	2.44	0.90	3.41	0.95	1.91	0.91	2.65
I-75	0.94	2.32	0.93	2.91	0.94	2.27	0.93	2.87
Ft. Myers	0.94	3.22	0.92	5.11	0.96	2.31	0.94	2.98
Cape Coral					0.97	2.46	0.97	2.95
Shell Point	0.89	3.58	0.88	3.79	0.94	2.78	0.92	2.90
Sanibel					0.84	2.03	0.86	2.80

Hydrodynamic Model Experiments

The total freshwater inflow entering the CRE was the same between the existing condition and the scenario where S-79 was removed. Salinity decreased slightly during the dry season without the control structure at the estuary head (**Figure 12A**). The relative difference in salinity was greater at I-75 (not shown) than at the Ft. Myers station with a more noticeable deviation in the bottom water. Salinity at Ft. Myers did not change significantly with the removal of the Sanibel Causeway (**Figure 12B**). However, there was a slight increase in salinity at Sanibel during the dry season (data not shown). While dry season salinity at Ft. Myers increased slightly when the oyster bar was reestablished, this effect diminished in the upstream direction (**Figure 12C**). In contrast, filling the navigational channel led to reductions in salinity throughout the CRE during the dry season

(**Figure 12D**). Finally, reintroduction of the predevelopment bathymetry resulted in significantly lower salinity in upstream regions of the estuary relative to the existing condition (**Figure 12E**). Except for the four drought years (2001, 2007, 2008, and 2011), the estuary would be nearly fresh upstream of the Ft. Myers station even during the dry season. Changes in both average surface and bottom salinities at I-75 and Ft. Myers were most pronounced in the scenarios that decreased the depth of the navigational channel or across the entire model grid (**Table 6**).

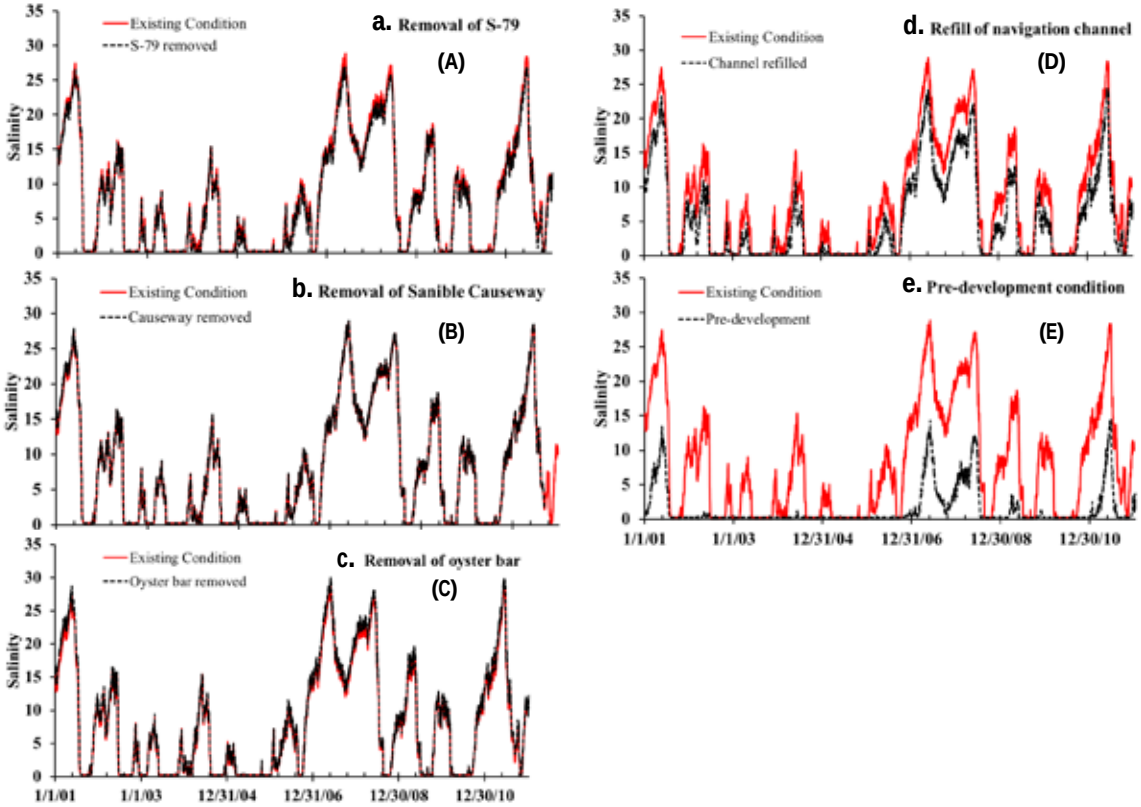

Figure 12. Comparison between average daily surface salinity at Ft. Myers (red line) and five different physical alteration experiments (black dash) from 2001 to 2010: (**A**) removal of S-79; (**B**) removal of Sanibel Causeway; (**C**) restoration of oyster bar at the mouth; (**D**) refill of the navigational channel; and (**E**) reestablishment of predevelopment bathymetry.

Table 6. Difference of monthly average surface (S) and bottom (B) salinity between each experiment and the existing condition at I-75 and Ft. Myers in May 2001, 2007, 2008, and 2011.

Scenario		2001		2007		2008		2011	
		I-75	Ft. Myers	I-75	Ft. Myers	I-75	Ft. Myers	I-75	Ft. Myers
S-79 Removal	S	-1.03	-0.84	-2.57	-1.49	-1.61	-1.04	-1.54	-0.95
	B	-2.56	-1.31	-3.27	-1.88	-2.59	-1.40	-2.62	1.59
Causeway Removal	S	0.14	0.15	0.16	0.16	0.12	0.14	0.15	0.17
	B	0.15	0.18	0.17	0.16	0.13	0.14	0.16	0.16
Restore Oyster Bar	S	0.75	0.49	1.33	0.95	1.38	1.02	1.46	1.02
	B	1.01	1.23	1.39	1.33	1.46	1.37	1.56	1.56
Refill Navigation Channel	S	-5.7	-4.5	-5.5	-4.5	-5.7	-5.0	-5.6	-4.7
	B	-4.8	-4.8	-5.1	-4.9	-5.7	-5.4	-5.0	-5.1
Predevelopment	S	-14.4	-14.8	-17.1	-15.3	-15.9	-14.1	-14.7	-14.7
	B	-15.4	-14.2	-19.1	-16.2	-17.9	-17.9	-17.4	-16.4

Theoretical Considerations for Salt Intrusion

In many estuaries, reduced freshwater inflow over time can result in landward salinity encroachment (Cloern and Jassby 2012). There have been many attempts to address the problem based on theoretical and experimental approaches. With a prismatic channel, analytical solutions of salt transport equations have been given by various authors (Ippen and Harleman 1961, Ippen 1966, Prandle 1985, 2004, 2009, Savenjie 1992, 2005, Kuijper and Van Rijn 2011). When averaged on tidal time scales, the one-dimensional salt continuity equation can be simplified to a balance between the seaward advective salt transport and the landward dispersive transport (Savenije 2005):

$$u_r S + D_x \frac{dS}{dx} = 0 \quad (1)$$

Where x is the distance from the mouth, u_r is the river discharge velocity, S is salinity, and D_x is the dispersive coefficient. Each parameter was averaged over multiple tidal cycles and the channel cross-sectional area. The transport due to advection is caused by the velocity associated with freshwater discharge, whereas the longitudinal dispersive transport is caused by tidally- and density-driven processes. Longitudinal dispersion in estuaries can be particularly difficult to measure and model (Jay et al. 1997, Austin 2004, Geyer et al. 2008, Spencer et al. 2014). Nevertheless, the theory can still provide qualitative guidance.

The most important parameters influencing salt intrusion are the tidal characteristics (tidal amplitude and peak tidal velocity), the river parameters (discharge and average cross-sectional velocity), and the geometric parameters (depth, width, and convergence length scale). Using a tidally averaged approach and assuming the following relation between the dispersion coefficient D_x and river discharge velocity u_r (Van Der Burgh 1972) results in **Equation 2**:

$$\frac{dD_x}{dx} = -Ku_r \quad (2)$$

where K is a calibration coefficient (Van Der Burgh coefficient) between 0 and 1. The salt balance equation can be solved and the maximum salt intrusion length L_{max} (defined as the salt penetration length at high slack water) can be expressed as **Equation 3** (Savenije 2005, Kuijper and Van Rijn 2011):

$$L_{max} = L_a \ln\left(1 + \frac{D_0 A_0}{K L_a Q_r}\right) \quad (3)$$

where L_a is the convergent length scale for the cross-section area $A = A_0 \exp(-x/L_a)$, A_0 is the cross-section area at the mouth, D_0 is the dispersive coefficient at the mouth, and Q_r is the river discharge. For prismatic estuaries, **Equation 3** is reduced to the following:

$$L_{max} = \frac{D_0 A_0}{K Q_r} \quad (4)$$

Savenije (2005) also found an empirical relationship for the dispersive coefficient at the mouth:

$$D_0 \sim 1400 \widehat{u_0} h_0 \quad (5)$$

where $\widehat{u_0}$ is the peak tidal velocity and h_0 is the depth at the mouth.

Thus, it is evident from **Equations 3** through **5** that salt intrusion length would increase significantly with increasing depth h and cross-section area A. This theoretical consideration is consistent with the numerical simulation results of the last two of scenarios of physical alteration (e.g. refilling the estuarine channel and return to the predevelopment bathymetry).

Discussion

This study applied a three-dimensional, curvilinear hydrodynamic model (CH3D) to investigate the impact of physical alterations on salinity in the CRE. Simulated salinity distributions and time series from five different model experiments representing physical alterations to the estuary were compared to those from the existing condition. Intra- and inter-annual variations in the model's existing salinity conditions were validated using extensive data collected from 2000 to 2011. With all forcing being kept the same, the modeled salinity of the existing conditions was compared with five cases in which historical physical alterations of the estuary were reversed, including (1) removal of the S-79 structure, (2) removal of the Sanibel Causeway, (3) backfill of the oyster bar, (4) backfill of the navigation channel, and (5) the predevelopment bathymetry.

Model results indicated that the construction of the Sanibel Causeway, the removal of the oyster bar near the estuarine mouth, and the S-79 water control structure had little effect on salinity of the CRE. Potential effects of these alterations were localized and spatially limited. In contrast, dredging the navigational channels greatly increased salinities throughout the estuary. Under the pre-development bathymetry, before dredging, salinity was dramatically lower in the estuary upstream of Fort Myers being nearly fresh in the dry season except for the drought years of 2001, 2007, 2008, and 2011. Dredging and deepening of the estuary was one of the primary activities that changed the pattern of salt transport in the estuary. This is consistent with the analytical theory about the significance of estuary depth and cross-sectional area in salt intrusion. There are two factors that could explain this difference. On the one hand, refilling the channel provided more resistance to salt intrusion; on the other hand, the volume of the estuary was significantly reduced, but the amount of freshwater input remained the same, resulting in reduced salinity in the estuary. Since these physical changes are unlikely to be reversed, the results may have important implications in the development of realistic inflow goals to protect the estuarine ecosystem. This modeling evaluation provides a framework for understanding the influence of different structural alterations on resulting salinity distributions. It should be recognized that these irreversible alterations act as constraints on the ability to restore historical hydrologic conditions to the CRE.

Component Study 2: Analysis of the Relationship between Freshwater Inflow at S-79 and Salinity in the CRE 1993–2013

Christopher Buzzelli

Abstract

The upstream migration of salt with reduced freshwater inflow alters the composition and productivity of oligohaline habitats in estuaries. This process can be problematic in subtropical estuaries with regulated freshwater inflow such as the CRE in southwestern Florida. This study component examined relationships between average monthly inflow (Q) and mid-estuary salinity (S) from 1993 to 2013. An exponential decay equation was fit to the inflow-salinity (Q-S) relationship for each water year (May 1 to April 30). Annual equations were used to estimate the inflow rate associated with a salinity of 10 at the Ft. Myers monitoring station (Q_{calc}). Inflows varied both intra- and inter-annually. Q_{calc} ranged from 70 cfs to 773 cfs with an average of 445 ± 218 cfs. At the estuary and annual scales, the quantity of fresh water to support a particular salinity target varied greatly. This variance was related to the variations in freshwater inputs from both the C-43 Watershed located upstream of S-79 structure and the downstream tidal basin.

Introduction

Life histories of many estuarine organisms are directly dependent upon temporal and spatial variations in salinity (Livingston et al. 1997, Palmer et al. 2011, Whitfield et al. 2012). The vertical and horizontal patterns of salinity can be quantified using lines of equal salinity (e.g. isohalines) whose positions fluctuate with freshwater inflow, tidal cycles, and meteorological phenomena (e.g. fronts, winds, and storms; Jassby et al. 1995). Upstream or downstream shifts in isohaline position can narrow the optimal habitat for estuarine organisms or move them further away from their optimal locations (Sklar and Browder 1998). Data analyses and research to provide guidelines for freshwater management should rely upon appropriate physical and ecological indicators and seek clear breakpoints in relationships between inflow, salinity, and biological responses (Montagna et al. 2002a). Therefore, isohaline position can be used as an indicator of ecological conditions in estuaries (Jassby et al. 1995).

The CRE has a watershed characterized by extensive agriculture and urbanization, is influenced by freshwater inflow from several sources, and contains valuable biological resources (Chamberlain and Doering 1998a, Doering et al. 2006, Balci and Bertolotti 2012). Through combinations of climatic variations, landscape modification, and managed operations, the CRE can experience variable freshwater inflow during the dry season. In many estuaries reduced freshwater inflow over time can result in the landward encroachment of salinity (Cloern and Jassby 2012). In the case of the CRE, upstream salt migration can reduce the extent of vegetated freshwater habitat (i.e., *Vallisneria americana*), impact community composition in the water column and benthos, and compress the oligohaline area of the estuary essential to a variety of faunal populations (Doering et al. 2002, Simpfendorfer et al. 2011, Palmer et al. 2011, Stevens et al. 2013).

Continuous salinity recorders have been in place near Fort Myers, Florida since 1992. The objective of this study was to quantify inter-annual variations in the estimated freshwater inflow from S-79 associated with a salinity of 10 (S_{10}) at the Ft. Myers station.

Methods

This analysis focused on the average daily freshwater inflow at the Franklin Lock and Dam (S-79; Q_{S79}; cfs) and did not include consider freshwater inputs from tributaries or groundwater downstream of S-79. Inflows from January 1, 1992, to May 1, 2013, were downloaded from the publicly available SFWMD database, DBHYDRO, which can be accessed at http://my.sfwmd.gov/dbhydroplsql/show_dbkey_info.main_menu. Average daily salinity determined at the Ft. Myers station (S_{FtM}) over the same period of record (POR) was downloaded and combined with the inflow data. The two data sets were used to generate a time series of average monthly values (**Figure 13A**). The overall relationship between average monthly inflow (Q_{S79}; cfs) and average monthly salinity at Ft. Myers (S_{FtM}) follows a negative exponential form (**Figure 13**; Qiu and Wan 2013):

$$S_{FtM} = a * e^{(-b*Q_{S79})} \quad (6)$$

The average monthly inflow and salinities were categorized by water year to derive 21 individual years of coupled inflow-salinity records (n = 12 per water year). Scatter plots similar to **Figure 13B** were generated for each water year (**Figure 14A-U**). The negative exponential curve fit to the scatter plots for each year resulted in estimates of r^2 and two equation parameters (a, b) to calculate salinity at the Ft. Myers station. There were five water years for which the relationship was unusable. The high inflows throughout WY1995 resulted in average monthly salinities < 5. Inflow and salinities in the dry (November–April) and wet (May–October) seasons were anomalous in WY2006 as tropical storms in 2005 led to extreme freshwater releases from Lake Okeechobee from late 2005 to the middle of 2006 (**Figure 13A**). Precipitous decreases to inflow in WY2007 due to drought rendered the curve-fitting procedure meaningless. Similarly, the greatly reduced inflow and exacerbated salinity in WY2008 resulted in an uncertain mathematical relationship. Finally, the salinity sensor was unavailable for several months in WY2010. The negative exponential equation for each of the remaining 16 water years was solved to predict Q_{S79} required for S_{10} (Q_{calc}):

$$Q_{calc} = \frac{\ln(S_{10}) - \ln(a)}{-b} \quad (7)$$

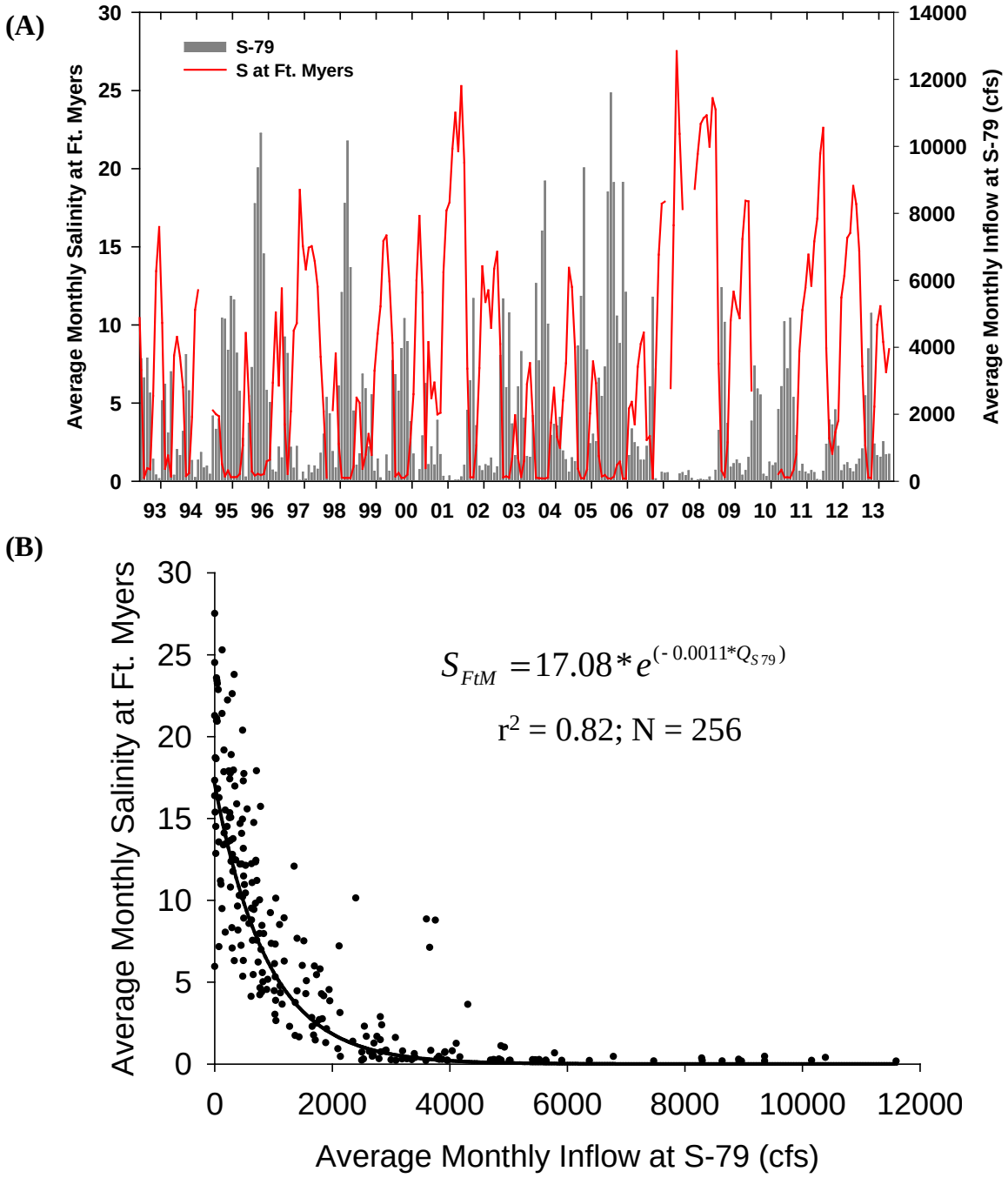

Figure 13. (**A**) Time series of average monthly inflow from the S-79 structure to the CRE and average monthly salinity at the Ft. Myers monitoring station. (**B**) Negative relationship between inflow (Q_{S79}) and salinity (S_{FtM}) represented by an exponential decay equation. All months from the period of record, WY1993–WY2013, are included.

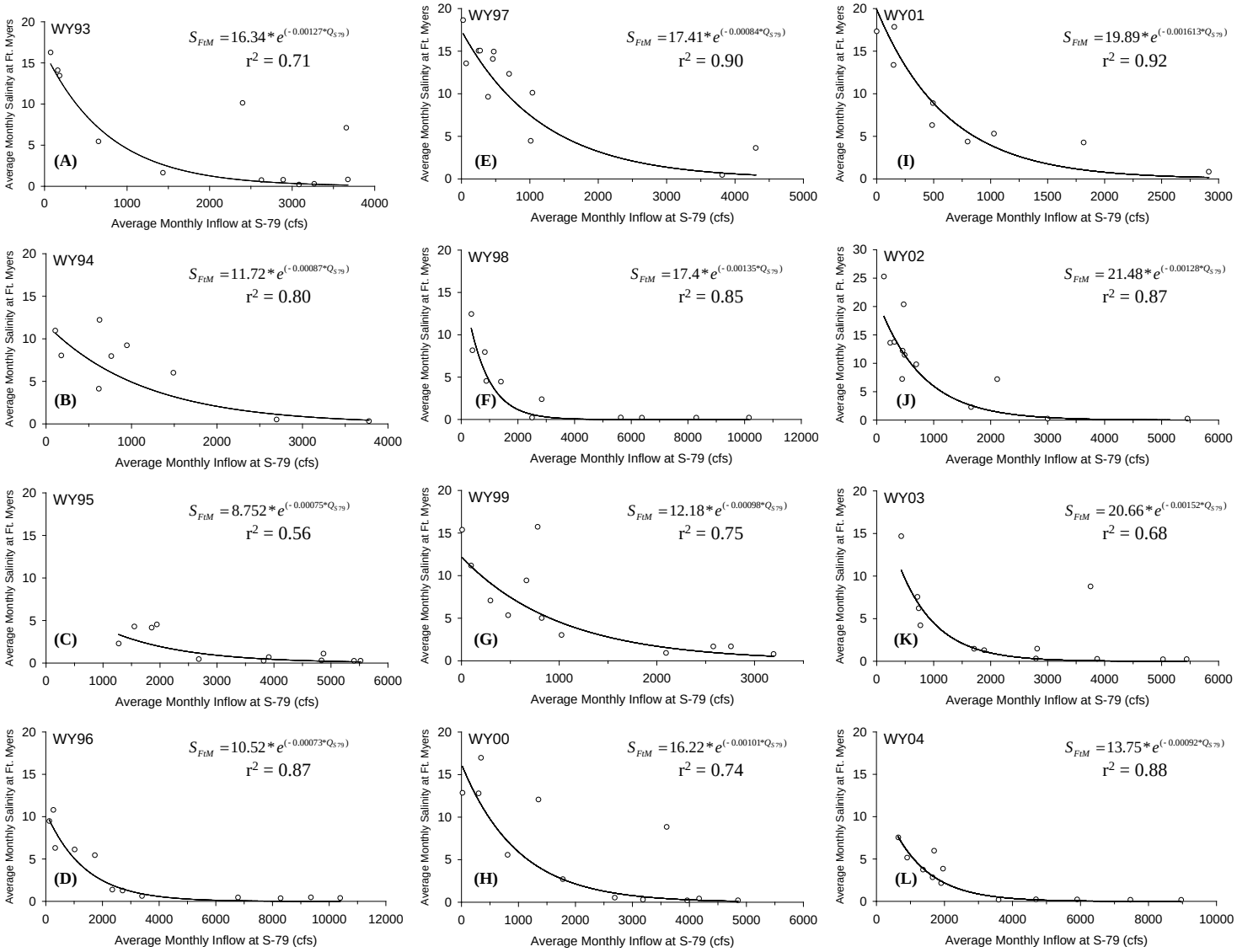

Figure 14A–L. Series of scatter plots and fitted exponential decay equations between average monthly inflow at S-79 (cfs) and average monthly salinity at the Ft. Myers monitoring station since WY1993.

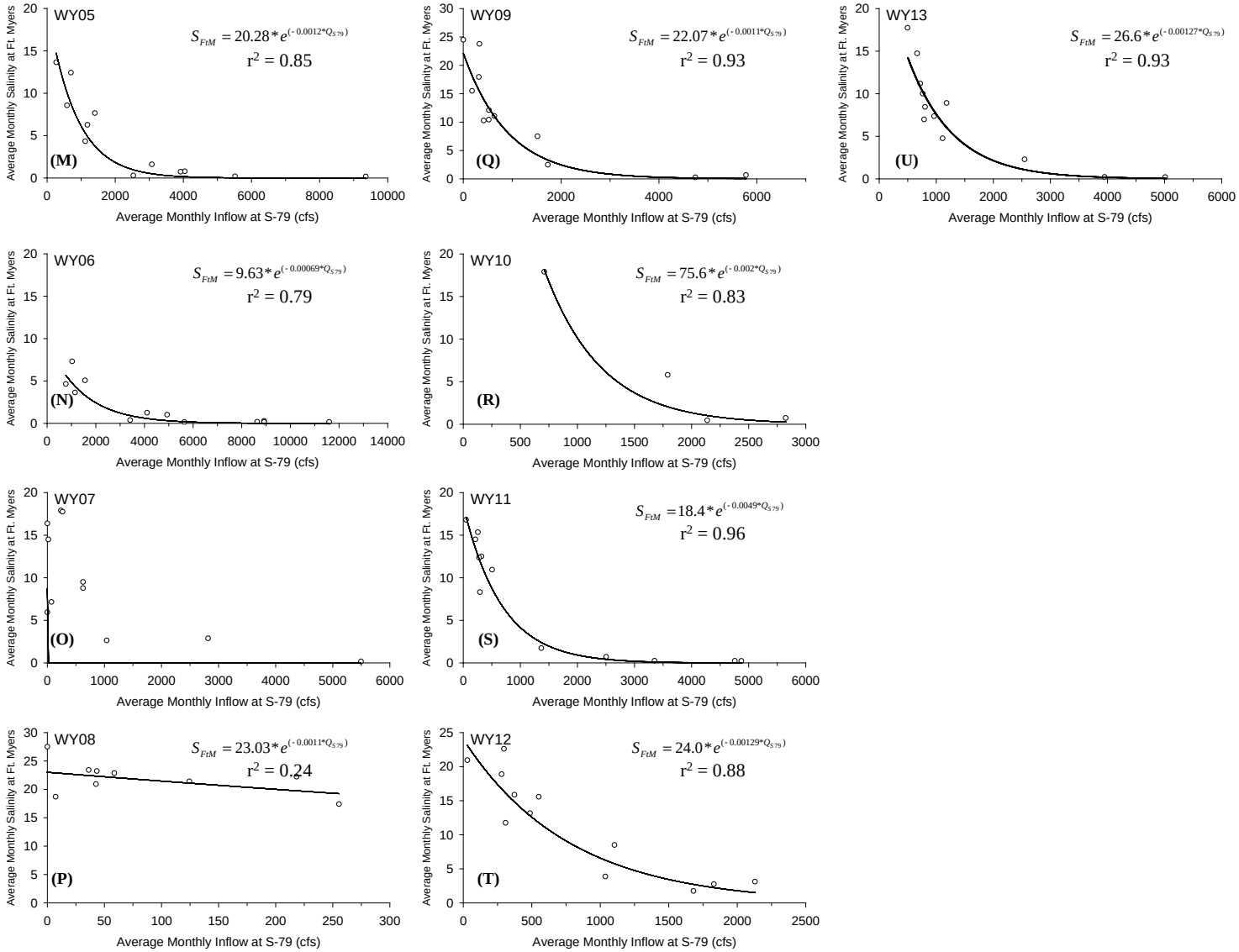

Figure 14M–U. Series of scatter plots and fitted exponential decay equations between average monthly inflow at S-79 (cfs) and average monthly salinity at Ft. Myers since WY1993.

Results

Average monthly inflows varied both intra- and inter-annually from WY1993 to WY2013 (**Figure 14A-U**). As noted, inflows were extremely low (< 300 cfs) in WY2008 (**Figure 14P**). The maximum monthly inflows were comparatively low in WY1993 (1,997 cfs), WY1994 (1,073 cfs), WY1997 (1,069 cfs), WY1999 (1,238 cfs), WY2000 (2,256 cfs), WY2001 (664 cfs), WY2002 (1,291 cfs), WY2003 (2,500 cfs), WY2009 (1,397 cfs), WY2011 (1,576 cfs), and WY2013 (1,585 cfs; **Table 7**). Average monthly salinity at the Ft. Myers station ranged from 5.5 to 11.0 among these years. By contrast, average monthly inflows were comparatively high in WY1996 (3,905 cfs), WY1998 (3,445 cfs), WY2004 (3,394 cfs), WY2005 (2,817 cfs), and WY2006 (5,074 cfs; **Table 7**). Average monthly salinities were 3.9, 3.8, 2.7, 5.1, and 2.0, respectively, for these water years under comparatively higher freshwater inflow.

The degree of fit (r^2) for the relationship between average monthly inflow and average monthly salinity at the Ft. Myers station ranged from 0.71 to 0.96 among 17 water years (**Table 7**). r^2 was lowest in WY1993 (0.71) and WY2003 (0.68) and greatest in WY2001 (0.92), WY2009 (0.93), WY2011 (0.96), and WY2013 (0.93). Q_{calc} to achieve S10 at Ft. Myers ranged from 70 cfs (WY1996) to 773 cfs (WY2013) with an average (± standard deviation) of 445 ± 218 cfs over all water years (**Figure 15**).

Discussion

This study demonstrated that the amount of freshwater inflow at the head of the CRE varies greatly both intra- and inter-annually. This has implications for attempts to establish inflow requirements to the estuary. The quantity of fresh water delivered from S-79 associated with a salinity target of 10 at the Ft. Myers station varied from 70 to 773 cfs depending upon the contribution from the downstream Tidal Basin. In fact, the amount of ungauged freshwater input from the Tidal Basin is likely to be a key component to the total freshwater budget for the estuary. Modeling of freshwater inputs from tributaries and groundwater in the downstream Tidal Basin is ongoing and these inputs have been incorporated into the CRE CH3D Model (Wan et al. 2013).

Table 7. Summary from analysis of average monthly inflow at S-79 (cfs) and average monthly salinity at Ft. Myers. An exponential decay curve was used to describe the relationship between the average monthly values for each water year. Table values for each water year include the average inflow (Q_{S79}) and salinity at Ft. Myers (S_{FtM}), curve fit parameters (r^2, a, and b), and the calculated inflow to achieve a salinity of 10 at Ft. Myers (Q_I).

Water Year	Q_{S79} (cfs)	S_{FtM}	r^2	a	b	Q_I (cfs)
1993	1,997	5.5	0.71	16.34	0.00127	386
1994	1,073	7.0	0.80	11.72	0.00087	183
1995	3,152	1.4				
1996	3,905	3.9	0.87	10.52	0.00073	70
1997	1,069	11.0	0.90	17.41	0.00084	657
1998	3,445	3.8	0.85	17.40	0.00135	410
1999	1,238	6.4	0.75	12.18	0.00098	201
2000	2,256	6.1	0.74	16.22	0.00101	479
2001	664	12.0	0.92	19.89	0.00161	426
2002	1,291	10.3	0.87	21.48	0.00128	597
2003	2,500	3.9	0.68	20.66	0.00152	477
2004	3,394	2.7	0.88	13.75	0.00092	346
2005	2,817	5.1	0.85	20.28	0.00120	589
2006	5,074	2.0				
2007	953	8.8				
2008	113	21.6				
2009	1,397	11.4	0.93	22.07	0.00110	720
2010	1,516	7.5				
2011	1,576	7.8	0.96	18.40	0.00487	125
2012	844	11.6	0.88	24.00	0.00129	677
2013	1,585	7.7	0.93	26.63	0.00127	773
Average	1,993	7.6				445 $\pm$ 218

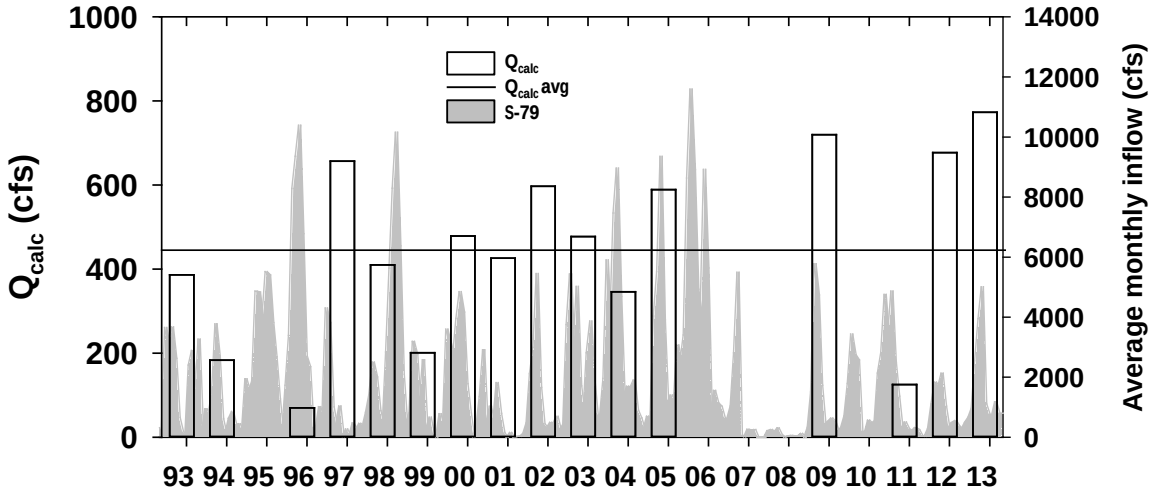

Figure 15. Time series of the calculated amount of freshwater inflow from S-79 associated with a salinity of 10 at Ft. Myers (Q_{calc}). The average Q_{calc} is shown (445 cfs).

Component Study 3: Relationships between Freshwater Inflows and Water Quality Attributes during the Dry Season in CRE

Christopher Buzzelli, Peter Doering, Teresa Coley, and Zhiqiang Chen

Abstract

Decreased flushing with reduced inflow can lead to the deposition of phytoplankton biomass and bottom water hypoxia in estuaries. This study component utilized event-scale water quality data, long-term monitoring of CHL, and simulation modeling of phytoplankton dynamics to evaluate low freshwater inflows that could contribute to water quality problems in the upper CRE. The highest CHL and lowest DO concentrations occur in the upper CRE under low inflows. Although more research is needed, it is hypothesized that dry season inflows of less than approximately 500–600 cfs may promote bottom water hypoxia in the deeper channel of the upper CRE. Field and model results indicated that CHL concentrations greater than the water quality standard of 11 µg L^{-1} were associated with inflows of 469 ± 689 cfs and 269 ± 493 cfs, respectively. Low level inflows (< 500 cfs) need to be further studied to better quantify the discharge required to mitigate the potential for hypoxia in the upper CRE.

Introduction

Bottom water hypoxia (DO concentrations £ 3 milligrams per liter [mg L^{-1}]) is increasingly common in many estuaries (Diaz and Rosenberg 2008, Committee on Environment and Natural Resources 2010). Recurring hypoxia negatively impacts benthic fauna, fish populations, fishery harvest, and ecosystem energy flow (Breitburg 2002, Powers et al. 2005, Diaz and Rosenberg 2008, Rabalais et al. 2010). The potential for bottom water hypoxia is directly related to phytoplankton blooms as phytoplankton detritus stimulates DO consumption below the pycnocline (Paerl et al. 2006, Livingston 2007, Kemp et al. 2009, Committee on Environment and Natural Resources 2010). Processes can be complex due to spatial and temporal lags among hydrodynamic drivers, phytoplankton production and deposition, and bottom water hypoxia.

Relationships between freshwater inflow and phytoplankton production in estuaries are dependent upon the time scales of transport, growth, and grazing (Cloern et al. 2014). Reduced inflow can promote phytoplankton blooms through longer water residence time, decreased vertical mixing, and enhanced light in the surface layer (Lancelot and Muylaert 2011, Wan et al. 2013, Cloern et al. 2014). Anthropogenic factors such as increased water temperature from climate change, reductions in filter feeders, and increased nutrient loads can stimulate phytoplankton production in excess of consumption (Kemp et al. 2009). Phyto-detritus not consumed or transported downstream reaches bottom sediments through vertical settling (Cloern et al. 2014).

Estuarine phytoplankton production can be viewed on annual, seasonal, and event (< 1 month) time scales (Cloern and Jassby 2009). Phytoplankton dynamics at the event-scale can be particularly acute in small estuaries with subtropical climate and managed freshwater inflows (Schlacher et al. 2008, Buzzelli 2011, Azevedo et al. 2014). Phytoplankton responses to pulsed river discharges are sometimes modulated by zooplankton grazing (Wolanski et al. 2004). However, low flow conditions favor phytoplankton growth in excess of loss, upstream migration of the chlorophyll *a* maximum

(CHL_{max}), and hypoxia in the upstream bottom water (Schlacher et al. 2008). Upstream encroachment of CHL_{max} is common for micro-tidal Gulf of Mexico estuaries with subtropical climates and vertical stratification under reduced flushing (Murrell et al. 2007). The CRE possesses many of these characteristics.

Changes to freshwater inflow have altered salinity regimes and the overall ecology of the estuary (Chamberlain and Doering 1998a, Barnes 2005). The CHL_{max} (~30 µg L^{-1}) moves upstream towards the water control structure at the estuarine head (S-79) under low inflows (0–500 cfs; Doering et al. 2006, Tolley et al. 2010, Radabaugh and Peebles 2012, Buzzelli et al. 2014a). When this occurs, the highest CHL and lowest DO concentrations can be coincidently located upstream (Doering and Chamberlain 1998). Like many estuaries, hypoxia develops through increased residence time, reduced vertical mixing, and increased deposition of phyto-detritus (Tolley et al. 2010, Radabaugh and Peebles 2012). This process was particularly evident in 2000 as the CRE experienced a decline in bottom water DO one to two months following a phytoplankton bloom (Doering et al. 2006). Reduced freshwater inflow results in the proliferation of diatoms in the upper CRE (Tolley et al. 2010). While this can stimulate the food web, unconsumed phyto-detritus can contribute to bottom water hypoxia.

There is limited information on the effects of low level freshwater inflows on patterns of salinity and water quality in the CRE. Additionally, it is very difficult to rely on the CHL concentration as an indicator of freshwater inflow. This is because CHL is itself an uncertain indicator of a variety of non-linearly related physical, biogeochemical, and biological processes (Buzzelli 2011, Cloern et al. 2014). The objective of this study component was to consider relationships between freshwater inflows and water quality attributes during the dry season. Of interest were freshwater discharges that position the CHL_{max} in the upper estuary, thus potentially enhancing deposition of phyto-detritus and hypoxic conditions in the bottom waters. This was accomplished through three synergistic approaches. First, fine-scale detection of water quality gradients with managed freshwater inflows (Adaptive Protocol Release Study [APRS]) was applied to better understand patterns at the event scale in the dry season. Second, analysis of long-term monitoring data provided a platform to examine patterns of CHL with intra- and inter-annual variations in inflow. Finally, a simulation model of phytoplankton dynamics was used to examine CHL patterns with variable transport and material cycling in the upper CRE over a range of scales.

Methods

Adaptive Protocol Release Study

This study presented a unique opportunity to evaluate the potential effects of short-term inflows on water quality and plankton abundances during the dry season. It was unique because it combined the operational capacity to regulate inflow through S-79 with ecological responses along the CRE salinity gradient and rapid in situ data acquisition (e.g. flow-through system; Madden and Day 1992, Lane et al. 2007, Buzzelli et al. 2014a).

The APRS focused on the event scale to assess potential effects of short-term pulses of fresh water on water column ecological attributes along the length of the CRE. A total of 23 APRS research cruises were conducted during in dry seasons (November–April) between January 2012 and April 2014. The cruises utilized a combination of continuous

flow-through technology and a series of vertical sampling stations. Cruises covered a total distance of ~42 km from S-79 to San Carlos Bay (**Figure 16**).

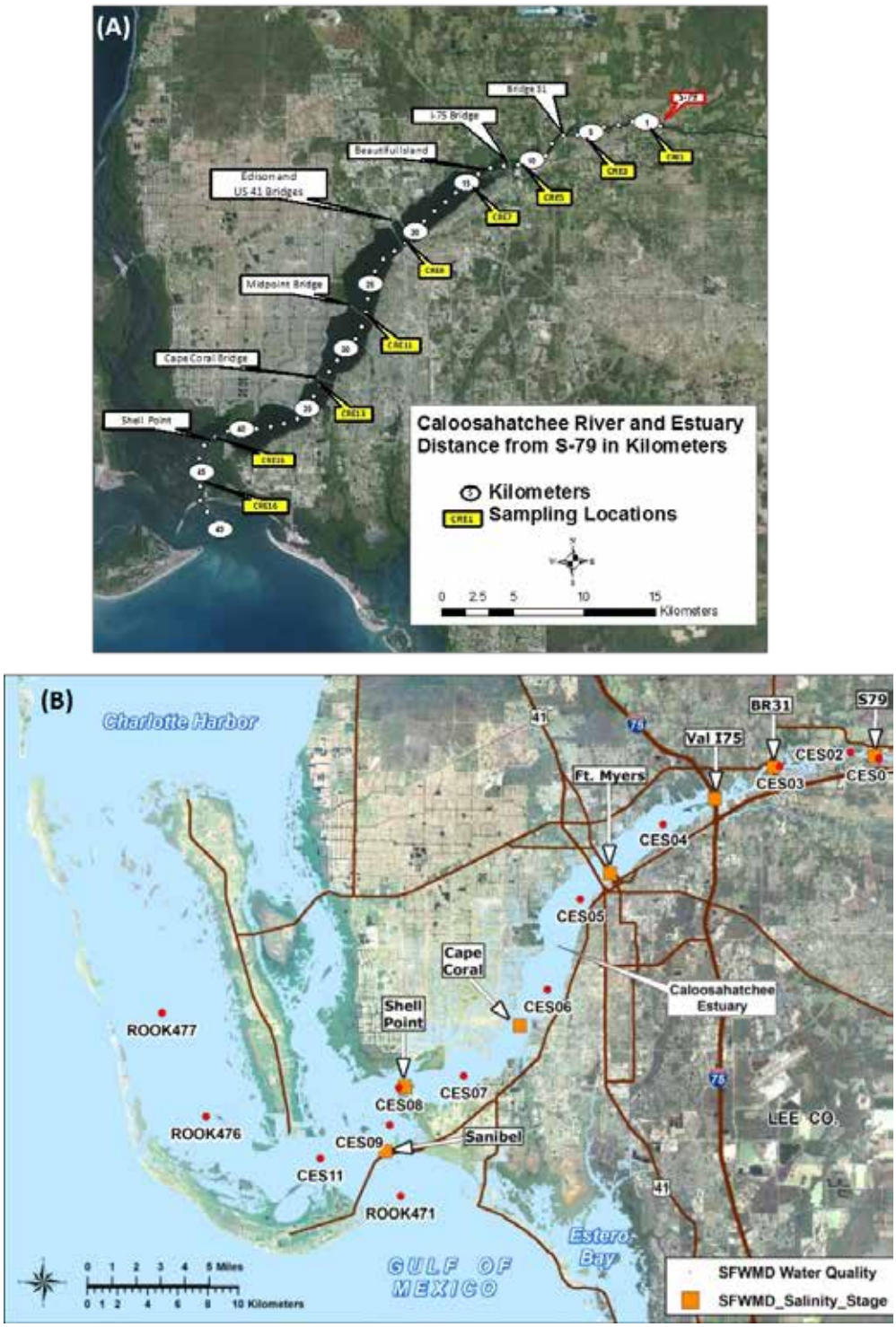

Figure 16. (**A**) Map of the CRE in Southwest Florida from the APRS showing the major structures (S-79 and bridges), the distance downstream of S-79 (white circles), and the locations for the nine vertical profiling stations (yellow call-outs). (**B**) Site map for monitoring in the CRE.

The flow-through system offers a novel method of acquiring in situ surface water data while the research vessel is under way. The system consists of an intake ram attached to the stern, a flow meter, a Trimble global position system (GPS), an YSI 6600 multi-probe instrument, a bathymetric profiler, and a laptop computer with Streamline GEO software. The YSI 6600 was set up to record temperature, salinity, pH, turbidity, DO, and in situ CHL every 5 seconds. The intake ram was at 0.5 m below the water surface with an in-line pump to ensure continuous water flow through the system. Streamline Geo software permitted integration of the GPS and surface water data into an ArcGIS shape file useful both to display surface water properties in real time and for the post-processing of spatial data. Approximately 7–8 hours were required to travel from S-79 to San Carlos Bay at an average speed of 15.2 km per hour resulting in an average distance of 15–26 m between surface water recordings (Buzzelli et al. 2014a).

Patterns of surface water salinity and CHL with distance downstream from S-79 from three dates in 2012 (March 8, March 21, and April 12) were included in this study. Since the cruises occurred approximately every two weeks, the downstream location of the maximum CHL concentration (CHL_{max}) on each date was plotted versus freshwater inflow at S-79 averaged over the previous 14 days. All the cruise dates from 2012 and 2013 were included in a separate assessment of the longitudinal variation in isohalines and the CHL_{max}. Cruise data taken under higher discharges in 2014 (0–2,030 cfs; 761 ± 569 cfs) were omitted from this analysis.

On each of the cruises, the research vessel stopped at several mid-channel stations along the mid-estuary axis to conduct vertical profiling of temperature, salinity, pH, DO, turbidity, and CHL with the YSI 6600 multi-probe instrument. Recordings using the multi-probe instrument occurred at 1-meter intervals between the surface and bottom allowing for instrument stabilization between successive recordings. The vertical profiles for salinity, CHL, and DO were interpolated in two-dimensions (distance and depth) using a kriging technique to compare patterns among the three selected cruise dates.

Long-Term Monitoring of CHL

Water quality concentrations are monitored at approximately monthly intervals at multiple locations in the CRE (stations beginning with CES; **Figure 16B**). These data are available from SFWMD's DBHYDRO database, which can be accessed via http://www.sfwmd.gov/dbhydroplsql/show_dbkey_info.main_menu. CHL concentrations at CES03 in the upper CRE from April 1999 to April 2014 were included in this assessment. Since the relationships between freshwater inflow and estuarine indicators are often lagged in time and space, CHL was related to inflow averaged over different time periods. The monitoring dates were combined with a freshwater inflow series at S-79, which included the inflow on the sampling date (0 day) and inflow averaged 7 to 35 days prior. The relationship between CHL concentrations at CES03 was plotted over all time periods. The combined CHL-inflow data set was queried to determine freshwater inflows associated with the Impaired Waters Rule (Rule 62-303.353, Florida Administrative Code) annual average CHL value of 11 µg L^{-1}. This exercise resulted in the determination of freshwater inflows linked to increased phytoplankton production in the upper CRE.

Segmented Simulation Model of the CRE

The CRE was split into three segments for development of a simulation modeling framework (Buzzelli et al. 2014b, 2014c). This model application focused on Segment 1 in the upper CRE (16.1 km from S-79; 1.5 x 10^7 square meters [m^2]; 2.1 x 10^7 m^3, see **Figure 16** for river km). The model framework includes a box model for transport, external inputs, forcing functions that drive model processes, and biogeochemical process equations and coefficients (Buzzelli et al. 2014b). The biogeochemical models use an integration interval of 0.03125 days (45 minutes) over simulations spanning 2,922 days from 2002 to 2009. The box model was driven by daily time series for freshwater inflow at the estuarine head and salinity for each segment and the downstream boundary. Physical transport of a water column constituent was the sum of advection, lateral inputs from tributaries and groundwater, and non-tidal dispersion. The time series for estuarine head from 2002 to 2009 (2,922 days) at S-79 was derived from DBHYDRO. The loadings of water column constituents at the upstream boundary were calculated as the product of the estuarine head and average monthly concentrations.

A watershed model was used to estimate the daily lateral input from tributaries and groundwater (Y. Wan, unpublished data). The loadings of water column constituents from the tributaries and groundwater were the product of the lateral inflows to each segment and the corresponding average monthly input concentration derived from Lee County, Florida monitoring stations. Time series for the average daily salinity of each segment were generated using a predictive statistical model developed for the CRE (Qiu and Wan 2013).

Each of the three segments included a water column submodel to simulate the concentration of phytoplankton carbon, organic nitrogen and phosphorus, ammonium, nitrate-nitrite, ortho-phosphate, and sediment microalgae. Biogeochemical processes were modulated by variations in temperature, depth, and submarine light. The total attenuation coefficient for submarine light contained contributions from pure water, color, turbidity, and CHL. Attenuation due to color was estimated using a negative exponential relationship with average salinity of the segment (McPherson and Miller 1994, Bowers and Brett 2008, Buzzelli et al. 2012). Time series for the average turbidity of each segment were derived from monitoring data available through DBHYDRO. Phytoplankton was a key variable since it receives external inputs of CHL from the watershed, is the primary sink for inorganic nitrogen and phosphorus, is the primary source of autochthonous organic nitrogen and phosphorus, is important in submarine light extinction, and serves as an ecological indicator (Doering et al. 2006, Buzzelli 2011, Buzzelli et al. 2014b). The amount of phytoplankton biomass (e.g. CHL) is calculated every time step depending upon five source terms (input from S-79, input from the Tidal Basin, production, resuspension from the bottom, and dispersion) and six sink terms (downstream outflow, dispersion, respiration, sinking, exudation, and grazing; **Figure 17**).

Dry season (November–April) results from the base model simulations (2002–2009) in Segment 1 were used in this study. Daily model predictions of CHL in the upper CRE were calibrated using monthly CHL concentrations averaged among the S-79, CES01, CES02, and CES03 locations (Buzzelli et al. 2014b). Similar to the field data, the model output was queried to determine freshwater inflows associated with the Impaired Waters Rule annual average CHL value of 11 µg L^{-1}. This exercise resulted in the determination of the desirable freshwater inflows below which there was the potential for phytoplankton blooms in the upper CRE.

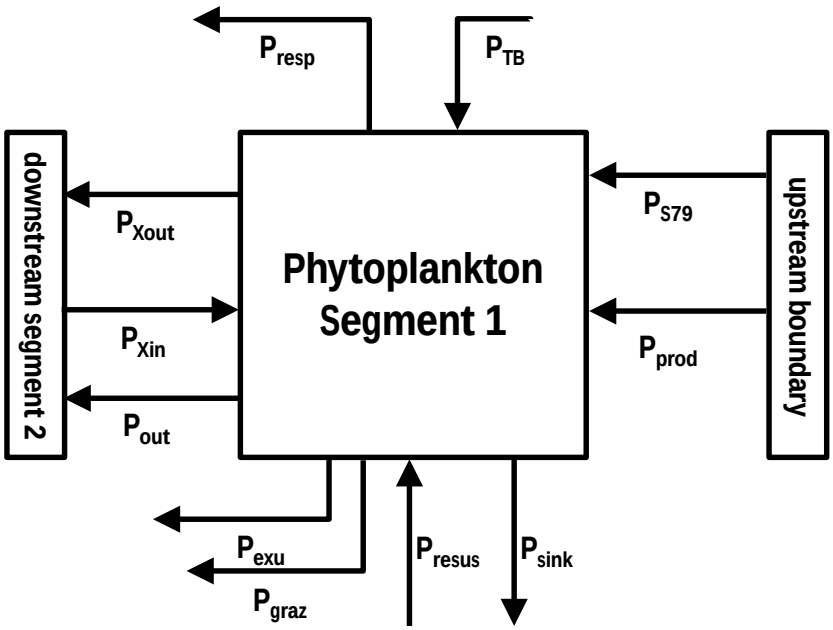

P_{in} = Input from upstream boundary
P_{prod} = Gross production
P_{TB} = Input from the tidal basin
P_{resp} = Respiration
P_{sink} = Sinking from water column
P_{resus} = Resuspension from bottom
P_{graz} = Loss to grazing
P_{exu} = Loss to exudation
P_{Xin} = Upstream non-tidal exchange
P_{Xout} = Downstream non-tidal exchange
P_{out} = Downstream transport

$$dPhytodt^{-1} = [(P_{S79} + P_{TB} + P_{prod} + P_{resus} + P_{Xin}) - (P_{out} + P_{Xout} + P_{resp} + P_{sink} + P_{exu} + P_{graz})]$$

Figure 17. Schematic and definition of process terms that influence phytoplankton biomass (e.g. CHL) in the simulation model for the CRE.

Results

Adaptive Protocol Release Study

Freshwater inflow to the CRE through S-79 declined from January to March 2012 before reaching 0.0 cfs on March 27, 2012 (Buzzelli et al. 2014a). Two-week average inflow decreased from 627.8 cfs to 556.3 cfs between March 8 and March 21 (**Table 8**). There were a total of 1,559, 2,177, and 2,085 surface water recordings along the length of the CRE on March 8, March 21, and April 12, respectively (Buzzelli et al. 2014a). These highly resolved spatial data permitted visualization of the longitudinal patterns of salinity and CHL with changes in freshwater inflow (**Figure 18**). The locations of the salinity of 10 isohaline moved upstream with reduced inflow; it was located 14.6 km from S-79 on March 8 but only 0.7 km from S-79 on April 12 (**Table 8**). Salinity ranged 5 to 6 from 0 to 14 km downstream before increasing from 6 to 35 over the remaining 26 km on March 8 (**Figure 18A**). There were obvious variations in salinity along the length of the CRE on this date. On March 21, salinity ranged from 6 to 7 over the initial 10 km after which it increased linearly with distance downstream. Finally, salinity at S-79 was ~10 on April 12 after the cessation of inflow. It increased gradually down to ~14 km before exhibiting a smooth, linear increase over the remaining length of the estuary.

Table 8. Results from the APRS on the CRE in the 2012 dry season. Included are the 14-day average inflow at S-79 (Q_{S79}), the location of the salinity of 10 isohaline in km from S-79 (S_{10}), and the location and value for the maximum concentration of chlorophyll *a* (CHL_{max}).

Date	Q_{S79} (cfs)	S_{10} (km)	CHL_{max} (km)	CHL_{max} (µg L^{-1})
3/8/12	627.8	14.6	12.9	11.1
3/21/12	556.3	11.1	12.8	10.2
4/12/12	0.0	0.7	2.6	25.6

Similar to the salinity of 10 isohaline, the CHL_{max} migrated upstream with reduced discharge. While it was located at 12.8 km downstream of S-79 on March 21, it moved upstream to 2.6 km as inflow decreased leading up to the April 12 cruise (**Table 8**). There was great variability in CHL (20–48 µg L^{-1}) from 0 to 10 km on April 12 compared to the previous two cruise dates (**Figure 18B**). Thus, the location of the CHL_{max} in the upper estuary increased dramatically from 10.2 µg L^{-1} on March 21 to 25.6 µg L^{-1} on April 12 (**Table 8**). CHL declined to 10–15 µg L^{-1} from 20 to 42 km downstream on all three cruise dates.

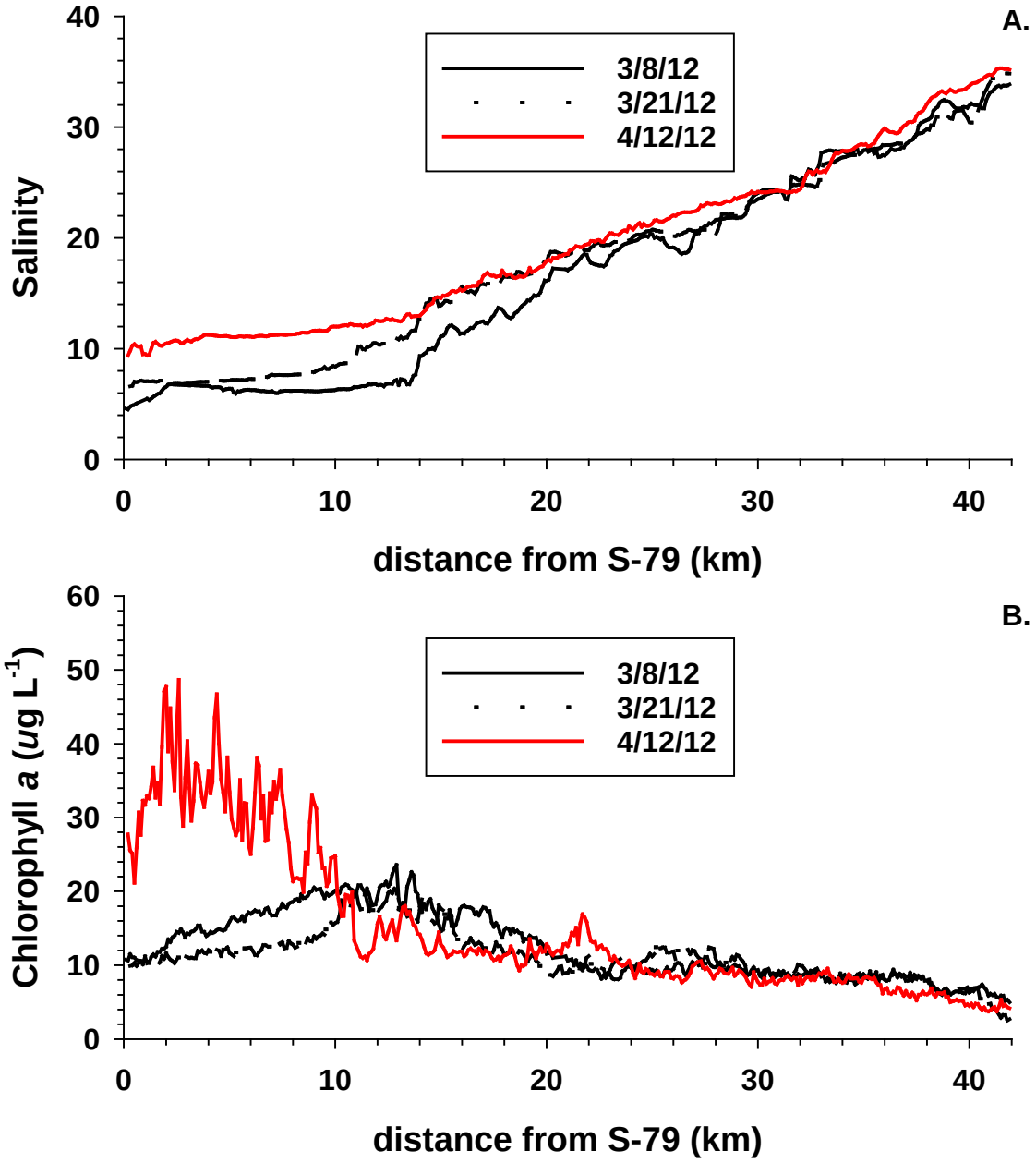

Figure 18. Results of the APRS from March 8, 2012, March 21, 2012, and April 12, 2012: (**A**) surface water salinity versus distance downstream of S-79; and (**B**) surface water CHL versus distance downstream of S-79.

Interpolated contour plots derived from the vertical profiles validated upstream salinity and CHL encroachment as inflow decreased (**Figure 19**). These profiles and plots illustrated depth-dependent patterns including a surface lens of fresh water that contributed to vertical salinity stratification on March 8 (**Figure 19**, top left; Buzzelli et al. 2014a). It appeared that the vertical stratification evident in March gave way to horizontal gradients as saltier water moved upstream by April (**Figure 19**, top center and top right). There appeared to be a topographic influence on hydrodynamic and biogeochemical processes due to the decrease in depth from 6 km (~7 m) to 15 km (~2.5 m) downstream of S-79.

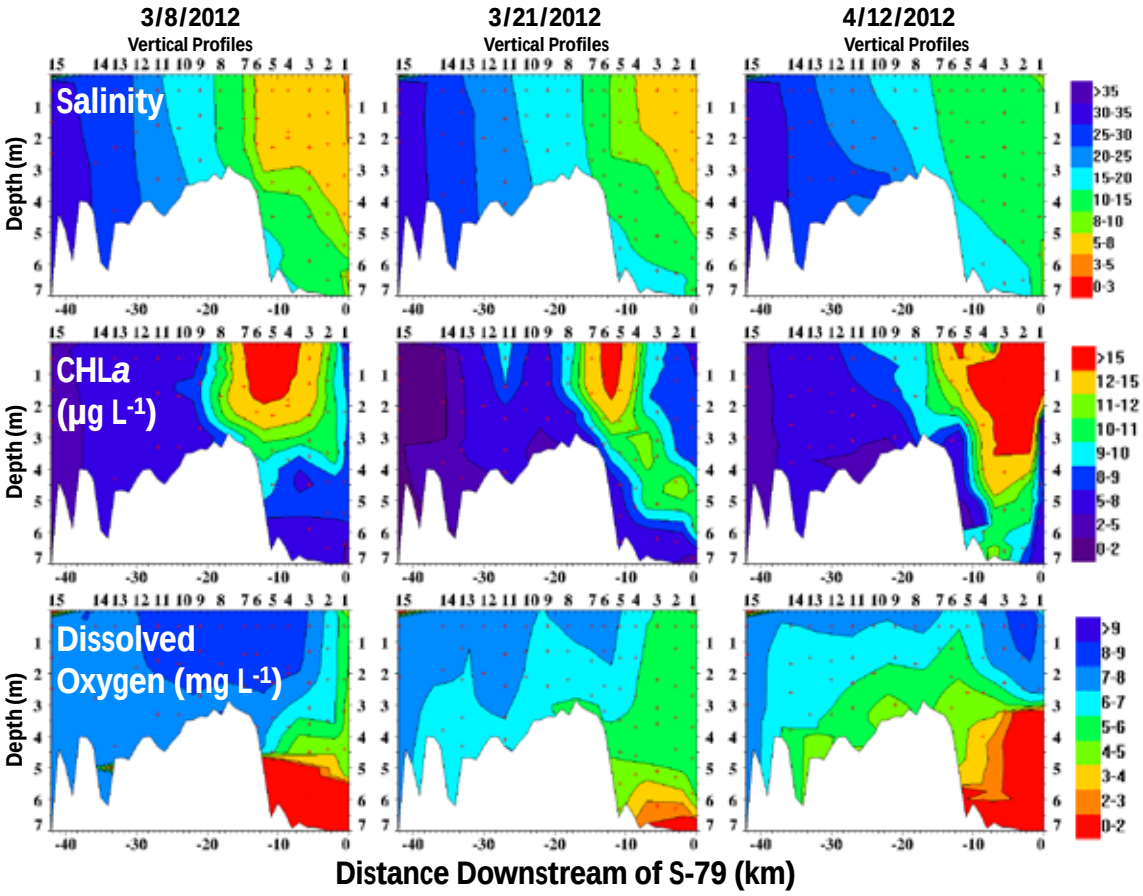

Figure 19. Interpolated depth versus distance contour plots derived from vertical profiling from the APRS for three different cruise dates. The APRS station designations shown in **Figure 16A** are provided along the top of each plot. The horizontal axis is oriented from right to left to represent distance downstream of S-79. The vertical axis is depth. The top three plots show salinity ranging from 0 to 3 to > 35.0. The middle three plots show CHL ranging from 0 to 2 to > 15.0. The bottom three plots show DO concentrations ranging from 0 to 2 to > 9.0.

The CHL_{max} was located ~13 to 20 km downstream under inflows of 500 to 1,000 cfs over all cruises in 2012 and 2013 (**Figure 20**). Thus, the CHL_{max} extended vertically down a couple of meters as it was located in a shallower area of the estuary. This was evident on March 8 followed by a slight deepening of the surface layer CHL_{max} on March 21 (**Figure 19** middle left and middle center). The estuarine water parcel containing a greater amount of phytoplankton biomass located farther upstream on April 12 extended much deeper in the water column (~4.5 m; **Figure 19**, right center). These attributes of depth, inflow, and primary production affect the potential for bottom water hypoxia in the upper CRE (**Figure 19**, bottom row). Although there were bottom water DO concentrations $\leq$ 3 mg L^{-1} on March 8 and March 21, the vertical and horizontal extent of bottom water hypoxia was much greater on April 12.

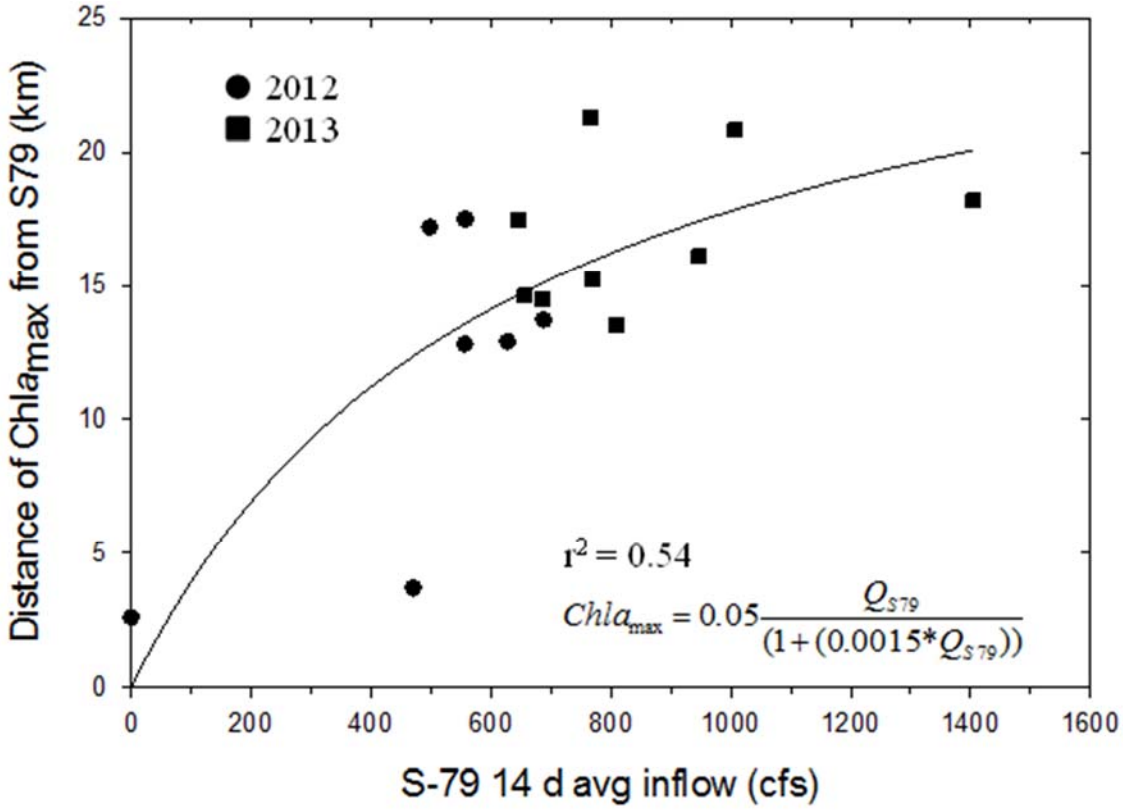

Figure 20. Hyperbolic relationship between average (avg) freshwater inflow 14 days (d) before cruise date for the APRS and the location of the CHL_{max} in surface water of the CRE. Results are from all cruises from dry seasons in 2012 and 2013 (n = 15).

Long-Term Monitoring of Chlorophyll a

CHL at CES03 (7 km downstream of S-79) ranged from a minimum of 0.3 µg L^{-1} to maximum values of 73.0 and 98.8 µg L^{-1} in the dry and wet seasons, respectively (**Table 9** and **Figure 21**. CHL was low (< 10 µg L^{-1}) from 2002 to 2006 but appeared to be more variable from 2007 to 2011. The highest values were observed on April 28, 2009 (73.0 µg L^{-1}) and July 20, 2011 (98.8 µg L^{-1}). The seasonally averaged concentrations were highly variable in dry and wet seasons (8.6 ± 10.2 and 12.2 ± 15.0, respectively). The coefficient of variation was > 100% in both seasons. Averaging inflow over an increasing number of days preceding the field sampling at CES03 did not improve the correlation between the observed CHL concentrations and freshwater discharge (**Figure 22**).

Table 9. Descriptive statistics for CHL (µg L^{-1}) at station CES03 in the CRE from April 1999 to April 2014. The data set was split into dry (November–April) and wet (May–October) seasons. Included are the number of samples, range, median, average and standard deviation (Avg ± SD), and the coefficient of variation expressed as a percentage (CV = (SD/Avg)*100).

Season	Number	Range	Median	Avg ± SD	CV (%)
Dry	93	0.3–73.0	5.5	8.6 ± 10.2	118
Wet	93	0.3–98.8	5.2	12.2 ± 15.0	123

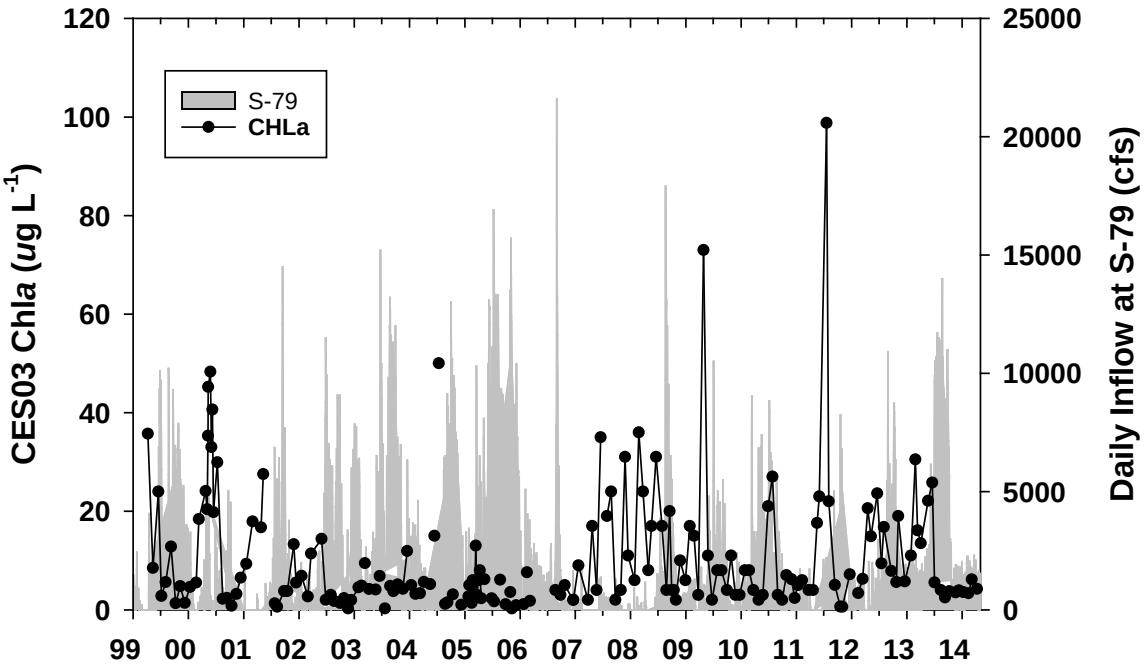

Figure 21. Time series of water column CHL observed at station CES03 in the upper CRE. Average daily inflow at S-79 (right axis) is shown in grey.

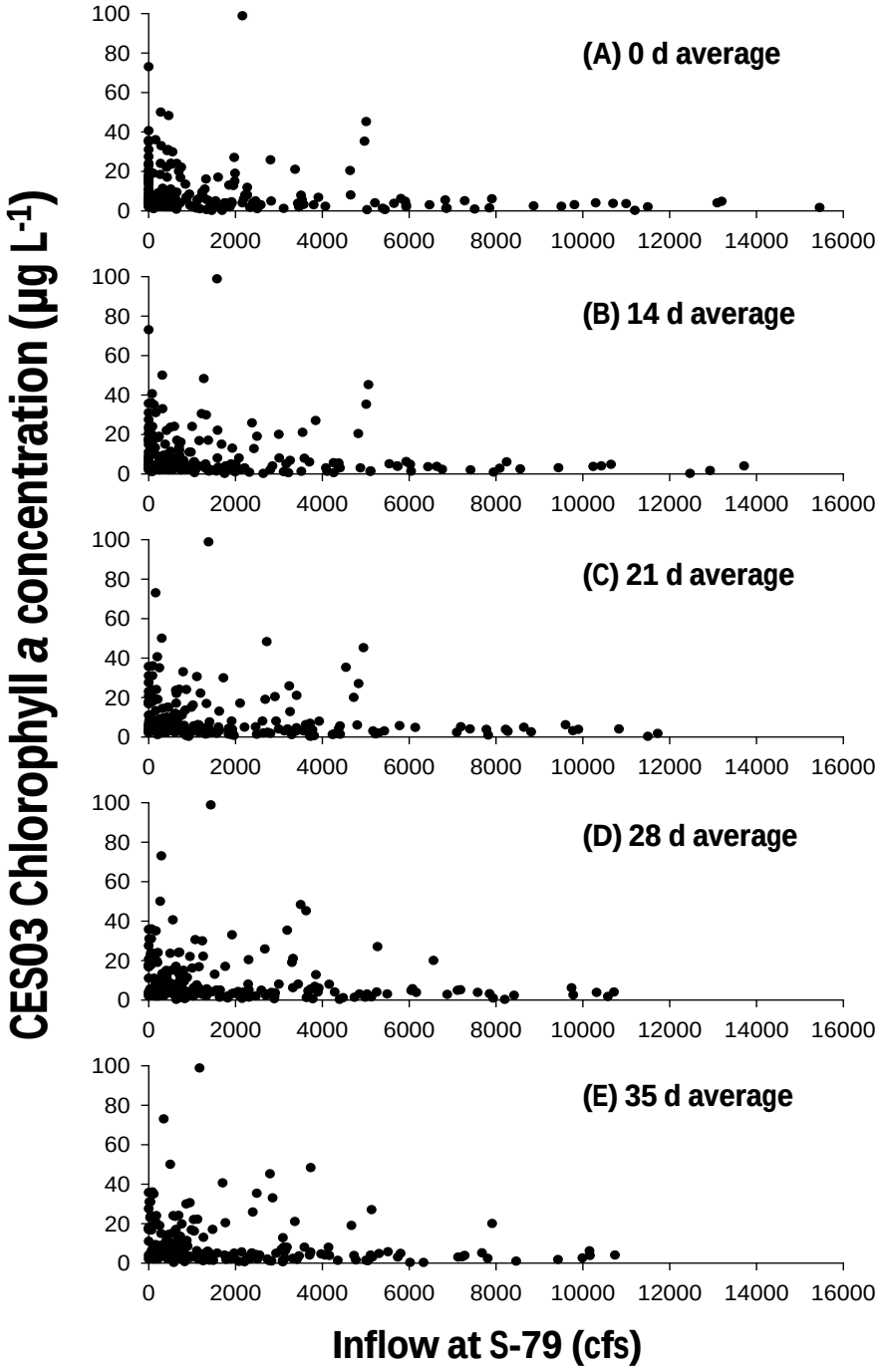

Figure 22. Scatterplots of water column CHL observed at station CES03 in the upper CRE versus the average daily inflow at S-79: (**A**) inflow on CES03 sampling date; (**B**) inflow averaged over 14 days (d) prior to the sampling date; (**C**) inflow averaged over 21 days prior to sampling date; (**D**) inflow averaged over 21 d prior to sampling date; (**E**) inflow averaged over 35 days prior to sampling date.

Segmented Simulation Model of the CRE

Average daily CHL concentrations predicted for the upper CRE ranged from 0.6 to 31.3 µg L^{-1} from 2002 to 2009 (**Figure 23**). The model was a reliable predictor as CHL approximated the average concentrations determined among multiple stations in the upper CRE (r = 0.61–0.76; **Table 10**). Values were generally higher in the wet season (14.2 ± 4.0 µg L^{-1}) compared to the dry season (6.8 ± 2.3 µg L^{-1}; **Table 10**). The simulation model predicted that average monthly CHL during the dry season in the upper CRE decreases exponentially with increased freshwater inflow (**Figure 24**). However, there was a wide range of CHL concentrations that were possible when inflows were <500 cfs.

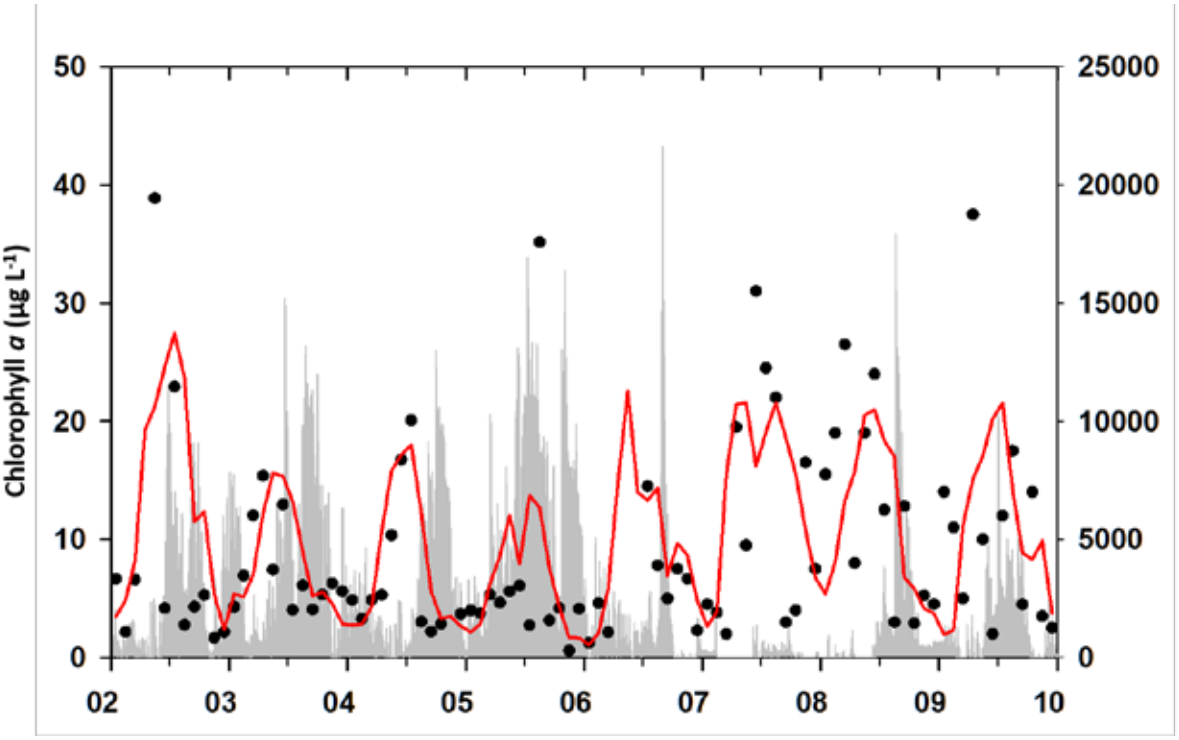

Figure 23. Time series of water column CHL concentration predicted for the upper CRE (0–16 km downstream of S-79) using the simulation model. Data points represent the average CHL concentration averaged among four stations in the upper CRE (S-79, CES01, CES02, and CES03). Also shown are daily average flows from S-79.

Table 10. Model calibration results to simulation CHL concentration (µg L^{-1}) in the upper CRE (0–16 km from S-79) from 2002 to 2009. Included are the average + standard deviation for pooled monitoring data (CES01, CES02, CES03, and S-79) and the model. The correlation coefficient (r) between the data and the model was calculated using monthly average concentrations (n = 96 months).

Season	Data	Model	r
Dry	7.4±4.5	6.8±2.3	0.61
Wet	9.4±3.9	14.2±4.0	0.76

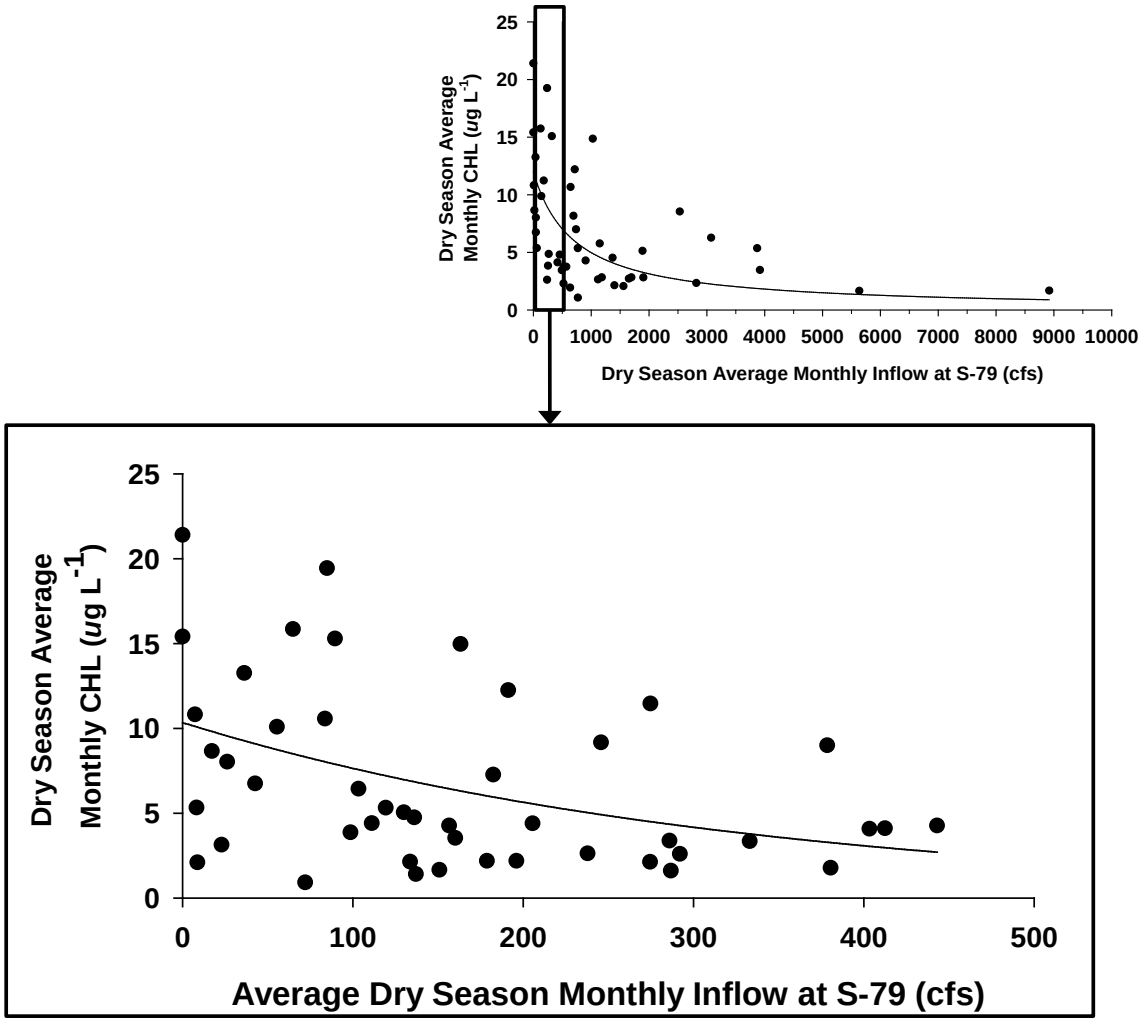

Figure 24. Results from simulation model of the CRE. Average monthly inflow at S-79 (cfs) versus average monthly CHL concentration (µg L^{-1}) in upstream Segment 1. The zoomed scatterplot highlights inflows < 500 cfs.

An upper threshold of 11.0 µg L^{-1} was used as a critical criterion to query both the field and model CHL concentrations in the dry season (**Table 11**). There were 24 measurements of CHL at CES03 that were > 11.0 µg L^{-1} (19.5% of all dry season measurements). Daily average inflows at S-79 ranged from 0 to 2,270 cfs averaging 469 ± 689 cfs over these measurements. For the model, there were 265 daily predictions of CHL in the upper CRE that were > 11.0 µg L^{-1} (18.3% of dry season simulation days). Inflow at S-79 ranged from 0 to 2,450 cfs averaging 269 ± 493 cfs for this subset of simulated days.

Table 11. Summary of daily average inflows at S-79 (cfs) when the CHL concentrations were > 11 µg L^{-1}. Results from both field monitoring (top row) and the upper segment of the CRE simulation model (bottom row; Buzzelli et al. 2014b). Water column CHL concentrations were determined at station CES03 from April 1999 to April 2014 (n = 259). Using the model, water column CHL concentrations were predicted for the upper CRE (0 to 16 km from S-79) every day from 2002 to 2009 (n = 2,120 days). Values include the averages and standard deviations (Avg ± SD) for CHL and the freshwater inflows from S-79 (Q_{S79}; cfs). Results are for dry season days only (November–April) for both the field (n = 123) and model (n = 1,450).

Source	Count	CHL ≥11 µg L^{-1} Avg ± SD	Q_{S79} (cfs) Avg ± SD
Data	24 (19.5%)	31.8 ± 51.4	469 ± 689
Model	265 (18.3%)	16.1 ± 3.8	269 ± 493

Discussion

Reduced freshwater inflow has clear biogeochemical implications for shallow, micro-tidal estuaries around the Gulf of Mexico (Murrell et al. 2007, Tolley et al. 2010). Internal cycling of materials becomes more important with reduced inflow, overall biological productivity can be severely inhibited as freshwater input declines (Livingston 2007). These attributes can favor phytoplankton production in excess of transport and grazing and the deposition of phyto-detritus in upstream sediments (Radabaugh and Peebles 2012, Cloern et al. 2014). Decreased vertical mixing coupled with enhanced deposition of organic matter can fuel hypoxia in the bottom water under reduced freshwater inflow (Doering et al. 2006, Murrell et al. 2007, Tolley et al. 2010).

Combined results suggested that daily inflows <500 cfs would result in the CHL_{max} located less than ~13 km downstream of S-79. This sequence would position the CHL_{max} above the deeper channel (~7 m) where bottom water DO concentrations ≤ 3 mg L^{-1} occur. Thus, diminished freshwater inflow could enhance both salinity stratification and the deposition of phyto-detritus (Murrell et al. 2007, Radabaugh and Peebles 2012). The possibility for hypoxia in the upper CRE is heightened given that both sediment organic content and rates of sediment oxygen demand are greater in the upper CRE (Buzzelli et al. 2013b). Finally, at the estuary scale there is increased heterotrophy (e.g. the respiration of organic matter) with reduced freshwater inflow (Buzzelli et al. 2013c).

Previous studies of the CRE have established (1) that high CHL in surface waters is correlated with low DO in bottom waters (2) hypoxia occurs most often in the upper estuary and (3) that both the magnitude and position of the CHL_{max} depend on freshwater inflow (Doering et al 2006, Wan et al 2013, Buzzelli et al. 2014a). Research into fine-scale responses of water quality to variable freshwater inflow (APRS) has provided some additional insight. While the APRS provides highly resolved spatial and temporal data, there have been limited surveys at very low inflows. More cruises need to be conducted at inflows of 0 to 500 cfs to better quantify the discharge required to mitigate the potential for hypoxia in the upper CRE. These efforts will improve the predictions of CHL_{max} and permit quantification of freshwater inflows required to avoid hypoxia in the upper CRE.

The model (< 269 cfs) and field (469 cfs) results indicated that freshwater inflows of < 500 were associated with CHL concentrations greater than the Impaired Waters Rule standard of 11.0 µg L^{-1}, annual average. Both the empirical and simulation estimates of the inflow magnitudes are valuable results of this study. Monthly monitoring of CHL

concentrations at specific locations provides an indicator of water quality, but does not account for dynamic changes in phytoplankton assemblages on scales of hours-weeks. Whereas CHL is regularly monitored as a proxy for biomass, phytoplankton production is modulated by non-linear interactions among several environmental drivers (Cloern et al. 2014). Additionally, many of these biogeochemical interactions are lagged in time and space.

In terms of water quality modeling, the many process-based parameters introduce uncertainty to the predictions. Confidence in model predictions is largely dependent upon the quality of both the experimental and calibration data (Buzzelli et al. 2014a).

While this modeling effort has great utility to evaluate estuarine responses over a range of inflow and nutrient loading conditions, it was highly aggregated spatially (Buzzelli et al. 2014a, 2014b). The development and implementation of a hydrodynamic-water quality modeling framework with greater spatial resolution could greatly benefit quantification of the inflows required to support optimal levels of phytoplankton and other water column indicators (Wan et al. 2012, Condie et al. 2012, Funahashi et al. 2013, Azevedo et al. 2014).

Component Study 4: Zooplankton Response to Freshwater Inflow in the CRE

Peter Doering

Abstract

Freshwater inflow to some estuaries, including the CRE, is regulated through control structures. Zooplankton assemblages provide an essential food web link whose position in the estuary fluctuates with inflow. Unfortunately, zooplankton habitat can be both impinged and compressed due to the presence of a water control structure as inflow is reduced in the dry season. This study assessed impingement and habitat compression for zooplankton under reduced inflow. Data used were from a CRE study conducted by Florida Gulf Coast University from 2008 to 2010. Zooplankton samples were collected monthly at each sampling site at night during a flood tide. The centers of abundance (COA) for the 13 taxa investigated migrated downstream and upstream as freshwater inflow increased and decreased, respectively. Both habitat compression and impingement were potentially harmful for zooplankton assemblages in the estuary. Impingement was possible if inflow from the S-79 structure ranged from 98 to 566 cfs and averaged 412 ± 165 cfs. Almost all taxa investigated (except *Menidia*) experienced habitat compression if the COA was < 12 km downstream of S-79.

Introduction

Like many drowned river-valley type estuaries, the CRE is funnel shaped, being narrow near its head waters and wide at its mouth. Typically, this geomorphology results in a longitudinal volumetric gradient increasing from the head to the mouth of the estuary. The COA for planktonic organisms have been shown to move upstream and downstream as freshwater inflow decreases and increases, respectively (Peebles et al. 2007). This response to inflow coupled with the geomorphology of the estuary means that the volume of open water habitat available to planktonic populations varies with freshwater inflow (Peebles and Greenwood 2009). If the longitudinal dispersion of the population remains constant, the volume of water available for occupancy decreases with diminished inflow and the upstream movement of the organisms. The crowding of organisms into a relatively confined space (habitat compression; Crowder 1986, Copp 1992, Eby and Crowder 2002) may result in increased predation and competition for limited food resources. Some organisms may be forced to utilize habitat that is physiologically suboptimal and this may result in lower growth and survival (Petersen 2003). Many estuaries, including the CRE, have water control structures (e.g. dams) that regulate freshwater inflow (Franklin Lock and Dam or S-79). These structures block upstream movement of planktonic organisms with reduced inflow and serve as barriers to adult fish migration (impingement; Peebles and Greenwood 2009). Impingement against a water control structure such as S-79 in the upper CRE can exacerbate habitat compression.

The objectives of this study were to demonstrate the compression of the zooplankton community with upstream translation in the CRE, demonstrate the occurrence of impingement of zooplankton against S-79, and determine the discharges at S-79 that promote habitat compression and impingement.

The source of data for the analysis was a 24-month study of plankton in the CRE conducted by Florida Gulf Coast University (May 2008–April 2010; Tolley et al. 2010). The overall goal of the project was to establish linkages between variability in freshwater inflow and ecosystem condition by characterizing and quantifying the responses of estuarine phytoplankton, zooplankton, and benthic microalgae. Major details of the study design and sampling routine, extracted from Tolley et al. (2010), are given below. The present analyses were conducted by SFWMD staff.

Methods

Florida Gulf Coast University Plankton Surveys 2008–2010

This study used distance upstream from the estuary mouth to reference stations and patterns. A total of seven zones were sampled from Point Ybel, Sanibel in San Carlos Bay to S-79. There were two stations (downstream and upstream) within each zone for a total of 14 stations per sampling (**Figure 25** and **Table 12**). The use of zones was not based on the identification of strata along the estuarine gradient but simply facilitated station location and sampling along the ~47-km transect. Zooplankton sampling sites were fixed for all collections. The position of the collection vessel was recorded at the beginning of each zooplankton tow using GPS. Mean distance between adjacent sampling sites was 3.26 ± 2.01 km. The system was sampled monthly for 24 months (May 2008–April 2010).

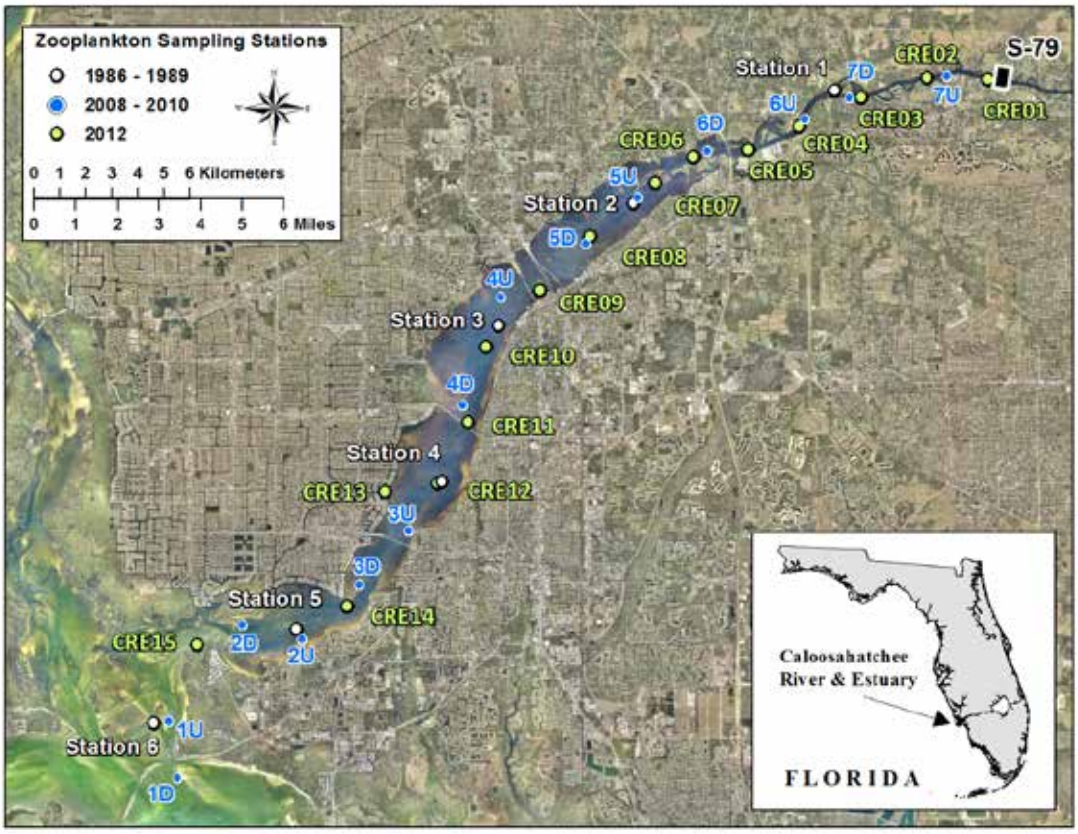

Figure 25. Zooplankton sampling stations within the CRE. The Franklin Lock and Dam are located at about 43.5 km upstream of Shell Point. Data collected from 2008 to 2010 was used in this study.

Table 12. Sampling stations for biological and water quality data (May 2008–April 2010). Depth represents the mean maximum water depth recorded at each station during biological sampling. (Note: D = downstream and U = upstream stations within each zone, with zones as described in the text.)

Zone	Station	River (km)	Latitude	Longitude	Depth
1	D	-5.9	26.4776	82.01157	2.92
	U	-3.6	26.49721	82.01514	3.09
2	D	2.5	26.53089	81.98688	3.96
	U	5.2	26.52616	81.96375	2.91
3	D	7.6	26.54528	81.94169	4.06
	U	10.6	26.56413	81.92283	3.88
4	D	16.2	26.60805	81.9022	3.73
	U	20	26.64585	81.88743	2.53
5	D	24.2	26.66452	81.85461	1.97
	U	26.9	26.68076	81.83474	2.03
6	D	30.2	26.69704	81.808	2.97
	U	34.4	26.70864	81.77011	4.38
7	D	37.1	26.71587	81.75259	3.83
	U	41.0	26.72397	81.71516	1.64

Zooplankton samples were collected monthly at each sampling site at night during a flood tide. Standard zooplankton collection gear consisted of a 500-micrometer Nitex mesh, 0.5-m mouth diameter, conical (3:1 aspect ratio) plankton net, equipped with a three-point bridle, 1-liter cod-end jar, 20 kilograms of weight suspended from the mouth ring, and a General Oceanics model 2030R flowmeter suspended at the center of the net's mouth. Deployment at each site consisted of a three-step oblique tow that divided fishing time equally between bottom, mid-depth, and surface waters. Tow duration was 5 minutes with tow speed estimated at 1.0–1.5 meters per second. Net position in the water column was regulated using a gunwale-mounted winch with metered tow line. Flowmeter readings were recorded before and after deployment to calculate the volume of water filtered during each tow.

Data Analysis

Longitudinal variations in the volume of the CRE were determined using interpolated bathymetry data and hypsometric assessment of distance downstream versus cumulative volume (similar to Buzzelli et al. 2013b). Bathymetry data are available by request from SFWMD. The volume of water contained in each 1-km segment of the estuary from S-79 to Shell Point was calculated.

Organisms captured were identified to the lowest practical taxon. Quality control and assurance procedures are described in Tolley et al. (2010). For each sampling event, the density-weighted COA (rkm_U) within the sampling space was calculated following Peebles et al. (2007) and Peebles and Greenwood (2009). The density weighted COA was calculated using **Equation 8**:

$$rkm_U = \sum (\mathrm{km} \cdot \mathrm{U}) / \sum \mathrm{U} \quad (8)$$

where U is the organism density (number per cubic meter [#/m^3]) at a station and *rkm* is the distance (km) of the station from Shell Point. $\sum$ U is the sum of organism density across all stations for each sampling date. For each sampling date, the quantity (km · U) is calculated for each station. These are summed and divided by $\sum$ U. rkm_U was correlated with freshwater discharge (Q) at S-79 averaged over the 1 to 120 days prior to sampling. A linear regression of rkm_U on transformed freshwater inflow (ln(Q+1)) was computed for the "lagged inflow" with the highest correlation coefficient (Tolley et al 2010). Inflows were calculated for lags of 60 days or less as these were considered most likely to be achievable through management of inflows at S-79. Inflows were averaged over 0, 3, 7, 14, 18, 20, 21, 30, 45, and 60 days prior to sampling.

Taxa used for the evaluation of impingement and habitat compression were selected from Tolley et al (2010). Tolley et al (2010) calculated regressions relating the location of the COA to natural log transformed freshwater inflow at S-79 for over 60 taxa (see Table 3.7.1.1 in Tolley et al. 2010). The 11 marine species with intercepts occurring furthest upstream (COA when inflow was 0 cfs) were evaluated for impingement and habitat compression (**Table 13**). Based on the regression equations (see Table 3.7.1.1 in Tolley et al. 2010), the calculated positions of these 11 species when inflow was 0.0 cfs was 67.3 km upstream of Shell Point or 24 km upstream of S-79. These responses made them good candidates to experience habitat compression and impingement. Because of their high relative abundance and importance in the food web (Tolley et al. 2010), adult (*Anchoa mitchilli*) and juvenile (*Anchoa spp*.) anchovies were also included in the analysis.

Table 13. List of organisms evaluated for potential habitat compression and impingement on S-79.

Taxon	Type
Clytia spp.	jellyfish
Lironeca spp.	isopod
Edotia triloba	isopod
Bowmaniella brasilliensis	mysid
Americamysis almyra adults	mysid
Americamysis spp. juveniles	mysid
Psuedodiaptomus pelgicus	copepod
Gobiosoma spp. postflexion larvae	fish
Menidia spp. preflexion larvae	fish
Gobiidae preflexion larvae	fish
Microgobius spp. postflexion larvae	fish
Anchoa mitchilli adult	fish
Anchoa mitchilli juveniles	fish

Potential habitat compression and impingement on S-79 were investigated using the spatial abundance quantile approach outlined by Peebles and Greenwood (2009). This approach utilizes the locations of the 10^{th} and 90^{th} deciles of cumulative abundance to assess impingement and habitat compression. Abundance, represented as organism density (#/m^3), was summed for each monthly survey to produce a total monthly value. Monthly density at individual stations was then summed sequentially in the upstream direction, and the resulting sums were expressed as a percentage of total monthly density. This process is analogous to creating a cumulative distribution curve or function, except that it sums

sequential density values from successive stations along a transect instead of summing data-class frequencies. The location (rkm) of the 10th (the lower decile) and 90th percentiles (the upper decile) of total monthly density were interpolated linearly. These linear interpolations were always made between the station with the highest percentile < 10 or < 90 and the next station upstream. The inter-decile range (IDR) is the distance in river km between the locations of the 10th and 90th abundance deciles. Monthly surveys were excluded from this analysis if > 10% of the catch was encountered at the downstream-most station, or if there were fewer than three stations with non-zero densities (Peebles and Greenwood 2009).

We tested the hypothesis that habitat volume decreases as the COA translates upstream (habitat compression). For each taxon investigated, the relationship between rkm_U and the two deciles was modeled using linear least squares regression (Peebles and Greenwood 2009). The positions of the 10th and 90th deciles were calculated for a series of rkm_U ranging from river km 15 to river km 40. In addition, the IDR was also calculated. For each rkm_U, the volume of water available for occupation (habitat volume) was calculated by combining estimates of estuarine segment volumes with the IDR. The segments containing the location of the upper and lower deciles were determined and the volumes of these and intervening segments summed to estimate the volume of water available for occupation. For each taxon investigated, this procedure yielded a series of rkm_U and potential habitat volumes occupied by 80% of the cumulative catch. This approach was used to determine if habitat volume decreases as rkm_U translates upstream or whether this decrease was offset by increased dispersion as measured by the IDR (Peebles and Greenwood 2009).

Impingement was assessed by examining the location of the upper abundance percentile (90th percentile) as a function of lagged freshwater inflow at S-79. Inflows were calculated for lags of 60 days or less as these were considered most likely to be achievable through management of inflows at S-79. Inflows were averaged over 0, 3, 7, 14, 18, 20, 21, 30, 45, and 60 days prior to sampling. For organisms whose location in the estuary moves upstream as freshwater inflow declines, impingement was indicated if a threshold inflow was reached at which the position of the 90th abundance decile ceases to change upon further reduction in inflow. Conversely, as inflows increased above this threshold impingement was relieved and the position of the 90th abundance decile moved downstream. This threshold inflow was determined by a change point analysis using the SAS NLIN procedure as described by Schwarz (2013). A conditional regression approach is employed (**Figure 26**):

$$\text{If } Y < CP \text{ then } Y = b; \text{ otherwise } Y = b + m\,(X - CP) \quad (9)$$

where Y is the location of the 90th decile in the estuary, X is lagged inflow, CP is change point or threshold inflow, b is the constant or river km where position of the 90th decile becomes independent of inflow, and m is slope or the rate at which the position of the 90th decile changes as inflows increase above the threshold.

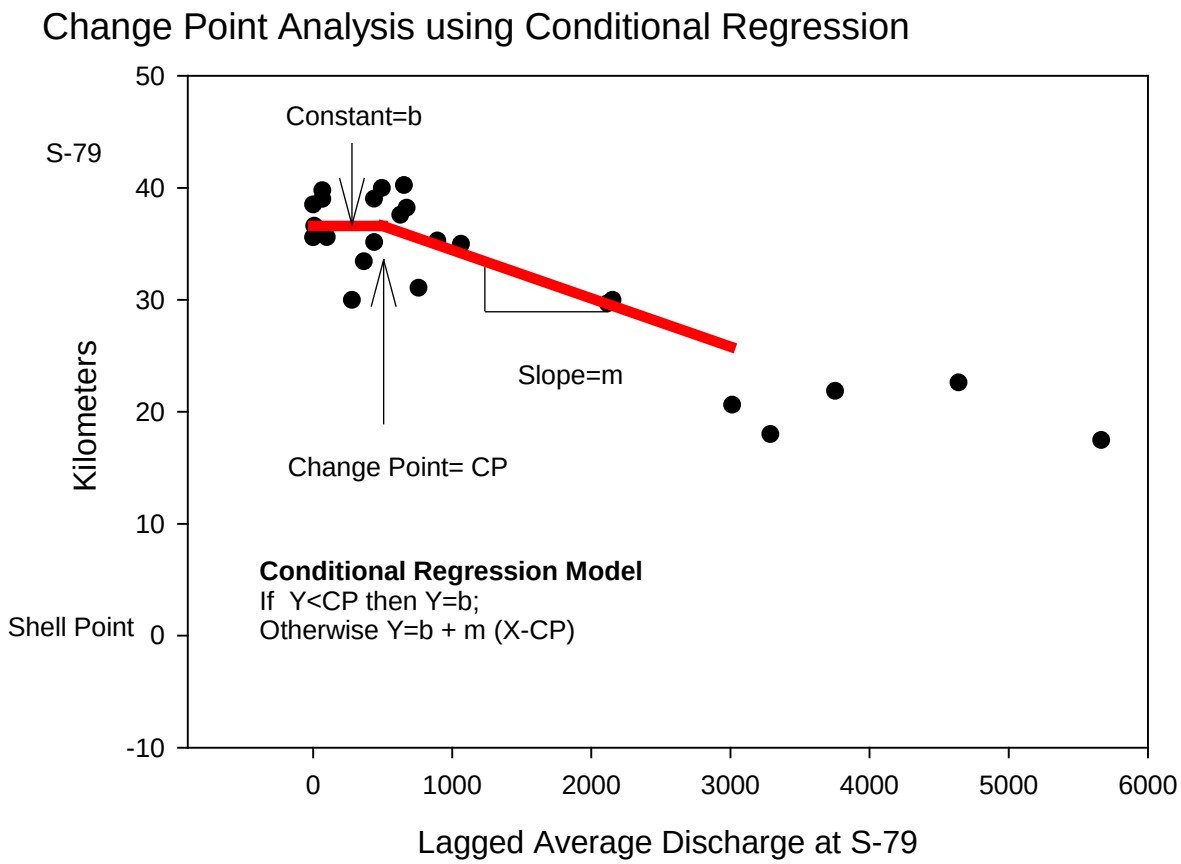

Figure 26. Change point analysis using conditional regression. The Y-axis is the position of the 90th abundance decile in the CRE. The x-axis is discharge averaged over a number of days before sampling, which ranged between 0 and 60.

Results and Discussion

Volume of 1-km increments ranged from 5.0 x 10^5 m^3 to 1.3 x 10^7 m^3 along the longitudinal gradient of the CRE (**Figure 27**). Volume was greatest ~2 to 3 km and 14 to 16 km upstream of Shell Point. There is a major constriction and reduction in the volume of individual segments upstream of about kilometer 30 (Beautiful Island).

The COA's for the 13 taxa investigated migrated downstream and upstream as freshwater inflow increased and decreased, respectively (**Table 14**). This response was revealed by the negative slope in regression relationships. Freshwater inflow at S-79 explained from 15% to 50% of the variability in location of the COA's of the various taxa. Most taxa responded to inflows averaged over 45 or 60 days. This agrees with a previous analysis of the data by Tolley et al. (2010) that found most taxa responding to inflows averaged over ~50 days. For twelve of the thirteen taxa, COA's were sometimes located upstream of river km 30, in the narrow region of the estuary where habitat volume is greatly reduced indicating the potential for both habitat compression and impingement (**Figure 28**). Inflows at S-79, required to locate the COA of each taxon at river km 30, ranged from 6.6 cfs to 1,362 cfs, and averaged (± standard deviation) 259 ± 378 cfs among the 13 taxa. The median was 128 cfs with 25th and 75th percentiles of 29.7 and 289 cfs, respectively.

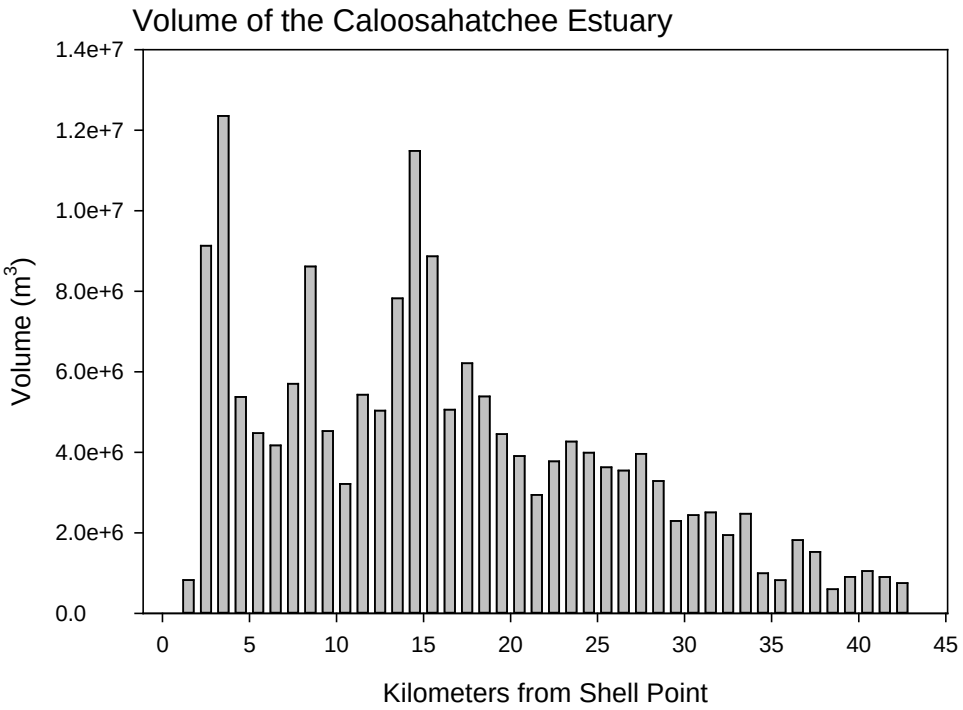

Figure 27. Volume of the CRE in 1-km increments, Shell Point (0 km) to the S-79 (43 km).

Table 14. Regression relationships between freshwater inflow at S-79 (x) and the location of the COA (rkmU; y) in the sampling space. n is the number of observations, a is the intercept, b is the slope, p is the level of statistical significance, and r^2 is the coefficient of determination. Days are the number of days prior to each sampling date that inflow (Q) was averaged. In general regression equations were of the form *rkmU* = a – b (ln(Q+1)) except where noted. Also given is the inflow required to locate the COA at 30 km upstream of Shell Point where volume of the estuary begins to increase.

Taxon	n	a	b	p	r^2	Days	30 km (cfs)
Lironeca spp.	24	36.73	-3.31	0.001	0.43	14	6.6
Edotia triloba	24	47.31	-3.89	0.001	0.41	45	85.0
Bowmaniensis brasilliensis	24	44.76	-4.31	0.002	0.36	45	29.7
Americamysis almyra adults	24	49.90	-3.51	0.002	0.35	45	288.9
Americamysis spp. juveniles	24	46.72	-3.44	0.004	0.32	45	128.1
Psuedodiapotomus pelagicus	22	44.10	-5.37	0.001	0.46	60	12.8
Gobiosoma spp. postflexion larvae	20	51.85	-5.91	0.008	0.33	60	39.4
Microgobius spp. postflexion larvae	17	71.82	-7.88	0.001	0.54	60	200.8
Gobiidae preflexion larvae	24	45.72	-5.21	0.001	0.36	60	19.5
Menidia spp. preflexion larvae	17	76.31	-7.36	0.005	0.38	60	540.8
Anchoa mitchilli adults [a]	24	3.50	0.00	0.002	0.34	14	518.4
Anchoa spp. juveniles [b]	24	31.88	0.00	0.065	0.15	3	1,362.3

a. $\ln(rkm_U) = a - b(Q)$
b. $rkm_U = a - b(Q)$

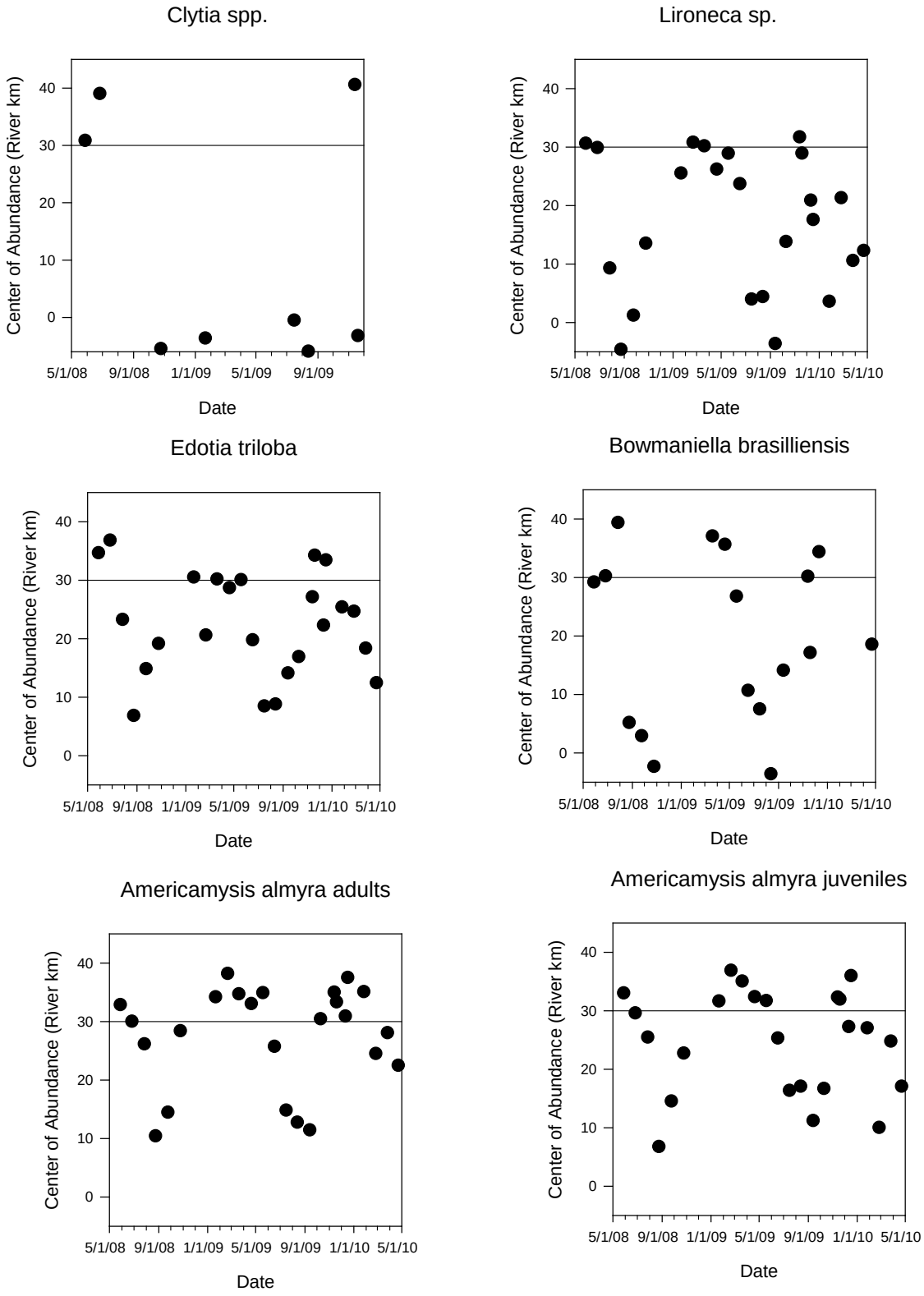

Figure 28. COA for various taxa during the study period. Upstream of the reference line at 30 km, habitat volume is reduced.

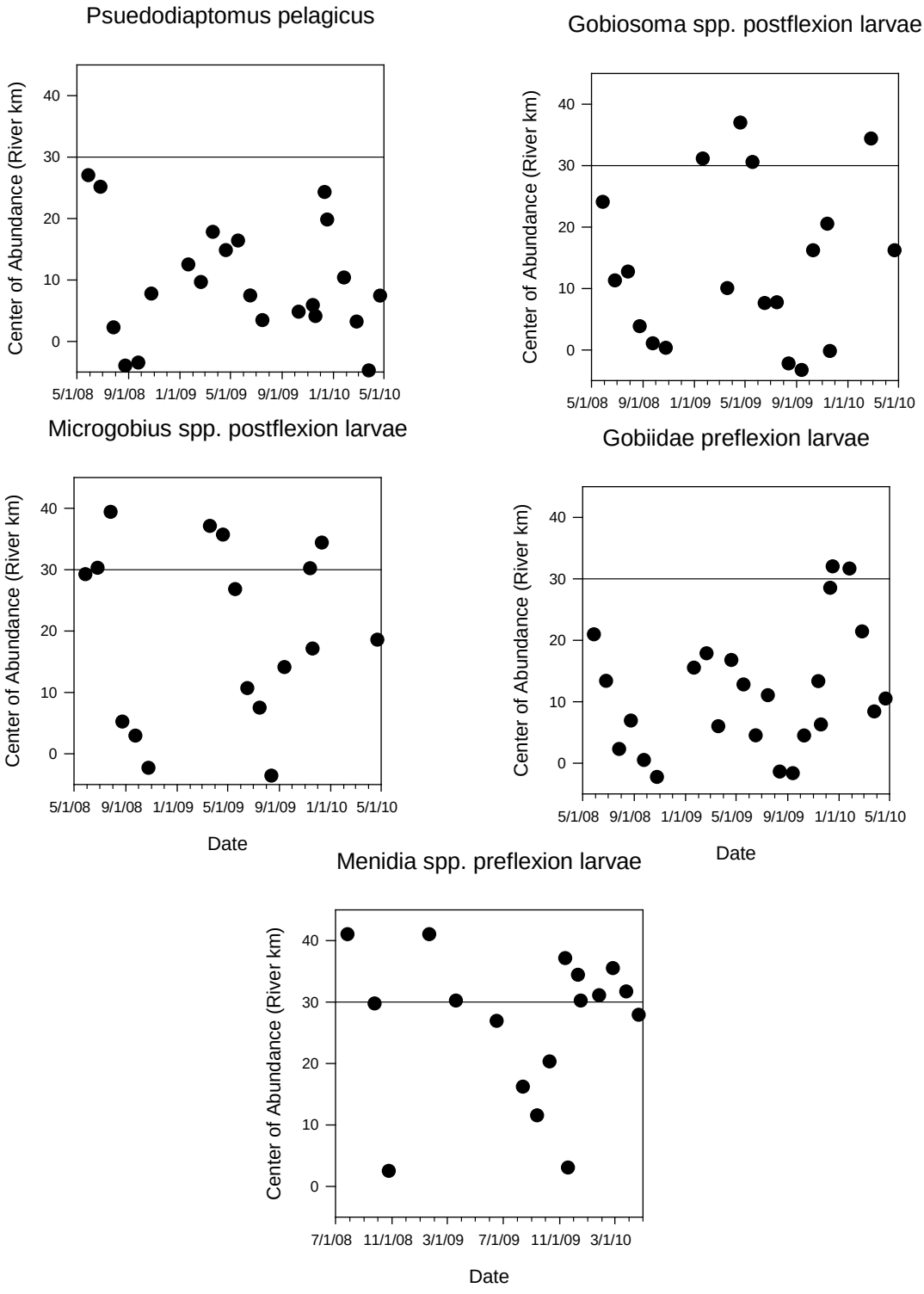

Figure 28. Continued.

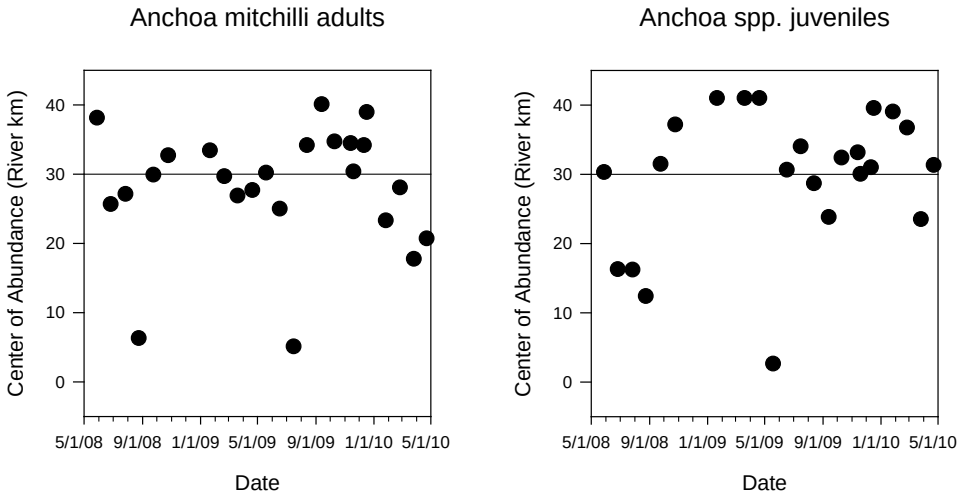

Figure 28. Continued.

In general, the positions of the 10th and 90th abundance deciles were linearly related to the location of rkm_U the distance-weighted COA (see regressions in **Table 15**). For *Menidia*, the 10th abundance decile was unrelated to rkm_U so its average position (12.9 km) was employed in calculations of habitat volume. The same situation obtained for *Gobiidae preflexion* larvae but the average position of the 10th decile was -2.3 km and outside the domain of the volume calculations. Neither decile was related to rkm_U for Clytia. Habitat volumes were not calculated for these latter two taxa.

Table 15. Linear regression relationships between the distance-weighted COA (x) and the location (river km) of the 10th (KM_10) and 90th (KM_90) abundance deciles (y). n is the number of observations, a is the intercept, b is the slope, and r^2 is the coefficient of determination. All regression were statistically significant at $p < 0.05$ except where noted (ns = not significant and * denotes $p < 0.10$).

Taxon	n	KM_10			KM_90		
		a	b	r^2	a	b	r^2
Clytia spp.	3			ns			ns
Lironeca spp.	16	-5.12	0.417	0.276	3.167	1.155	0.902
Edotia triloba	24	-4.27	0.81	0.759	0.7899	1.163	0.877
Bowmaniensis brasilliensis	23	-4.95	0.625	0.655	4.022	1.115	0.811
Americamysis almyra adults	24	-12.32	1.07	0.796	11.48	0.764	0.828
Americamysis spp. juveniles	24	-12.57	1.04	0.695	15.58	0.669	0.637
Psuedodiapotomus pelagicus	14	-5.73	0.681	0.604	1.099	1.026	0.762
Gobiosoma spp. postflexion larvae	10	-10.3	0.733	0.686	17.17	0.759	0.466
Microgobius spp. postflexion larvae	6	-9.05	0.739	0.554*	4.69	1.05	0.856
Gobiidae preflexion larvae	15			ns	19.8	0.71	0.461
Menidia spp. preflexion larvae	4			ns	4.64	1.05	0.958
Anchoa mitchilli -adults	17	-13.34	1.018	0.489	13.8	0.732	0.833
Anchoa spp. -juveniles	17	-3.38	0.588	0.223	27.3	0.347	0.681

Habitat compression due to translation of rkm_U upstream was assessed graphically (**Figure 29**). Mysids (*Americamysis, Bowmaniella*) exhibited both a shrinking habitat volume and a contracting IDR as rkm_U progressed upstream. For these species, a change in the habitat volume curve was evident between rkm_U of 25 and 30. By contrast, for the isopods (*Lironeca* and *Edotia*) and the copepod (*Pseudodiaptomus*), habitat volume showed curvature. For *Edotia* and *Pseudodiaptomus*, peak habitat volumes occurred when the COA was ~20 km and decreased further upstream despite monotonic expansion of the IDR (**Figure 29**). For *Lironeca* habitat, volume remained fairly constant to about 30 km where it began to decline with further upstream translation of the COA (**Figure 29**). The fish taxa exhibited various patterns. Like the mysids, both habitat volume and the IDR decreased as rkm_U moved upstream for the two *Anchoa* groups. The habitat volumes occupied by *Gobiosoma* and *Microgobius* decreased despite an increasing IDR. For both of these species, there is a distinct increase in the slope of the habitat volume curve at an rkm_U of 30 km.

It is noteworthy that taxa exhibiting downward curvature in their habitat volume plots also had monotonically increasing IDRs (*Gobiosoma*, *Microgobius*, *Lironeca*, *Edotia*, and *Psuedodiaptomus*). Such curvature may indicate that at least over part of the range examined (15 to 40 km) increases in dispersion compensated for loss of volume associated with upstream translation of the population. *Menidia* was the only taxon where both habitat volume and the IDR increased as rkm_U translated upstream. Increases in dispersion offset decreases in volume associated with geomorphology. The habitat volume plot was also curved indicating a progressive decline in the rate of increase. This decline in the rate of increase may have resulted from the interplay between a constant rate of IDR expansion and an increasing rate of decline in habitat volume associated with the funnel shape of the estuary. The incremental increases in IDR in the upper estuary were less effective at offsetting decreases in habitat volume than in the lower estuary.

The conditional regression model used to evaluate impingement yielded a statistically significant demonstration of impingement for all taxa examined except *Psuedodiaptomus pelagicus* (copepod), *Clytia* (jellyfish), and *Menidia* spp. preflexion larvae. This result does not imply the absence of impingement for these two taxa, but more likely reflects the small number of observations that could be used in the analysis of deciles. The model explained between 40 and 89% of the variation in location of the 90th decile for the remaining taxa. Lagged inflows averaged 22.5 days and ranged between 3 and 60 days (**Table 16**). Impingement was evident following change point analysis of *Americamysis almyra* (adults) and *Edotia triloba* (**Figure 29**).

Of the three parameters in the conditional regression model, estimates of threshold inflow had large errors compared to estimates of the constant and slope. In most cases, the 95% confidence intervals bracketing the threshold inflow overlapped zero. Thus, for any one taxon, the river kilometer at which impingement occurs, where position of the 90th decile becomes independent of inflow, was estimated more robustly then the threshold inflow at which impingement begins to occur.

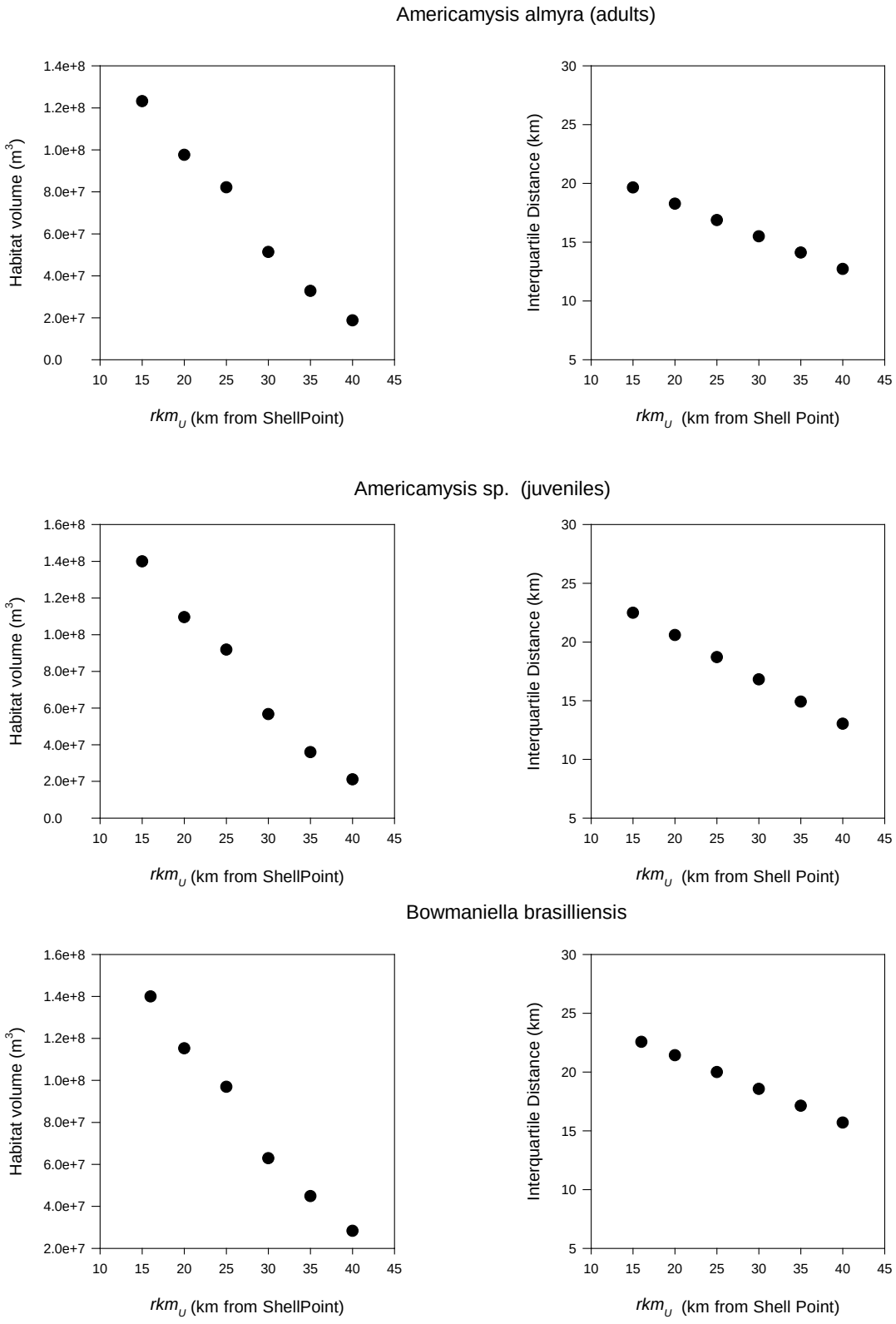

Figure 29. Potential habitat volume as a function of the position of rkm_U (left) for different taxa. IDR as a function of the position of rkm_U (right).

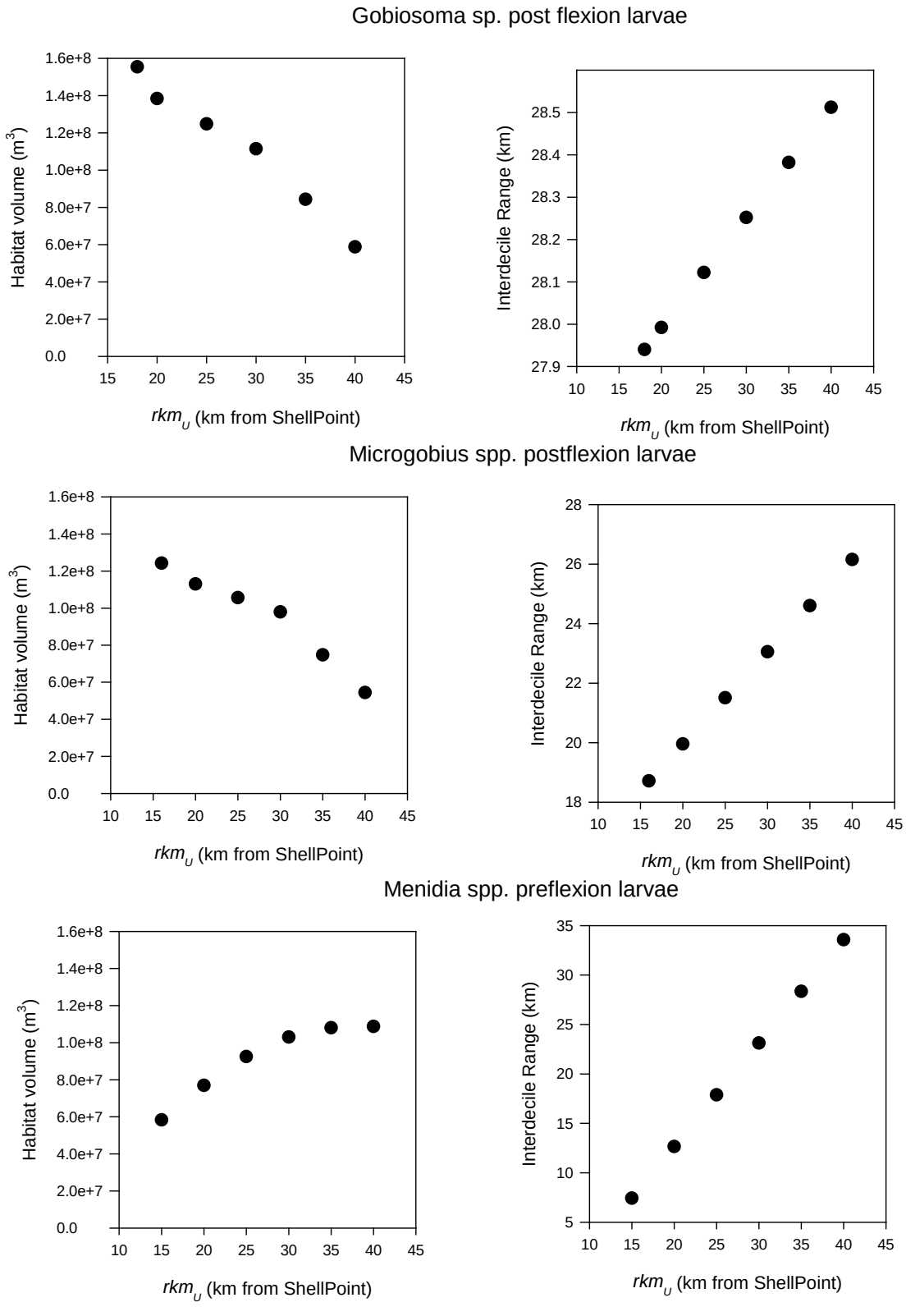

Figure 29. Continued.

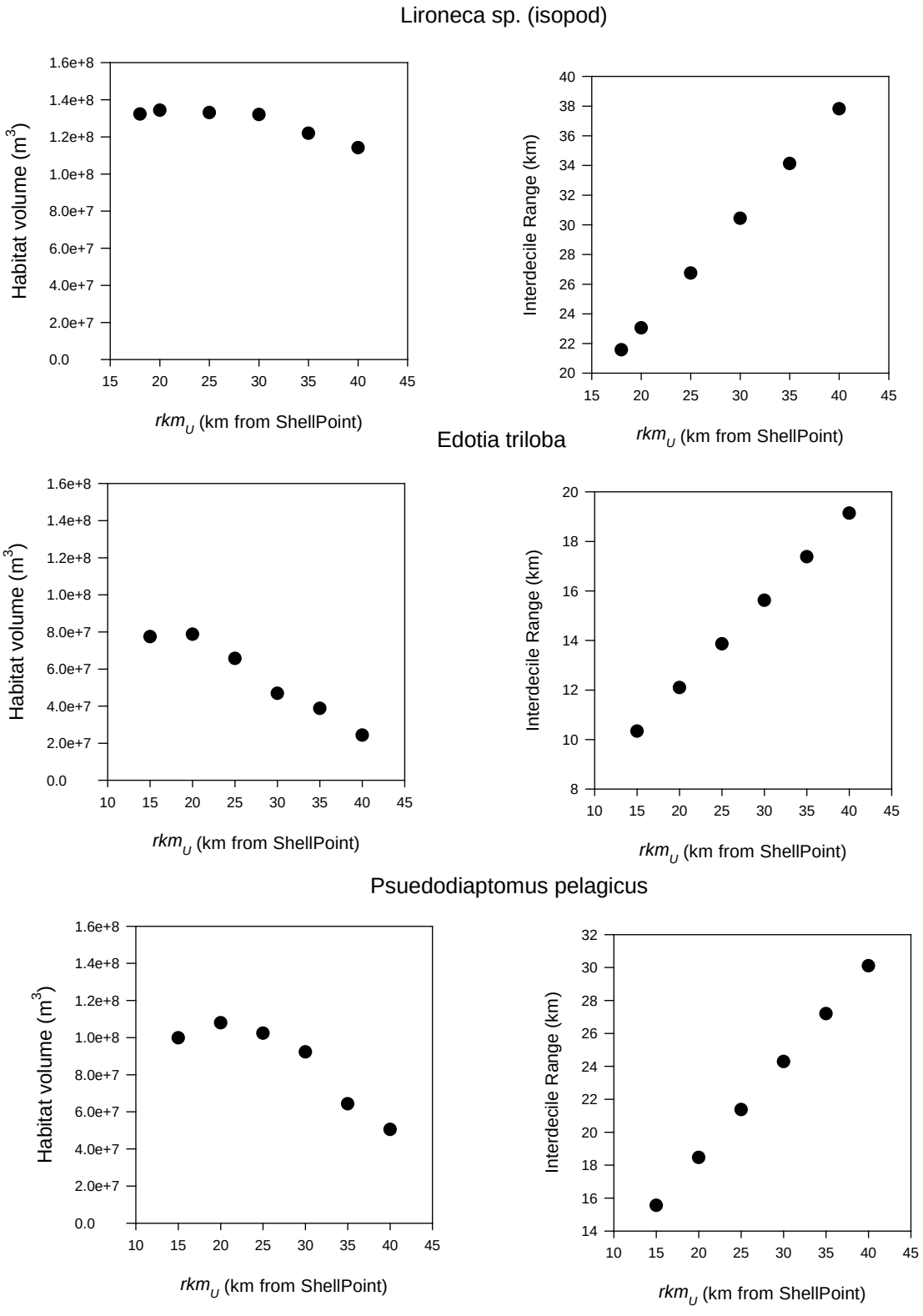

Figure 29. Continued.

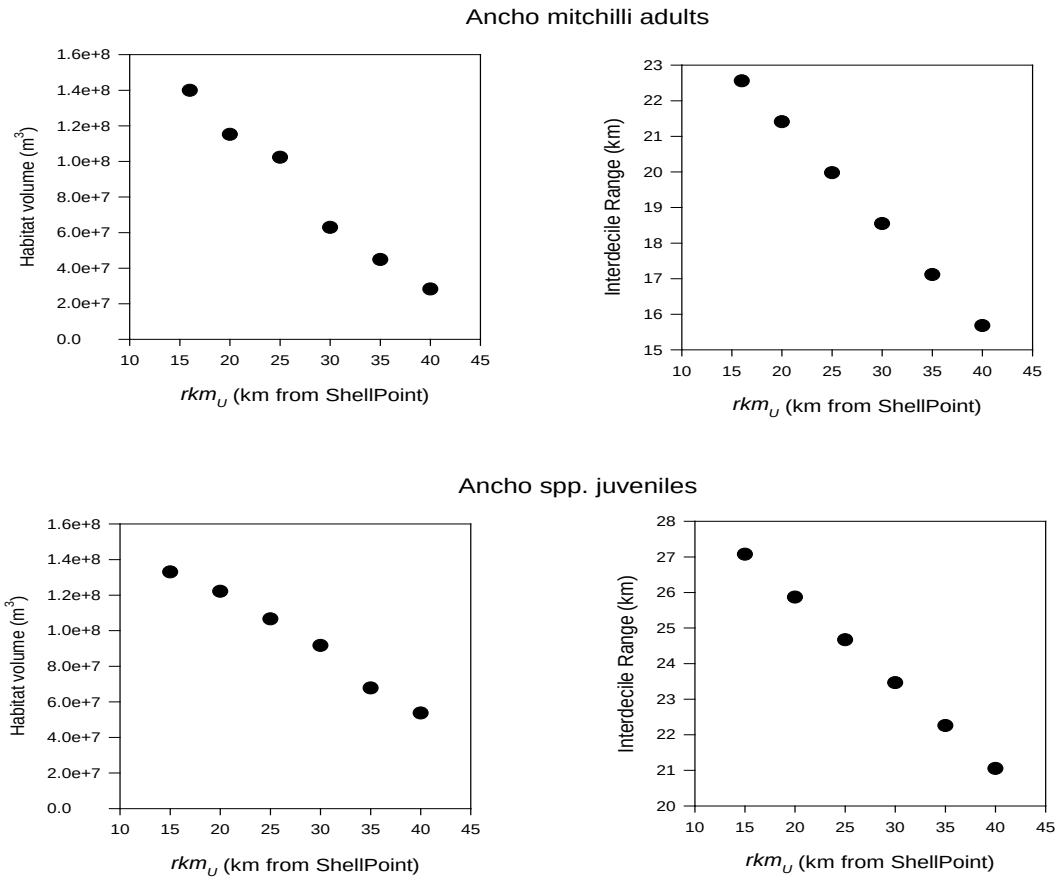

Figure 29. Continued.

Estimates of threshold inflows for the two *Anchoa mitchilli* groups and Godiidae preflexion larvae were an order of magnitude higher than for other taxa. According to the equations given in Tolley et al (2010), inflows of these magnitudes (2,200–4,200 cfs over 7–30 days) would position the COA for most marine zooplankton far downstream. Results for these taxa were not considered further. Despite the substantial error surrounding any single estimate of threshold inflow, the estimates for the remaining seven taxa were fairly consistent with a mean of 412 cfs (± 40%), a median of 476 cfs and a range of 97.9–565.6 cfs (**Table 16**). The location at which impingement occurred averaged 34.5 km upstream of Shell Point or about 8 km downstream of S-79.

Impingement was possible if inflow ranged and averaged 98–566 cfs and 412 ± 165 cfs, respectively. Inflows at which habitat compression occurred were less obvious. We do know that the volume of the estuary becomes very much smaller in the narrow region upstream of about river km 30. Almost all taxa investigated (except *Menidia*) experienced habitat compression if the COA was upstream of this point. This position in the river was associated with a clear increase in the rate of habitat compression (*Lironeca*, *Gobiosoma*, and *Microgobius*) or a distinct change in the habitat compression curve (e.g. *Americamysis* and *Bowmaniella;* **Figure 29**). Inflows associated with an rkm_U of 30 are 125 to 290 based on the median and 75th percentile and about 250 cfs based on the mean (**Table 14**).

Table 16. Results of change point analysis to evaluate impingement on the Franklin Lock and Dam (S-79). Constant is the river km where the location of the 90th abundance quantile stops changing as inflows decrease, indicating impingement. CP is the inflow at which the 90th decile begins to move downstream as inflow increases. U and L indicate upper and lower limits of the 95% confidence interval. Decile data for *A. mitchilli* adults were natural log transformed for the analysis. Results for Anchoa and Gobiidae not included in calculation of means and standard deviations.

Taxon	n	Days	Constant (km)	95%L	95%U	CP (cfs)	95%L	95%U	beta2	Standard Error	R^2
Clytia spp.	3										
Menidia spp.	4										
Psuedodiaptomus pelagicus	20										
Anchoa mitchilli adults (ln)	17	18	35.51	33.44	37.71	4277.0	4178	4377	-0.0026	0.0294	0.639
Anchoa mitchilli juveniles	19	7	37.79	36.1	39.5	3826.5	-1167	8820	-0.0017	0.000810	0.407
Gobiidae preflexion larvae	15	30	33.36	30.4	36.35	2219.7	-180	4620	-0.0189	0.0227	0.611
Lironeca spp.	16	3	32.18	24.5	39.86	476.3	-1323	2275	-0.0065	0.00188	0.516
Edotia triloba	24	60	31.8	25.7	38	452.1	-1286	2190	-0.0053	0.00168	0.404
Bowmaniella brasilliensis	23	14	29.13	23.3	34.91	512.2	-1041	2065	-0.0064	0.00197	0.454
Americamysis almyra adults	24	14	36.6	34.5	38.7	500.2	-322	1322	-0.0043	0.000572	0.805
Americamysis juveniles	24	14	36	33.5	38.5	565.6	-423	1554	-0.0042	0.000684	0.731
Gobiosoma postflexion larvae	10	45	37.6	23	52.2	97.9	-2615	2811	-0.0058	0.00109	0.783
Microgobius postflexion	6	20	38.1	28.6	47.6	280.2	-1763	2323	-0.0089	0.00209	0.895
			34.49			412.07					
			3.43			164.92					

Addendum to Component Study 4

Gelatinous Predators and Habitat Compression

At least two physical attributes of the CRE may influence the effects of freshwater discharge on zooplankton: its shape and the dam at its head. Despite the alterations that have been made to the CRE, its geomorphology reflects the typical funnel shape of a drowned river valley. The Franklin Lock and Dam separates the freshwater Caloosahatchee River from the downstream estuary. The COA of many estuarine plankters has been shown to move downstream as river flows increase and upstream as they decrease (Peebles et al. 2007). At low flows, some organisms will become concentrated in the narrow region of the estuary located more than 30 km upstream of Shell Point. At even lower flows, their upstream progress may be blocked and organisms will be impinged on the lock and dam (S-79) located about 43 km upstream of Shell Point (Peebles and Greenwood 2009). The crowding of organisms in a relatively confined space, termed habitat compression (Crowder 1986, Copp 1992, Eby and Crowder 2002) may result in increased predation and competition for limited food resources. In addition, some organisms may be forced to utilize habitat that is physiologically suboptimal and this may result in lower growth and survival (see Petersen 2003).

The purpose of this analysis was to evaluate the potential for overlap between gelatinous predations and potential prey in the narrow region of the estuary upstream of km 30 where habitat compression might occur. Examination of Table 3.7.1.1 in Tolley et al (2010) revealed that for all but one of the 61 taxa examined, the COA moved downstream as discharge increased. Time lags (number of consecutive days prior to sampling used to calculated mean inflow) associated with the responses were variable, but most taxa (92%) responded to inflows averaged over periods of < 2 months, and 32% of the responses corresponded to flows averaged over 6 to 8 weeks. In contrast, the COA for the tanaidacean, *Hargeria rapax*, progressed upstream as flows increased.

At low freshwater inflows, the COA for several taxa occurred (see **Table 17** below) in the narrow portion of the upper CRE (> 30 km upstream of Shell Point and < 13 km downstream of S-79). As discussed earlier, this is a region of potential habitat compression where competition and predation may be increased. The presence of two gelatinous (jelly fish) predators, *Clytia* and *Mnemiopsis*, in this region (**Table 17**) supports the increased predation hypothesis.

Relationships between the location of the COA and freshwater inflow for taxa that occurred upstream of km 30 and, therefore, were likely to experience habitat compression are summarized in **Table 17**. These relationships have been extracted verbatim from Table 3.7.1.1 in Tolley et al. (2010). The predatory jellyfish, *Clytia*, occurs upstream of km 30 at discharges less than 175 cfs. The comb jelly, *Mnemiopsis*, reaches this location at a discharge of 9 cfs. Habitat compression is unlikely to increase the chances of predation by *Mnemiopsis* except at very low discharges. While habitat compression may still occur for many species, flows greater than 175 cfs should keep the COA of *Clytia* out of the narrow area upstream of km 30, reducing the risk of increased predation.

Table 17. Response COA (*kmU*) to freshwater inflow using natural-log transformed inflow values for inflow data recorded at S-79. Regression statistics are sample size (*n*), intercept, slope and coefficient of determination r^2 as %. Days is the number of consecutive daily inflow values used to calculate mean inflow. All regressions are significant at $p < 0.04$. The last columns give the calculated discharge at S-79 necessary to position a given taxa 30 km upstream of Shell Point (or 13 km downstream of S-79) at Stations 5D and 5U, respectively.

Taxon	n	Intercept	Slope	r^2	Days		KM 30 (cfs)
Microgobius spp. postflexion larvae	17	79.3	-8.81	63	55		269
Lironeca sp. (isopod)	24	69.99	-7.84	56	51		164
Gobiosoma spp. postflexion larvae	20	62.12	-7.22	41	57		86
Bowmaniella brasiliensis	24	65.56	-7.2	64	50		140
Pseudodiaptomus pelagicus	22	55.3	-6.9	69	57		39
Menidia spp. preflexion larvae	17	75.09	-6.81	57	67		751
Edotia triloba (isopod)	24	65.25	-6.33	65	51		262
Gobiidae preflexion larvae	24	51.73	-5.94	44	59		39
Americamysis almyra	24	63.51	-5.35	49	51		525
Americamysis spp. juveniles	24	59.76	-5.22	48	50		299
Cumaceans	24	37.13	-4.04	66	48		6
Gobiidae flexion larvae	23	39.45	-4.31	20	66		9
Syngnathus louisianae juveniles	12	37.21	-3.96	53	1		6
Microgobius spp. flexion larvae	18	43	-3.59	26	80		37
Tinectes maculatus postflexion larvae	12	33.48	-2.87	49	2		3
Anchoa mitchilli adult	24	40.01	-1.82	16	17		245
Argulu sp. Branchiuran	16	42.19	-2.39	18	92		164
Median		**55.30**	**-5.35**		**51**		**140**
75%					**59**		**262**
Average					**50**		**179**
Clytia sp.	8	96.03	-12.78	79	50		175
Mnemiopsis spp.	8	35.53	-2.53	88	1		9

Component Study 5: Ichthyoplankton Response to Freshwater Inflow in the Caloosahatchee River Estuary

Cassondra Thomas, Christopher Buzzelli and Peter Doering

Abstract

Ichthyoplankton communities are key components of food webs in the upper, oligohaline reaches of most estuaries. This study analyzed historical (1986–1989) data to evaluate effects of salinity and freshwater inflow on ichthyoplankton communities in the CRE. Abundance of ichthyoplankton was greatest when the 30-day inflows at S-79 averaged between 151 and 600 cfs. Juvenile fish appeared to prefer salinities < 10 and their abundance was centered just downstream of Station 2 near Beautiful Island. Flows at S-79 associated with a salinity of 10 near Beautiful Island averaged 237.5+ 255.5 cfs. Flows less than this could result in loss of favorable habitat.

Introduction

Ichthyoplankton (e.g. larval fishes and fish eggs) are a relatively small but vital component of total zooplankton in estuaries (Able 2005, Sutherland et al. 2012). They feed on smaller plankton and serve as a food source for larger animals. Because they swim poorly or not at all they are sensitive to freshwater inflow (Gillson 2011). Ichthyoplankton assemblages can indicate the status and reproductive potential of adult fish populations in estuaries. This means that when fish such as anchovies and sardines are spawning, ichthyoplankton samples can provide a relative index of population size.

It is important to understand the factors that influence fish populations in small, subtropical estuaries with managed freshwater inflow like the CRE in Southwest Florida (Stevens et al. 2013). Freshwater discharge influences ichthyoplankton location within an estuary and habitat overlap predators (Gillson 2011, Tolley et al. 2012). Additionally, the plankton food sources for fish and decapod larvae (phytoplankton and zooplankton) are also directly impacted by freshwater inflow in the CRE (Chamberlain et al. 2003).

The objective of this research component was to assess the associations between freshwater inflow and ichthyoplankton abundance and community structure in the CRE. Ichthyoplankton data collected between 1986 and 1989 were used in this assessment.

Methods

Nocturnal samples were collected monthly from 1986 to 1989 at six stations within the CRE (**Figure 30**). Paired 0.5-millimeter conical zooplankton nets with a 505-micrometer mesh were towed obliquely with a flowmeter (meter per second) affixed to one net opening (square meter [m^2]) to measure the water volume sampled (cubic meters per second). In the laboratory, the samples were sorted to the lowest possible taxonomic level and quantified. They were then grouped into the following categories for analysis: total, eggs, post-yolk sac larval, juvenile, by family, eggs by family, crab, and shrimp. Crabs and shrimp data were included in total ichthyoplankton abundance but not life stage data presentation. Life stage categories were based on Hubbs (1943).

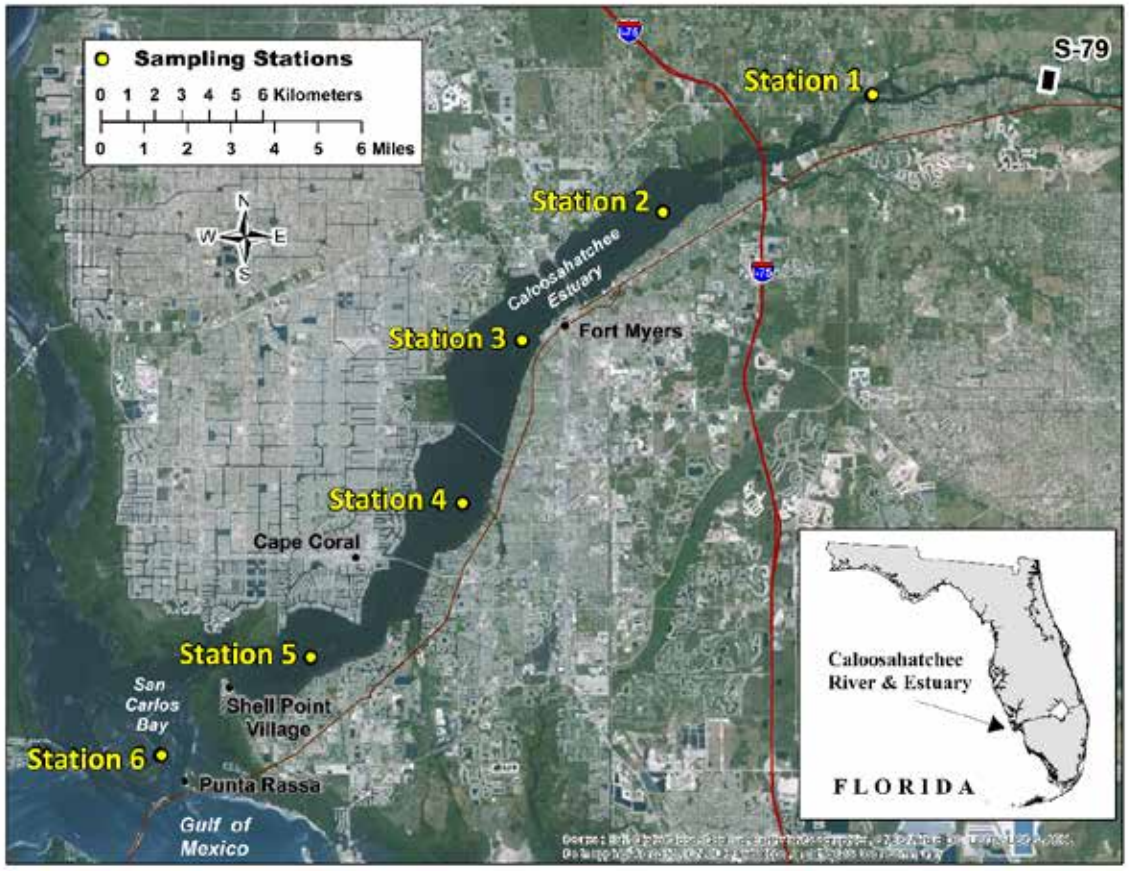

Figure 30. Map of ichthyoplankton sampling stations from 1986 to 1989 in the CRE.

Freshwater inflow volume to the CRE was measured daily at S-79. Salinity values at each station were predicted using an auto-regressive approach that combined hydrodynamic and time series modeling (Qiu and Wan 2013). Salinities were averaged over 1-, 5-, 7-, 14-, 21-, and 30-day periods prior to the day of sampling. Freshwater inflow was averaged over the same temporal series and grouped into several categories: (1) 0–150 cfs, (2) 151–300 cfs, (3) 301–600 cfs, (4) 601–1,200 cfs, (5) 1,201–2,500 cfs, and (6) > 2,500 cfs following Chamberlain et al. (2003). Due to infrequent sampling events in the second inflow category when averaged over 30 days, Categories 2 and 3 were combined.

The salinity envelop was assessed using the running median of abundance at different salinities. A running median is a smoothing technique that was used to determine the median value of abundance for a particular salinity, and then the median was graphed over all salinities in the data set. This approach removes the influence of outliers and is appropriate when the distribution around the mean is not normal.

Untransformed data were evaluated a priori using principle components analysis and pairwise correlations. Additional statistical analyses included one- and two-way analysis of variance (ANOVA), analysis of covariance (ANCOVA), and nonlinear regressions were performed on log(x+1) transformed abundance data. Tukey's honestly significant difference was used to determine differences between groups. Essential independent variables included sampling station, month, season (dry season is November–April; wet

season is May–October), and freshwater inflow category. Interactions detected in two-way ANOVAs were assessed for "clumping" of results (i.e. upper estuary versus lower estuary; lower inflows versus higher inflows; and continuous months). In addition, ANCOVAs were run to test for significance of slope and intercept.

The COA was calculated following Peebles et al. (2007) and Peebles and Greenwood (2009) using **Equation 10**:

$$rkm_U = \Sigma(\text{km} * \text{U})/\Sigma\ \text{U} \quad (10)$$

where U is the organism's density (#/m^3) at a station and rkm is the distance (km) of the station from the S-79 structure. ΣU is the sum of organism density across all stations for each sampling date. For each sampling date, the quantity (km * U) is calculated for each station. These are summed and divided by ΣU.

Results and Discussion

Total ichthyoplankton abundance most closely correlated to 30-day average inflow and salinity ($p = 0.0002$ and $p < 0.0001$, respectively). Abundance was highest at Stations 5 and 6 ($p < 0.0001$, one-way ANOVA) favoring a more marine ichthyoplankton assemblage (**Figure 31**). Abundances were greatest when inflows ranged from 151 to 600 cfs ($p < 0.0001$, one-way ANOVA) and declined with increasing freshwater discharge (**Figure 32**). There were no seasonal signals for total ichthyoplankton or individual taxa.

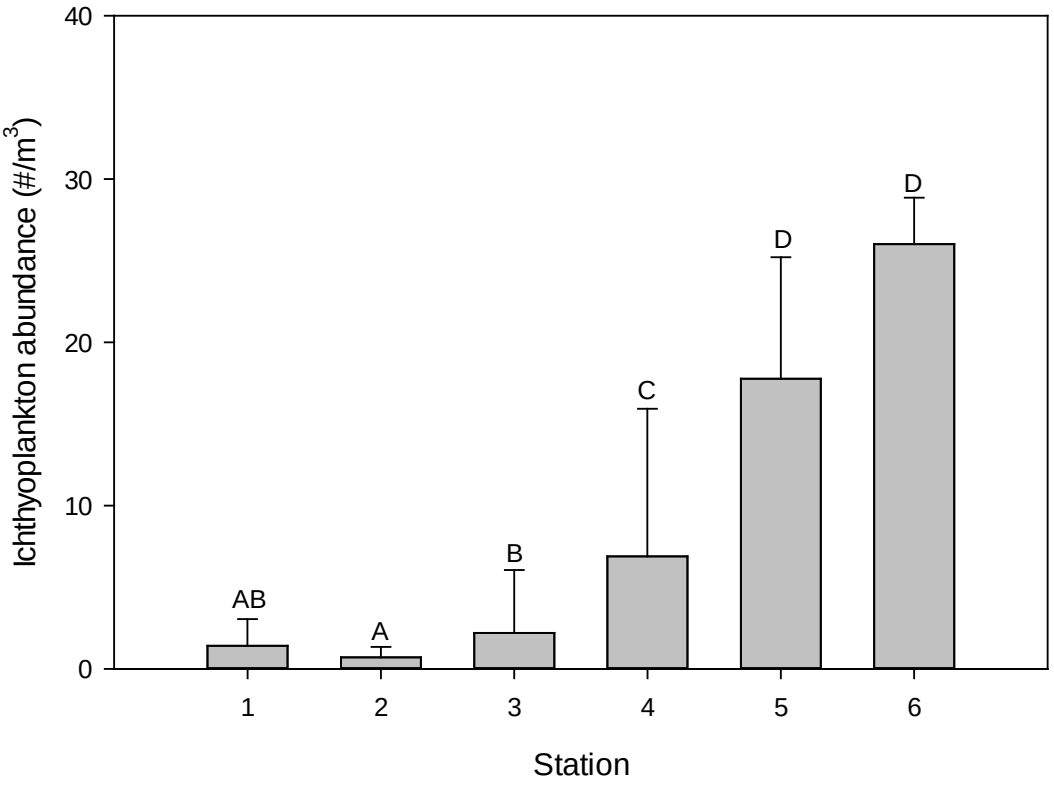

Figure 31. Ichthyoplankton abundance (number per cubic meter [#/m^3]) across stations. Bars with the same letters are not significantly different ($p > 0.05$). Data were retransformed from log(x+1) transformed analysis.

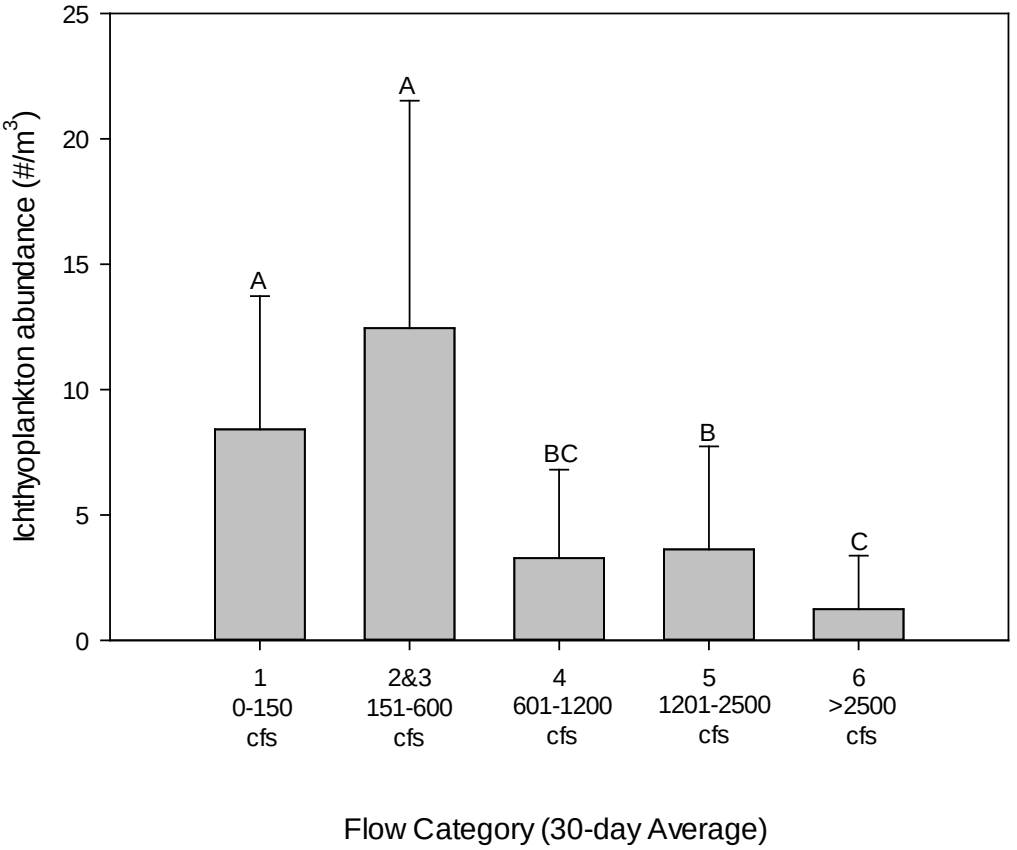

Figure 32. Ichthyoplankton abundance (number per cubic meter [#/m³]) under different inflow regimes (1 = 0–150 cfs; 2 and 3 = 151–600 cfs; 4 = 601–1,200 cfs; 5 = 1,201–2,500 cfs; 6 > 2,500 cfs) (1986–1989 study). Bars with the same letters are not significantly different ($p > 0.05$). Data were retransformed from log(x+1) transformed analysis.

Although eggs and post-yolk sac larva were primarily located in the lower estuary at high abundances, juvenile fishes were located in the upper estuary regardless of month (**Figure 33**). This assemblage was dominated by *Anchoa mitchilli* (bay anchovy), which Kimura et al. (2000) noted disperse up-estuary in the Chesapeake Bay to seek lower salinities if the timing of recruitment occurs when salinities are > 18 in the lower estuary. It was likely that those remaining in the downstream estuary did not successfully recruit to the juvenile stage. Thus, the upper estuary is an important nursery for juvenile fish.

Most juvenile fish were found associated with salinities ranging from 0 to 10 (**Figure 34**). Juvenile fish were most abundant in the upper and mid-estuary. The COA of the juvenile fish ranged from 7 to 30 km downstream of S-79 and averaged 18.9 km (just downstream of Station 2) (**Figure 35**). Using the density-weighted salinity (S_U) as a covariate, higher inflows result in the COA being located further downstream ($p < 0.0001$, ANCOVA model, $p < 0.0001$ intercept, $p = 0.9024$ slope; **Figure 35**). These regressions can be used to locate the COA over a range of 30-day average salinity values for particular flow classes. For example, the COA ranged from 7 to 20 km downstream when the S-79 inflow rate was < 600 cfs (lowest flow categories). This result suggested that hydrodynamics were important to the location of the COA, and that juvenile fish location could serve as an indicator for freshwater inflow.

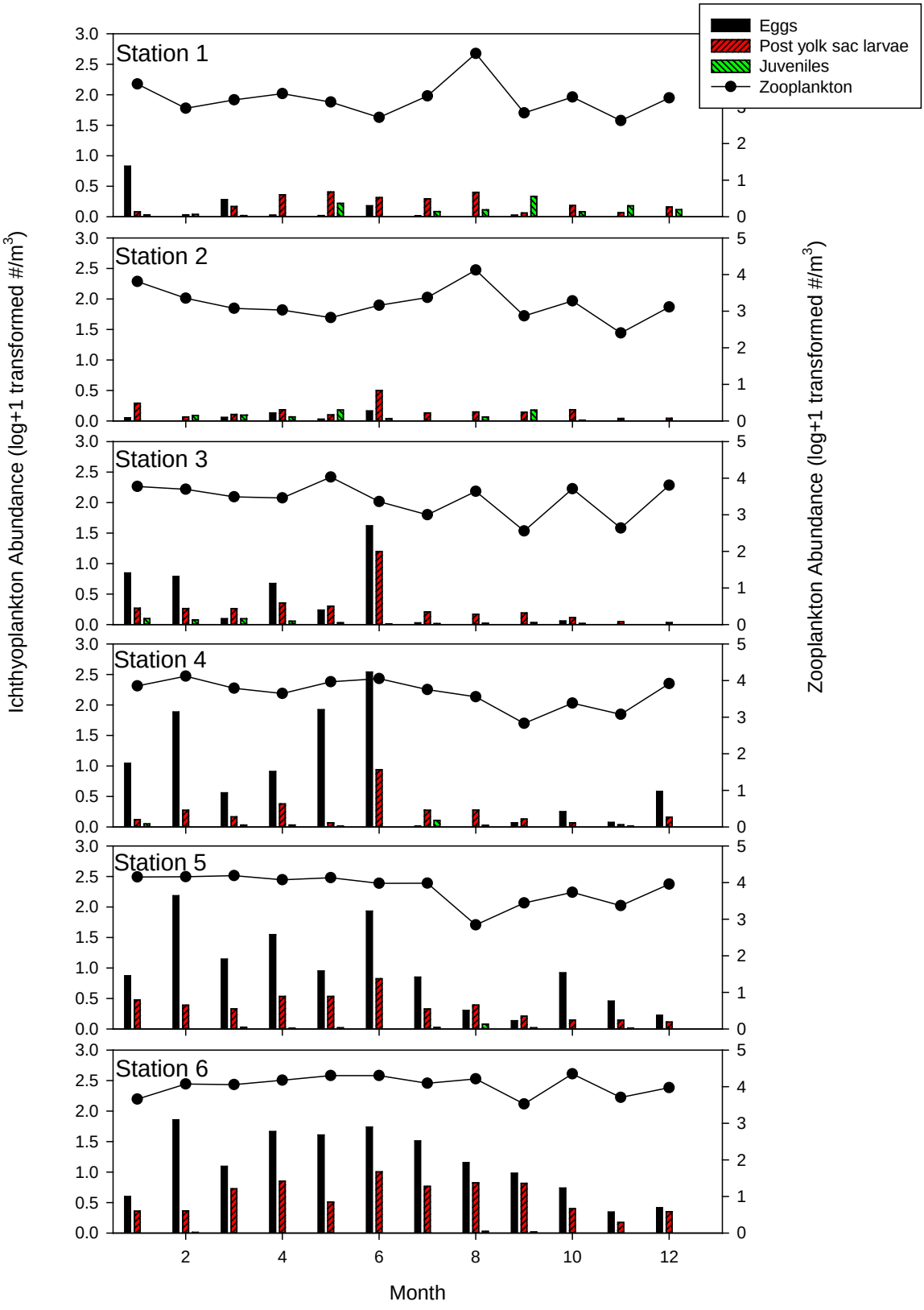

Figure 33. Ichthyoplankton abundance of different life stages at each station over different months compared to abundance of zooplankton (1986–1989 study).

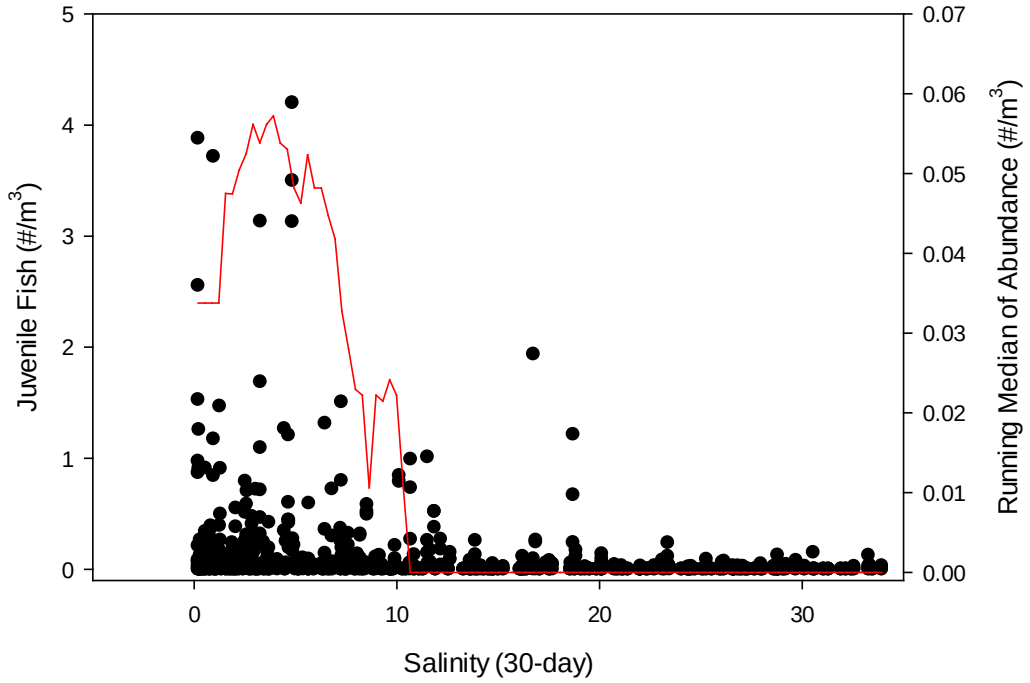

Figure 34. Juvenile fish abundance (number per cubic meter [#/m^3]) relative to 30-day average salinity and the running median of abundance (right axis; red line) to establish a salinity envelope of preference.

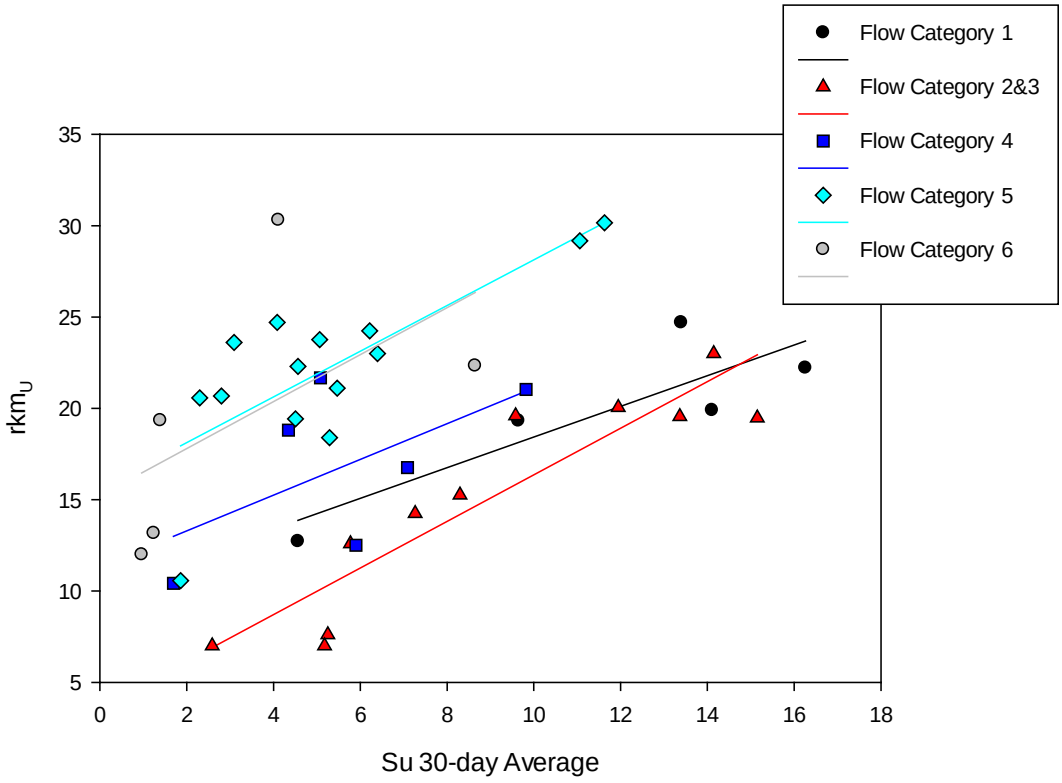

Figure 35. COA for juvenile fish compared to density-weighted salinity at different inflow regimes (1 = 0–150 cfs; 2 and 3 = 151–600 cfs; 4 = 601–1,200 cfs; 5 = 1,201–2,500 cfs; 6 > 2,500 cfs) (1986–1989 study).

Juvenile fish were most frequently found in salinities ranging from 4 to 6 with frequency of occurrence declining at salinities that were > 10 (**Figure 36**). Given that the juvenile fish prefer salinity value < 10 and had an average COA just downstream of Station 2, potential habitat loss was assessed by determining the flow at which salinity exceeded 10 at Station 2. Out of the five years of study, there were 11 months where the 30-day average salinity was > 10 at Station 2. The 30-day average inflows associated with these salinity values ranged from 12.3 to 1,357 cfs and averaged 237.5 ± 255.5 cfs. Inflow rates less than this average are likely to result in habitat loss for juvenile fish as the fish need to move upstream toward the S-79 structure to seek their preferred salinity range.

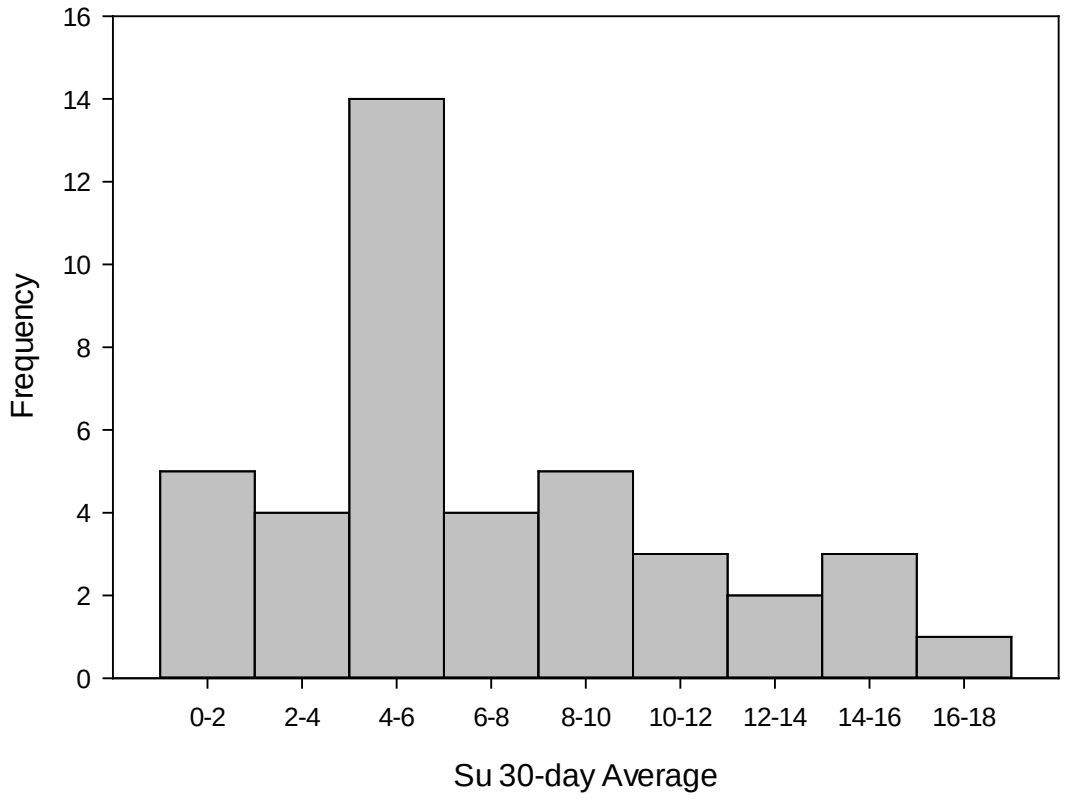

Figure 36. Frequency distribution of density-weighted salinity for juvenile fish.

Component Study 6: Summary and Interpretation of Macrobenthic Community Properties Relative to Salinity and Inflow in the CRE

Christopher Buzzelli

Abstract

The composition, distribution, and density of benthic invertebrate communities (macrofauna) can be used as indicators of salinity and inflow for estuaries. The goal of this study component was to explore the relationships between inflow, salinity, and benthic macrofauna in the CRE. Benthic samples were collected every 2 to 4 months at seven stations during two periods (February 1986–April 1989 and October 1994–December 1995). The abundance, diversity, and composition of the macrofaunal community were determined relative to observed fluctuations in salinity. Four distinct zones emerged based on salinity ranges and the composition of the macrobenthic community. Conditions conducive to maintain the characteristic community observed during the sampling periods in the most upstream zone (salinity = 0 to 4 and 0 to 7 km from S-79) occurred on 54% of dry season days from 1993 to 2012. The indicator inflows (Q_I) ranged from 0 to 3,720 cfs and averaged 501 ± 525 cfs for the days where salinity was 3 to 4 (n = 181).

Introduction

Alterations to the quality, quantity, timing, and distribution of inflows are extremely important to the health and function of an estuary (Montagna et al. 2013). Within the CRE, changes in freshwater inflows have altered salinity regimes and the ecology of the estuary (Chamberlain and Doering 1998a, Barnes 2005). Changes in freshwater inflows and salinity have been shown to change the distribution and dynamics of many taxa and communities in the CRE including submersed vegetation (Doering et al. 2001, 2002, Lauer et al. 2011), oysters and dermo disease (La Peyre et al. 2003, Barnes et al. 2007, Volety et al. 2009), fauna inhabiting oyster reefs (Tolley et al. 2005, 2006), and fishes (Collins et al. 2008, Heupel and Simpfendorfer 2008, Stevens et al. 2010, Simpfendorfer et al. 2011, Poulakis et al. 2013).

Benthic organisms are ideal biological indicators of changes in water quality because they have limited mobility, long lifespans relative to plankton, and sensitivity to changes in water and sediment quality (Montagna et al. 2013). Many studies have used benthic communities as indicators of freshwater inflow and estuarine status (for a summary see Montagna et al. 2013). Macrobenthic communities have been used as indicators in Rincon Bayou, Texas (Montagna et al. 2002b) and other Texas estuaries (Palmer et al. 2011), Southwest Florida (Montagna et al. 2008, Palmer et al. 2011), and the St. Johns River Estuary in northeastern Florida (Mattson et al. 2012).

The goal of this research component was to explore the relationships between freshwater inflow, salinity patterns, and the distribution, density, and composition of benthic macrofaunal communities in the CRE (Montagna and Palmer 2014). This assessment was based on a more comprehensive analysis of macrofaunal communities and salinity patterns in the CRE (Montagna and Palmer 2014). Specifically, this effort emphasized the potential effects of reduced dry season inflow on salinity patterns in the upper CRE.

Methods

The study was designed by Robert Chamberlain, SFWMD, to investigate benthic macrofauna distributions as a function of salinity and to compare variability between dry (November–April) and wet (May–October) seasons. Benthic samples were collected at seven stations (B1–B7; **Figure 37A**) during two periods: from February 1986 to April 1989 (Period 1) and from October 1994 to December 1995 (Period 2). Sampling occurred every two months at Stations 1 through 6 and every four months at Station 7 during Period 1. Four stations (2, 4, 5, and 6) were sampled in Period 2 for 12 of 15 months. The environmental conditions were different between the two sampling periods. While relatively low inflow rates characterized Period 1, extremely high inflow rates occurred during Period 2.

Benthic samples were collected using a Wildco® petite ponar grab (0.02323 m^2). Five replicates were collected at each station within a 30–50-m diameter. The sediment at each station consisted of predominantly sand and shell hash. Samples were sieved in the field on a 500–micrometer screen, preserved in formalin buffered by Epsom salt, and stained with Rose Bengal. Invertebrates were separated from the sieved substrate by either SFWMD (Period 1) or Mote Marine Laboratory (Period 2) and stored in ethanol. Staff from Mote Marine Lab identified the dominant taxa (95% of organisms) to the species level and the remaining taxa to genera or higher taxa groups.

Salinity values along the length of the CRE from 1980 to 2000 were estimated using a time series modeling technique that accounted for spatial distribution of salinity in the estuary and driving factors such as freshwater inflows, rainfall, and tide (Qiu and Wan 2013). This model output has been calibrated to local salinities and uses a linear reservoir model to simulate Tidal Basin flows (Wan and Konyha 2015).

Macrofaunal diversity was calculated using Hill's N1 diversity index because it has units of number of dominant species (Hill 1973). Differences in macrofauna characteristics among stations were tested on two subsets of the data because the sampling design was uneven. The first subset included all seven stations for ten months in Period 1 (dry season only). The second subset included four stations (2, 4, 5, and 6) across all months (except November 1987) and encompassed both sampling periods. Differences in macrofauna characteristics among stations were determined using two-way ANOVA with station and month-year as treatments. A linear contrast was added to the ANOVA on the second subset (four stations and all dates) to test for differences among sampling periods. Post-hoc Tukey tests were run to test for differences among stations and station-period interactions.

Macrofaunal community structure was analyzed using non-metric multi-dimensional scaling (MDS) using a Bray-Curtis similarity matrix among stations to create a MDS plot (Clarke 1993, Clarke and Warwick 2001). Relationships within each MDS were highlighted through cluster analysis using the group average method. Significant differences between each cluster were tested with the SIMPROF permutation procedure with a significance level of 5% ($p = 0.05$). Where stations were sampled in both time periods, differences in community structure and species assemblages between periods and among zones were tested using ANOSIM and SIMPER in Primer (Clarke 1993). Data were $\log_e(x + 1)$ transformed prior to multivariate analysis to decrease the effect of numerically dominant species on community composition (Clarke and Gorley 2006). This information was used to help characterize salinity zones for the CRE in both dry and wet seasons.

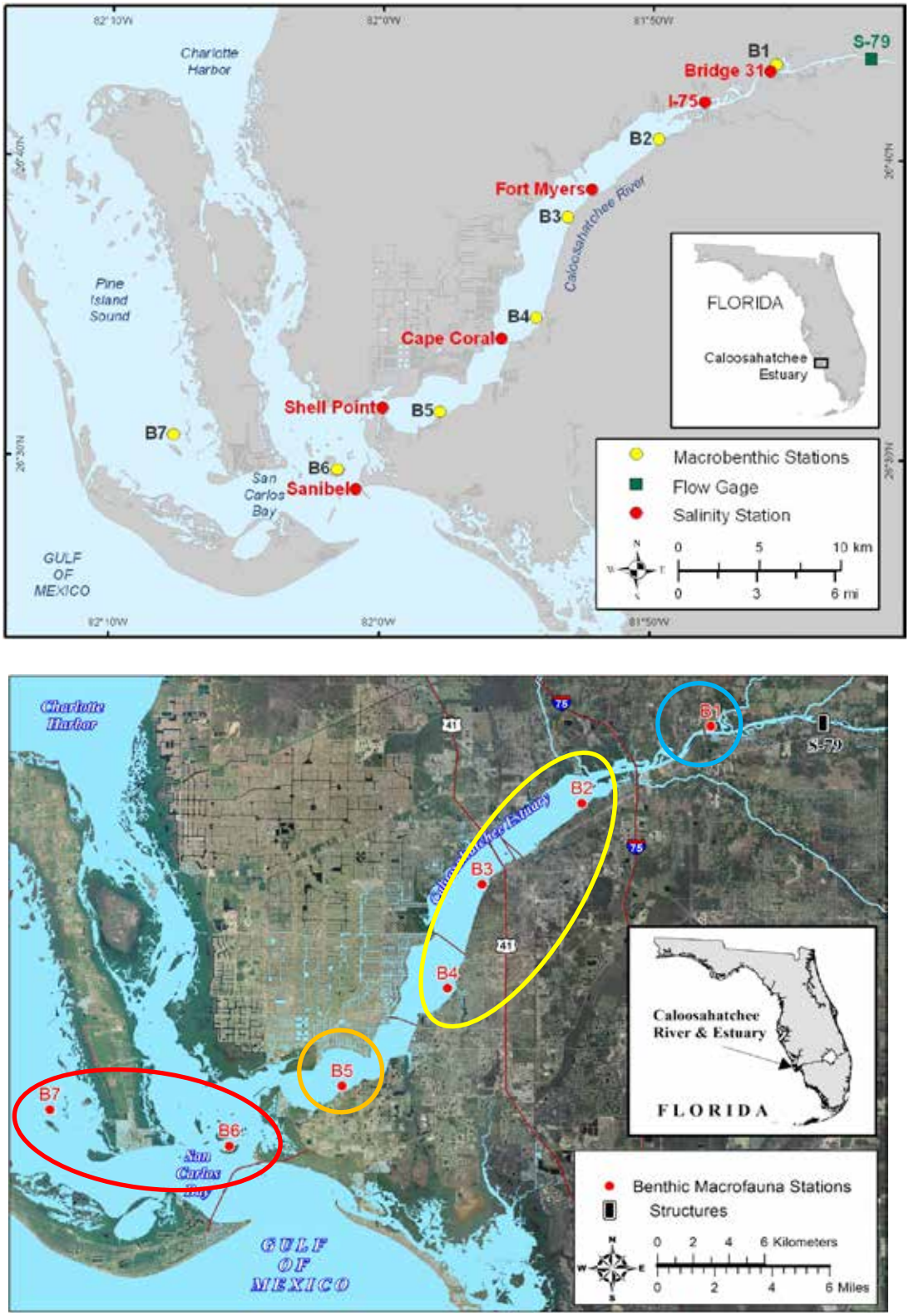

Figure 37. (**A**) Location map for macrobenthic sampling in the CRE. Included are sampling macrobenthic stations (B1 through B7; yellow), the long-term salinity stations (red), and the upstream location of freshwater inflow (S-79; green). (**B**) Map of the CRE with the macrobenthic sampling stations (B1 through B7; red) and four estuarine zones determined in this study.

The benthic community in the uppermost CRE (0–7 km from S-79) should be most sensitive to reduced freshwater inflow. Salinity responds quickly to changes in discharge in this part of the estuary. Changes in the number of low salinity species indicate a change in hydrologic conditions. The MDS analysis provided a target salinity range of 0–4 for the macrobenthic communities in the upper CRE (Montagna and Palmer 2014). Thus, salinities > 4 may lead to changes in the oligohaline benthic community.

Long-term salinity data collected at Bridge 31 (BR31) in the upper CRE was used to assess estuarine conditions for macrofauna communities in the most upstream portion of the estuary (**Figure 37A**). Average daily salinity at this location from January 22, 1992, to August 16, 2012, was merged with average daily freshwater inflow at S-79. These data were categorized by water year and season (dry versus wet) with analyses focused on the dry season days throughout the period of record (POR). The number and percentage of dry season days where salinity values ranged from 0 to 1, 1 to 2, 2 to 3, and 3 to 4, and > 4 were calculated along with the averages and standard deviations for salinity and freshwater inflow associated with each of these salinity classes. The freshwater inflows on the days where salinity was assumed to be the highest level tolerated by the expected macrofauna species (salinity = 3 to 4) were queried from the data set. The range and average and standard deviation of associated freshwater inflows were calculated from these selected days.

Results and Discussion

There was clear zonation of benthic communities along the salinity gradient in the CRE (**Figure 37B**). This zonation was evident when comparing N1 diversity and multivariate community structure of the communities along the length of the CRE. The positive relationship between salinity and diversity on a spatial salinity gradient is common in many estuaries due to the increasing abundance of marine species in downstream locations (Whitfield et al. 2012).

In the current study, 34 taxa were identified as being indicators of salinity (**Table 18**). Two taxa served as indicators of limnetic conditions (salinity < 0.5), 6 taxa indicated oligohaline conditions (salinity 0.5 to 5), 11 indicated mesohaline conditions (salinity 5 to 18), 10 indicated polyhaline conditions (salinity 18 to 30), and 5 provided an indication of euhaline conditions (salinity 30 to 40) according to the Venice salinity classification system (**Table 18**; Anon 1958, Cowardin et al. 1979).

Table 18. Summary of dominant macrobenthic taxa and relationship with salinity in the CRE (Montagna and Palmer 2014).

Taxa Name	Higher Taxa Group[1]	Lower Taxa Group[2]	Parameters					p Value
			a (Peak Abundance)	b (Skewness)	c (Salinity)			
					Estimate	90% Low	90% High	
Ceratopogonidae sp.	Insecta	Diptera	29	3.93	0.0	-1.7	1.8	0.0364
Amphicteis floridus	Polychaeta	Ampharetidae	137	2.10	0.4	-0.3	1.0	< 0.0001
Edotia sp. 1	Crustacea	Isopoda	546	1.16	0.8	0.5	1.2	0.0008
Edotia spp.	Crustacea	Isopoda	253	1.53	1.0	0.2	1.7	0.0016
Tellina texana	Bivalvia	Veneroida	1139	-1.38	1.6	0.5	2.7	0.0002
Tubificidae w/o cap. setae	Clitellata	Oligochaeta	1034	1.94	1.9	0.6	3.2	< 0.0001
Neanthes succinea	Polychaeta	Nereididae	109	1.26	2.2	0.0	4.3	0.0131
Streblospio benedicti	Polychaeta	Spionidae	970	1.48	2.7	1.0	4.4	< 0.0001
Eteone heteropoda	Polychaeta	Phyllodocidae	128	0.68	5.2	3.2	7.2	0.0022
Assiminea succinea	Gastropoda	Neotaenioglossa	6.2×10^{10}	-0.04	5.9	5.1	6.8	< 0.0001
Mulinia lateralis	Bivalvia	Veneroida	1347	-0.65	6.8	0.6	13.0	0.0772
Tellina versicolor	Bivalvia	Veneroida	16711	-0.09	7.0	6.7	7.2	< 0.0001
Stylochus sp.	Platyhelminthes	Polycladida	51	0.77	8.8	5.7	11.8	< 0.0001
Tagelus plebeius	Bivalvia	Veneroida	57497727	-0.04	10.1	9.9	10.2	< 0.0001
Ischadium recurvum	Bivalvia	Mytiloida	1016692	0.05	10.1	9.7	10.5	< 0.0001
Lucina nassula	Bivalvia	Veneroida	36	-0.63	13.0	-3.1	29.1	0.0075
Ampelisca spp.	Crustacea	Amphipoda	3469	0.36	15.0	12.1	17.9	0.0003
Paraprionospio pinnata	Polychaeta	Spionidae	290	0.95	15.8	9.5	22.1	< 0.0001
Mysella sp. A	Bivalvia	Veneroida	1828	-0.04	17.0	16.7	17.4	0.0063
Odostomia sp.	Gastropoda	Heterostropha	220	0.11	20.4	19.9	21.0	0.0032

Table 18. Continued.

Taxa name	Higher Taxa group[1]	Lower Taxa Group[2]	Parameters					
			a (Peak Abundance)	b (Skewness)	c (Salinity)			
					Estimate	90% Low	90% High	p Value
Mysella planulata	Bivalvia	Veneroida	115	0.35	21.5	14.2	28.7	0.0302
Caecum pulchellum	Gastropoda	Neotaenioglossa	124	0.10	21.7	20.2	23.1	0.0067
Aglaophamus verrilli	Polychaeta	Nephtyidae	22	0.58	23.5	8.7	38.4	0.001
Phascolion strombus	Sipuncula	Golfingiiformes	119	0.15	24.8	22.7	26.9	0.0211
Listriella barnardi	Crustacea	Amphipoda	864	-0.04	26.0	24.1	27.2	0.0005
Parvilucina multilineata	Bivalvia	Veneroida	51	0.24	26.1	23.8	28.4	< 0.0001
Ampelisca sp. 3	Crustacea	Amphipoda	153	0.15	26.5	23.7	29.3	0.004
Sthenelais sp. A (or spp.)	Polychaeta	Sigalionidae	72	0.23	26.9	22.4	31.3	0.0015
Kalliapseudes sp. 1	Crustacea	Tanaidacea	188	0.12	27.6	26.4	28.9	0.0012
Schistomeringos rudolphi	Polychaeta	Dorvilleidae	103	0.03	30.1	29.7	30.4	0.0041
Spiochaetopterus oculatus	Polychaeta	Chaetopteridae	425	0.01	30.7	30.3	31.1	0.001
Molgula occidentalis	Ascidiacea	Pleurogona	519	-0.03	31.4	31.1	31.8	0.0006
Eusarsiella texana	Crustacea	Ostracoda	310	-0.03	31.6	31.2	32.1	< 0.0001
Grubeulepis mexicana	Polychaeta	Eulepethidae	110	0.04	32.1	31.8	32.5	0.027

While the Venice system is widely used to divide an estuary into salinity-based zones, it is not biologically relevant in all cases. It is often more practical to divide an estuary into several overlapping zones that are based on the abundances of organisms along a salinity gradient (Bulger et al. 1993). This study applied a combination of these two classification schemes to specify four zones to describe the distribution and composition of macrobenthic communities in the CRE (**Table 19**). These zones, based on dry season salinities, were designated Bulger Zone 1 (salinity of 0.2–4.2), oligohaline zone 2 (2.6–12.5), mesohaline zone 3 (15.1–24.9), and polyhaline zone 4 (28.0–34.7).

Table 19. Seasonal ranges for salinity zones in the CRE based on classifications provided by Bulger et al. 1993.

Zone	Dry	Wet
Bulger Zone 1	0.2–4.2	0.2–0.2
Oligohaline	2.6–12.5	0.2–3.1
Mesohaline	15.1–24.9	7.9–13.9
Polyhaline	28.0–34.7	21.0–30.5

Despite the loss of several macrobenthic species in high flow relative to low flow periods, the abundance of several mobile invertebrates and fish have been documented to decrease during low flow periods in Southwest Florida estuaries (Flannery et al. 2002). Mobile species with decreases during low flow periods include bay anchovy and sand seatrout juveniles, mysids, and grass shrimp. A previous study on fish and mobile aquatic invertebrates (blue crab [*Callinectes sapidus*] and pink shrimp [*Farfantepenaeus duorarum*]) separated the CRE into three zones, with the lower, middle and upper zones incorporating the reach of the benthic stations in the current study of stations 4 and 5, 2 and 3, and 1, respectively (Stevens et al. 2010).

Salinity observations at BR31 from WY1993–WY2012 provided a platform to explore long-term, dry season variations in inflow and salinity conditions in the Bulger Zone (0.2 to 4.2; **Table 20**; **Figure 38A**). Average dry season salinity varied from 0.3 (WY1995) to 13.3 (WY2001) averaging 4.5 ± 4.8 over all dry season days (n = 3,591). Periods of reduced salinity coincided with increased inflows in the dry seasons of WY1994–WY1996, WY1998, and WY2003–WY2006. The percentage of dry season days where salinity was within the desired range indicative of the Bulger Zone as defined for macrobenthic communities ranged from 0.0% (WY1997, WY2001, WY2007, and WY2008) to 96–99% (WY1995 and WY2003–WY2006; **Figure 38B**). Salinity was within the desired 0 to 4 range on ~54% of dry season days at BR31 with percentages of 38.7%, 5.8%, 4.6%, and 5.0% for the 0 to 1, 1 to 2, 2 to 3, and 3 to 4 salinity categories, respectively (**Table 20**). This means that salinity values were in excess of 4 on ~46% of the dry season days. The inflow rate ranged from 0 to 3,720 cfs and averaged 501 ± 525 cfs for the days where salinity was 3 to 4 (n = 181).

Benthic communities are not only indicators of a salinity gradient, but are part of the food chain for many mobile aquatic species. Providing sufficient inflows to the CRE promotes spatial salinity gradients that are favorable for a wide range of benthic and water column communities. Reduced dry season freshwater inflows can cause freshwater and low salinity species and habitats in the upper CRE to be lost or reduced in size as these

habitats are destroyed or relocated upstream (Chamberlain and Doering 1998a). Maintaining low salinity habitat is integral for at least part of the life cycle of mobile species such as *Callinectes sapidus* (blue crab), *Carcharhinus leucas* (bull shark), and *Pristis pectinata* (smalltooth sawfish; Hunt and Doering 2013) and many other species in the CRE (Stevens et al. 2010).

Table 20. The number and percentages of dry season days for average daily salinity values at BR31 over a series of salinity class criteria (0 to 1, 1 to 2, 2 to 3, 3 to 4, > 4, and all dry season days) from WY1993 to WY2012.

Salinity Class	Number	Percentage (%)	Salinity	Inflow S-79 (cfs)	
			Avg ± SD	Range	Avg ± SD
0 to 1	1,388	38.7	0.3 ± 0.2	0 to 15,700	3,074 ± 2,777
1 to 2	208	5.8	1.5 ± 0.3	0 to 6,990	782 ± 980
2 to 3	165	4.6	2.5 ± 0.3	0 to 4,260	596 ± 782
3 to 4	181	5.0	3.5 ± 0.3	0 to 3,720	501 ± 525
>4	1,649	45.9	9.0 ± 3.6	0 to 4,410	239 ± 465
All Dry Season Days	3,591	100.0	4.5 ± 4.8	0 to 15,700	1,366 ± 2,201

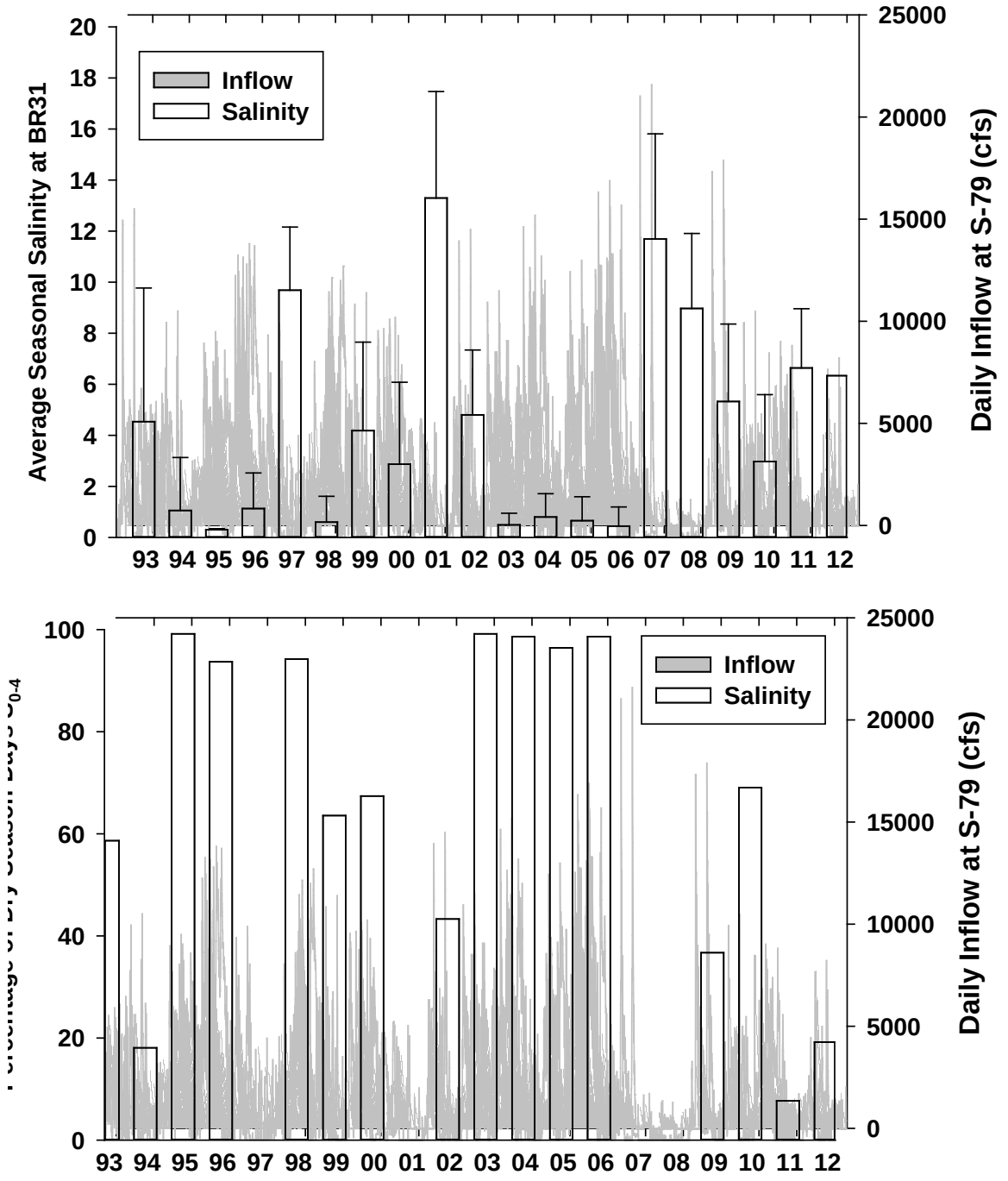

Figure 38. (**A**) Long-term average salinity in the dry season at Bridge 31 in the upper CRE (open bars; left axis) superimposed on daily freshwater inflow at S-79 (grey fill; right axis). (**B**) The percentage of dry season days where salinity ranged from 0 to 4 ($S_{0\text{-}4}$) at Bridge 31 in the upper CRE (open bars; left axis) superimposed on daily freshwater inflow at S-79 (grey fill; right axis).

Component Study 7: Relationships between Salinity and the Survival of *Vallisneria americana* in the CRE

Christopher Buzzelli, Peter Doering, Zhiqiang Chen, and Yongshan Wan

Abstract

Vallisneria americana is sensitive to increased salinity in many estuaries, including the CRE. Much of the *Vallisneria* observed from 1993 to 1999 in the CRE has been lost since droughts in 2001 and 2007–2008. This study examined relationships between *Vallisneria* and salinity through change-point analysis, assessment of long-term patterns of abundance, and exploration of the effects of salinity exposure time. Change-point analysis revealed salinity thresholds of 4, 9, and 15. Dry season average daily salinity was ~5 and rarely exceeded 10 when *Vallisneria* was abundant from 1993 to 1999. Indicator inflows (Q_I) ranging from 0 to 3,160 cfs and averaging 545 ± 774 cfs were associated with dry season salinity values of 9 to 10 (sample size [n] = 63) at Fort Myers from 1993 to 1999. In contrast, *Vallisneria* was virtually absent from 2007 to 2013 as dry season average daily salinity exceeded 10. Negative changes in shoot density can be rapid as ~50 to 60% of the aboveground material was lost if salinity was > 10 for two to three weeks. These results highlight the effects of both the magnitude and duration of environmental conditions that can inhibit *Vallisneria* survival in the CRE.

Introduction

Vallisneria is a freshwater species of SAV commonly found in many lakes, rivers, and upper reaches of estuaries (Kraemer et al. 1999, Bortone and Turpin 2000, McFarland 2006). *Vallisneria* is dioecious, perennial, and capable of extensive clonal growth through the formation of belowground stolons (Lovett-Doust and LaPorte 1991). Northern populations overwinter as a dormant winter bud buried in the sediments (Titus and Hoover 1991). In South Florida, populations do not completely die back in winter as plants actively grow year round (Dawes and Lawrence 1989, Doering et al. 1999).

Vallisneria habitats are ecologically and economic important components in many estuaries (Wigand et al. 2000, Rozas and Minello 2006, Hauxwell et al. 2007). However, the survival of *Vallisneria* in estuaries can be modulated by interactions among salinity intolerance, submarine light limitation, and grazing by herbivores (Kraemer et al. 1999, Hauxwell et al. 2004, Dobberfuhl 2007, Moore et al. 2010). In particular, there have been many laboratory experiments to evaluate the responses of *Vallisneria* to altered salinity (**Table 21**). Bourn (1932, 1943) reported that growth stopped at 8.4, while Boustany et al. (2010) found limited growth at 8.0. Haller (1974) reported growth at 10.0 but death at 13.3. While growth was minimal or zero when salinities ranged from 10.0 to 15.0, values > 15.0 caused mortality (Haller 1974, Doering et al. 2001, 2002, French and Moore 2003, Frazier et al. 2006, Boustany et al. 2010, Lauer et al. 2011). It is widely accepted that salinity > 10.0 can be damaging to the survival of *Vallisneria*.

Table 21. Summary of *Vallisneria* salinity tolerances from a variety of studies in different locations.

REFERENCE	LOCATION	CONDITIONS	RESPONSE
PLANTS			
Bourn 1932, 1943	Back Bay, VA	Static, acute 2-month exposure, outdoors, 11 salinity treatments	Growth stopped at a salinity of 8.4 in both winter and summer.
Haller 1974	Fort Lauderdale, FL	Static, acute 4-week exposure in greenhouse, 6 salinity treatments	Growth lower at salinities of 6.66 and 10 than at 0.17 and 3.33. Death at salinities of 13.32 and 16.65.
Twilley and Barko 1990	Potomac River, VA	Static, 5-week exposure outdoors, slowly raise salinity to treatment levels, 5 salinity (maximum 12) and 2 light treatments	No effect on growth at salinities of 0 to 12 regardless of light.
Doering et al. 1999	CRE, FL	Flow through mesocosms, 6-week exposure, artificial light, indoors, slowly raise salinity; 5 salinity treatments (maximum 15)	Growth declined with increasing salinity, nil or very slow at a salinity of 15.
Doering et al. 2002	CRE, FL	Flow through mesocosms, 5–6-week exposures, artificial light, indoors, slowly raise salinity; 10 salinity treatments (maximum 30)	Growth low or ceased at salinities of 10 and 15, mortality at salinities > 15.
French and Moore 2003	Maryland	Static, outdoor mesocosms exposure 7-month growing season, 4 salinity treatments (maximum 15), 3 light levels	Growth minimal at salinities of 10 and 15.
Boustany et al. 2010	St. Johns River, FL	Static, greenhouse, 10-week exposure, 10-week recovery, 3 salinity treatments (maximum 18), 3 light levels	Survived a salinity of 8, but growth was limited. Aboveground biomass perished after 10 weeks at a salinity of 18, 20% of these plants recovered after 10 weeks.
DURATION			
Doering et al. 2001	CRE, FL	Flow through mesocosms, 0- to 70-day exposure to 18, 30-day recovery, artificial light, indoors, slowly raise salinity	Declines in blades and shoots observed after 5-day exposure. Statistically significant declines at 20- to 70-day exposures. Viable plants after 70 days.
Frazier et al. 2006	Kings Bay, Florida	Static, acute, 4 salinity treatments (maximum 25), 3 durations of exposure, 28-day recovery	100% mortality at a salinity of 25 after 1-, 2- , or 7-day exposure. 75% mortality at a salinity of 15 after a 7-day exposure. Exposure to a salinity of 5 had no effect on growth.
FLOWERING			
French and Moore 2003	Maryland	See French and Moore 2003 above	No flowering at salinities of 10 or 15 regardless of light level.
Doering et al. unpublished 1999	CRE, FL	See Doering et al. 1999 above	Female structures at salinities of 0 and 3. Male structures at salinities of 0, 3, and 9. Neither structures at salinities of 12 or 15.
SEEDS			
Nosach 2007	CRE, FL	Petri dishes, laboratory incubator, 3 temperature, 2 light, and 4 salinity (maximum 15) treatments	Seeds germinated at all salinities although rate declined as salinity increased. Temperature had the greatest effect with highest germination at 30° C.
Jarvis and Moore 2008	Tidal tributary of the Potomac River, MD	Field characterization and laboratory experiments: (A) Salinity at 4 levels 1 to 15 in petri dishes; (B) temperature at 4 levels 13 to 29 °C in petri dishes; (C) dark and light for oxygenated and hypoxic in 250 milliliter serum bottles; and (D) 4 treatments of varying sediment composition and 6 burial depths	Increased salinity had significant negative effect on germination with the threshold between salinities of 5 and 10. Seed viability was maintained at salinity > 10. Temperature exhibited a strong influence on germination with the highest germination occurring at > 22°C. Oxygenation enhanced germination while light and burial depth (0.2 to 10 centimeter) had no effect.

Salinity also influences flowering and seed production in the life history of estuarine *Vallisneria* populations. French and Moore (2003) noted that flowering did not occur in salinity treatments of 10 and 15. Although the data were not included in Doering et al. (1999), they observed female flowers at 0 and 3, but not at 9 or above. Male flowers occurred at salinity values of 0, 3, and 9 but not when salinity was 12 or 15. Nosach (2007) examined the effects of temperature, light, and salinity on germination of *Vallisneria* seeds. Although seeds germinated across all salinities in this study (0 to 15), the best conditions for seed germination occurred at a temperature of 30 degrees Celsius (°C) and salinities < 5. Jarvis and Moore (2008) found that *Vallisneria* germination occurred best at temperatures > 22ºC and was significantly greater in salinity treatments of < 1 and 5 compared to the 10 and 15 treatments. Non-germinated seeds provide a pathway for revegetation by remaining viable throughout most environmental conditions.

The growing season for *Vallisneria* in the CRE in Southwest Florida lasts from March to September, with peak shoot density occurring in June or July (Bortone and Turpin 2000). Shoot density begins to decline in late summer as the production of male and female flowers is greatest in September or October. Blade length increases from March to September or October, sometimes to over a meter, and declines into the winter. Overwintering rosettes have short blades, 10 centimeters or less in length (Bortone and Turpin 2000).

Historically, there was abundant *Vallisneria* habitat in the upper CRE (Kraemer et al. 1999, Bortone and Turpin 2000, Doering et al. 2002, Bartleson et al. 2014). Published qualitative observations supported the presence of *Vallisneria* in the early 1960s (Gunter and Hall 1962, Phillips and Springer 1960). *Vallisneria* was present in the CRE from the mid-1980s until quantitative monitoring began in January 1998 (Bortone and Turpin 2000). Hoffacker (1994) conducted a visual census from July to October 1993 characterizing coverage as dense, moderate, or scattered. *Vallisneria* coverage was dense in the upper estuary between the Railroad Trestle near Beautiful Island and the Edison Bridge at Fort Myers (**Figure 39**). The maximum downstream extent (Whiskey Creek) was documented in the Hoffaker map. When considered along with quantitative monitoring, it appears that there were dense beds of *Vallisneria* in the upper CRE from 1993 to 1999.

The management of freshwater inflow through the Franklin Lock and Dam at the head of the CRE (S-79; **Figure 40**) is an important influence on circulation and transport in the CRE. Reduced freshwater inflow during the dry season (November–April) permits upstream encroachment of salt water (Wan et al. 2013, Buzzelli et al. 2014a). Superimposed on intra-annual variations and water management are droughts such as the one in 2000–2001 when increased salinity led to widespread loss of *Vallisneria*. Rainfall for the CRE MFL Watershed (**Figure 1A**) averages 51.1 inches annually. In 2001, the rainfall was only 35.8 inches, which was representative of a 1-in-25 year drought event. Another drought event occurred in 2007 that was equivalent to a 1-in-10 year drought. Additionally, for many years since 2000, dry season rainfall has been well below normal. As a result of multiple drought events and deficits in dry season rainfall, freshwater inflows in the CRE have been reduced.

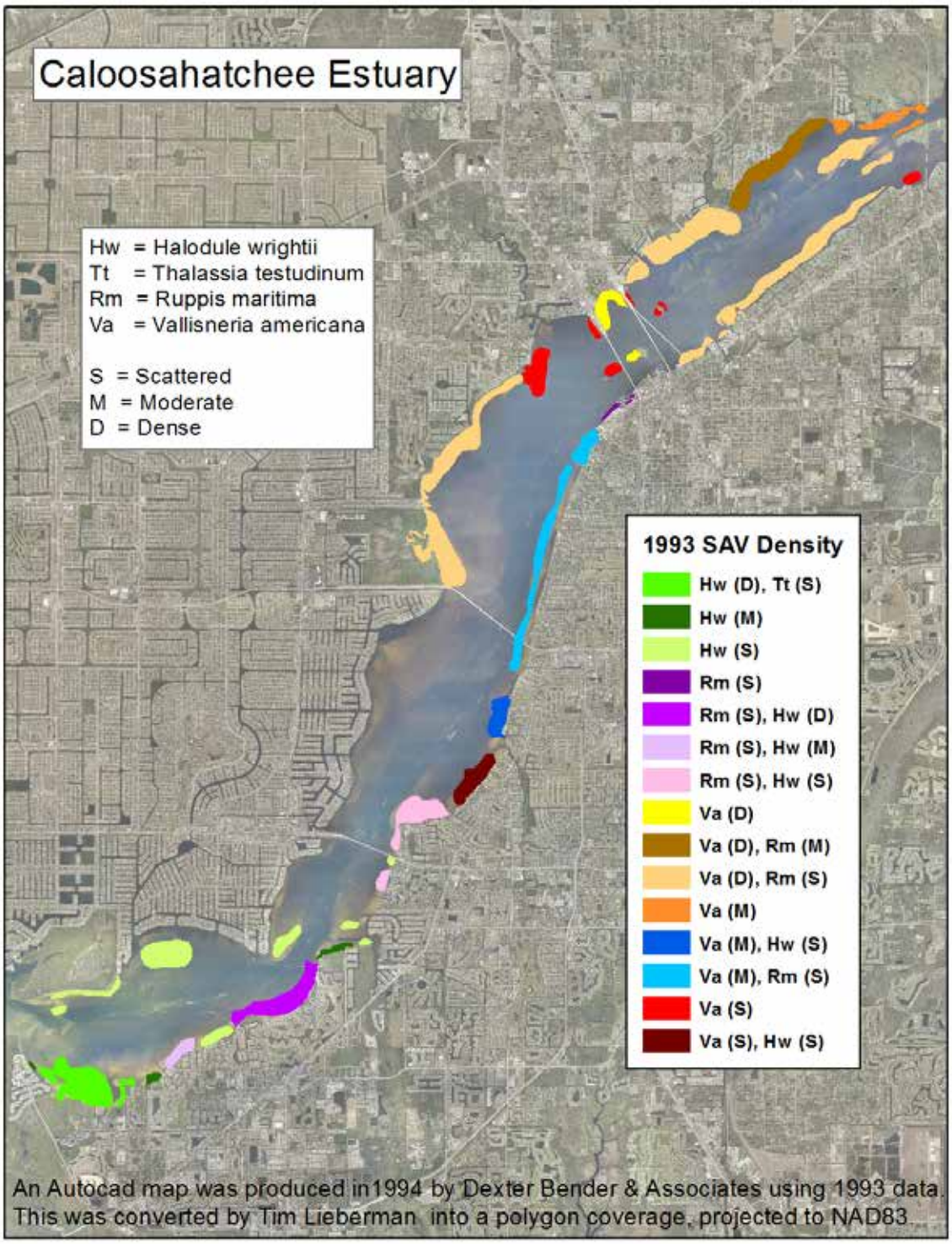

Figure 39. 1993 map of SAV habitat density in the CRE from Hoffaker (1994).

Based on accumulated knowledge, this study assumed that salinity is the dominant driver for *Vallisneria* survival. This phenomenon was explored through local observations and data to assess survival of *Vallisneria* with fluctuating salinity using three separate approaches. The first was a statistical approach that applied Bayesian change-point analysis to determine the critical salinity values for *Vallisneria* (Beckage et al. 2007). This method uses piecewise regression to identify abrupt changes in sequential data (e.g. time series). The second was an assessment of long-term patterns of *Vallisneria* shoot densities and salinity. This approach provided an historical perspective that could help explain the present status of the resource. The relationship between the duration of super critical salinity and the proportional mortality of *Vallisneria* shoots was examined in the third approach.

Methods

Vallisneria Monitoring in the CRE

Quantitative monitoring of *Vallisneria* started in 1998 at Sites 1 through 4 (**Figure 40**). Researchers established paired, perpendicular 100-m transects at each site. On each sampling date, the number of blades, shoots, and flowers were counted in five separate, random 0.1-m^2 quadrats along each transect (n = 10 = 5 quadrats x 2 transects; Bortone and Turpin 2000; Doering et al. 2002). Blade length and width were also determined in each quadrat. Field monitoring methods were changed in 2008 to a gridded presence/absence method where the number of cells containing shoots within a 1-m^2 quadrat was counted at multiple, randomly distributed sites. Because Site 3 was discontinued in 2003, there are three sites (1, 2, and 4) where shoot densities were monitored at approximately monthly intervals from 1998 to 2007. Data from Sites 1 and 2 were used in this study. Site 4 was omitted because *Vallisneria* presence was extremely variable at this most downstream station.

Salinity Monitoring in the CRE

Since 1992, SFWMD has monitored salinity at several locations in the CRE at 15-minute intervals (**Figure 40**). Salinity is determined at two depths (20 and 80% of depth relative to mean sea level) using in situ data recorders. Daily average surface salinity recorded at the Ft. Myers station from May 1, 1992 to April 30, 2014 was obtained from DBHYDRO (http://www.sfwmd.gov/dbhydroplsql/show_dbkey_info.main_menu). Missing daily salinity values (1,058 of 8,035 days) were estimated using an autoregressive model (Qiu and Wan 2013).

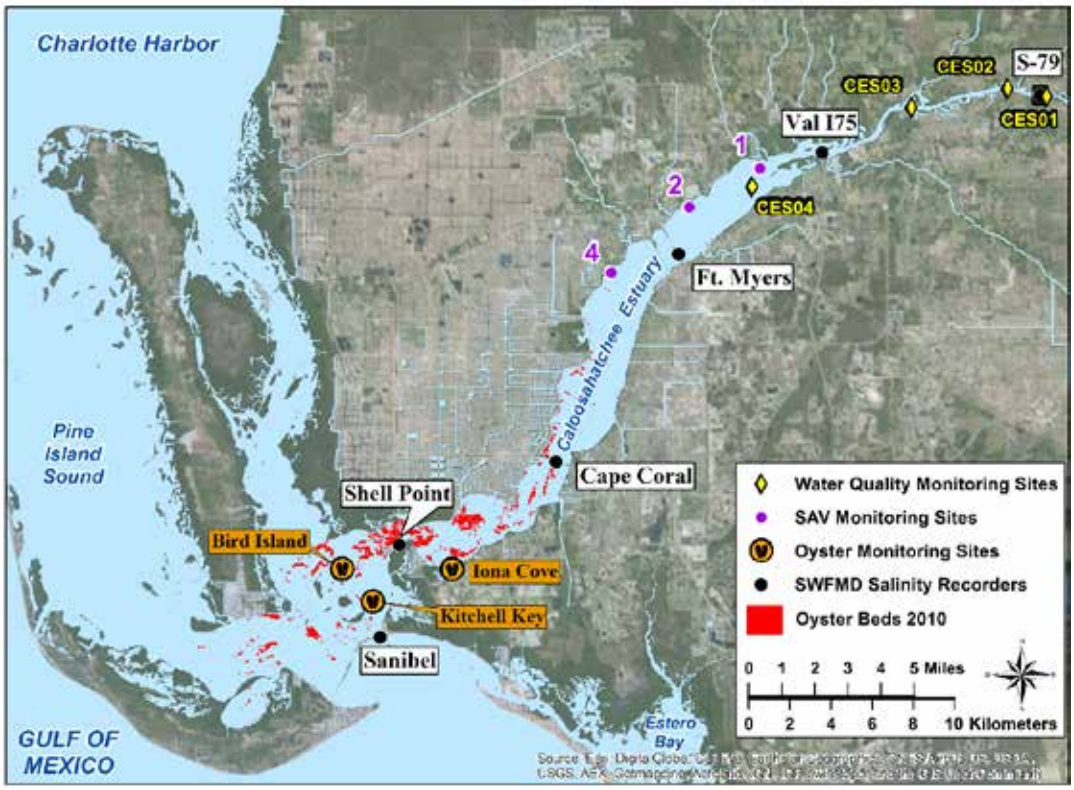

Figure 40. Location map for the CRE including the S-79 water control structure, water quality monitoring sites, SAV monitoring sites (upper CRE), and the location of continuous salinity recorders.

Data Analyses

Both salinity and *Vallisneria* shoot count data were expressed as a time series of water years. A water year spans May 1 to April 30 to include both wet (May–October) and dry (November–April) seasons representative of the subtropical climate of South Florida. There were a few different approaches to assess *Vallisneria*-salinity relationships.

First, salinity thresholds were quantified by applying Bayesian change-point analyses to the merged salinity-*Vallisneria* data (Qian et al. 2004, Ruggieri 2012). Change-point analyses successively split the data into two groups. At each split, the statistical properties (e.g. posterior means) of the two groups are evaluated to determine the likelihood (probability) that each group is statistically similar unto itself and at the same time statistically distinct from the opposing group. The most probable change point was considered to represent a change point threshold of salinity with uncertainty quantified by constructing a high density credible interval around this threshold. The Bayesian change point package in "R" was used (http://cran.r-project.org/web/packages/bcp/; Erdman and Emerson 2007). Shoot density data were log transformed to normalize the distribution. In addition, shoot density data were binned based on integer salinity values from 1 to the maximum salinity observed. The procedure results in posterior means and a probability distribution over salinity groups. Change points of salinity were chosen as salinities where there was maximum probability of difference among adjacent data groups at each split.

Second, historical differences in indicators of *Vallisneria* abundance and salinity were assessed to better understand the conditions that either promote or inhibit *Vallisneria*. This was accomplished by defining two equivalent time periods each containing seven wet and six dry seasons for analysis of salinity patterns. The two periods were May 1, 1993–October 31, 1999 (WY1994 to wet season of WY2000), and, May 1, 2007–October 31, 2013 (WY2008 to wet season WY2014). Salinity patterns during these time periods were qualitatively compared to shoot densities from Site 2. Data from the first period (WY1993–WY1999) were queried to extract the dry season days where salinity at the Ft. Myers station was 9 to 10. These inflows were assumed to be below the desirable limit to maintain favorable salinity conditions.

Finally, the effects of exposure time on the survival of *Vallisneria* were examined using the observed shoot densities at Sites 1 and 2 and the Ft. Myers salinity record. The 30-day moving average salinity was calculated. Four time periods among the two sites were selected to assess decreases in shoot density with critical salinity values. Not all high salinity (30-day average salinity > 10) events were included in the data set. Two episodes occurring between March and June 2002 were excluded because initial shoot density was too low (£11 shoots per m^2) to quantify a decline. An episode that occurred in 1999 also was not included. While plants did decline, the decline itself began well before salinity at Ft. Myers reached 10 and other factors either singly or in combination with salinity may have been responsible. For the remaining intervals, the shoot density on the first day was used as the initial condition. The number of days where the 30-day moving average salinity exceeded 10 (x) was paired with the percent of shoots remaining relative to the initial conditions (y) and modeled using a negative exponential curve.

Results

Salinity at the Ft. Myers station varied on seasonal, annual, and multi-annual time scales (**Figure 41A**). It was greatest in the dry season peaking at ~26 and 27 in 2001, 2007, and 2008. Values were generally lowest from 2003 to 2006. Average shoot densities ranged from 0 to 370 and 0 to 1,200 shoots per m^2 at Sites 1 and 2 (**Figure 41B**). Shoots were abundant from 1998 to 2000 with densities at Site 2 much greater than those observed at Site 1. Shoot densities were much reduced and similar between the two sites in 2000 before dropping to near zero from 2001 to 2004. Density increased slightly to 0 to 200 shoots per m^2 from 2004 to 2006 before again falling to zero in 2007.

The Bayesian change-point analysis resulted in clear salinity thresholds of 4, 9, and 15 (**Figure 42**). These values reinforce previous findings where salinity values that were ³ 5 impaired growth, those ³ 10 stopped growth, and salinity values ³ 15 caused mortality. The first threshold (4) was associated with the highest shoot densities. The most pronounced change point of salinity was around 9 (posterior probability of 86%) with the 95% credibility limit from 8 to 10. Salinity values > 9 were associated with decreased densities from 200 to 100 shoots per m^2. The inflection point around a salinity of 15 had a probability of 0.6 and a 95% credibility limit of 14 to 16. Salinity values > 15 were associated with decreased densities to < 40 shoots per m^2.

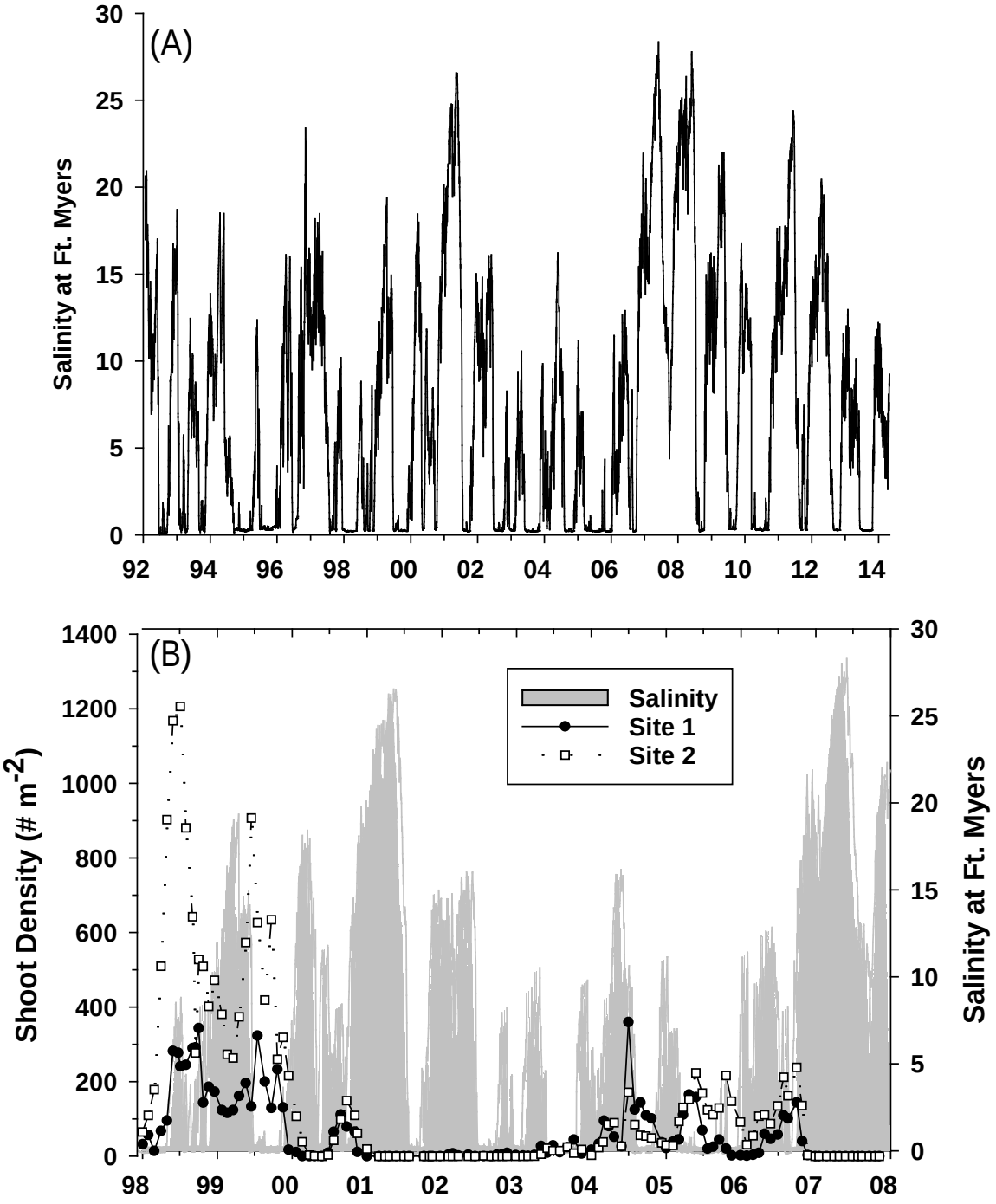

Figure 41. (**A**) Time series of daily average surface water salinity at the Ft. Myers station from January 1992 to April 2014. (**B**) Time series of average *Vallisneria* shoot densities (# m^{-2}) at Sites 1 (filled circle) and 2 (open square) in the CRE from 1998 to 2007. Average daily surface salinity at Ft. Myers is shown as the grey filled time series (right axis).

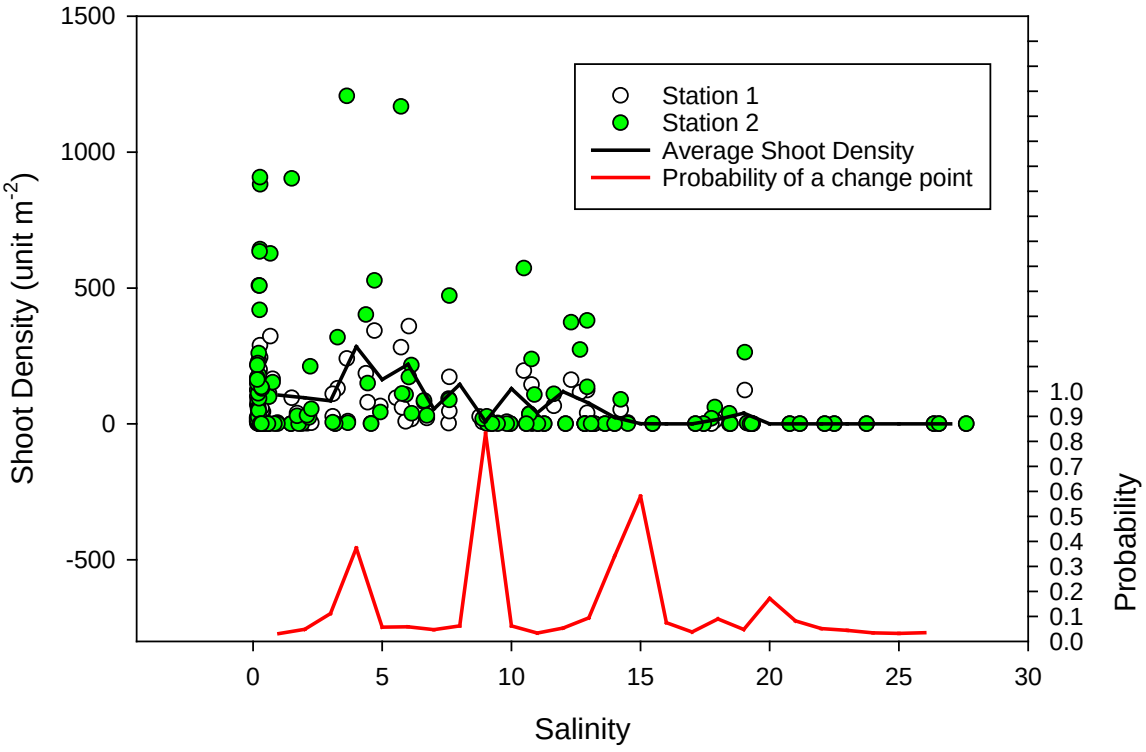

Figure 42. Combination plot showing *Vallisneria* shoot densities (unit per m^2 [unit m^{-2}]; left axis) from monitoring Sites 1 and 2 as a function of the 30-day moving average salinity at Ft. Myers. The red line depicts the probabilities of break points in the relationship between shoot density and salinity.

Anecdotal, observational, and quantitative information indicated large differences in *Vallisneria* distribution and density between the two time periods (WY1993–WY1999 and WY2007–WY2013; **Figure 42**). The Hoffaker map (1994; **Figure 39**) revealed extensive *Vallisneria* habitat throughout the upper half of the CRE. Personal observations by SFWMD staff (P. Doering and R. Chamberlain) confirmed dense beds of *Vallisneria* from the WY1995–WY1997 period. Shoot densities derived from in situ counts ranged from 200 to 900 shoots per m^2 from WY1998 to WY2000 across the habitat area. Both the distribution and abundance declined through 2001 reaching ~0.0 from 2002 to 2003. There were small observable increases in shoot density from WY2004 to WY2007. However, monitoring conducted since WY2008 indicated that *Vallisneria* has been mostly absent except for a minor appearance in WY2011.

Daily surface salinity at the Ft. Myers station over the entire period of record (May 1, 1993–April 30, 2014) averaged 7.17 ± 7.09 (n = 8,035). During the period when *Vallisneria* beds were likely extensive and dense (WY1993–WY1999), daily salinity averaged 5.4 ± 5.4 (n = 2,375; **Table 22**). In contrast, salinity during the period when *Vallisneria* was virtually absent (WY2007–WY2013) averaged 10.0 ± 8.0 (n = 2,376). One-way ANOVA showed these averages to be significantly different ($p < 0.001$). In general, *Vallisneria* requires salinities below 10 for a sustainable population (French and Moore 2003). Average seasonal salinity exceeded this value only once during the first period when *Vallisneria* was abundant (dry season 1997; **Figure 43**). During the more recent period when *Vallisneria* was sparse or absent, average salinity exceeded this threshold in five of six dry

seasons and three of six wet seasons. Freshwater inflows ranging and averaging 0 to 3,160 and 545 ± 774, respectively, were associated with dry season salinity values of 9 to 10 (n = 63) at the Ft. Myers station in Period 1 when *Vallisneria* was abundant (WY1993–WY1999).

Table 22. Descriptive statistics for salinity values at the Ft. Myers station. Two equal subsets of data were extracted from the long-term (1992–2014) time series. Period 1 was from May 1, 1993, to October 31, 1999. Period 2 was from May 1, 2007, to October 31, 2013.

Salinity	Period 1	Period 2
Number	2,375	2,376
Range	0.03–23.4	0.15–28.3
Average + Standard Deviation	5.4 ± 5.4	10.0 ± 8.0
Median	3.6	10.3

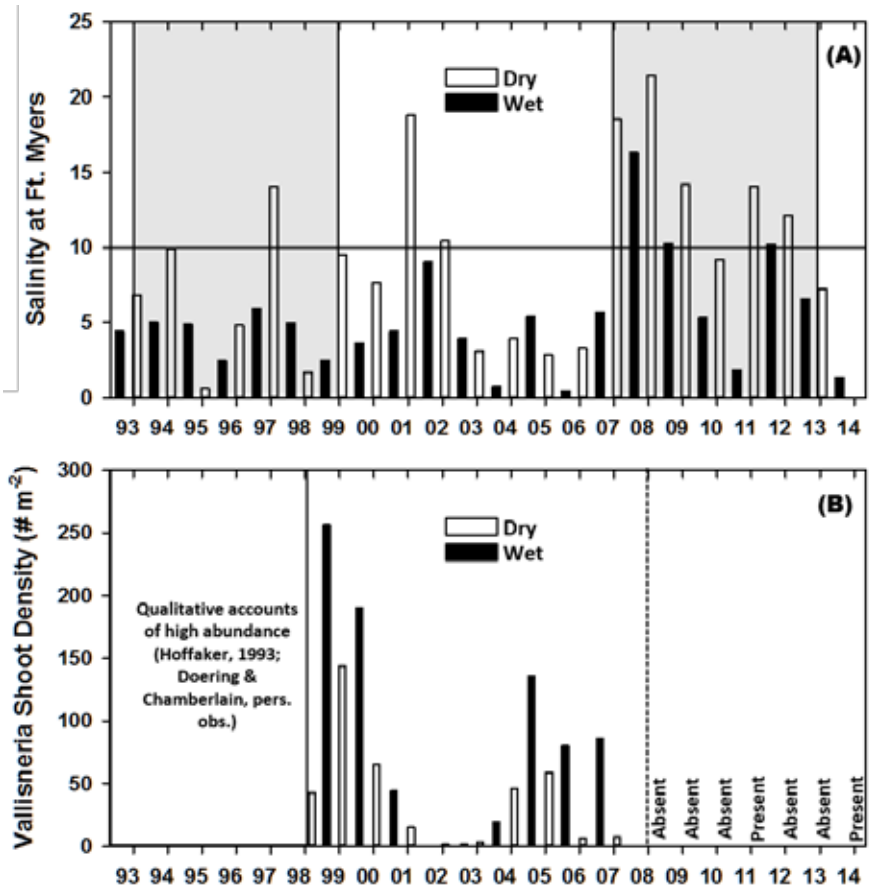

Figure 43. (**A**) Time series of average seasonal salinity at the Ft. Myers station from 1993 to 2014. The shaded areas mark two separate seven-year periods (1993–1999; 2007–2014). (**B**) Time series of average seasonal shoot density from 1998 to 2007. Data before this period were qualitative. Monitoring methods changed to detect presence versus absence since 2008.

Vallisneria shoot density decreased precipitously with increased duration of 30-day average salinity values in excess of 10 at the Ft. Myers station (**Table 23** and **Figure 44**). The negative exponential relationship suggests that a 50% reduction in plant density would occur after 14 days, an 85% reduction after 42 days, and a 95% reduction after 63 days. Examination of the upper confidence limit on the mean prediction of the equation revealed that significant mortality occurred after 4 days (95% confidence interval no longer overlaps 100% remaining).

Table 23. Time periods and data used to calculate percent change in *Vallisneria* shoot densities relative to salinity criteria at the Ft. Myers station. See text and **Figure 44** for details and results.

Station 1 Start	End	Initial Shoots	Days	% Remaining	Comment
2/27/2000	3/16/2000	10.5	19	0	Not used
11/18/2000	3/26/2001	79	11	83	
			24	17	
			70	0	
5/20/2004	6/23/2004	52	36	50.7	
11/12/2006	1/24/2007	143.9	10	28	
			37	1.7	
Station 2 Start	**End**	**Initial Shoots**	**Days**	**% Remaining**	**Comment**
2/27/2000	4/20/2000	107	19	36	
			34	1.6	
11/18/2000	3/26/2001	149	11	74	
			24	56	
			70	18	
			127	0	
5/20/2004	6/23/2000	90	36	29.78	
11/12/2006	1/24/2007	238.3	10	56.95	
			37	1.0	

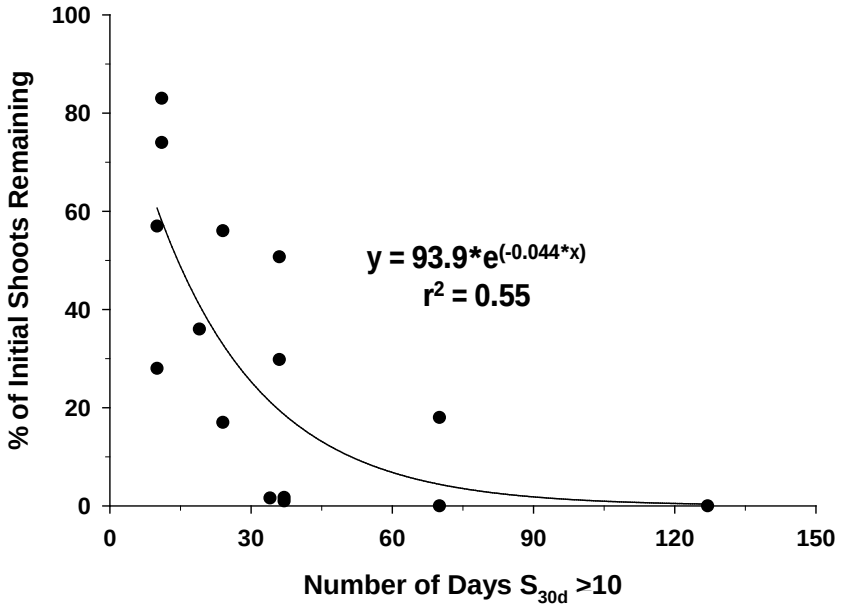

Figure 44. Proportional mortality plot showing the number of days where salinity at the Ft. Myers station was > 10 versus the percent of initial shoots remaining. See text and **Table 23** for details of analysis.

Discussion

This study represents an important step towards an improved understanding of the survival of *Vallisneria americana* in the CRE in Southwest Florida. This understanding builds upon a foundation of original accounts, local surveys, quantitative monitoring, mesocosm experiments, statistical analyses, and simulation modeling (Hoffaker 1994, Doering et al. 1999, Bortone and Turpin 2000, Doering et al. 2002, Bartleson et al. 2014, Buzzelli et al. 2015b). While estuarine *Vallisneria* is sensitive to multiple environmental factors (e.g. light, grazing, and temperature), it appears that the dominant driver is salinity (French and Moore 2003, Dobberfuhl 2007, Boustany et al. 2010, Lauer et al. 2011).

Salinity is a conservative property of estuaries that, while uninfluenced by biogeochemical processes, varies over many time scales through complex hydrodynamic processes. These processes integrate rainfall, surface inflows, groundwater discharge, wind events, and tidal exchanges to establish salinity conditions (Zheng and Weisberg 2004) and modulate biological processes (Jassby et al. 1995, Livingston et al. 1997, Whitfield et al. 2012). Thus, estuaries are very sensitive to anthropogenic changes in freshwater inflow (Alber 2002). Physical alterations such as dredging and dams change natural inflows, impact mixing with the coastal ocean, and dramatically affect salinity and water quality in the estuary (Day et al. 1989, Zhu et al. 2015). Discharge, salinity gradients, biogeochemical properties, and biological attributes of the CRE are greatly influenced by a combination of subtropical climatic variability and landscape-scale water management (Tolley et al. 2005, Volety et al. 2009, Buzzelli et al. 2013c, Wan et al. 2013).

The location of particular isohalines in estuaries can be used as an indicator of ecological conditions (Jassby et al. 1995). In the case of the CRE, a salinity of 10 at the Ft. Myers station has been established as a benchmark for water management (Balci and Bertolotti 2012). The long-term salinity record at Ft. Myers provides an excellent indication of the environmental suitability for *Vallisneria* in the upper CRE. Increasing salinity thresholds of 4 to 5, 8 to10, and > 15 serve to slow growth, inhibit survival, and cause mortality in estuarine populations of *Vallisneria*, respectively (Bourn 1932, 1943, Haller 1974, Doering et al. 2001, 2002, French and Moore 2003, Frazier et al. 2006; Boustany et al. 2010, Lauer et al. 2011).

This study demonstrated that differences in salinity between two time periods (1993–1999 and 2007–2013) may have contributed to observed differences in density and spatial extent of *Vallisneria* in the upper CRE. During the initial period when *Vallisneria* beds were dense and widespread, salinity was ~5 and seasonally averaged salinity rarely exceeded 10 for a sustainable population. There was a 40% reduction in freshwater inflow to the upstream estuary during the second seven-year period. Reduced freshwater inflow is an important driver leading to increased salinity in the CRE. When *Vallisneria* was virtually absent in the second period, salinity was ~10 with multiple wet and dry seasonal exceedances of this threshold.

It is not surprising that the *Vallisneria* habitat in the CRE has trouble recovering from repeated, severe drought-induced stress in 2001 and 2007–2008. Salinity in the CRE has been much higher since 2007 as compared to the last known period of *Vallisneria* abundance (WY1993–WY1999). Additionally, approximately half of the standing stock could be lost if salinity at the Ft. Myers station is greater than 10 for 14 consecutive days. Loss of mature shoots inhibits the potential to reestablish viable habitat through vegetative

and reproductive growth. The cumulative impacts of anthropogenic changes, increased salinity, decreased shoot density, and shrunken habitat extent have created circumstances that greatly inhibit the recovery of *Vallisneria* habitat in the CRE.

Component Study 8: Development and Application of a Simulation Model for *Vallisneria americana* in the CRE

Christopher Buzzelli, Peter Doering, Yongshan Wan, and Teresa Coley

Abstract

Monitoring of *Vallisneria americana* densities in the upper CRE from 1998 to 2007 was accompanied by mesocosm experiments to determine relationships between salinity and growth. This study built upon these efforts by developing a simulation model to examine the effects of temperature, salinity, and light on *Vallisneria* survival and biomass in the upper CRE from 1998 to 2014. The effects of salinity on *Vallisneria* mortality were explored using an eight-year experimental model based on favorable conditions from 1998 to 1999. Using the experimental model, the dry season salinity was systematically increased in 5% increments until the net annual biomass accumulation of *Vallisneria* was negative. A five-fold increase in grazing was required to stabilize model biomass under optimal conditions. A 55% salinity increase to 12 promoted shoot mortality in the experimental model. Annual inflow-salinity relationships for the Ft. Myers station were used to estimate that dry season inflows ranging from 15.2 to 629.0 cfs and averaging 342 ± 180 cfs were associated with a salinity of 12 at Ft. Myers. Model results suggested that an estimated 85.4 and 86.7% of the shoots were lost in the dry seasons of 2001 and 2007, respectively.

Introduction

Vallisneria is a freshwater species of SAV commonly found in many lakes, rivers, and upper reaches of estuaries (Bortone and Turpin 2000, McFarland 2006). *Vallisneria* habitat in estuaries is desirable since it supports a variety of ecologically and commercially important fauna (Wigand et al. 2000, Hauxwell et al. 2004, Rozas and Minello 2006). Because it is a freshwater organism that can extend into oligohaline estuarine areas, *Vallisneria* is very responsive to fluctuations in salinity (Doering et al. 2002, Boustany et al. 2010).

There have been many laboratory experiments to evaluate the responses of *Vallisneria* to altered salinity. Salinity values in excess of 8 to 15 can be stressful and result in net mortality depending upon exposure time (Doering et al. 1999, Doering et al. 2001, French and Moore 2003, Boustany et al. 2010, Lauer et al. 2011). Bourn (1932, 1943) reported that growth stopped at 8.4, while Boustany et al (2010) found limited growth at 8.0. Haller (1974) reported growth at 10.0 but death at 13.3. While growth was minimal or zero when salinities ranged from 10.0 to 15.0, values > 15.0 caused mortality in several studies (Haller 1974, Doering et al. 2001, French and Moore 2003, Frazier et al. 2006, Boustany et al. 2010, Lauer et al. 2011). It is generally accepted that salinity > 10.0 is detrimental to *Vallisneria*.

Water clarity is a complicating factor that can affect the survival and growth of *Vallisneria* in estuaries. Submarine light penetration in the upper part of estuaries is affected by colored dissolved organic matter, which is directly proportional to freshwater inflow (McPherson and Miller 1994, Bowers and Brett 2008, Buzzelli et al. 2014b). *Vallisneria* requires ~9 to 14% of surface irradiance with total light extinction coefficients of 3 to 4 per m being most favorable (French and Moore 2003, Dobberfuhl 2007, Boustany

et al. 2010, Moore et al. 2010). The obvious implication is that the low salinity necessary for *Vallisneria* survival in oligohaline estuarine areas is usually accompanied by decreased light levels.

The growing season for *Vallisneria* in Southwest Florida lasts from March to September, with maximum shoot density and biomass occurring in July–August (Bortone and Turpin 2000). Published qualitative observations supported the presence of *Vallisneria* in the early 1960s (Gunter and Hall 1962, Phillips and Springer 1960) and the 1980s (Bortone and Turpin 2000). Hoffacker (1994) conducted a visual census from July to October 1993 that documented widespread coverage with variable density. The negative response of *Vallisneria* to increased salinity makes it an excellent ecological indicator for freshwater management (Doering et al. 2002). It provides a useful indicator because its sensitivity provides insight into environmental conditions that trigger problems at the habitat scale (Dale and Beyeler 2001).

The distribution and density of *Vallisneria* habitat is variable in the upper CRE in Southwest Florida (Kraemer et al. 1999, Bortone and Turpin 2000, Doering et al. 2002, Bartleson et al. 2014). The decreased availability of fresh water in the dry season (November–April) can lead to reduced freshwater inflow and the upstream encroachment of saline water (Wan et al. 2013, Buzzelli et al. 2014a). These attributes were particularly acute during droughts in 2001 and 2007–2008 when salinity increases in the upper CRE led to widespread loss of *Vallisneria*.

The goal of this study was to develop a simulation model for *Vallisneria* in the CRE (Buzzelli et al. 2012, 2014b). There has been much environmental monitoring since initial efforts to use *Vallisneria* as an indicator of freshwater inputs over a decade ago. These data provide an empirical foundation for ongoing management, and, the creation of a mathematical model to forecast potential responses to proposed management actions. The objectives were to develop and test a simulation model of *Vallisneria* responses to environmental variables (temperature, salinity, and light) and evaluate the salinity and inflow conditions that support viable oligohaline (0–10) SAV habitat in the upper CRE.

Methods

Study Site

The CRE is bounded upstream by S-79 and extends ~42 km downstream to the mouth near the Sanibel Bridge (**Figure 45**). The surface area of the CRE is 67.6 km^2 (6,764 hectares = 16,715 acres) with an average depth of 2.7 m (Buzzelli et al. 2013b). Average flushing time ranges from 5 to 60 days (Wan et al. 2013, Buzzelli et al. 2013c). A variety of physical, chemical, and biological variables are regularly monitored by SFWMD and other organizations. Discharge from S-79 has been recorded since 1966 and is reported here as the daily mean average inflow rate in cfs. Salinity has been monitored at multiple locations since the 1990s (S-79, Val I75, Ft. Myers, Cape Coral, Shell Point, and Sanibel; **Figure 45**). The distribution and density of SAV have been determined at the upper stations (1, 2, and 4) since 1998 and the in the lower estuary (5, 6, 7, and 8) every two months since 2004. This study focused on SAV Site 1 because of its upstream location near Beautiful Island and proximity to the Ft. Myers salinity monitoring location.

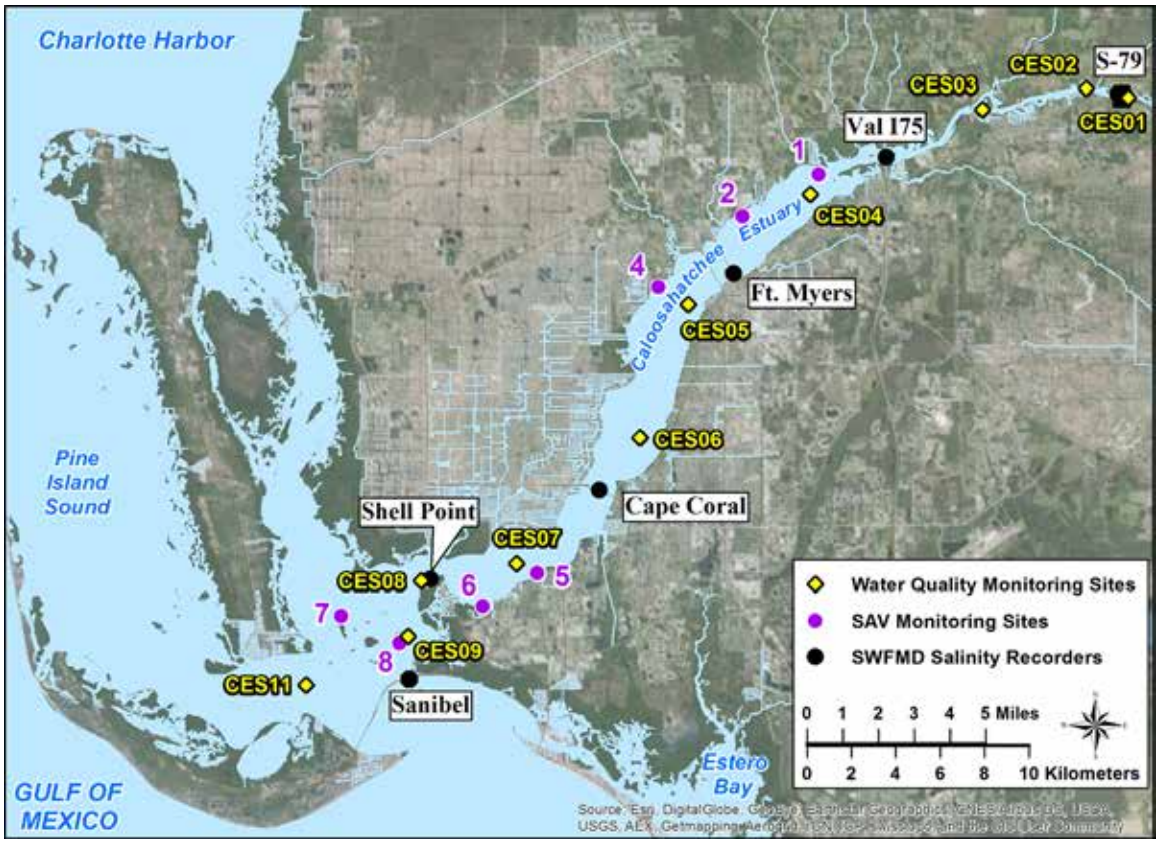

Figure 45. Location map for the CRE including the S-79 water control structure, water quality monitoring sites, SAV monitoring sites, and the location of continuous salinity recorders.

Empirical Data

Daily average surface salinity recorded at the Ft. Myers station from May 1, 1992, to April 30, 2014, was obtained from the DBHYDRO, which is accessible from the following link: https://www.sfwmd.gov/science-data/dbhydro). Missing daily salinity values (1,058 of 8,035 days) were estimated using an autoregressive model (Qiu and Wan 2013).

Researchers established paired, perpendicular 100-m transects at the beginning of the SAV monitoring period for each site. On each sampling date the number of blades, shoots, and flowers were counted in five separate, random 0.1-m^2 quadrats along each transect (n = 10 = 5 quadrats x 2 transects; Bortone and Turpin 2000, Doering et al. 2002). Blade length and width were also determined in each quadrat. SAV shoot counts, length, width, and dry weight biomass were monitored approximately bi-monthly at Site 1 from 1998 to 2007.

Both salinity and *Vallisneria* shoot count data were expressed as a time series of water years. Each water year includes wet (May–October) and dry (November–April) seasons representative of the subtropical climate of South Florida. Mesocosm experiments provided data used to generate a linear regression between shoot densities and aboveground biomass (Doering et al. 1999, 2001). This relationship was used to convert shoot densities (number per square meter [# m^{-2}]) observed at Site 1 to biomass (grams dry weight per square meter [gdw m^{-2}]) and generate a time series of shoot biomass from 1998 to 2007. This time series was used to calibrate model predictions of shoot biomass. The regression

relationship also was used to convert predicted shoot biomass back to shoot density for various applications.

Model Boundaries

Vallisneria habitat near Beautiful Island in the upper CRE provided the spatial reference for the model (Doering et al. 2001). The model was developed to represent changes in biomass at Site 1 over an 18-year period from 1997 to 2014 (6,574 days or 216 months). The integration interval was 0.75 hours (0.03125 day; Buzzelli et al. 2012, 2014b). The first year of simulation time (1997) was used to stabilize the model and was not included in reporting and interpretation. The model output (1998–2014) was summed or averaged to depict daily, monthly, seasonal, and annual (calendar and water year) time scales.

Model Mathematical Structure

Water temperature (T_w), submarine light (Iz), and salinity (S) were the important environmental drivers for the *Vallisneria* model (**Figure 46**, **Table 24**, and **Table 25**). A daily time series of T_w at the Ft. Myers station from 1998 to 2012 was derived from continuous monitoring (**Figure 47A**). Missing temperature data were estimated using an interpolation method (Baldwin and Hunt 2014). Temperature influences both the photosynthesis-irradiance relationship (fT_{shoot}) and the effective rate of respiration (**Table 24**, **Table 25**, and **Figure 47B**).

Daily salinity at SAV monitoring Site 1 (S_{val}) was predicted using a method derived through integrated hydrodynamic and time series modeling (**Figure 48A**; Qiu and Wan 2013). The method combines empirically derived freshwater inflow through S-79, estimated freshwater input through combined tributaries and groundwater inflows from the downstream Tidal Basin, and daily salinity data observations from the I-75 Bridge in the upper CRE to generate a continuous time series of salinities at Site 1 (Qiu and Wan 2013). S_{val1} was used to influence rates of *Vallisneria* gross production and loss. A salinity range of 0 to 10 decreased and increased the model rates of gross production and mortality, respectively (**Figure 48B**).

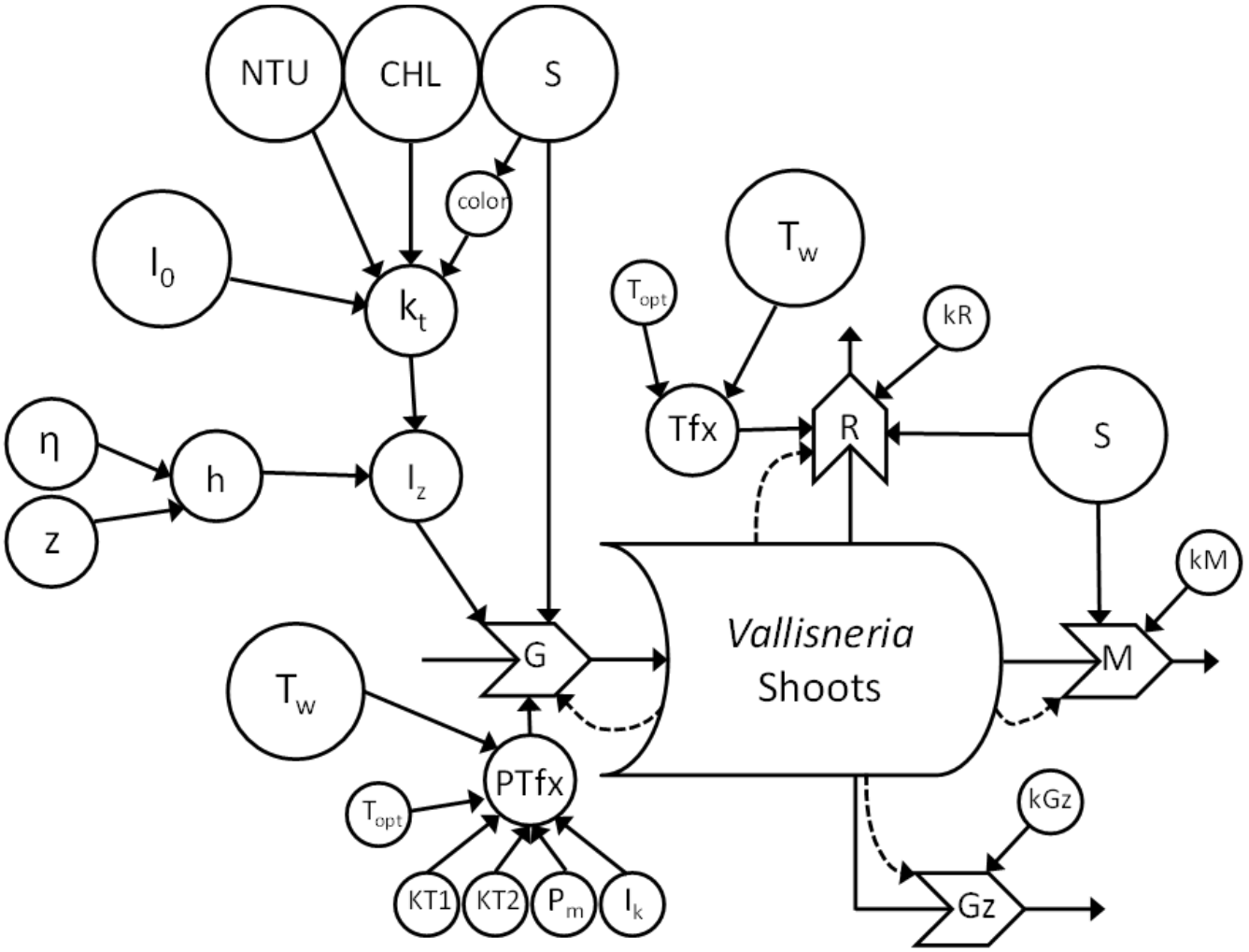

Figure 46. Conceptual model for response of *Vallisneria* shoots to variable water temperature (T_w), irradiance at the bottom (I_z), and salinity (S). See **Error! Reference source not found.** and **Table 25** for model equations and coefficients, respectively. Surface irradiance (I_0), turbidity (NTU), chlorophyll *a* (CHL), and color were used to calculate I_z. S was used as a term to estimate color. Depth (h) was calculated using water level (η) and sediment elevation (z). A suite of coefficients—optimum temperature (T_{opt}), *Vallisneria* constants for photosynthesis (KT1) and (KT2), maximum rate of photosynthesis (P_m), and the half-saturation irradiance value (I_k)—are combined with T_w and shoot biomass to calculate gross production (G). Respiration (R) is influenced by a temperature effect (Tfx) and S. S also influences the rate of shoot mortality (M). Loss due to grazing (Gz) is a function of the shoot biomass and the basal grazing rate (kGz).

Table 24. List of equations to simulate dynamics of *Vallisneria americana* shoot biomass. See Buzzelli et al. (2012, 2014b) for mathematical details.

Description	Equations
(1) Photoperiod ($P_{photo;}$ hrs)	$P_{photo} = 12 - 2 * \cos(\frac{2 * \pi * day}{365})$
(2) Surface irradiance ($I_{0;}$ µmole m^{-2} s^{-1})	$I_0 = MAX[(I_{amp} * \cos(\frac{2 * \pi * (hour - 12)}{2 * P_{photo}})), 0.0]$
(3) M_2 water level (η; m)	$\eta = MSL + (AM2 * \cos(2 * \pi * (\frac{hour - PhM2}{TM2})$
(4) Water Depth (h; m)	$h = \eta - z$
(5) Light extinction coefficient (k_t; m^{-1})	$k_t = k_w + [k_{color}] + [a_{NTU} * NTU] + [a_{CHL} * CHL]$
(6) Light extinction color (k_{color}; m^{-1})	$k_{color} = a_{color} * e^{(-b_{color} * S)}$
(7) Light at bottom ($I_{z;}$ µmole m^{-2} s^{-1})	$I_z = I_0 * e^{(-k_t * h)}$
(8) Percentage of surface light at bottom ($\%I_{z;}$)	$\%I_z = (\frac{I_z}{I_0}) * 100$
(9) *Vallisneria* shoot ($C_{shoot;}$ gC m^{-2})	$\frac{dC_{shoot}}{dt} = G_{shoot} + N_{shoot} - R_{shoot} - M_{shoot} - Gz_{Shoot}$
(10) *Vallisneria* shoot growth (G_{shoot})	$G_{shoot} = P_m * [\frac{I_z}{(I_k + I_z)}] * fS_{gross} * fT_{shoot} * [1 - (\frac{C_{shoot}}{C_{max}})] * C_{shoot}$
(11) *Vallisneria* photosynthesis T effect (Tfx_{shoot})	$fT_{shoot} = IF(T_w \le T_{opt}) e^{-kT1 * (T - T_{opt})^2}$
	$fT_{shoot} = IF(T_w > T_{opt}) e^{-kT2 * (T_{opt} - T)^2}$
(12) *Vallisneria* new shoots (N_{shoot}; gC m^{-2} d^{-1})	$N_{shoot} = C_{shoot} * kN$
(13) *Vallisneria* shoot respiration (R_{shoot}; gC m^{-2} d^{-1})	$R_{shoot} = C_{shoot} * [kR * e^{KfB(T_w - T_{opt})}]$
(14) *Vallisneria* shoot mortality (M_{shoot}; gC m^{-2} d^{-1})	$M_{shoot} = C_{shoot} * kS_{loss} * fS_{loss}$
(15) *Vallisneria* shoot grazing (Gz_{shoot}; gC m^{-2} d^{-1})	$Gz_{shoot} = kGz * C_{shoot}^2$

Key to units: µmole m^{-2} s^{-1} – micromoles per square meter per second; gC m^{-2} – grams shoots per square meter; gC m^{-2} d^{-1} – grams shoots per square meter per day; hrs – hours; m – meters; and m^{-1} – per meter.

Table 25. List of *Vallisneria* model coefficients. See Buzzelli et al. (2012, 2014b) for mathematical details.

Parameter	Value	Unit	Description	Source
I_{amp}	1000	µmole m^{-2} d^{-1}	Amplitude of surface irradiance	local data
MSL	0.0	m	Mean sea level	***
TM2	12.42	hours	Period of M2 tide	NOAA Ft. Myers
AM2	0.111	m	Amplitude of M2 tide	NOAA Ft. Myers
PhM2	1.43	radians	Phase angle of M2 tide	NOAA Ft. Myers
z	-0.75	m	Sediment elevation of habitat	USGS bathymetry data
k_w	0.15	m^{-1}	Attenuation due to water	Calculated from Gallegos 2001
a_{NTU}	0.062	NTU^{-1}	Attenuation factor for turbidity	McPherson and Miller 1987
a_{CHL}	0.058	m^3 mg^{-1}	Attenuation factor for chlorophyll *a*	McPherson and Miller 1987
a_{color}	2.89	m^{-1}	Constant for salinity-color relationship	McPherson and Miller 1987
b_{color}	0.096	m^{-1}	Constant for salinity-color relationship	McPherson and Miller 1987
T_{opt}	28	°C	Optimum temperature for rate processes	Bartleson et al. 2014
KtB	0.069	$°C^{-1}$	Rate constant for temperature effect	Buzzelli et al. 1999
P_m	0.02	d^{-1}	Vallisneria max photosynthetic rate	Blanch et al. 1998
I_k	56	µmole m^{-2} d^{-1}	Vallisneria light constant	Blanch et al. 1998
kT1	0.004	unitless	Vallisneria temperature constant for photosynthesis	Buzzelli et al. 1999
kT2	0.006	unitless	Vallisneria temperature constant for photosynthesis	Buzzelli et al. 1999
kN	0.01	unitless	Vallisneria source of new shoots	Calibration
kR	0.001	d^{-1}	Vallisneria shoot respiration rate	Calibration
kS_{los}	0.01	d^{-1}	Vallisneria loss rate with salinity	Calibration
kGz	0.0002	m^2 gdw^{-1}	Vallisneria shoot grazing rate	Calibration
C_{init}	15	gdw m^{-2}	Vallisneria initial shoot biomass	Calibration - CRE data
C_{max}	100	gdw m^{-2}	Vallisneria maximum shoot biomass	Calibration - CRE data

Key to units: °C – degrees Celsius; $°C^{-1}$ – per degrees Celsius; µmole m^{-2} d^{-1} – micromoles per square meter per day; µmole m^{-2} s^{-1} – micromoles per square meter per second; d^{-1} – per day; gdw m^{-2} – grams dry weight per square meter; m – meters; m^{-1} – per meter; m^2 gdw^{-1} – square meters per grams dry weight; m^3 mg^{-1} – cubic meters per milligram; and NTU^{-1} – per turbidity.

Key to agencies: NOAA – National Oceanic and Atmospheric Administration and USGS – United States Geological Survey.

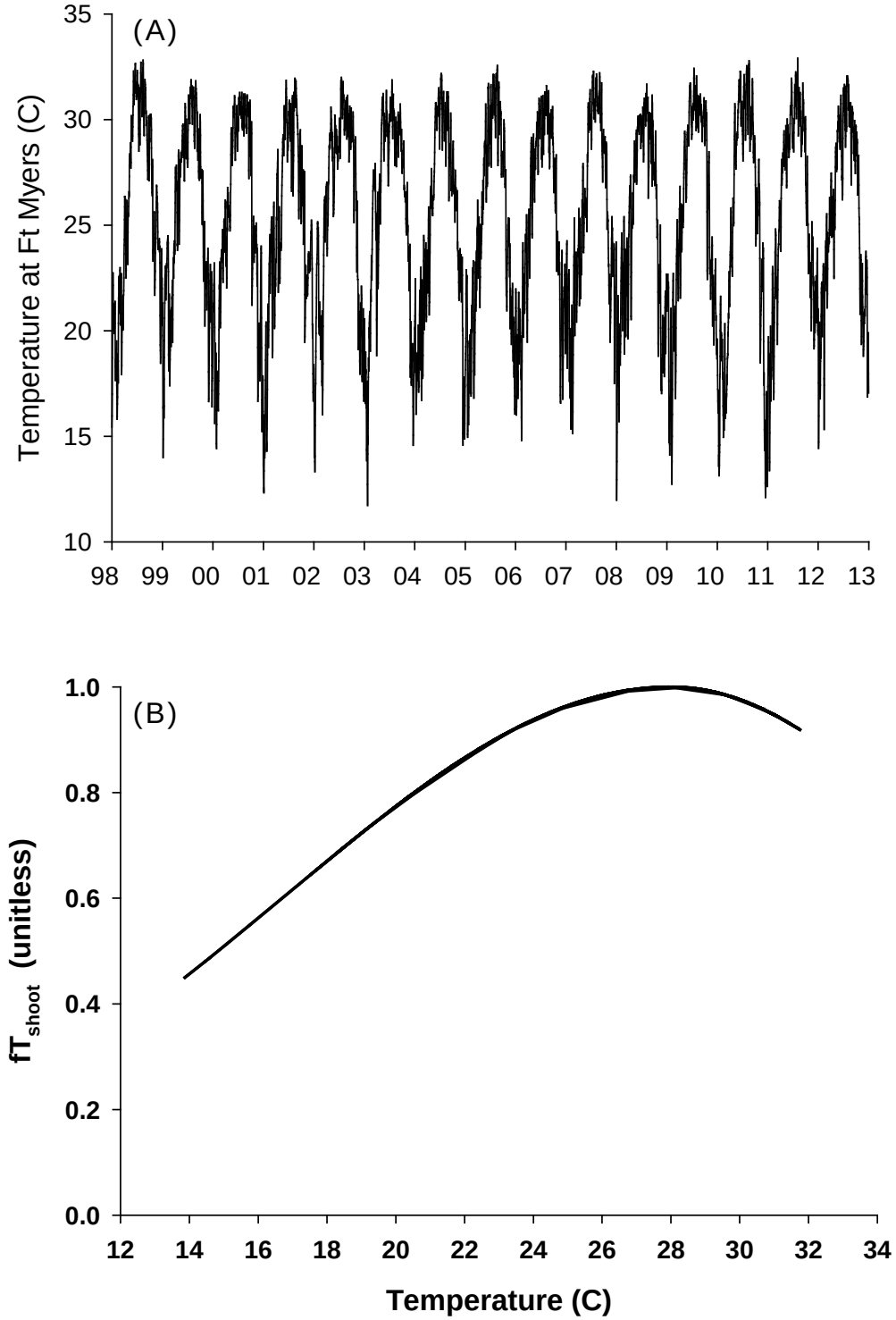

Figure 47. (**A**) Time series of daily water temperature in °C at the Ft. Myers station from 1998 to 2012. (**B**) Relationship between water temperature in °C and the shoot gross production rate (fTshoot).

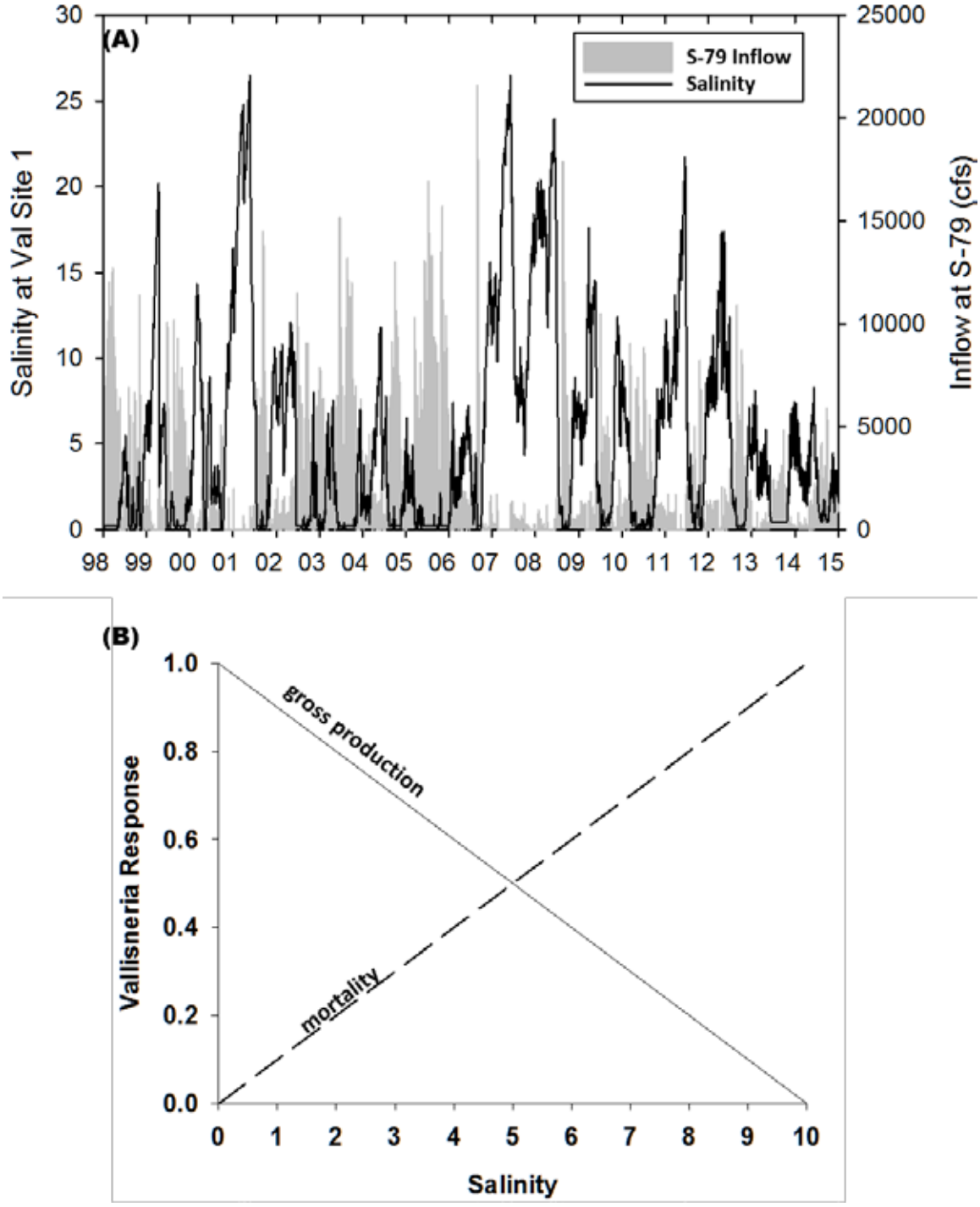

Figure 48. (**A**) Time series of daily salinity predicted for SAV monitoring Site 1 from 1998 to 2014 (black line; left axis) and freshwater inflow at S-79 (cubic meters per second [$m^3\ s^{-1}$]; grey fill; right axis). (**B**) Scalar multiplier for the negative effects of salinity on gross photosynthesis (fS_{gross}; solid) and positive effects on shoot mortality (fS_{loss}; dashed).

Irradiance at the water surface (I_0) and photoperiod (P_{photo}) were necessary to simulate variations in light (**Tables 24** and **25**). Surface light was attenuated by water depth and the total attenuation coefficient to derive irradiance at the bottom (I_z). Variable water level (η) was calculated hourly based on the amplitude (AM2), period (TM2), and phase of the M2 tide (PhM2) determined for the Ft. Myers station (**Tables 24** and **25**). Depth (h) was calculated as the difference between η and the base elevation of the habitat (z). The total attenuation coefficient for submarine light (k_t) contained contributions from pure water (k_w), color, turbidity (NTU), and chlorophyll *a* concentration (CHL) (Christian and Sheng 2003). Attenuation due to color (k_{color}) was estimated using a negative exponential relationship with salinity (**Tables 24** and **25**); McPherson and Miller 1994, Buzzelli et al. 2012). Time series for monthly average NTU and CHL were derived from monitoring data at station CES04 (**Figure 49A** and **49B**). These data are available through DBHYDRO (https://www.sfwmd.gov/science-data/dbhydro). There were specific coefficients for each of the attenuation components: k_w, attenuation factor for turbidity (a_{NTU}), attenuation factor for chlorophyll *a* (a_{CHL}), and constants for salinity-color relationship (a_{color} and b_{color}); (**Table 25**). I_z in µmoles per square meter per second (µmoles m^{-2} s^{-1}) was calculated as an exponential decline with h depending upon k_t (**Tables 24** and **25**). The percentage of surface irradiance at the bottom (%I_0) is simply a ratio between the half-saturation irradiance value (I_k) and I_0 multiplied by 100 (**Tables 24** and **25**).

The equations for *Vallisneria* were similar to those used in modeling of seagrass communities in the Southern Indian River Lagoon and the lower CRE (Buzzelli et al. 2012, 2014b). Changes in the aboveground biomass of *Vallisneria* (C_{shoot}) resulted from gross production (G_{shoot}), respiration (R_{shoot}), salinity-based mortality (M_{shoot}), and herbivorous grazing (Gz_{shoot}; **Table 24**). G_{shoot} included terms for the maximum rate of photosynthesis (P_m), light limitation using I_k, gross production ($fS_{gross;}$ **Figure 48B**), photosynthesis-irradiance relationship (fT_{shoot}), and C_{shoot} (Buzzelli et al. 2012, 2014b). The rate was also scaled using the maximum biomass (C_{shoot}/C_{max}). P_m and I_k were set at 0.02 per day and 56 µmoles m^{-2} s^{-1}, respectively (**Table 25**; Blanch et al. 1998). R_{shoot} included a basal rate of respiration (kR) and an exponential increase with water temperature (T_w; **Table 25**). M_{shoot} was calculated using the basal rate of mortality (kM) combined with shoot mortality (fS_{loss}; **Figure 48B**). Finally, the Gz_{shoot} was the product of a basal grazing rate (kGz) and the square of C_{shoot} (**Tables 24** and **25**).

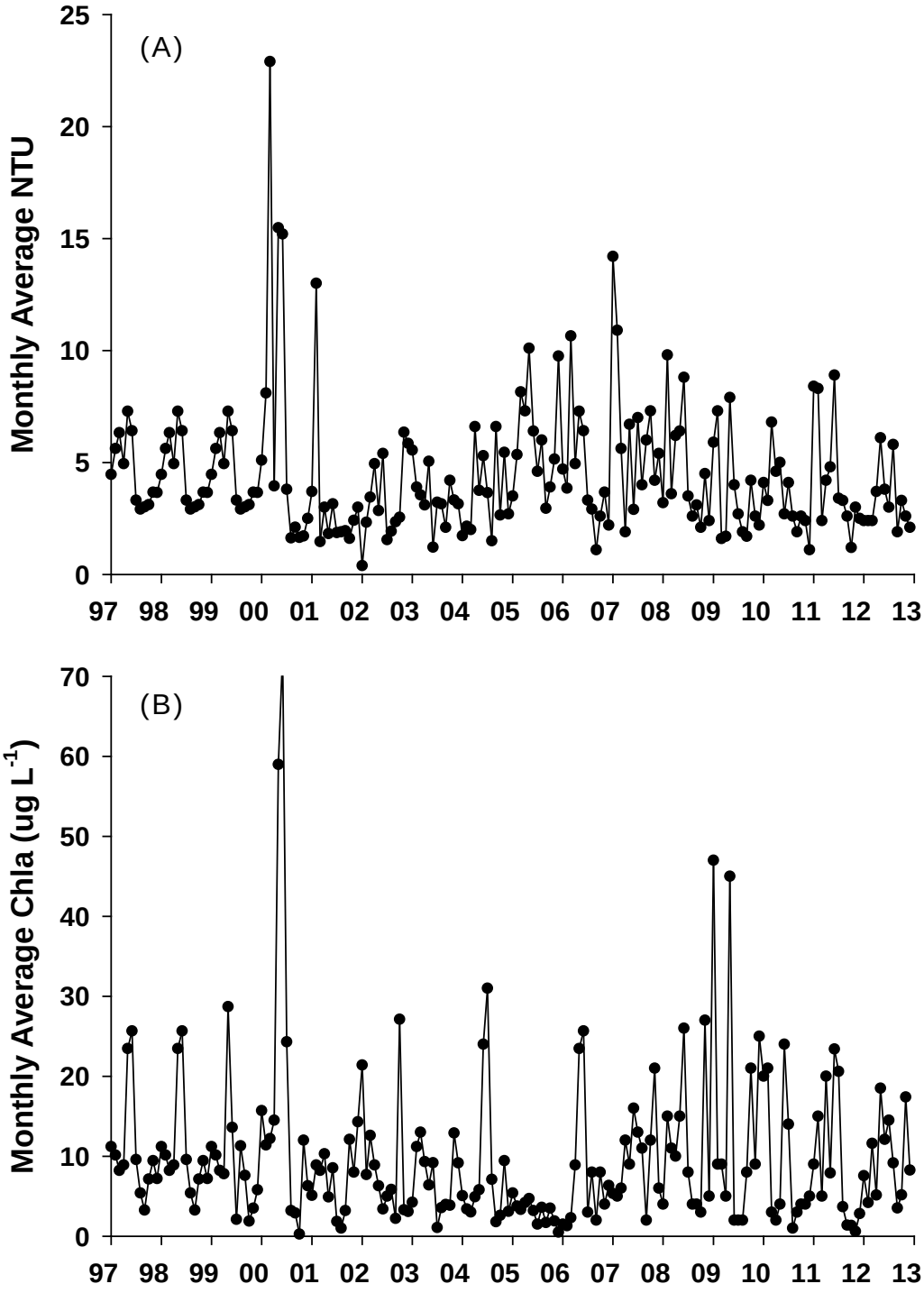

Figure 49. Monthly time series at CES04 monitoring site in the CRE for (**A**) turbidity (NTU) and (**B**) CHL.

Model Calibration, Sensitivity, and Application

Vallisneria occurs naturally in a wide range of freshwater and estuarine environments from Maine to Texas and inland to the Mississippi River (McFarland 2006). Despite its prevalence, there have been few physiological studies through which to obtain essential rate constants for model development. Calibration exercises were mindful of the spatial variations in patch densities inherent in the natural community, unavoidable sampling bias during routine monitoring, variability in the mesocosm-derived relationship between shoot densities and biomass, and the lack of information on rates of mortality and grazing specific to the CRE.

The goal of calibration was to provide the best approximation of the biomass time series derived for Site 1 near Beautiful Island in the upper CRE. The simulation of *Vallisneria* shoot biomass was calibrated by adjusting initial biomass values (C_{init}), the salinity-specific loss rate (kS_{loss}), and kGz. C_{init}, P_m, kR, kS_{loss}, and kGz were varied by ±10% and ±50% relative to the base model values in a series of sensitivity tests.

In order to help describe the conditions that account for *Vallisneria* survival versus loss, the environmental variables (inflow, temperature, salinity, and light) and *Vallisneria* shoot biomass were evaluated for each dry season from 1998 to 2014. An eight-year experimental model was generated by looping the favorable environmental conditions (salinity, turbidity, and CHL) from the 1998–1999 calendar years (2 year x 4 loops = 8 year simulations). Salinity values for each day in the dry season were systematically increased by 5% to 75% at 5% intervals over 16 model runs (base model + 15 separate simulations; 7 of which are shown in **Figure 50**). In order to identify the S-79 inflows associated with net morality of *Vallisneria*, the daily dry season salinity was systematically increased until shoot biomass at the end of the simulation was less than that at the beginning (i.e. net mortality). The resulting dry season salinity increase that led to net mortality was used to estimate the freshwater inflows using the annual regression equations from Component Study 2. Finally, the model was used to calculate the percentage of shoots lost based on the number of consecutive days where salinity was ³ 10 in multiple dry seasons.

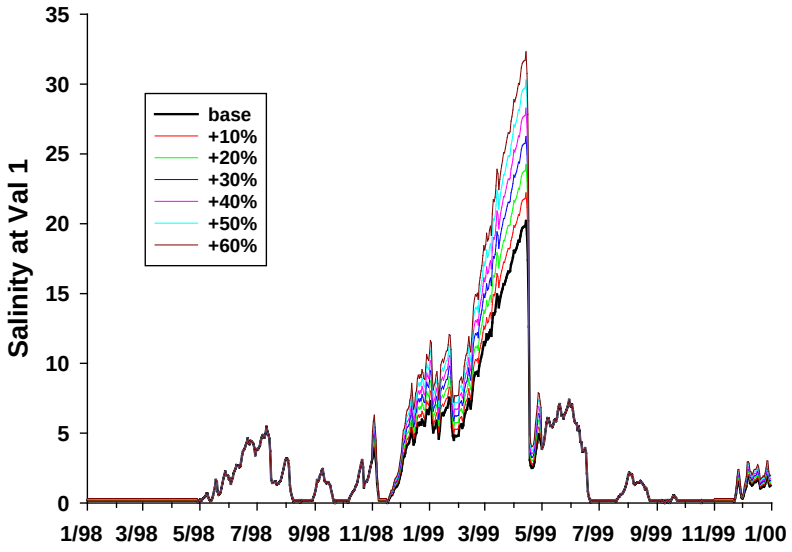

Figure 50. Time series of altered daily salinity in the dry season as input to the 1998–1999 loop model.

Results

The model output was sensitive to changes in C_{init}, P_m, kR, kS_{loss}, and kGz. Predicted shoot biomass declined by -19.5% and -69.2% when P_m was decreased by -10% and -50%, respectively (**Table 26**). The effects of increasing P_m by +10% and +50% were comparatively greater as model shoot biomass increased by +25.1% and +201.0%. Predicted shoot biomass increased by +8.6% and +52.9% when kR was decreased by -10% and -50%, respectively (**Table 26**). The effects of increasing kR by 10% and 50% led to shoot biomass decreases of -7.7% and -32.0%. Adjustments in C_{init} had diminished effects on predicted shoot biomass relative to the other parameters. Decreased values for kS_{loss} resulted in the greatest relative increase in predicted biomass (72.7% and 861.5%). The effect of increasing kS_{loss} was less dramatic (-36.0% and -81.9%). Finally, decreasing kGz by -10% and -50% increased shoot biomass by 8.9% and 70.9%, respectively. Increasing kGz had a reduced negative effect (-7.5% and -28.5% for +10% and +50% increase in kGz).

The average inflow rate through S-79 overall dry seasons averaged 1,172 cfs ranging from 52 ± 151 cfs (2008) to 5,596 ± 3,655 cfs (1998; **Table 27**). S_{val1} averaged 6.9 ± 2.9 ranging from 1.2 (1998) to ~16.5 (2001 and 2008). An average of ~7% of surface irradiance reached the bottom including a minimum of 3.3% under the greatest inflows (1998) and a maximum of 15.7% when inflow was low (2001). Submarine light extinction ranged from a maximum of ~8.0 per meter (m^{-1}) (~0% surface irradiance) in 2000 to < 1.0 m^{-1} (> 30% surface irradiance) in 2001, 2008, and 2011 (**Figure 51**). Light availability for *Vallisneria* was generally inversely related to freshwater inflow due to the dominant role of color (McPherson and Miller 1994, Buzzelli et al. 2014b, Chen et al. 2015). The exception occurred in May–June 2000 when the relative influences of both CHL and turbidity enhanced light extinction (**Figure 49**).

Average *Vallisneria* shoot density at Site 1 was variable ranging from 0.0 to 325 shoots per square meter (m^{-2}) from 1998 to 2007 (**Figure 52A**). Average density peaked in the wet seasons of 1998–1999 (200–300 shoots m^{-2}) and 2005–2006 (100–200 shoots m^{-2}). There was a decline approaching 0.0 in the 2000 dry season followed by an increase (~100 shoots m^{-2}) in the wet season before minimal shoots were observed from 2001 to 2003. Shoot density increased in the subsequent wet seasons before dry conditions in 2007 and into 2008 triggered widespread loss of shoots. The relationship between shoot density and biomass was used to generate the time series of aboveground biomass used to calibrate the model (gdw m^{-2}; $r^2 = 0.82$; **Figure 52B** and **C**).

The model provided a reasonable approximation of the shoot biomass converted from the observed densities (**Figure 53**). Although the model was sensitive to parameter values and over-predicted the biomass for the 2006 dry season, it was a responsive indicator of changes in salinity. This was evident throughout the simulation period culminating in a slight increase in shoot biomass as conditions improved from 2013 to 2014.

Table 26. Results of sensitivity tests for the effects of physiological coefficients on predicted *Vallisneria* shoot biomass. The maximum rate of photosynthesis (P_m; per day), the basal rate of respiration (kR; per day), the initial shoot biomass (C_{init}; gdw m^{-2}), the shoot loss rate due to salinity (kS_{loss}; per day), and the basal grazing rate (kGz; square meter per grams dry weight [m^2 gdw^{-1}]) were varied by +10% and +50% in independent model simulations. Simulations spanned 18 years (1997–2014 = 6,574 days). Provided are the coefficient values, the predicted biomass ranges (C_{shoot}; gdw m^{-2}), the average and standard deviations (Avg ± SD) of predicted biomass (gdw m^{-2}), and the percent difference between the base model values (base) and each sensitivity test averaged over all simulation days (%Difference = ((observed – expected)/expected)*100).

Coefficient	Sensitivity Test	Coefficient Value	Range	Avg ± SD	%Difference
P_m	Base	0.020			
	-10%	0.018	0.1–32.0	5.0 ± 5.8	-19.5%
	-50%	0.010	0.0–14.9	2.2 ± 2.7	-69.2%
	+10%	0.022	0.15–38.1	6.7 ± 7.2	25.1%
	+50%	0.030	0.2–45.8	10.5 ± 9.7	201.0%
kR	Base	0.001			
	-10%	0.0009	0.1–36.1	6.1 ± 6.7	8.6%
	-50%	0.0005	0.2–38.8	7.2 ± 7.4	52.9%
	+10%	0.0011	0.1–34.6	5.6 ± 6.4	-7.7%
	+50%	0.0015	0.1–31.1	4.6 ± 5.6	-32.0%
C_{init}	Base	15.0			
	-10%	13.5	0.1–35.3	5.7 ± 6.5	-0.9%
	-50%	7.5	0.1–35.3	5.3 ± 6.3	-5.6%
	+10%	16.5	0.1–35.3	5.9 ± 6.6	0.8%
	+50%	22.5	0.1–35.3	6.1 ± 6.7	3.4%
kS_{loss}	Base	0.01			
	-10%	0.009	0.2–36.6	7.1 ± 6.9	72.7%
	-50%	0.005	1.9–39.3	14.0 ± 7.5	861.5%
	+10%	0.011	0.0–33.5	4.8 ± 6.0	-36.0%
	+50%	0.015	0.0–14.9	1.8 ± 2.8	-81.9%
kGz	Base	0.0002			
	-10%	0.00018	0.1–38.6	6.3 ± 7.1	8.9%
	-50%	0.0001	0.2–60.9	9.6 ± 11.0	70.9%
	+10%	0.00022	0.1–32.6	5.4 ± 6.1	-7.5%
	+50%	0.0003	0.1–24.9	4.2 ± 4.7	-28.5%

Table 27. Dry season (November–April) average and standard deviations (Avg ± SD) for model variables from WY1998 to WY2014. Variables include freshwater inflow at S-79 (Q_{S79}) and the tidal basin (Q_{TB}; cfs), salinity at *Vallisneria* monitoring site 1 (S_{val1}), temperature at Ft. Myers (T; °C), total light extinction coefficient (k_t; m^{-1}), the percentage of surface light at the bottom ($\%I_0$; unitless), and model *Vallisneria* shoot biomass (C_{shoot}; gdw m^{-2}). The range of model *Vallisneria* shoot biomass for each dry season is also provided. See text for description of model input and response variables.

WY	Q_{S79} (cfs) Avg ± SD	Q_{TB} (cfs) Avg ± SD	S_{val1} Avg ± SD	T Avg ± SD	k_t Avg ± SD	$\%I_0$ Avg ± SD	C_{shoot} Range	C_{shoot} Avg ± SD
1998	5,596±3,655	1,024±679	1.2±1.9	21.3±2.5	3.6±0.5	3.3±1.4	7.8–12.2	9.2±2.8
1999	737±1,606	344±460	7.7±5.6	22.8±3.0	2.6±0.8	8.0±5.4	7.8–17.5	14.1±3.1
2000	1,412±1,766	147±135	5.5±4.6	21.7±2.9	3.5±1.0	4.3±2.5	7.6–18.5	13.5±3.4
2001	61±269	146±148	16.6±5.3	21.1±3.9	1.5±0.5	15.7±6.2	2.5–7.5	5.8±1.7
2002	440±462	125±110	7.4±2.4	22.5±3.5	2.5±0.4	7.6±2.9	1.5–3.0	2.5±0.4
2003	1,809±1,948	306±271	2.7±2.4	21.7±3.9	3.2±0.6	4.9±2.4	2.2–4.9	3.9±0.9
2004	1,358±1,360	198±190	2.8±2.0	21.1±2.9	2.9±0.4	5.3±1.7	9.8–16.4	13.6±1.7
2005	2,212±1,991	185±209	1.8±1.5	21.1±3.0	3.2±0.4	4.2±1.0	11.3–18.7	15.5±1.8
2006	3,273±3,552	185±220	2.0±1.8	21.7±3.1	3.5±0.4	3.5±1.0	17.2–35.3	26.6±5.3
2007	128±262	120±102	14.7±3.9	21.5±2.4	1.8±0.3	11.9±2.9	3.5–17.1	10.3±4.6
2008	52±151	148±132	16.5±2.2	22.2±2.7	1.9±0.5	11.4±3.5	0.3–1.1	0.8±0.3
2009	426±340	130±121	8.1±3.1	20.9±3.0	2.9±1.2	7.5±5.9	0.2–0.4	0.3±0.1
2010	1,117±1,448	344±401	5.6±3.7	20.4±3.3	2.9±0.8	5.9±2.6	0.2–0.4	0.3±0.1
2011	268±371	164±171	8.7±2.2	21.2±4.4	2.6±0.5	7.0±2.8	0.4–1.3	0.9±0.3
2012	488±695	256±304	8.2±3.9	22.4±2.5	2.4±0.5	8.4±3.3	0.2–0.8	0.5±0.2
2013	371±534	162±141	4.0±1.6	21.7±2.6	3.5±0.8	4.0±2.6	0.3–0.5	0.4±0.1
2014	168±145	168±145	4.0±1.5	22.2±2.8	3.2±0.5	4.6±1.4	1.4–2.0	1.6±0.2
Total	1,172±1,117	244±154	6.9±2.9	21.6±3.1	2.8±0.6	6.9±2.9		7.1±1.6

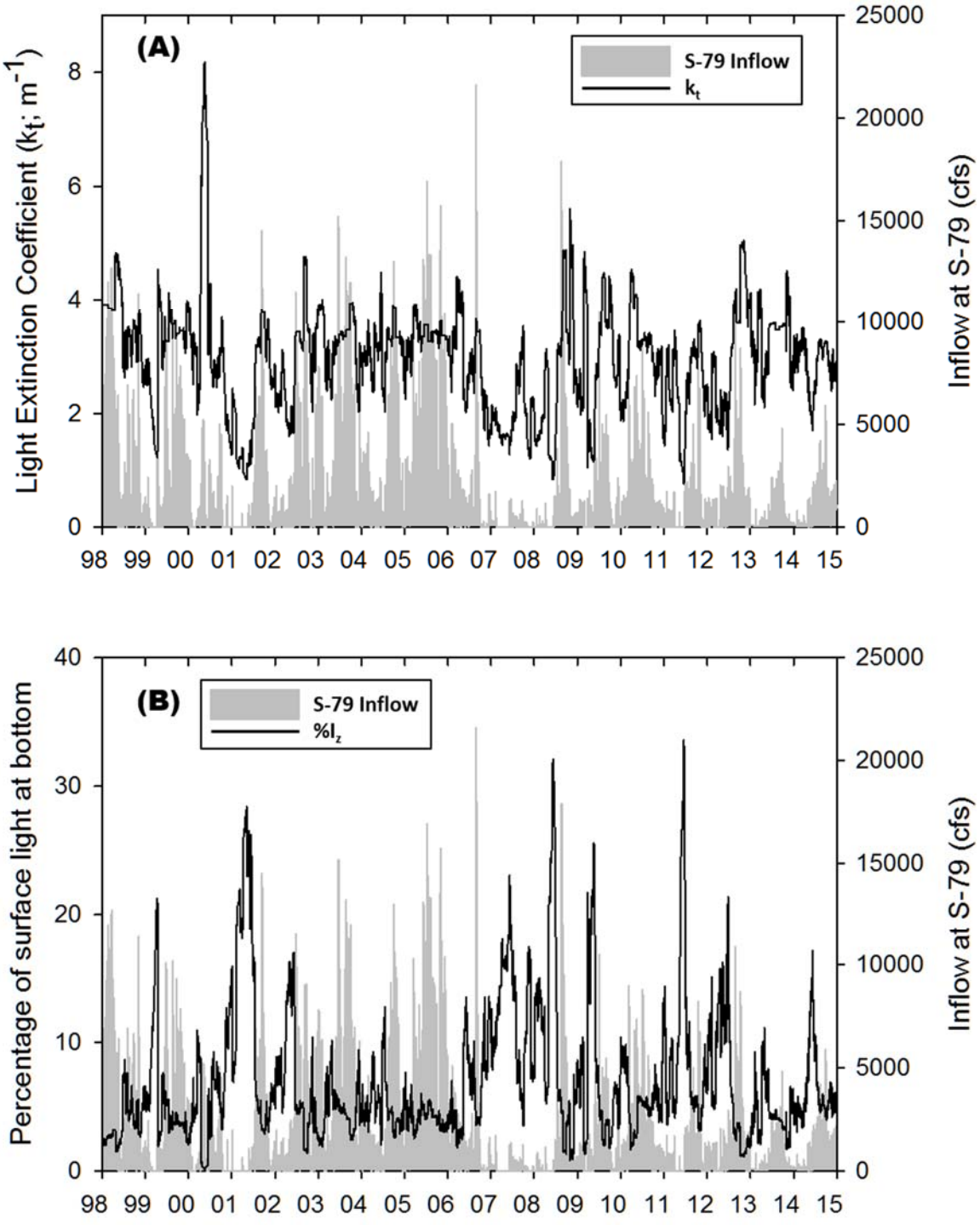

Figure 51. (**A**) Time series of the submarine light extinction coefficient (k_t; m^{-1}; left axis) and daily freshwater inflow at S-79 (cfs; right axis). (**B**) Time series of the percent of light at the bottom ($\%I_0$; left axis) and daily freshwater inflow at S-79 (cfs; right axis).

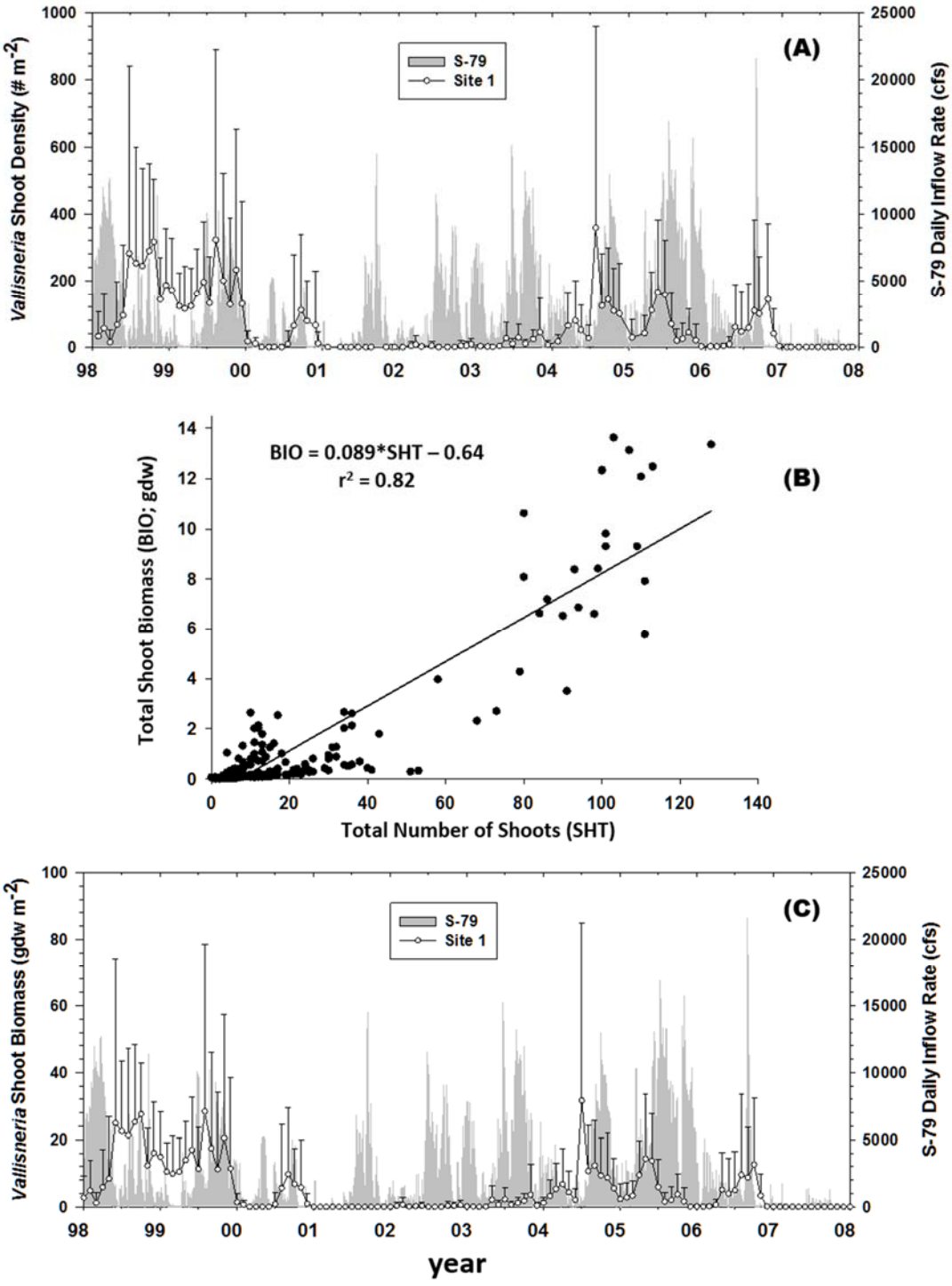

Figure 52. (**A**) Time series of *Vallisneria* shoot density (average + standard deviation) from Site 1 near Beautiful Island in the CRE. (**B**) Linear regression between total number of *Vallisneria* shoots and total dry weight biomass of shoots (grams dry weight [gdw]) from controlled mesocosm experiments. (**C**) Time series of Site 1 *Vallisneria* shoot biomass (average + standard deviation) derived by converted shoot density using the regression equation.

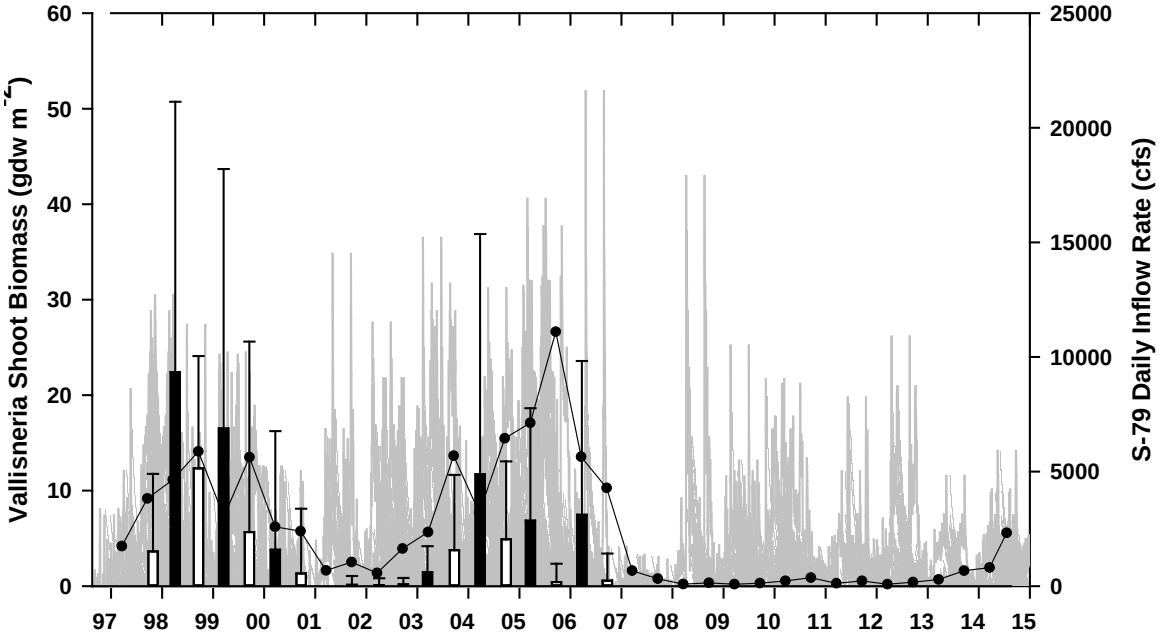

Figure 53. Time series (1998–2014) of average seasonal *Vallisneria* shoot biomass from the model superimposed on average seasonal values at Site 1 (1998–2008). Daily inflow at S-79 shown as shaded area with right axis.

Conditions from 1998 to 1999 were conducive for survival and growth of *Vallisneria* in the upper CRE (**Table 27**). Salinity increases of 5% per trial led to a linear reduction in model biomass over the eight-year experimental simulations (**Figure 54**). A 55% increase in dry season salinities resulted in a net decrease in shoot biomass at the end of the experimental simulation. The model experiment predicted that an average dry season salinity of 12 will result in net mortality of *Vallisneria* in the CRE. This value was used to estimate the associated freshwater inflows from the annual inflow-salinity relationships derived in Component Study 2. Estimated inflows associated with *Vallisneria* mortality ranged from 15 to 629 cfs (n = 14) averaging 342 ± 180 cfs.

The number of consecutive days where S_{val1} was ³ 10 ranged among 10 days (2002), 40–48 days (1999, 2000, 2009, and 2012), and 145–182 days (2001, 2007, and 2008; **Table 28**). Model results suggested that an estimated 17.6% of the *Vallisneria* shoots were lost when salinity was ³ 10 for 10 consecutive days. This value increased to 85.4% (2001) and 86.7% (2007) when salinity was elevated for a majority of the dry season. Due to the losses in 2007, initial shoot density was not great enough to calculate changes with extended times of increased salinity in 2008–2012.

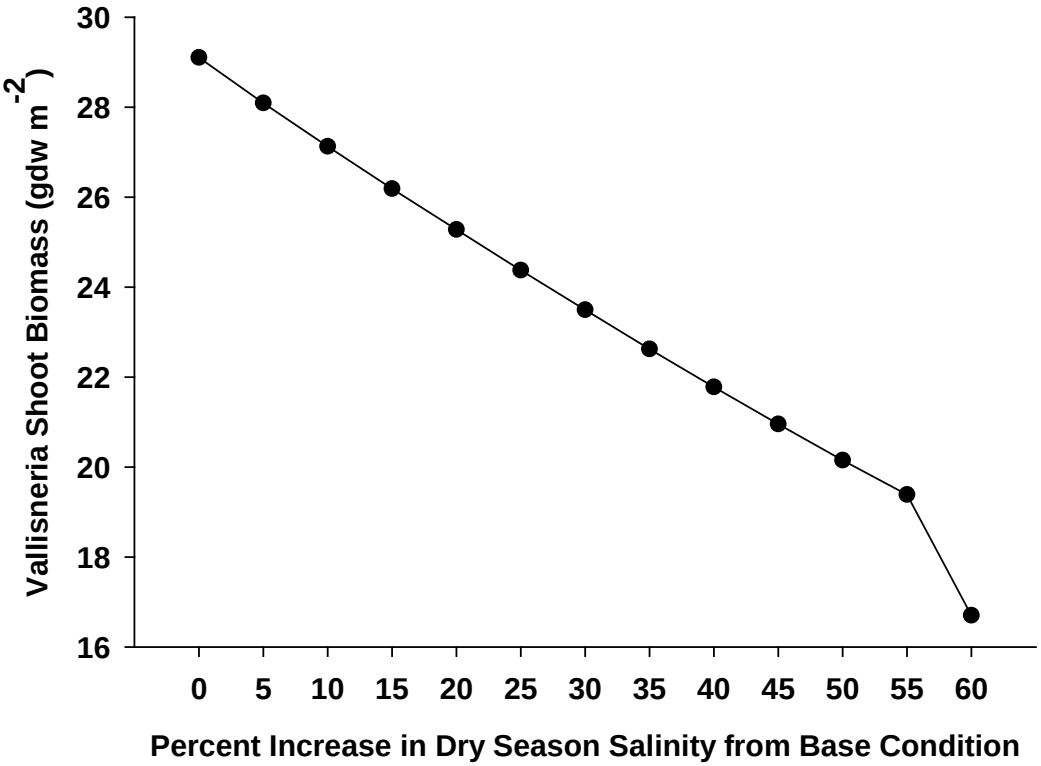

Figure 54. Plot of percent increase in dry season salinity versus average shoot biomass. A 55% increase in dry season salinity values resulted in net mortality of *Vallisneria*.

Table 28. Results from a simulation model of *Vallisneria*. Shown are dry seasons with average daily salinities ³ 10 at Monitoring Site 1 in the CRE from WY1999 to WY2012. All values based on daily salinity ³ 10 including the total number of days in the dry season, the average and standard deviation (Avg ± SD) of salinity for those days, the initial and final dates bracketing consecutive days where salinity was ³ 10, the initial shoot density, and the percentage of initial shoots lost during the consecutive days. The model biomass reaches a minimum of 0.1 gdw m^{-2}, which converts to ~8 shoots m^{-2}.

Water Year	Total Number of Days S_{val1} ³ 10	Salinity Avg + SD	Initial Date	Final Date	Consecutive Days S_{val1} ³ 10	Initial Shoot Density (# m^{-2})	% Shoots Lost
1999	53	15.4 ± 3.0	3/1/99	4/17/99	48	283	54.8%
2000	42	12.3 ± 1.2	2/17/00	3/29/00	42	222	47.3%
2001	150	18.3 ± 4.2	12/6/00	4/30/01	145	110	86.7%
2002	19	10.5 ± 0.4	4/21/02	4/30/02	10	11	17.6%
2007	174	14.9 ± 3.8	11/7/06	4/30/07	174	72	85.4%
2008	182	16.5 ± 2.2	11/1/07	4/30/08	182	9	5.4%
2009	46	12.8 ± 1.7	3/10/09	4/30/09	46	-	-
2010	26	11.1 ± 0.6	11/10/09	12/5/09	26	-	-
2011	47	11.7 ± 1.3	4/12/11	4/30/11	18	-	-
2012	50	12.9 ± 2.1	3/16/12	4/24/12	40	-	-

Discussion

The incorporation of the environmental requirements of *Vallisneria* into a resource-based approach to estuary and water management is very unique in estuarine science (Doering et al. 2002). This uniqueness emerges because (1) freshwater inflow from S-79 has been regulated since 1966; (2) low freshwater inflow in the dry season can lead to increased salinity throughout the estuary; (3) historically, *Vallisneria* habitat has been an important ecological resource in the upper CRE; and (4) *Vallisneria* sensitivity to salinity at weekly–annual time scales makes it an excellent indicator of managed freshwater inflows. This study built upon existing information to derive a model to simulate the responses of *Vallisneria* to environmental drivers (i.e. temperature, salinity, and light; Doering et al 1999, 2002, French and Moore 2003, Bartleson et al. 2014). Ecological modeling provides a pathway to incorporate the effects of multiple non-linear variables, evaluate different management alternatives, and build consensus among a variety of stakeholders (Costanza and Ruth 1998, Urban 2006, Buzzelli et al. 2015b).

The *Vallisneria* model exhibited greater sensitivity to changes in parameter values than equivalent models of seagrasses in South Florida (Buzzelli et al. 2012, 2014b). The enhanced sensitivity of the *Vallisneria* model resulted because small changes in salinity (i.e. 4 to 5) triggered large changes in photosynthesis and mortality (> 10%). By comparison, the same salinity change would alter these rates by < 3% in the model of the seagrass *Syringodium filiforme* (Buzzelli et al. 2012). Since the P_m was determined experimentally (Blanch et al. 1998), calibration focused on adjusting the basal loss rates of mortality (kS_{loss}) and grazing (kGz) to best approximate the observed shoot attributes. The present model calibration provides a suitable representation of the responses of *Vallisneria* to fluctuations in salinity from 1998 to 2014.

The combination of the environmental drivers, field monitoring data, and the calibrated model indicated that salinity was indeed the key variable affecting the survival and growth of *Vallisneria*. Although only 3 to 8% of submarine light reached the bottom, dry season salinity conditions in 1998–2000 and 2004–2006 promoted the production of shoot biomass. In contrast, an average of 11 to 15% of submarine light was available in the drought years of 2001 and 2007–2008 when *Vallisneria* declined. There were intra- and inter-annual patterns between inflow, salinity, and *Vallisneria*. Periods where *Vallisneria* biomass increased generally spanned 4 to 6 months indicative of wet season conditions with increasing freshwater inflow and decreasing salinity. Each of these periods of favorable conditions started in June or July with salinity values ranging from ~1.0 to 2.0. Periods where *Vallisneria* biomass decreased generally spanned 6 to 8 months indicative of dry season conditions that extended into May–July of the following calendar year.

The model provided an effective tool to explore and quantify both freshwater inflow and the duration of high salinity conditions that contribute to the mortality of *Vallisneria* in the CRE. While the field monitoring and Ft. Myers salinity data were used to estimate that inflows of at least 545 ± 774 cfs were associated with *Vallisneria* survival from 1993 to 1999 (Component 7), the model was used to specify the freshwater inflow associated with net mortality (342 ± 180 cfs). Furthermore, the model results demonstrated that ~50% of the *Vallisneria* shoots were lost when salinity in the *Vallisneria* habitat near Beautiful Island was ³ 10 for ~1 month. These results provide a quantitative base to assess freshwater inflow requirements for the CRE.

Component Study 9: Assessment of Dry Season Salinity and Freshwater Inflow Relevant for Oyster Habitat in the CRE

Christopher Buzzelli, Cassondra Thomas, and Peter Doering

Abstract

Short- and long-term alteration of salinity distributions in estuaries with variable freshwater inflow affects the survival, abundance, and extent of oyster habitat. The objective of this study was to evaluate salinity conditions at two locations (Cape Coral and Shell Point) in the CRE. Salinity data from the 2006–2014 dry seasons (November–April) were categorized relative to oyster habitat criteria and related to freshwater inflow. Daily salinity was within the appropriate range for oysters (10– 25) on 70.1% of the observations. Daily inflow ranged from 0 to 2,000 cfs and averaged 296 ± 410 cfs when salinity ranged from 20 to 25 at Cape Coral in the dry season. The influence of the marine parasite *Perkinsus marinus* (Dermo) is limited due to the subtropical climate where temperature is low when salinity is high (dry season) and temperature is high when salinity is low (wet season). Overall salinity patterns were favorable for oyster survival at the upstream extent of oyster habitat in the CRE.

Introduction

The distribution and abundance of eastern oyster (*Crassostrea virginica*) habitat provides an ecosystem-scale indication of estuarine status (Kemp et al. 2005). Oysters filter suspended solids coupling the benthos to the water column while providing habitat for a variety of fauna (Tolley et al. 2006, Coen et al. 2007). The survival and growth of oysters are influenced by covariations in temperature, salinity, food supply, and mortality (Stanley and Sellers 1986, Bataller et al. 1999). Oyster habitat is declining worldwide through multiple interactive factors including over-harvesting, disease, sedimentation, and altered salinity patterns (Beck et al. 2011).

Salinity is a primary environmental factor affecting the eastern oyster in the Gulf of Mexico estuaries with optimal values varying from 10 to 30 (Shumway 1996, Livingston et al. 2000, Barnes et al. 2007, Wang et al. 2008; **Table 29**). A functioning oyster habitat is composed of the population cohorts (larvae, juvenile, and adults), protistan parasites (e.g. *Perkinsus marinus* or Dermo), the epibiotic community, and resident and transient consumers each with particular life histories and salinity tolerances (Dekshenieks et al. 2000, Tolley et al. 2006). Because the oyster life cycle is sensitive to both the timing and magnitude of variations in salinity, evaluating potential responses of oyster habitat to variable freshwater inflow offers a biotic tool for water management (Chamberlain and Doering 1998b, Volety et al. 2009).

Table 29. Summary of salinity tolerances for different oyster life stages.

Life Stage	Salinity Ranges			Citation
	Optimal	Sub-Optimal	Lethal	
Spawning	[3] 12		0–10,40	Woodward-Clyde 1999, RECOVER 2014
Egg Development	23–29	5–32		Clark 1935
Larvae	23–27	12–32	< 12	Kennedy 1991, Dekshenieks et al. 1993, 1996
Spat				
Survival	10–27.5	5–32	< 5	Loosanoff 1953, RECOVER 2014
Setting	16–18	9–29		Loosanoff 1965, Kennedy 1991
Juvenile				
Survival	10–20	5–32		Woodward-Clyde 1999
Predation Avoidance	< 20		20–25	Butler 1954, Wells 1961, Mackin and Hopkins 1962, Galtsoff 1964, Zachary and Haven 1973
Adult				
Survival	10–30	5–40	< 7	Loosanoff 1953, Mackin and Hopkins 1962, Brown and Hartwick 1988, Fisher et al. 1996
Disease avoidance	< 5			La Peyre et al. 2009

Conventional wisdom suggests reduced freshwater inflow leads to increased salinity, which negatively impacts oyster populations (Powell et al. 2003, Turner 2006). The introduction of marine parasites and predators is assumed to account for oyster losses (Stanley and Sellers 1986, Livingston et al. 2000, Powell et al. 2003, LaPeyre et al. 2003, Buzan et al. 2009, Petes et al. 2012). However, while episodic freshwater inputs reduce parasite activity, oyster filtration rates also can be suppressed by decreased salinity (Pollack et al. 2011). The ability of oysters to close their shells and alter pumping rates allows them to survive under fluctuating salinities (Loosanoff 1953, Davis 1958, Andrews et al. 1959). Patterns can be complicated as both oyster condition and long-term harvests around the Gulf of Mexico are positively correlated to salinity (Turner 2006, Guillian and Aguirre-Macedo 2009).

Turner (2006) hypothesized that the effects of salinity on oyster yields depend upon both the historical conditions and current trajectory for salinity in a particular estuary. It has been suggested that increasing total freshwater input to the Gulf of Mexico estuaries for natural resource protection probably would not increase estuarine oyster harvests (Hofstetter 1977, Turner 2006). Therefore, short- and long-term alteration of salinity distributions in Gulf of Mexico estuaries with variable inflow can have implications for oyster survival, abundance, and habitat extent (Chamberlain and Doering 1998a, Wang et al. 2008, Volety et al. 2009, Pollack et al. 2011).

The objective of this research component was to evaluate salinity conditions at two locations with oyster habitat in the CRE. The two locations are Cape Coral and Shell Point near the mouth of the CRE (**Figure 55**). Salinity data from the 2006–2014 dry seasons (November–April) were categorized relative to oyster habitat criteria and related to freshwater inflow at S-79 at the head of the CRE.

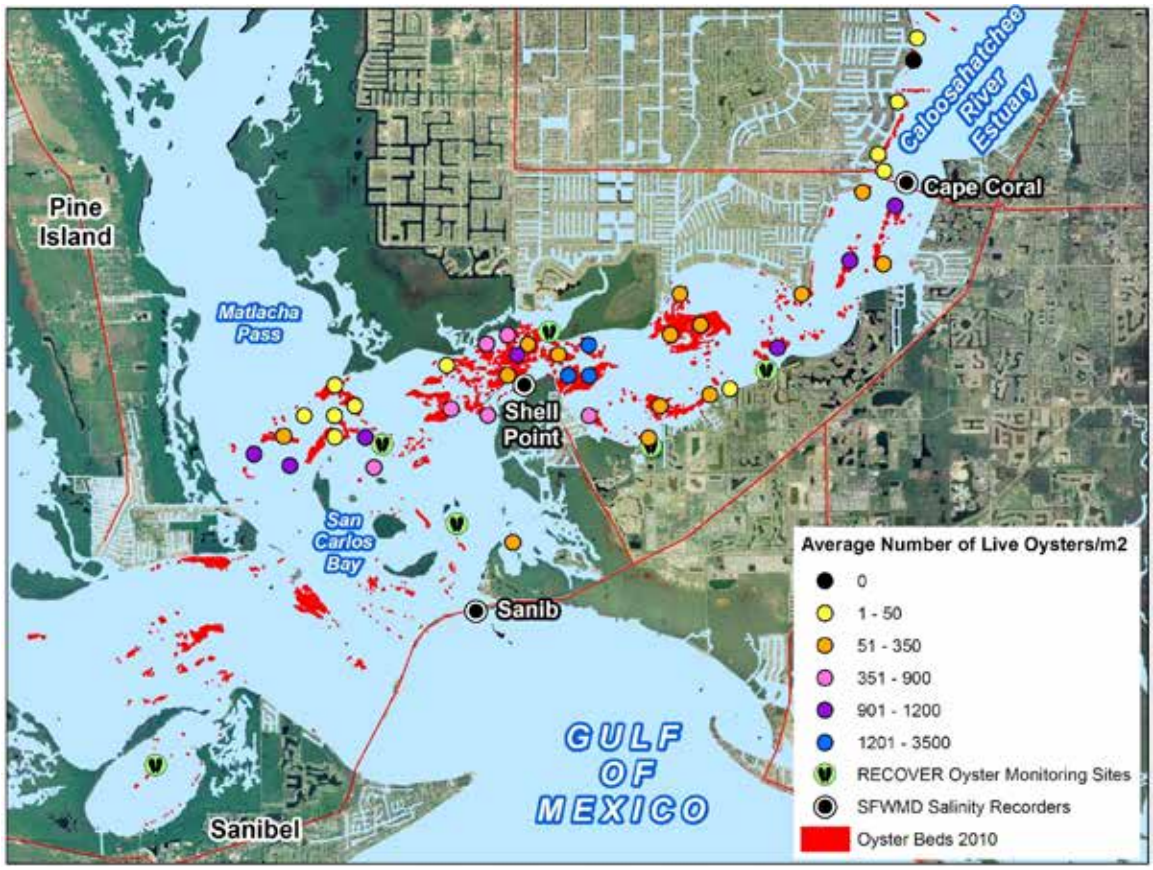

Figure 55. Location map for Cape Coral and Shell Point sampling sites, oyster habitat derived from side-scan mapping (red), and average densities (colored circles) in the lower CRE.

Methods

Oyster habitat in the CRE was mapped in 2010 using side-scan sonar as part of CERP (RECOVER 2012). This effort resulted in estimates of the extent and magnitude of oyster habitat. The benthic sampling effort used a four-prong approach: (1) calibration of the side-scan sonar and Quester Tangent Sideview Classification software in known oyster reef areas with varying substrate types, (2) remote sensing, (3) field intensive ground truth data to classify benthic habitat types, and (4) extensive mapping and quantitative assessment of live and dead reefs and oyster shell lengths of live oyster reefs. The mapping effort resulted in an estimated 847 acres (3.7%) of bottom classified as "oyster" habitat in the lower CRE. Although there were isolated patches located in the middle estuary, the upstream limit for mapped oyster habitat was near Cape Coral. Oyster habitat was denser and more widespread near Shell Point (**Figure 55**).

Salinity data collected at Cape Coral and Shell Point were used to assess estuarine conditions for oyster habitat. The POR for salinity data matched that for the monitoring of oyster population attributes in the CRE (2005–2014). Average daily salinity values at these locations were merged with average daily freshwater inflow at S-79. These data were used to generate time series (daily) and regressions between inflow and salinity at each station (monthly). Additionally, the data were categorized by water year and season (dry versus wet) with analyses focused on the dry season days.

In general, oyster growth and survival are maximized if salinity varies from 10 to 25 (**Table 29**; Loosanoff 1953, Shumway 1996, Dekshenieks et al. 2000, Barnes et al. 2007). A conceptual model of oyster responses to salinity and freshwater inflow was developed for the CRE (**Figure 56**; Buzzelli et al. 2013d). Based on this conceptualization, salinity data at Cape Coral and Shell Point were split into five categories: < 10, 10–15, 15–20, 20–25, and > 25. The number and percentage of dry season days where salinity values were within each of these categories were calculated. The averages and standard deviations for salinity and freshwater inflow associated with each of these salinity classes were also calculated for each of the downstream locations. The freshwater inflow associated with dry season salinity values of 20 to 25 at the upstream extent of oyster habitat (e.g. Cape Coral) was quantified.

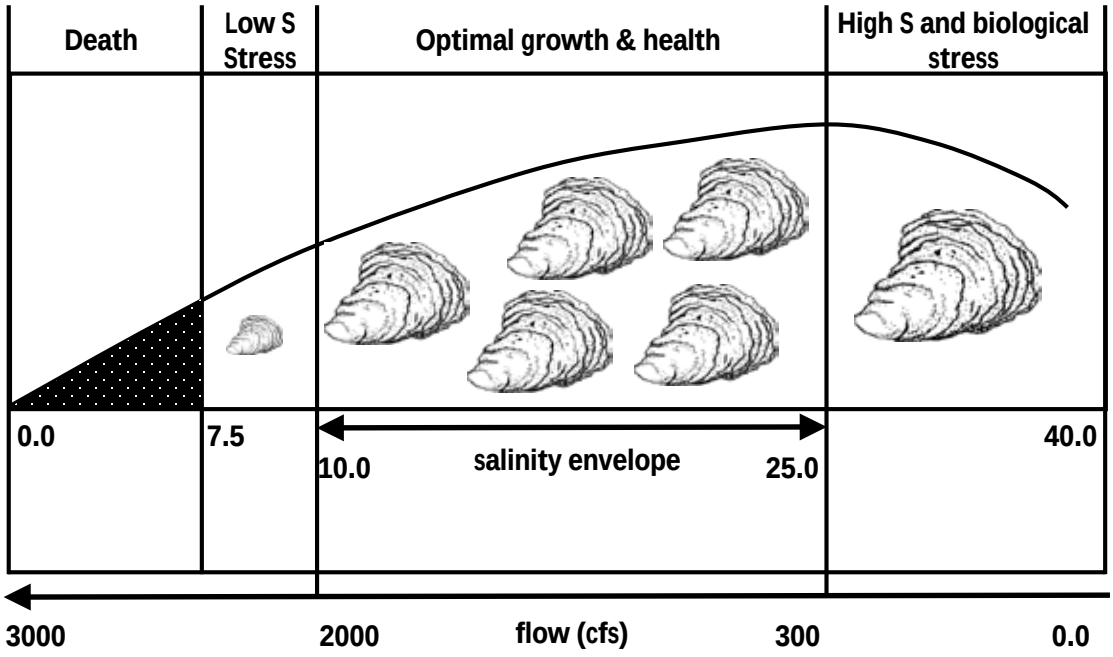

Figure 56. Conceptual model of the effects of salinity (S) on oyster survival and growth. Generalized freshwater inflows that could account for the target salinity range are shown at the bottom.

Results

Freshwater inflow ranged from near zero to > 20,000 cfs throughout the POR (**Figure 57**). Salinity at both locations increased with decreased inflow as the highest values were observed from January 2007 to August–September 2008. On average, salinity at Shell Point was ~1.5 times greater than at Cape Coral. Dry season salinity ranged from 1.1 to 32.2 and averaged 19.8 ± 5.7 at Cape Coral (**Table 30**). Wet season salinity at Cape Coral ranged from 0.1 to 33.0 and averaged 12.6 ± 9.9. At Shell Point, salinity ranged from 12.0 to 36.9 and averaged 29.1 ± 4.1 in the dry season and 1.0 to 37.4 and 23.4 ± 8.6 in the wet season.

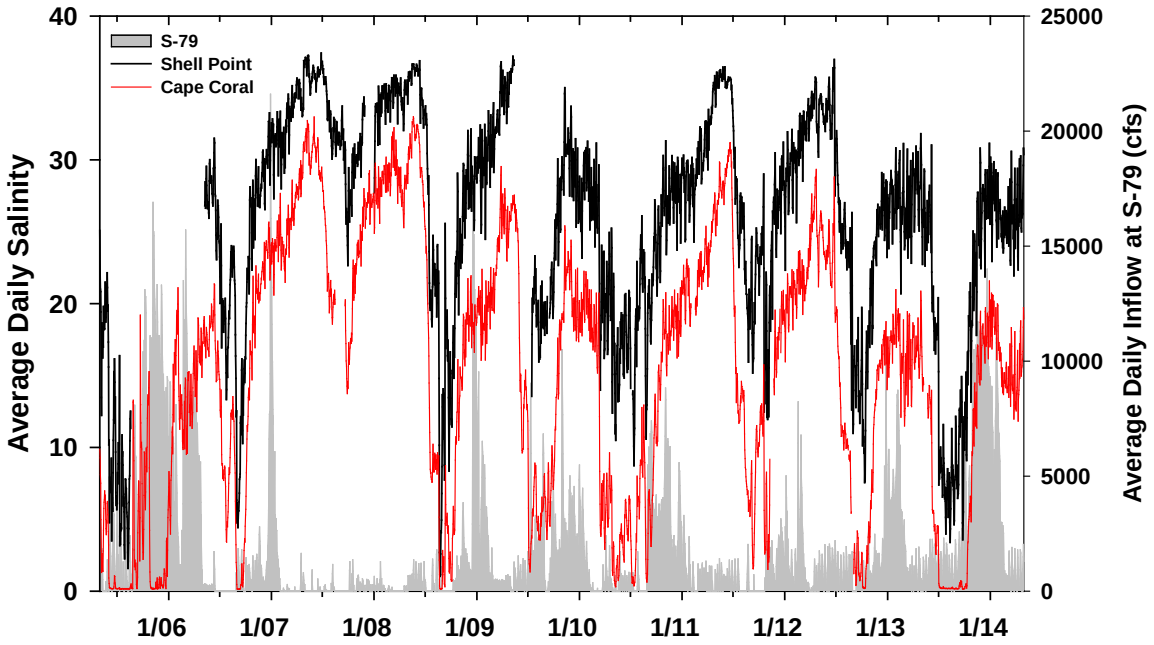

Figure 57. Time series of average daily freshwater inflow at S-79 (cfs; right axis; shaded fill) and salinities at Cape Coral (red) and Shell Point (black) from May 1, 2005, to April 30, 2014.

Table 30. Seasonal ranges, averages (Avg), and standard deviations (SD) for salinity values recorded at Cape Coral and Shell Point from 2005 to 2014.

Station	Season	Range	Avg ± SD
Cape Coral	Dry	1.1–32.2	19.8 ± 5.7
	Wet	0.1–33.0	12.6 ± 9.9
Shell Point	Dry	12.0–36.9	29.1 ± 4.1
	Wet	1.0–37.4	23.4 ± 8.6

Salinity was < 10 at Cape Coral for 234 or 13% of dry season days from 2005 to 2014 (**Table 31**). By contrast, there were 299 days (16.8%) where salinity was > 25 at this location. The average and standard deviation for freshwater inflow were 90 ± 273 cfs when dry season salinity was > 25. Daily salinity was within the desired range for oyster survival (10 to 25) on 70.1% of the observations. Daily inflow ranged from 0 to 2,000 cfs and averaged 296 ± 410 cfs when salinity ranged from 20 to 25 at Cape Coral in the dry season. While dry season salinity was never < 10 at Shell Point, it exceeded 25 for 1,266 or 83.3% of the days (**Table 32**). Salinity at Shell Point was within the 10 to 25 range on 16.8% of the days within the period of record.

Table 31. The number (n) and percentages (%) of dry season days with measured average (Avg) daily salinity values (± standard deviation [SD]) at Cape Coral that were < 10, 10–15, 15–20, 20–25, and > 25 from 2005 to 2014. Included are descriptive statistics (range; Avg ± SD) for salinity and freshwater inflow at S-79 (cfs) for each salinity class.

Salinity Class	n	%	Salinity		Inflow at S-79	
			Range	Avg ± SD	Range	Avg ± SD
<10	234	13.1	0.15-10.0	4.5 ± 3.3	0–15,700	4,002 ± 2,984
10–15	221	12.4	10.1-15.0	13.2 ± 1.4	0–9,030	1,068 ± 981
15–20	606	34.0	15.0-20.0	17.6 ± 1.4	0–6,990	670 ± 693
20–25	422	23.7	20.0-25.0	22.3 ± 1.4	0–2,000	296 ± 410
>25	299	16.8	25.0-32.2	27.7 ± 1.6	0–2,030	90 ± 273
Total	1782	100.0	0.15-32.2	18.1 ± 7.1	0–15,700	967 ± 1,721

Table 32. The number (n) and percentages (%) of dry season days with measured average (Avg) daily salinity values (± standard deviation [SD]) at Shell Point that were < 10, 10–15, 15–20, 20–25, and > 25 from 2005 to 2014. Included are descriptive statistics (range; Avg ± SD) for salinity and freshwater inflow at S-79 (cfs) for each salinity class. (Note: NA – not applicable.)

Salinity Class	n	%	Salinity		Inflow at S-79	
			Range	Avg ± SD	Range	Avg ± SD
<10	0	0.0	NA	NA	NA	NA
10-15	13	0.9	10.3–14.9	13.1 ± 1.4	264–10,030	4,696 ± 2,760
15-20	62	4.1	15.1–20.0	17.9 ± 1.4	256–5,990	2,537 ± 1,449
20-25	179	11.8	20.1–25.0	23.2 ± 1.3	0–9,030	1,243 ± 1,203
>25	1266	83.3	25.0–36.9	30.0 ± 3.0	0–6,990	428 ± 567
Total	1520	100.0	10.3–36.9	28.6 ± 4.4	0–15,700	967 ± 1,721

Discussion

Overall salinity patterns were favorable for oyster survival at the upstream extent of oyster habitat in the CRE (i.e. Cape Coral). Dry season salinity averaged 19.8 and was within the 10 to 25 range ~70% of the time. Oyster habitat is more widespread with average densities of ~1,000 oysters m^{-2} in the lower CRE around Shell Point. This is despite the fact that salinity exceeded 25 for > 80% of the time in this location. Thus, the assertion that salinity values > 25 are potentially detrimental to oysters in the lower CRE was difficult to support.

The historical contention that increased salinity can negatively affect oyster populations may not be relevant for oyster habitat in the CRE. This contention is supported by studies in the northern Gulf of Mexico that demonstrated that an upper salinity threshold of 17 to 25 could damage oysters in Apalachicola Bay (Petes et al. 2012). Damage occurs through the increased activity and prevalence of the marine, oyster-specific disease Dermo as an impediment to the health, distribution, and density of oysters. However, this may be limited in the CRE due to the subtropical climate where temperature is low when salinity is high (dry season), and temperature is high when salinity is low (wet season). This contrast greatly inhibits the impact of Dermo. In fact, laboratory experiments, field studies, and simulation models support this understanding (LaPeyre et al. 2003, Buzzelli et al. 2013d). While Dermo can be detected in large percentage of individual oysters from the monitoring locations in the lower CRE, infection intensity levels are generally very low (RECOVER 2014).

Using oyster habitat properties as indicators of inflow and salinity in the CRE might be limited. First, the influence of freshwater inflow on salinity is reduced in polyhaline (18 to 30) areas of estuaries including the CRE (Qiu and Wan 2013). This is due to the effects of tidal exchange and wind on patterns of circulation. Most of the oyster habitat is located ~40 km downstream from the dominant source of freshwater inflow (S-79). Second, the effects of the marine parasite Dermo on oyster populations are muted. Third, the role of predators with increased salinity in the CRE is largely unknown.

Component Study 10: Ecohydrological Controls on Blue Crab Landings and Minimum Freshwater Inflow to the CRE

Peter H. Doering and Yongshan Wan

Abstract

A long-term record (28 years) was used for blue crab landings in the CRE to establish relationships between (1) changes in hydrology and changes in water resource function and (2) the magnitude of the functional loss and time to recover. Annual catch per unit effort (CPUE), computed from monthly landings of crabs and measures of fishing effort, represented the resource function. Annual landings expressed as both unadjusted and de-trended CPUE were found to be significantly correlated with hydrologic variables, rainfall and freshwater inflow, during the previous year's dry season. Increases in CPUE from one year to the next were also positively related to dry season rainfall in the first of the two years. Geometric mean functional regressions and Monte Carlo simulations were used to identify the dry season rainfall associated with losses of water resource function (CPUE) that required 1, 2, or 3 years of average dry season rainfall to recover. A spectral analysis indicated that time series of both dry season rainfall and blue crab catch had periodicities of 5.6 years. A Monte Carlo analysis revealed that the rainfall associated with two and three year recoveries had return intervals of 5.8 and 8.2 years, respectively.

Introduction

Estuaries are among the most productive (Nixon et al. 1986) and economically important ecosystems on earth, supporting both commercial and recreational fisheries (Copeland 1966, Seaman 1988). The critical role of freshwater inflow in supporting estuarine productivity is well recognized (Copeland 1966, Nixon 1981, Nixon et al. 2004, Wetz et al. 2011, Montagna et al. 2013). In the early 1970s, Sutcliffe (1972, 1973) presented correlations between discharge from the St. Lawrence River and lagged landings of lobster, halibut, haddock, and soft shell clams from the Gulf of St. Lawrence. These relationships established a link between freshwater discharge and production at higher trophic levels.

Since that time, numerous studies have found similar correlations between river discharge or rainfall and recruitment or catch of fish and shell fish (Drinkwater and Frank 1994, Robins et al. 2005) including in Florida for pink shrimp (Browder 1985), blue crabs, and oysters (Meeter et al. 1979, Wilber 1992, 1994). Reductions in freshwater inflow from droughts (Dolbeth et al. 2008, Wetz et al. 2011) and the construction of dams (Aleem 1972, Baisre and Arboleya 2006) have been associated with reduced fisheries landings. These studies suggest that correlations between river flow and rainfall and fish catch are real rather than spurious. While the underlying mechanisms accounting for these correlations are not clearly understood, Robins et al. (2005) reviewed the literature and identified the following three hypotheses: (1) The food chain hypothesis is basically an agricultural argument whereby nutrients in freshwater discharge enhance food supplies resulting in better growth and survival (e.g. Loneragan and Bunn 1999); (2) a hydrodynamically-based alternative argues that freshwater discharge and the associated circulation may increase the size of retention areas and enhance recruitment (Gillanders and Kingsford 2002); and

(3) inflows may change spatial distribution and influence catchability (Loneragan and Bunn 1999).

In the State of Florida water resource protection rules are often based on harm standards. An MFL protects a water body from "significant harm" caused by further withdrawals. Significant harm "means the temporary loss of water resource functions, which result from a change in surface or ground water hydrology, that takes more than two years to recover…" (Subsection 40E-8.021(31), Florida Administrative Code). Establishing a water resource protection rule requires quantitative relationships between (1) changes in hydrology and changes in resource function and (2) the magnitude of resource loss and time to recover. Most of the MFLs that SFWMD has established contain a "return frequency" (SFWMD 2014). This concept recognizes that significant harm may happen naturally, at a frequency associated with the occurrence of a particular level of drought.

Most approaches to establishing freshwater inflow requirements are ultimately resource based by quantifying the relationships between freshwater inflow, estuarine conditions, and biological resources (Chamberlain and Doering 1998b, Alber 2002, Palmer et al. 2011). The freshwater requirements of estuarine fisheries are often included in the planning, allocation, and management of water resources (Robins et al. 2005). The fisheries themselves can be economically important. Their dependence on freshwater inflow is comprehensible to a wide variety of stakeholders (Alber 2002) and illustrates both the ecological and economic importance of freshwater supplies to estuaries (Copeland 1966).

In this component, we established quantitative relationships between hydrologic variables (rainfall and freshwater inflow) and commercial blue crab landings in Lee County, Florida. Secondly, we related reductions in catch to recovery time under average hydrologic conditions. Lastly, we analyzed periodicity in the time series of hydrologic and crab catch data to investigate return frequency.

The blue crab is an estuarine dependent macroinvertebrate that supports valuable recreational and commercial fisheries along the Atlantic and Gulf coasts (Guillory 2000, Mazzotti et al. 2006, Murphy et al. 2007). Blue crab, common in the crab trap fishery in the CRE, has historically had large and consistent landings within the estuary (Mazotti et al. 2006). It is classified as "highly abundant" by NOAA's Estuarine Living Marine Resources program (Nelson 1992). In 2003, licensed crab fishers in Lee County numbered 183 and the number of licensed crab traps was over 63,000 (FWRI 2003). This fishery expends a large effort and yields large numbers of crabs for local and distant consumers while supporting a valuable local economic employment opportunity.

Methods

Study Area

The CRE, a portion of the C-43 Canal (upstream of S-79), and Lee County are located on the southwest coast of Florida (**Figure 58**). The C-43 Canal runs 67 km from Lake Okeechobee to the Franklin Lock and Dam (S-79). S-79 separates the fresh water from the CRE, which terminates 42 km further downstream at Shell Point. The system has been altered to provide for navigation, water supply, and flood control on both a local and regional scale (Chamberlain and Doering 1998a, Doering et al. 2006). The river has been straightened and deepened and three water control structures (S-77, S-78 and S-79) have

been added (Antonini et al. 2002). The Franklin Lock and Dam (S-79) was added in part to act as a salinity barrier at the head of the estuary (Flaig and Capece 1998). The historic river (now the C-43 Canal) has also been artificially connected to Lake Okeechobee to convey releases of water to tide for the purpose of regulating water levels in the lake. The estuarine portion of the system has also been modified: a navigation channel has been dredged (Antonini et al. 2002) and a causeway has been built across the mouth of San Carlos Bay.

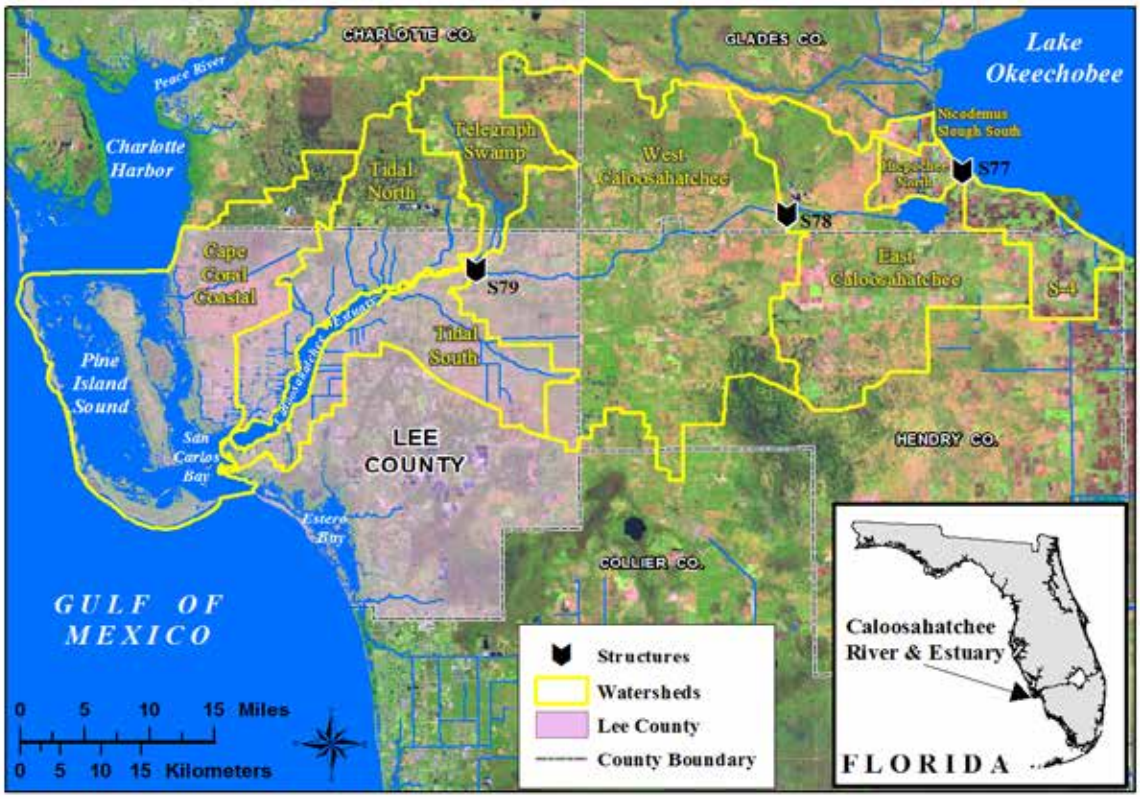

Figure 58. Location of Lee County and the Caloosahatchee River and CRE. Over 60% of land area in Lee County drains into the CRE and San Carlos Bay.

Inflow Characteristics

Major surface water inflows to the estuary come from Lake Okeechobee, the C-43 Basin upstream of S-79 (S-4 Basin, and East and West Caloosahatchee subbasins) and the Tidal Basin (i.e. the Telegraph Swamp, Tidal North, and Tidal South subbasins) located between S-79 and Shell point (**Figure 58**). Over the long term (1997–2014) the annual total surface water inflow from these three sources averages 1.8×10^6 ac-ft with 31.6% coming from Lake Okeechobee, 47.6 % from the Caloosahatchee Basin, and 21% from the Tidal Basin (Buzzelli et al. 2015a).

Data Sources

Monthly landings of blue crabs in Lee County for the period of November 1984 through December 2013 were obtained from the Florida Fish and Wildlife Conservation Commission's Florida Wildlife Research Institute in St. Petersburg, Florida (**Figure 59**). Fisherman are asked to report the weight of hard and soft shell crabs caught and the number

of traps pulled on a per trip basis. The number of traps pulled is not always reported and is estimated when missing (Murphy et al. 2007). Daily rainfall (inches) for Lee County and daily discharge (cfs) at S-79 were obtained from SFWMD's DBHYDRO (https://www.sfwmd.gov/science-data/dbhydro). Inflows from the Tidal Basin were predicted using a rainfall-runoff model calibrated to five years of measured discharge data from tidal creeks (Wan and Konya 2015). Total discharge to the estuary was taken as the sum of discharge at S-79 and inflows from the Tidal Basin.

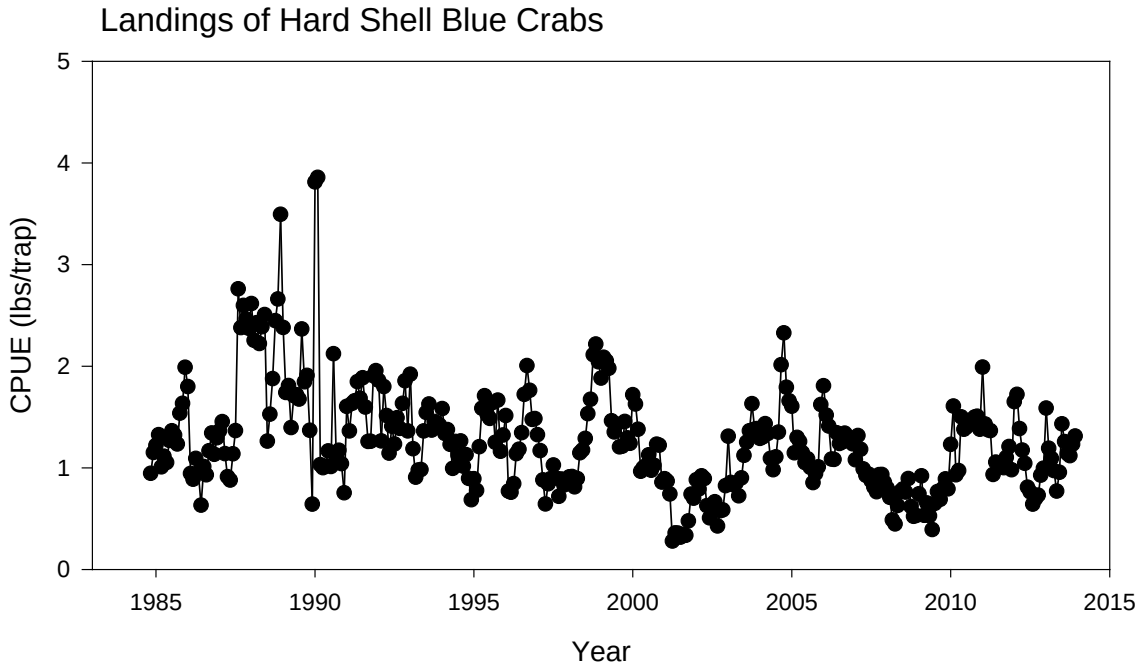

Figure 59. Monthly landings of hard shell blue crabs in Lee County Florida. Data from the Florida Fish and Wildlife Conservation Commission's Florida Wildlife Research Institute. (Note: lbs/trap – pounds per trap.)

Relationships between Hydrologic Variables and Blue Crab Catch

All time series were expressed in terms of water years. For example the water year 1998 begin on May 1, 1997, and ends April 30, 1998. The advantage of defining the time series on the basis of water year is that each 12-month period contains one full wet season (May–October) and one full dry season (November–April). The POR for analysis was 28 years (WY1986–WY2013). Monthly landings of crabs (pounds [lbs] hard, lbs soft) and measures of fishing effort (number of trips and number of traps pulled) were summed to produce annual totals. From these, annual estimates of CPUE were computed. CPUE was defined as lbs of crab (hard or soft) per trap (e.g. lbs of hard shell crabs per total number of traps pulled). Rainfall in Lee County, discharge at S-79, and total discharge (Tidal Basin + S-79) were also expressed on both an annual and seasonal (dry and wet) basis. To allow for examining the effects of previous years of rainfall and discharge on a current year's CPUE, the POR for hydrologic variables ran from WY1981 to WY2013.

Statistical Analyses

Statistical analyses were conducted using SAS version 9.3. Following Wilber (1994), annual estimates of CPUE for hard and soft shelled crabs were tested for association with

rainfall in Lee County and discharge (at S-79 and total discharge) at annual lags of zero to five years by calculating the Pearson Correlation coefficient. A lag of 0 indicates that the current year's CPUE was paired with the current year's rainfall or discharge. At a lag of 1, CPUE was correlated with the previous water year's rainfall or discharge.

When a correlation using unadjusted data was statistically significant, each time series involved was tested for long-term trend (linear increase or decrease over time) using least squares linear regression. If significant, a de-trended time series was obtained from the residuals of the least squares regression of CPUE on rainfall or flow. This procedure yielded a time series of deviations from the long-term mean (de-trended residuals). The time series were also tested for autocorrelation at a lag of one year. If statistically significant, autocorrelation was removed by subtracting the previous year's value from the value of a variable for a given year. Correlations between CPUE and hydrologic factors were reevaluated using the corrected time series.

Relationships between CPUE and hydrologic factors (rainfall and discharge) were quantified using a geometric mean functional regression (Ricker 1973), which provides an estimate of central tendency. This approach is appropriate when there is error in both X and Y. In order to evaluate periodicity, a spectral analysis (Proc Spectral in SAS) was conducted. Following Chatfield (1989), any trend (monotonic increase or decrease over time) was removed before analysis using least squares linear regression.

Loss of Water Resource Function and Recovery in Relation to Rainfall

In order to estimate the rate of recovery of CPUE, we developed a relationship between magnitude of the loss of resource function and recovery time. In the case of the blue crab fishery, the water resource function was expressed as CPUE. Loss of resource function was therefore a decrease in CPUE. In quantifying the relationship between loss of resource function and recovery time, three assumptions were made: (1) loss of resource function occurred when CPUE fell below the long-term annual mean of 1.26 pounds per trap (lbs/trap) (2) recovery occurred under average hydrologic conditions; and, (3) recovery was achieved when CPUE returned to the long-term annual mean.

To determine rate of recovery, instances from the POR (WY1986–WY2013) in which CPUE increased from one year to the next were extracted, expressed as an annual rate of increase in CPUE, and regressed on rainfall occurring during the first of the two years. This relationship was then used to estimate the change in CPUE associated with one year of average rainfall.

The loss in resource function or deviation from the long-term mean that can be recovered in one year was the estimated change in CPUE associated with one year of average rainfall. The loss that can be recovered in two years was twice the change in CPUE associated with one year of average rainfall, and so on.

The actual value of the CPUE that takes one year to recover to the long-term mean was the long-term mean minus the change in CPUE associated with one year of average rainfall. For a two-year recovery, the value of the CPUE was the long-term mean minus twice the change in CPUE associated with one year of average rainfall.

The above analysis of the rainfall associated with loss of blue crab CPUE and recovery was, to a certain extent, limited by the quantity of data within the POR. The time series did not include a sufficient number of events to quantify these relationships simply by

examining the record itself. As an alternative, we conducted Monte Carlo simulations, to acquire the frequency or probability of rainfall associated with CPUE recovery times of two and three years. Monte Carlo simulations have been used widely in fishery and hydrological research for assessing a model's outputs with different types and levels of variability or uncertainty in the model's inputs (e.g. Restrepo et al. 1992, Punt 2003, and Petrie and Brunsell 2011). In order to conduct a Monte Carlo simulation, an underlying probability distribution was specified. A normality test (Shapiro-Wilk's test (W) along with the normal quantile plot) of the Lee County dry season rainfall data from 1965 to 2013 indicated that the variability of the dry season rainfall can be well described by a log-normal distribution (**Figure 60**; W = 0.98, p = 0.752, and α = 0.05). Monte Carlo simulations were conducted based on this dry season rainfall probability distribution to generate ten sets of 10,000 years of dry season rainfall.

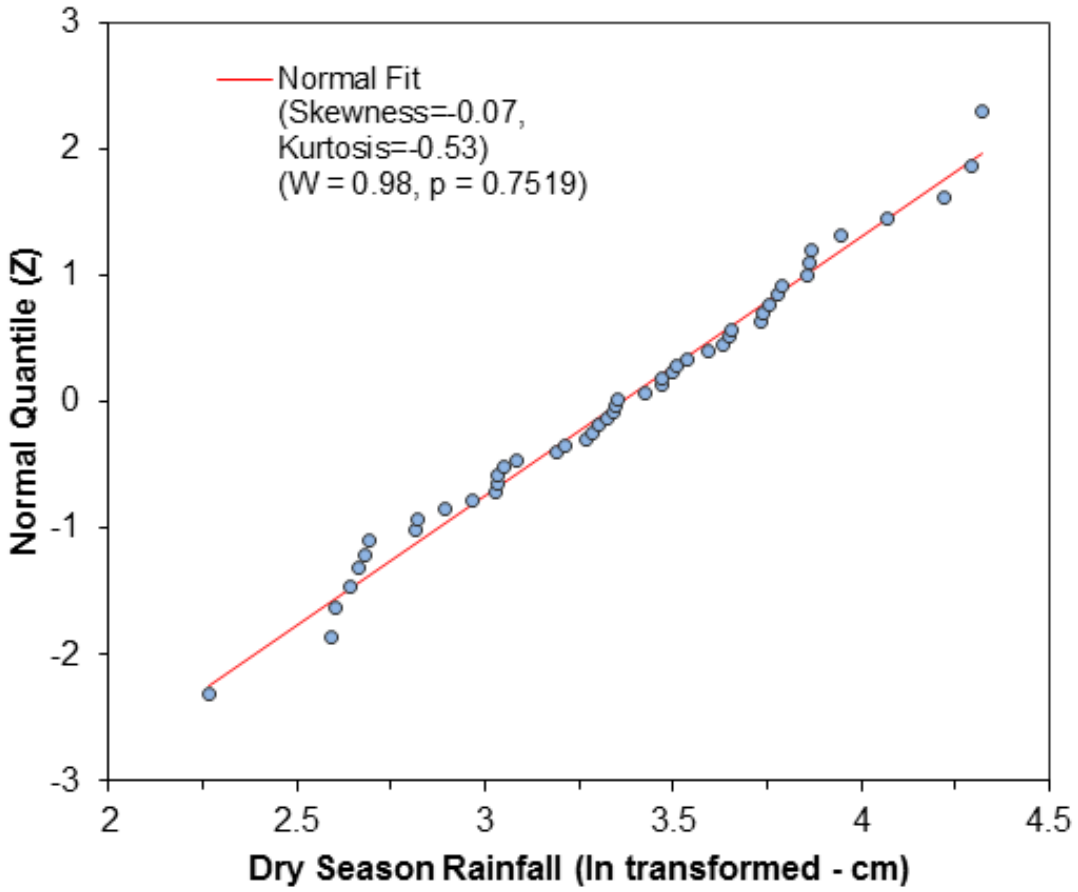

Figure 60. Normality test of natural log-transformed dry season rainfall during WY1966–WY2013. (Note: cm – centimeters.)

The functional regression equation relating annual CPUE and Lee County rainfall was used to predict blue crab CPUE with the generated rainfall data as inputs. The years with CPUE lower than the long-term (WY1986–WY2013) mean CPUE followed by successive two or three years of recovery back to normal were identified, respectively. The average dry season rainfall for these years and associated average return interval and probability of occurrence at least once in ten years were calculated.

Determination of Flow Associated with Rainfall

To convert estimates of rainfall associated with various recovery times to discharge (S-79 or total), regression analysis was performed. To maximize the probability of detecting a statistically significant relationship between discharge and rainfall, a longer POR (WY1967–WY2013) was used in this analysis.

Results

Relationships between Hydrologic Variables and Blue Crab Catch

Annual rainfall in Lee County averaged about 55 inches and ranged from a low of 41 inches in WY1981 to a high of 81.5 inches in WY1983. About 76% of the total annual rainfall occurred in the wet season and 24% in the dry season (**Table 33**). Dry season rainfall ranged from a low of 3.8 inches in WY2009 to a high of 29.6 inches in WY1998 (**Figure 61A**). Annual discharge at S-79 averaged 1,764 cfs (**Table 33**) ranging from a low of 113 cfs in WY2008 to a high of 5,044 cfs in WY2006. Daily average discharge at S-79 during the wet season (2,294 cfs) was nearly twice the average dry season discharge (1,238 cfs). Dry season discharge at S-79 ranged from a low of 52 cfs in WY2008 to a high of 5,616 cfs in WY1998. Total discharge averaged 2,267 cfs on an annual basis with Tidal Basin inflows adding about 500 cfs to the discharge at S-79. Daily total discharge averaged 3,055 cfs in the wet season and 1,480 cfs in the dry season, with Tidal Basin inflows contributing 760 and 245 cfs in the wet and dry seasons, respectively (**Table 33**).

Table 33. Annual and seasonal (wet versus dry) rainfall (inches) in Lee County and discharge (cfs) at the Franklin Lock and Dam (S-79) and total discharge to the estuary (sum of S-79 and Tidal Basin). Values are average (standard deviation). POR was WY1981–WY2013.

	Annual	Wet Season	Dry Season
Lee County Rainfall	55.2 (9.2)	42.3 (7.7)	12.8(5.9)
Discharge at S-79	1,764 (1208)	2,294 (1413)	1,235 (1445)
Total Discharge	2,267(1332)	3,055(1586)	1,480 (1599)

Annual landings in Lee County were dominated by hard shelled crabs with soft shelled crabs averaging only 3% of the total catch in lbs (**Table 34**). The CPUE for hard shelled crabs was also higher than for soft shelled crabs. On an annual basis, CPUE for hard shelled crabs averaged 1.26 lb/trap and ranged from a high of 2.1 lb/trap in 1989 to a low of 0.70 lb/trap in 2002 (**Figure 61B**). For soft shelled crabs, CPUE averaged 0.75 lb/trap (**Table 34**), ranging from a high of 1.58 lb /trap in 1989 to a low of 0.05 lb/trap in 2004.

Table 34. Mean annual landings in pounds per year (lbs/yr) of hard and soft shell blue crabs for WY1986–WY2013. Values are average (standard deviation).

	Landings lbs/yr	CPUE lbs/trap
Hard Shell	1,315,808 (711,508)	1.26 (0.35)
Soft Shell	36,515 (38,465)	0.75 (0.43)

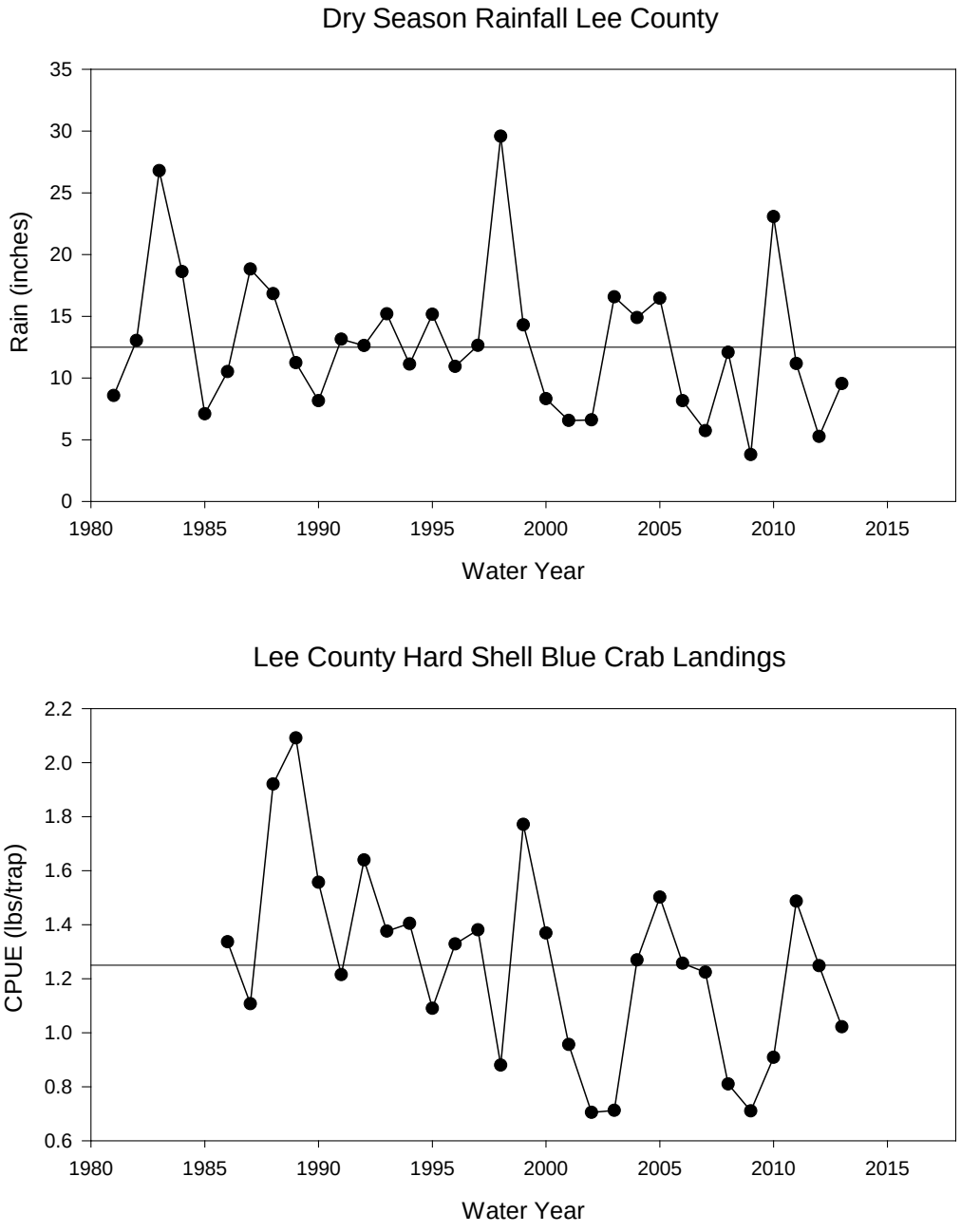

Figure 61. (**A**) Dry season (November–April) rainfall in Lee County. (**B**) Annual landings of hard shell blue crabs.

CPUE for hard and soft shelled crabs were tested for association with rainfall and discharge (S-79 and total) at annual lags of 0 to 5 years. Statistically significant ($p < 0.05$) correlations between CPUE and rainfall or discharge were found only when hydrologic variables were lagged by one year. Further, only correlations with dry season rainfall or discharge, lagged by one year, were statistically significant (**Table 35**). Therefore, the CPUE during the current year was positively associated with rainfall or discharge during the previous year's dry season. Of the three hydrologic variables tested, dry season rainfall explained the most variance in CPUE. A linear functional regression indicated that dry season rainfall explained about 45% of the variability in CPUE of hard shelled crabs, with CPUE increasing at a rate of 0.063 lbs/trap per inch (lbs/trap/inch) of rain (**Figure 62**). The 95% confidence interval (Ricker 1975) for the slope was 0.046 to 0.084 lbs/trap/inch of rain.

Table 35. Correlation of unadjusted hydrologic variables with unadjusted estimates of CPUE. n = 28 in all cases. Statistical significance: * $p < 0.10$, ** $p < 0.05$, and ***$p < 0.01$.

Variable	Annual CPUE Hard (lbs/trap)	Annual CPUE Soft (lbs/trap)
Lee County Rainfall		
Water Year (Lag 1)	0.216	-0.085
Wet Season (Lag 1)	-0.251	-0.309
Dry Season (Lag 1)	0.673***	0.399**
Discharge at S-79		
Mean Water Year (Lag 1)	0.289	0.091
Mean Wet Season (Lag 1)	0.083	-0.161
Mean Dry Season (Lag 1)	0.424**	0.345*
Total Discharge = S-79 + Tidal Basin		
Mean Water Year (Lag 1)	0.293	0.094
Mean Wet Season (Lag 1)	0.058	-0.177
Mean Dry Season (Lag 1)	0.450**	0.369*

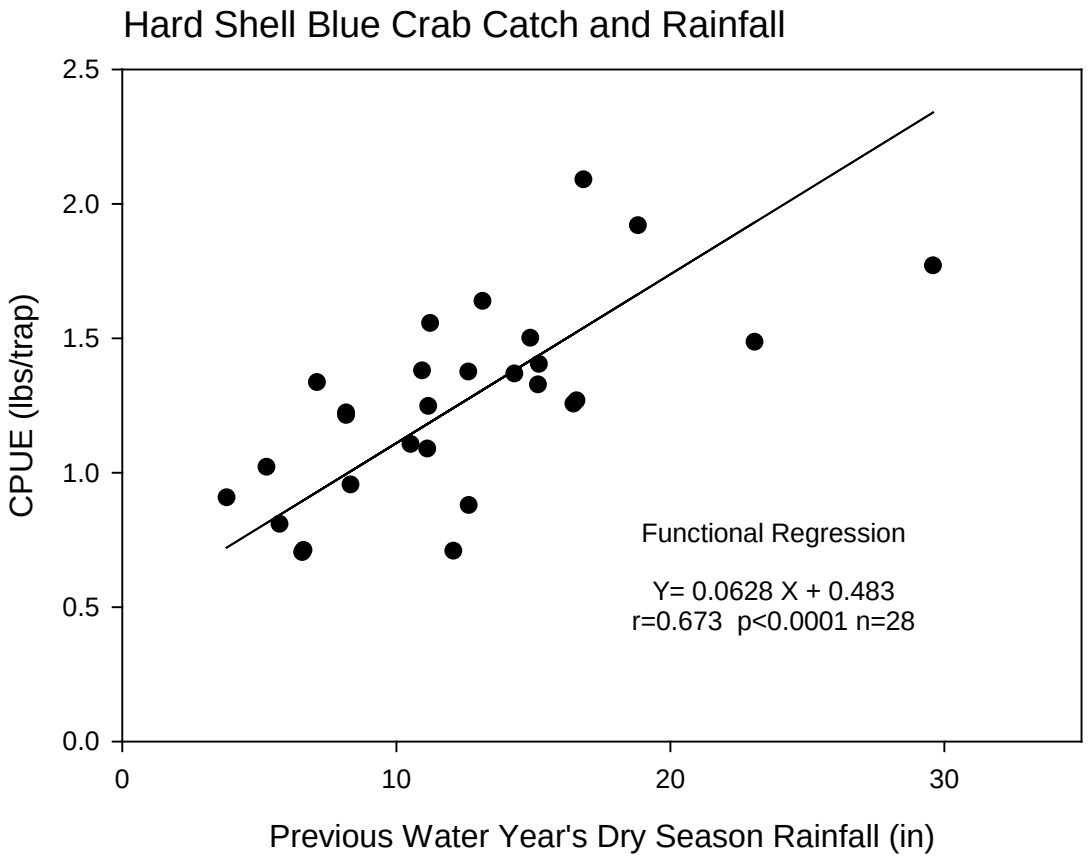

Figure 62. Functional regression of hard shell blue crab landings on the previous year's dry season rainfall (unadjusted data).

Long-term trend and autocorrelation may lead to spurious correlations between two time series (Chatfield 1989). For example, two variables that are both decreasing over time may appear correlated even though decreasing trends may have different causes. Linear regressions of dry season rainfall, total discharge and discharge at S-79 on water year were not statistically significant indicating that these time series showed no long-term trends. CPUE for both hard and soft shelled crabs exhibited significant, declining trends over time. Only CPUE for soft shelled crabs had significant autocorrelation at a lag of one year. In other words, for this variable, the current year's CPUE appeared dependent on the previous year's CPUE. When corrections for long-term trend and autocorrelation at lag 1 were made as appropriate, CPUE for both hard and soft shelled crabs were still correlated with dry season rainfall or discharge at a lag of 1 year (**Table 36**). Because soft-shelled crabs accounted for a small percentage of the total catch and because correlations between discharge and CPUE were relatively weak, further analysis focused on hard-shelled crabs and dry season rainfall.

Table 36. Correlations between hydrologic variables and CPUE after adjustment for long-term trend (de-trended) and autocorrelation (corrected) as appropriate. Included are correlations lagged by one year for dry season (November–May) Lee County rainfall, freshwater discharge through S-79, and total discharge calculated as the sum of S-79 and the Tidal Basin. Statistical significance: * $p < 0.10$, ** $p < 0.05$, and *** $p < 0.01$.

Variable	Annual CPUE	
	Hard (lbs/trap) (de-trended)	Soft (lbs/trap) (de-trended corrected)
Lee County Rainfall		
Dry Season (Lag 1)	0.696 ***	0.495***
Discharge at S-79		
Mean Dry Season (Lag 1)	0.468 **	0.426**
Total Discharge = S-79 + Tidal Basin		
Mean Dry Season (Lag 1)	0.497***	0.447**

Loss of Water Resource Function and Recovery in Relation to Rainfall

Year-to-year increases in unadjusted (not de-trended) CPUE for hard shelled crabs (n = 12) over the period WY1986–WY2013 were expressed as an annual rate of increase in CPUE and associated with dry season rainfall occurring in the first of the two years (**Figure 63**). The functional regression of annual rate of increase in CPUE on dry season rainfall was statistically significant (**Figure 63**, $p < 0.005$, $R^2 = 0.570$). For the average dry season rainfall (WY1986–WY2013) of 12.45 inches per year, this relationship yielded an annual increase of 0.22 CPUE per year. The deviation from the long-term mean that would be recovered after one year of average rainfall was therefore 0.22 CPUE. For two and three year recoveries, the deviations were 0.44 CPUE and 0.66 CPUE, respectively (**Table 37**.) Given a long-term (WY1986–WY2013) average of 1.26 CPUE, the actual CPUE associated with a one-, two-, or three-year recovery are given in **Table 37**. Using the equation in **Table 35**, the previous year's dry season rainfall associated with these CPUE was calculated. The rainfall corresponding to recoveries of one to three years ranged from 8.9 inches (1 year) to 1.9 inches (3 years).

With the Monte Carlo analysis, recovery periods of two and three years back to the average CPUE (1.26 lb/trap) were considered to estimate the dry season rainfall associated with each. Results, summarized in **Table 36**, were based on about 750 observations of recoveries requiring two to three years in each of the ten Monte Carlo runs. Average dry season rainfall associated with a deviation below the long-term average CPUE that took two years to recover was 7.1 inches. The average dry season rainfall associated with a deviation requiring three years to recover was 6.4 inches (**Table 36**).

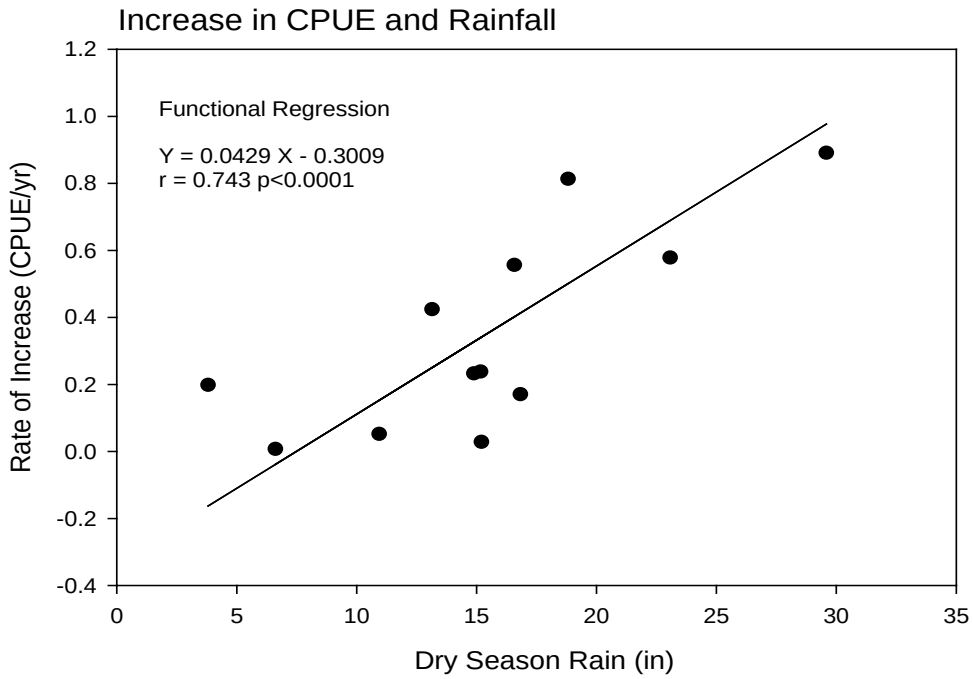

Figure 63. Functional regression of the increase in CPUE from one year to the next on the dry season rainfall occurring during the first of the two years. Data from **Figure 61**.

Table 37. Estimates of the preceding water year's dry season rainfall (Lee County) that produce annual catches of hard shelled crabs that will return to the long-term mean CPUE (1.26 lbs/trap) after one to three years of average dry season rainfall (12.45 inches). Estimates were made using a regression technique and a probabilistic Monte Carlo approach. Also given are the dry season discharge at S-79 and total discharge (S-79 + Tidal Basin) associated with the dry season rainfall in Lee County.

Method	Rainfall (inches)	CPUE (lbs/trap)	Years to Recover	Discharge S-79 (cfs)	Discharge Total (cfs)
	8.9	1.04	1	543	675
Regression	5.4	0.82	2	360	453
	1.9	0.66	3	239	304
Monte Carlo	7.1	0.97	2	440	552
	6.4	0.93	3	407	512

It is important to note that lagged (by 1 year) total dry season discharge and lagged dry season discharge at S-79 were also significantly related to CPUE for hard shelled crabs (**Table 36**). However, neither of these variables was related to year-to-year increases in CPUE as was the case for dry season rainfall (**Figure 63**). Thus a parallel analysis employing flow instead of rainfall could not be accomplished. Both flow variables were related to dry season rainfall in the current year. The data could be described by non-linear, exponential relationships that explained more than 60% of the variance (**Figure 64**).

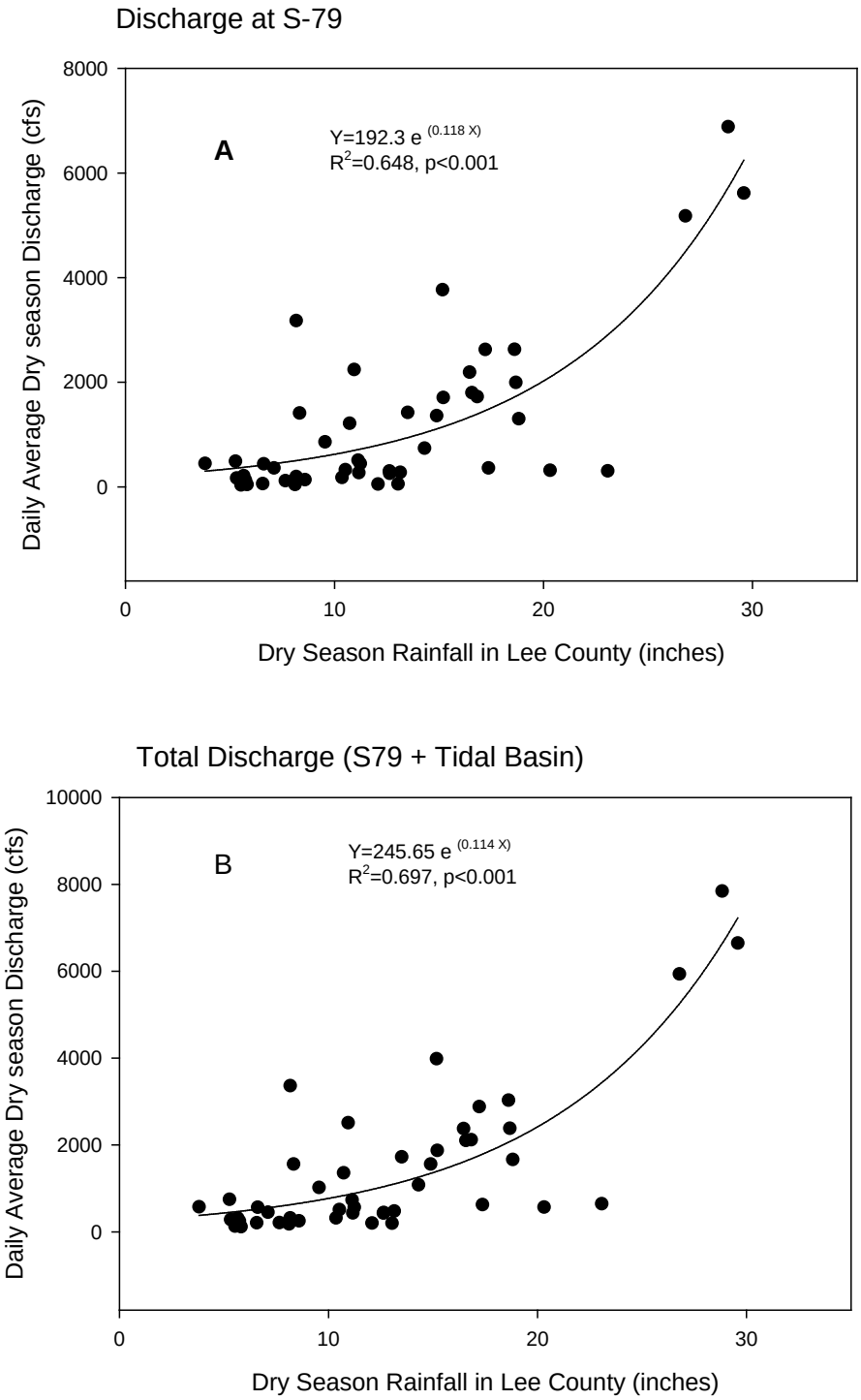

Figure 64. Exponential relationships between dry season rainfall in Lee County and discharge to the CRE at S-79 (top panel) or total discharge (bottom panel).

The exponential relationships were used to convert the estimates of dry season rainfall to inflow. The average daily dry season discharge at S-79 associated with one-, two-, or three-year recoveries ranged from 239 to 543 cfs (**Table 37**). Accounting for additional inflow from the Tidal Basin resulted in flows ranging from 304 to 675 cfs (**Table 37**).

Return Frequency

Results of the spectral analysis indicated that both dry season rainfall and CPUE showed statistically significant fluctuations with a period of 5.6 years (**Figure 65**). Analysis of the results of the Monte Carlo simulations indicated that the average rainfall with a two-year recovery of 7.1 inches has a return interval of 5.8 years, very close to the results of the spectral analysis (**Table 38**). The average rainfall with a three-year recovery was 6.4 in with a return interval of 8.2 years (**Table 38**). The probability for such dry season rainfall < 6.4 inches to occur at least once in ten years is still high (73%).

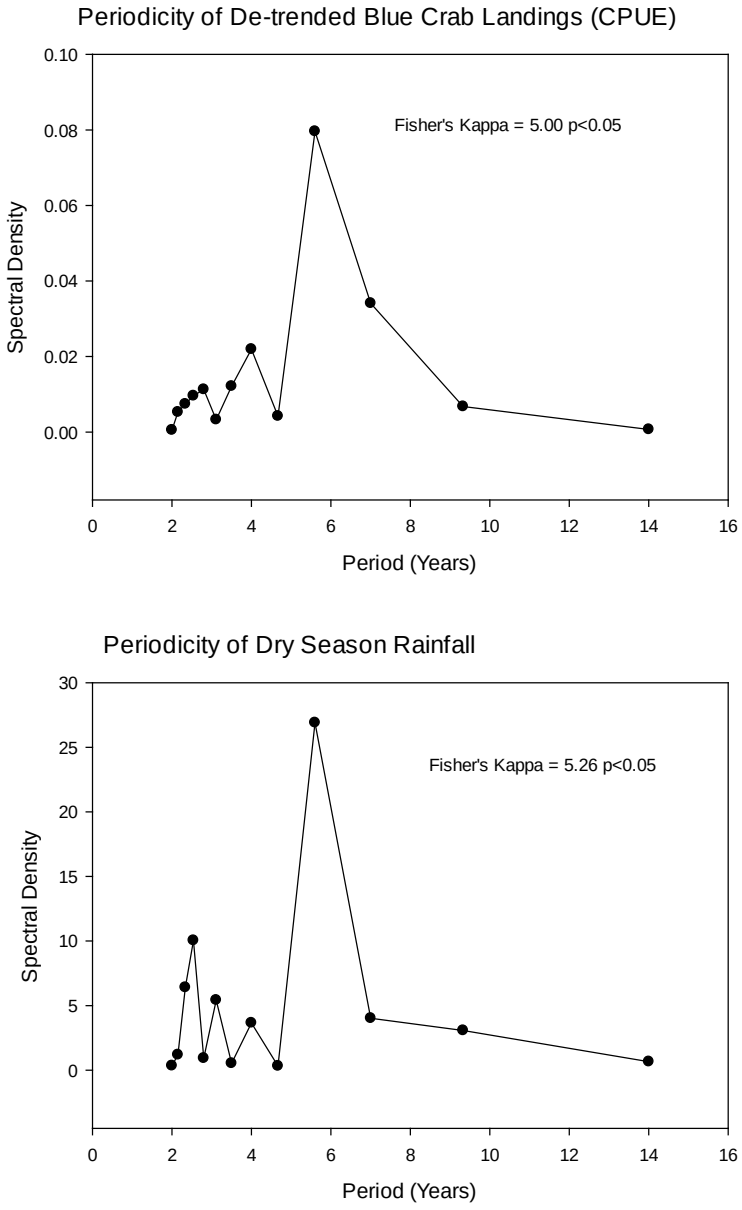

Figure 65. Results of spectral analysis. Periodicity of de-trended blue crab landings (top panel) and dry season rainfall (bottom panel) in Lee County for WY1986–WY2013. Results indicate that both time series show major fluctuation with a period of about six years.

Table 38. Average dry season rainfall for potential significant harm and associated return interval and probability of occurrences from Monte Carlo simulations.

Simulation	1	2	3	4	5	6	7	8	9	10	Mean
Dry Season Rainfall with 2-year Recovery (inches)	7.1	7.1	7.1	7.1	7.2	7.2	7.1	7.1	7.1	7.0	7.1
Average Return Interval (year)	5.8	5.5	5.9	5.8	5.7	5.5	6.0	5.9	5.8	6.0	5.8
Probability of 1-in-10 Year Occurrence (%)	85	87	84	85	86	87	84	85	85	84	85
Dry Season Rainfall with 3-year Recovery (inches)	6.4	6.1	6.2	6.7	6.6	6.5	6.0	6.5	6.5	6.4	6.4
Average Return Interval (years)	8.3	9	9.4	7.4	7.6	7.7	8.9	7.9	7.9	8.2	8.2
Probability of One in Ten Years Occurrence (%)	72	69	68	77	76	75	70	74	74	73	73

Discussion

The blue crab is an estuarine dependent species that utilizes the full range of salinity from oligohaline conditions to > 30 during its life time (Perry and McIlwain 1986, Longley et al. 1994). Salinities > 20 are required for successful reproduction and larval development (Sandoz and Rogers 1944, Perry and McIlwain 1986). Juveniles may use low salinity (< 15) regions of estuaries as nurseries (Van Engel 1958, Posey et al. 2005). During a three-year monitoring program in the CRE, Stevens et al (2008) observed recruitment of juvenile crabs (< 40 millimeter carapace width) primarily between November and April, with highest numbers in February, March, and April. Most of these were caught in low salinity conditions (0.5 to 5). There is also partitioning of the estuarine salinity gradient according to sex, with adult males remaining in low salinity waters, while mature females prefer the higher salinities found in lower estuarine and coastal regions (Perry and McIlwain 1986).

Given the dependence on a wide range of salinity for successful completion of its life cycle, it is not surprising that the productivity of blue crabs in an estuary may be influenced by freshwater inflow. Lower abundances of blue crabs have been associated with drought conditions in South Carolina (Childress 2010) and several Texas estuaries (Palmer et al. 2011). Commercial landings provide a convenient measure of productivity (Wilber 1994). Results from this study agreed with previous investigations that have reported positive relationships between freshwater inflow and landings of blue crabs (Meeter et al. 1979, Rogers et al. 1990, Wilber 1994, Guillory 2000). Wilber (1994) suggested three possible explanations for such relationships: (1) increased fresh water will reduce estuarine salinity and provide more low salinity habitat for juvenile crabs; (2) increased flows may further broadcast cues that may attract females from offshore, thus increasing the brood stock; and (3) higher inflows increase nutrient and detrital loading and thus directly or indirectly enhance food supply.

The long-term and inter-annual patterns that we observed for Lee County landings agree well with those observed statewide in Florida. In their recent assessment of the blue crab fishery in Florida, Murphy et al (2007) characterized the fishery as follows:

> Commercial landings in Florida have shown a general decreasing trend since the mid 1980's. Superimposed on this pattern are large oscillations often related to extended years of drought when blue crab production is apparently low and wet years when blue crab production is apparently high.

The period of record analyzed here (WY1986–WY2013) exhibited a decreasing long-term trend with much of the inter-annual variability (45%) explained by rainfall. The lower the rainfall and inflow during the dry season, the lower the following year's production of blue crabs. A similar lagged relationship between annual crab landings and the previous year's inflow from the Apalachicola River was observed by Wilber (1994). Blue crabs in the Gulf of Mexico reach harvestable size within a year of age (Perry 1984 as cited in Wilber 1994). The positive correlations between crab landings and river flows lagged by one year may reflect a positive influence of fresh water on juvenile crabs that reach harvestable size the following year (Wilber 1994). In this study, current annual landings were correlated with the previous year's dry season rainfall and inflow. The recruitment of juvenile blue crabs during the dry season (November–April) in the CRE may explain this correlation (Stevens et al. 2008).

Two key relationships are required to establish resource protection criteria: relationships between (1) changes in hydrology and changes in water resource function and (2) the magnitude of the functional loss and time to recover. In this component we have established a relationship between CPUE, which is the resource function, and dry season rainfall during the preceding water year, which represents the hydrology of the system. Since rainfall and freshwater flow were also related, changes in CPUE can also be related to a flow variable (e.g. discharge at S-79 and total discharge). We have also related the loss of water resource function to recovery time. Functional loss is defined as a negative deviation from the long-term mean CPUE. Recovery is achieved when the CPUE returns to the long-term mean. We have identified the CPUE that should recover to the long-term mean with one, two, or three years of average rainfall. Lastly, we have examined return frequency using spectral analysis and a Monte Carlo analysis.

Component Study 11: Relationships between Freshwater Inflow, Salinity, and Potential Habitat for Sawfish (*Pristis pectinata*) in the CRE

Christopher Buzzelli, Peter Doering, Yongshan Wan, and Detong Sun

Abstract

The smalltooth sawfish is an endangered species that historically ranged from Texas to North Carolina. The distribution and abundance of sawfish have declined due to overfishing and habitat loss. Presently, the CRE is an important sawfish nursery. Juvenile sawfish habitat can be characterized as nearshore environments < 1 m in depth, where salinities range from 12 to 27. This study quantified sawfish habitat with variable inflow to the CRE in the dry season using a combination of bathymetric analyses and hydrodynamic modeling. Inflows of 150–300 cfs positioned the 12 and 27 salinities in the shallowest part of the estuary (10 to 30 km downstream). Specifically, the area of sawfish habitat was greatest (5.7 km^2) when inflow through the S-79 structure was 270 cfs in the dry season. Under reduced inflow, the habitat migrated into the channel above Beautiful Island where it was compressed against S-79. Higher inflows pushed the position of salinity of 27 (S_{27}) out of the estuary.

Introduction

Fluctuations in freshwater inflows over time scales ranging from weeks to years have altered salinity regimes and impacted the ecological integrity of the CRE (Chamberlain and Doering 1998a, Barnes 2005). Changes in freshwater inflows and salinity have been shown to affect the distribution and dynamics of many taxa and communities including phytoplankton and zooplankton (Tolley et al. 2010, Radabaugh and Peebles 2012), SAV (Doering et al. 2001, 2002, Lauer et al. 2011), oysters and their pathogens (La Peyre et al. 2003, Barnes et al. 2007, Volety et al. 2009), fauna inhabiting oyster reefs (Tolley et al. 2005, 2006), and fishes (Collins et al. 2008, Heupel and Simpfendorfer 2008, Stevens et al. 2010, Simpfendorfer et al. 2011, Poulakis et al. 2013).

The balance between downstream transport of fresh water and the upstream encroachment of salinity creates gradients that influence all biogeochemical and biological processes and patterns. The gradient can be represented by lines of equal salinity (e.g. isohalines) whose positions fluctuate up and down the estuary with freshwater inflow(s), tidal cycles, and meteorological phenomena (e.g. fronts, winds, and storms). Particular isohalines provide indications of desirable (or undesirable) salinity conditions for sentinel organisms or communities (Jassby et al. 1995).

The smalltooth sawfish (*Pristis pectinata*) is an endangered species that historically ranged from Texas to North Carolina in the eastern United States (Simpfendorfer et al. 2011, Norton et al. 2012). The distribution and abundance of sawfish have declined due to overfishing and widespread habitat loss. The patterns of decline in the largetooth sawfish (*P. pristis*) are similar to smalltooth sawfish (Fernandez-Carvalho et al. 2014). Presently, sawfish populations are limited to habitats in Southwest Florida from Charlotte Harbor to the Dry Tortugas, including the CRE (NOAA 2009).

Little was known about sawfish feeding, reproduction, or habitat usage prior to designation as an endangered species in 2003 (Norton et al. 2012). More recently the CRE has been recognized as an essential nursery for neonates and juvenile sawfish (Simpfendorfer et al. 2011, Carlson et al. 2014). A suite of research studies was conducted to examine the distribution, location, and activity of juvenile sawfish in southwestern Florida and improve the existing understanding of the relationships between population dynamics, environmental conditions, and management actions (Poulakis et al. 2014).

Sawfish, cownose rays (*Rhinoptera bonasus*), and bull sharks (*Carcharkinus leucas*) are important components of the elasmobranch community in the CRE (Collins et al. 2008, Ortega et al. 2009, Heupel et al. 2010, Poulakis et al. 2011). Like many estuarine organisms, salinity is a key driver for these fish populations (Jassby et al. 1995, Collins et al. 2008, Heupel and Simpfendorfer 2008, Ortega et al. 2009). Migration within the estuary is modulated through a combination of osmotic regulation and the availability of prey resources (Poulakis et al. 2013). Individual cownose rays followed their preferred salinity range further upstream with decreasing freshwater discharge (Collins et al. 2008). A similar situation exists for bull sharks, which utilize the CRE as a nursery for at least 18 months, prefer salinities of 7 to 20, and move upstream with reduced inflow (Heupel and Simpfendorfer 2008).

Smalltooth sawfish generally prefer salinities of 12 to 27 but can survive and grow over a wider range (Poulakis et al. 2013). The desirable habitat for sawfish has been described as adjacent to red mangroves where nearshore depths are £ 0.9 m (Poulakis et al. 2011, Norton et al. 2012, Carlson et al. 2014). Sawfish spend their first few years of life in the CRE. Recent studies have shown that small sawfish (< 1 m) grow very fast over the full range of salinity conditions. While medium-sized fish (< 1.5 m) respond to changes in salinity lagged on a 90-day time scale, the largest fish (> 1.5 m) with the widest home range are more likely to be influenced by prey availability (Poulakis et al. 2013). Additionally, the average daily activity space (0 to 4 km) is correlated to sawfish body length (60 to 260 centimeters) as larger individuals can tolerate greater variations in salinity (Carlson et al. 2014).

Similar to cownose rays and bull sharks, increased salinity promotes upstream migration of juvenile sawfish away from downstream hot spots (Poulakis et al. 2013). Whereas juvenile sawfish can be found throughout the CRE, there are documented hotspots for smalltooth sawfish: Iona Cove, Glover Bight, the Cape Coral Causeway, and the US 41 Bridges near Fort Myers (Poulakis et al. 2014). Many sawfish are located in the lower estuary (Iona Cove and Glover Bight) when salinity is favorable, but migrate further upstream (US 41 Bridges) as salinity increases. This is potentially problematic for two reasons. First, the upper CRE from S-79 to Beautiful Island is much deeper and narrower with greatly reduced nearshore shallow habitat. Second, upstream migration into a bathymetrically compressed habitat potentially places juvenile sawfish in closer proximity to larger predators such as bull sharks (Poulakis et al. 2011).

It is possible that environmental factors other than salinity (i.e., temperature, DO, depth, shoreline attributes, and food availability) influence the distribution of juvenile sawfish (Poulakis et al. 2014). Although the endangered status of sawfish inhibits traditional dietary assessments, anecdotal evidence points to pink shrimp, blue crabs, fishes (clupeids, carangids, mullet, pinfish, mojarras, and kingfish), and stingrays as prey items. As opposed to stationary organisms such as oysters and benthic macrofauna, identification

of essential habitat based on bathymetric and salinity attributes can be tenuous for mobile fish populations (Norton et al. 2012). This study recognizes the inherent complexity in linking freshwater discharge, salinity distributions, and sawfish habitat requirements. Thus, the objective of this effort was to quantify the extent of the nearshore habitat potentially available to sawfish under reduced inflow to the CRE.

Based on knowledge of the CRE morphology and inflow-salinity relationships, this study hypothesized that there would be a dry season inflow that would maximize the area where salinity ranged from 12 to 27 in shallow environments £ 1.0 m (**Figure 66A**). While inflows less than the critical value allow salinity to encroach upstream where there is less shallow habitat, higher inflows may narrow the available habitat within the CRE (**Figure 66B**). This study combined sawfish salinity requirements, bathymetric data for the CRE, and low inflow salinity distributions predicted using a three-dimensional hydrodynamic model, CH3D (**Figure 67**).

Methods

Bathymetric Analyses

Three separate bathymetric data sets were merged to create a digital elevation model of the CRE (**Figure 67**). Data collected in the estuary between Beautiful Island and Shell Point by the USACE (2000) and the United States Geological Survey (2002) were combined with data collected between S-79 and Beautiful Island by SFWMD (2014). Aerial photography was digitized to provide a shoreline boundary for the digital elevation model. The digital elevation model was divided into 42 1-km segments between S-79 and Shell Point. The area and volume of the 0- to 1-m depth contour was quantified for each of the 42 segments.

Hydrodynamic Modeling

The CH3D model, originally developed by Sheng (1986), is a non-orthogonal curvilinear grid model capable of simulating complicated hydrodynamic processes including wind- and density-driven processes and tidal circulation. The model has a robust turbulence closure scheme for accurate simulation of stratified flows in estuaries and coastal waters (Sheng 1986, 1987). The non-orthogonal nature of the model enables it to represent the complex geometry of a tidal estuary such as the CRE. The model includes a circulation model to simulate 3-D hydrodynamics and a salinity model to simulate salt transport. The model is driven by external forcing prescribed at the boundaries including tidal forcing at the ocean boundary, freshwater inflow from the watershed, and meteorological forcing including wind and rainfall. The CH3D model has been successfully developed for many water bodies including east coast Florida estuaries such as the Indian River Lagoon, St. Lucie Estuary (Sun 2009), and Loxahatchee River Estuary (Sun 2004).

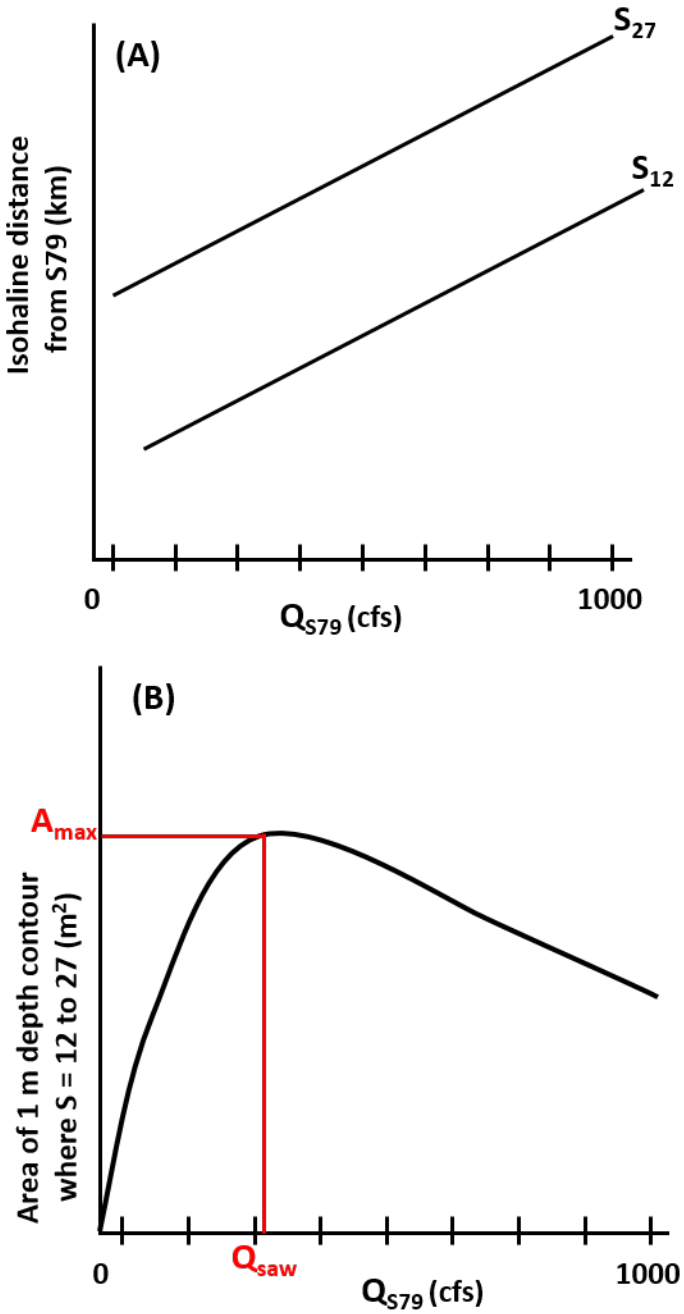

Figure 66. (**A**) Hypothetical relationship between inflow at S-79 (Q_{S79}; cfs) and the downstream locations of the position of salinity S_{12} to S_{27}. (**B**) Hypothetical relationship between inflow at S-79 and the area for sawfish in the CRE. (Note: A_{max} – maximum area; Q_{saw} – inflow that maximizes habitat area and S – salinity.)

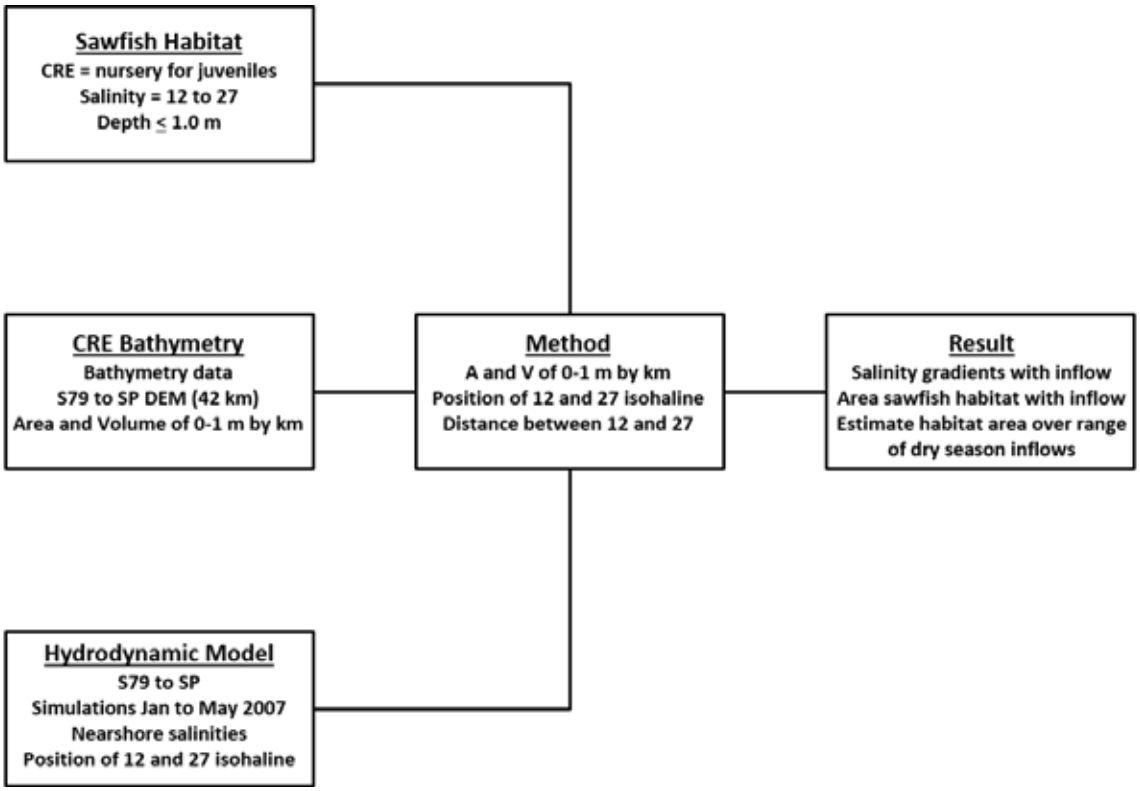

Figure 67. Schematic of method used to combine sawfish habitat requirements, the bathymetry of the CRE, and the hydrodynamic model (CH3D) to estimate A_{saw}. (Note: A – A_{saw}, sawfish habitat area; V – V_{saw}, sawfish habitat volume; DEM – digital elevation model; Jan – January; and SP – Shell Point.)

The CRE CH3D model was developed from the Charlotte Harbor CH3D model (Sheng 2002). The original Charlotte Harbor model was calibrated using two months of hydrodynamic and salinity data collected during summer 1986 at six stations located in and around Pine Island Sound and the Peace River. SFWMD extended the model to the CRE using 16 months of continuous salinity monitoring data (Qiu 2002, SFWMD 2003). The CRE CH3D model was further calibrated with three years of salinity observations (October 2001–December 2004) at five stations in the estuary for the evaluation of various alternative plans of the Southwest Florida Feasibility Study and the Caloosahatchee River (C-43) West Basin Storage Reservoir (Sheng and Zhang 2006, Qiu et al. 2007, USACE and SFWMD 2010). An external peer review of the CH3D model was conducted in 2006 for this application (Qiu 2006). The latest calibration of the model was conducted with data collected up to 2010 at seven locations in the estuary to support the development of the Lake Okeechobee Adaptive Protocols (SFWMD 2010, Wan et al. 2013).

The CRE CH3D model domain covers the entire estuarine system, including CRE, Charlotte Harbor, Pine Island Sound, San Carlos Bay, Estero Bay, and the major tributaries, as well as about 30 km offshore in the Gulf of Mexico. In the horizontal dimension, the grid has 166 x 128 elements allowing fine enough resolution to represent the numerous islands, including the islands of the Sanibel Causeway. The higher resolution within the CRE and San Carlos Bay (50 to 100 m) provides a more detailed representation of the

complex shoreline and the navigation channel. Five vertical layers evenly spaced over the water column enable simulation of density stratification within the estuary.

The hydrodynamic model was applied in a test mode to generate salinity distributions over a range of S-79 inflows indicative of the dry season. Sawfish habitat was defined as the area (A_{saw}) (or habitat volume [V_{saw}]) of the estuary where depth was £ 1 m and surface water salinity ranged from 12 to 27 (**Figure 67**). WY2007 was selected as the test case because it is within the POR for which the model has been calibrated and freshwater inflow was near the long-term minima. Simulations were from January 1, 2007, to May 31, 2007. The existing boundary conditions included empirical inputs for water level at the ocean boundary, rainfall, and wind at the surface, and estimated Tidal Basin runoff. These boundary conditions were applied over the entire simulation period. While observed S-79 freshwater inflows were applied from January 1, 2007, to February 28, 2007, a constant inflow was applied for the remaining time for each model simulation. This method was used because the model dynamics had to be established before the inflows could be manipulated. A total of seven simulations were performed for constant flow at S-79 of 0, 150, 300, 450, 650, 800, and 1,000 cfs. Based on long-term inflow records from WY1966 to WY2014, May has the lowest average rate of discharge through S-79 (761 ± 569 cfs). Thus, salinities from May 2007 from each of the simulations were used in sawfish habitat calculations.

Data Analyses

Surface salinities predicted for the nearshore areas using the hydrodynamic model along the northern and southern shorelines were averaged between S-79 and Shell Point. The average nearshore surface salinity then was plotted versus distance downstream of S-79 to visualize the salinity gradient for each of the seven constant inflows. Similarly, the area and volume of 0- to 1-m depth contour from the bathymetric analysis were plotted versus distance. The downstream positions of the 12 and 27 isohalines (S_{12} and S_{27}) were plotted versus the series of constant inflows. A_{saw} was derived by summing the area of bottom £ 1 m between S_{12} and S_{27} (millions of $m^2 = 10^6$ $m^2 = 1$ km^2). V_{saw} (millions of $m^3 = 10^6$ m^3) was calculated similarly as the volume of the 0- to 1-m depth contour for each km of estuary located between S_{12} and S_{27} was summed. A_{saw} and V_{saw} were plotted versus each of the constant inflows. A polynomial curve was fit to the scatterplot between A_{saw} and inflow at S-79 (Q_{S79}; cfs) as a tool to predict the A_{saw} as a function of dry season inflows.

Results

Depth ranges from 0.5 to 6.5 m in the CRE (**Figure 68A**). Approximately 58% of the CRE is < 1.0-m depth (**Figure 68B**; Buzzelli et al. 2013b). The area of the 0- to 1-m depth contour within each 1 km segment ranged from 0.01 x 10^6 to 0.53 x 10^6 m^2 (**Figure 69**). These shallow depths were more prevalent from ~10 to 20 km downstream of S-79. Although the values increased with decreasing discharge, salinity was stable and nearly constant from S-79 and ~10 km downstream (**Figure 70**; Buzzelli et al. 2014a). When there was no inflow, salinity was > 20 from 0 to 10 km before increasing to 35 near Shell Point. Similarly, salinity was > 14 in the upper CRE with 150 cfs of inflow. Because salinity was > 12 at S-79 for both of these inflow classes, the potential area of sawfish habitat was estimated to extend from the water control structure to the downstream location of S_{27}.

Conversely, salinities were < 27 throughout the CRE for the 1,000-cfs inflow class. Thus, A_{saw} could not be estimated for the highest inflow tested since S_{27} was located outside of the estuary domain.

The distance between the S_{12} and S_{27} ranged from ~19 km when inflow was 0 cfs to 26.7 km when inflow was 150 cfs (**Figure 71A**). This finding led to maximum values for A_{saw} (5.7 km^2) and V_{saw} (2.8 x 10^6 m^3; **Figure 71B**). A polynomial curve was fit to the relationship between A_{saw} and inflow at S-79 to estimate sawfish habitat area over a full range of inflows indicative of the dry season (**Figure 71C**). A_{saw} was maximized when inflow was 270 cfs.

Discussion

An estimated 95% of the historical smalltooth sawfish population from Texas to North Carolina has been lost (Heupel et al. 2007, Norton et al. 2012). Salinity tolerance, food availability, and protection from predators are among the variables that characterize sawfish habitat. Although they can have widespread distribution depending upon age, *Pristis pectinata* can be found across a wide range of salinity values though they generally prefer 12 to 27 (Poulakis et al. 2013). This study connected knowledge of sawfish habitat requirements with spatial analyses of the bathymetry and a three-dimensional hydrodynamic model to estimate changes in sawfish habitat area in the CRE with inflow in the dry season.

Combined bathymetric and modeling results suggested that the maximum A_{saw} occurred when the inflow was 270 cfs in May 2007. May 2007 was selected because there was no freshwater input through S-79 and occurred in one of the driest years on record. This inflow (270 cfs) would position the 12 to 27 salinity range ~10 to 30 km downstream of S-79 (above Beautiful Island to Cape Coral). Sawfish habitat area between S-79 and Shell Point would be greatest under these conditions (~5.5 km^2). Less than 270 cfs could confine the sawfish habitat to the deeper upper CRE where there is much less shoal area, and lead to habitat compression against the structure. Upstream migration into a bathymetrically compressed habitat potentially places juvenile sawfish in closer proximity to larger predators such as bull sharks (Poulakis et al. 2011). At the other end, dry season inflows > 800 cfs should push the S_{27} out of the CRE and extend the sawfish habitat into San Carlos Bay.

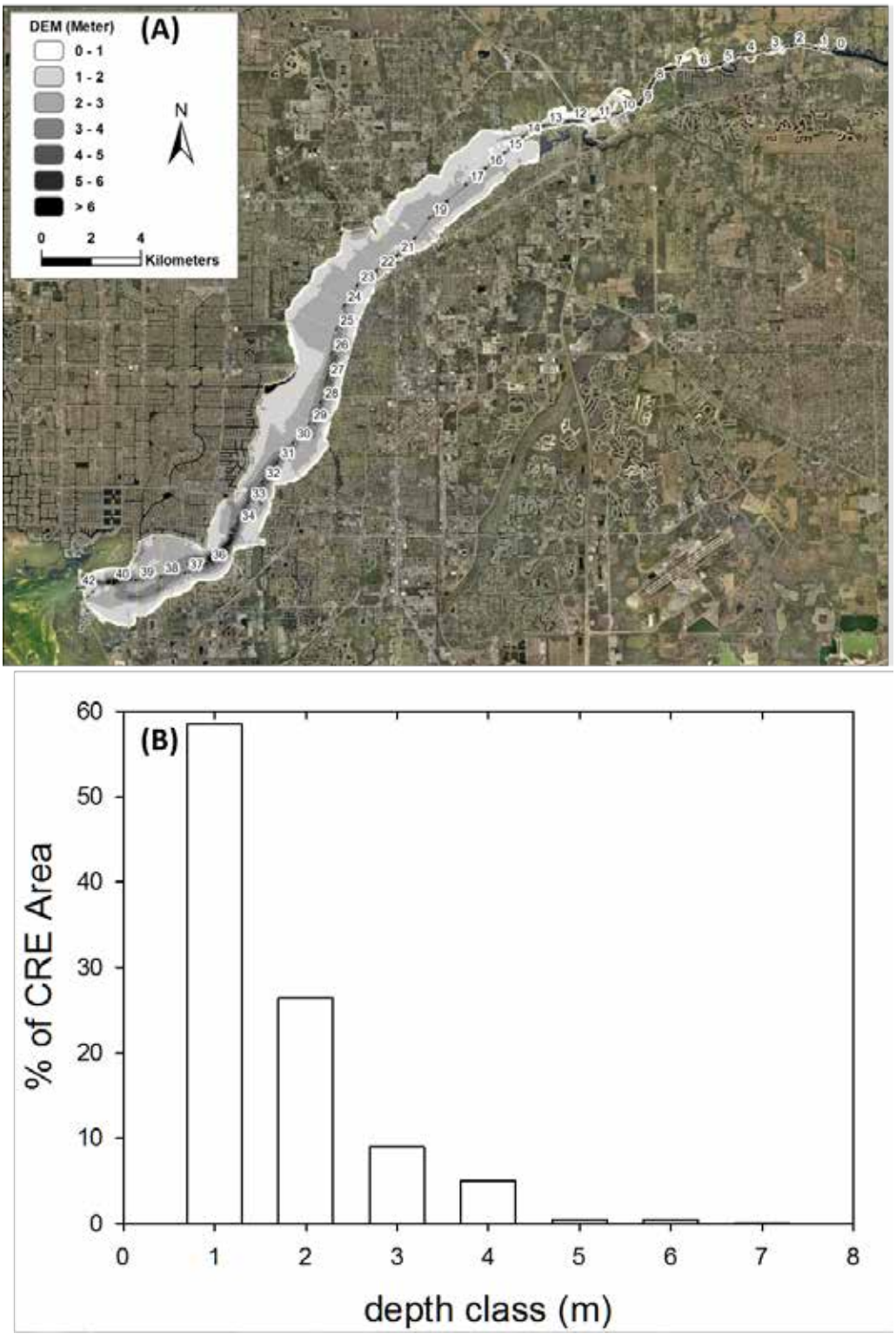

Figure 68. (**A**) Bathymetric contour map for the CRE. (**B**) Frequency histogram depicting the bottom area for each of several CRE depth classes.

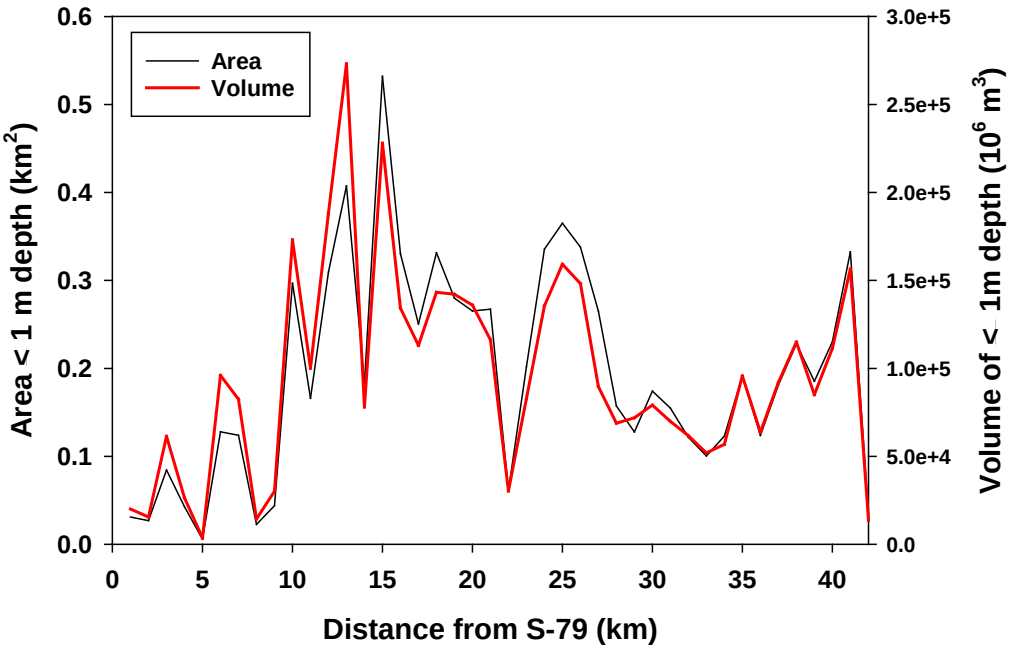

Figure 69. Results of bathymetric analyses depicting the area (km^2) and volume (106 m^3) of the 0- to 1-m depth contour relative to distance downstream of S-79.

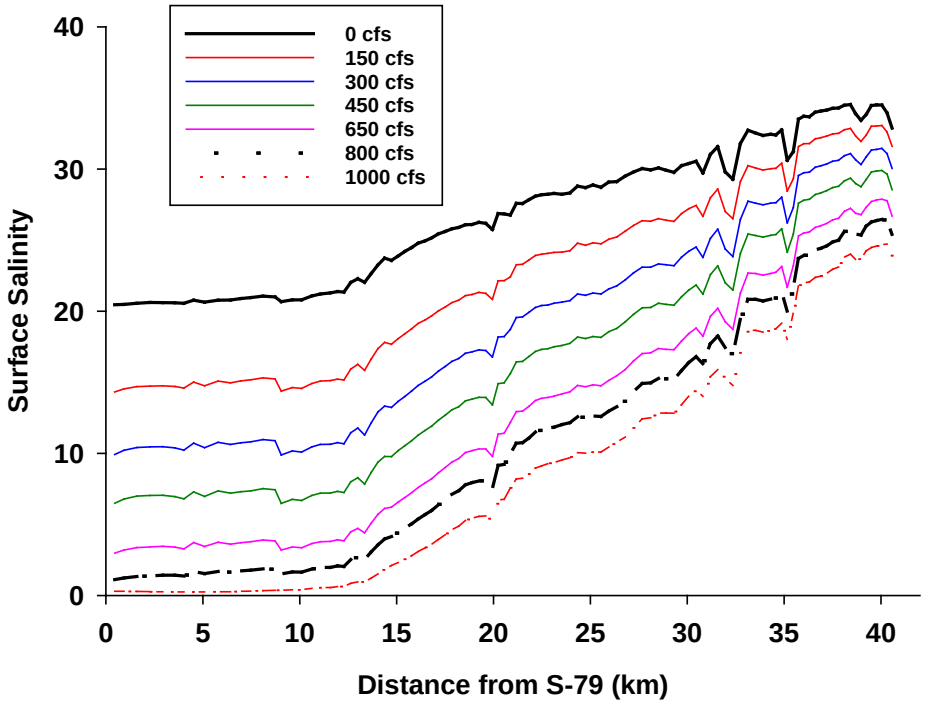

Figure 70. The gradient in average salinities in nearshore environments predicted over a range of inflows (0, 150, 300, 450, 650, 800, and 1,000 cfs) from May 2007.

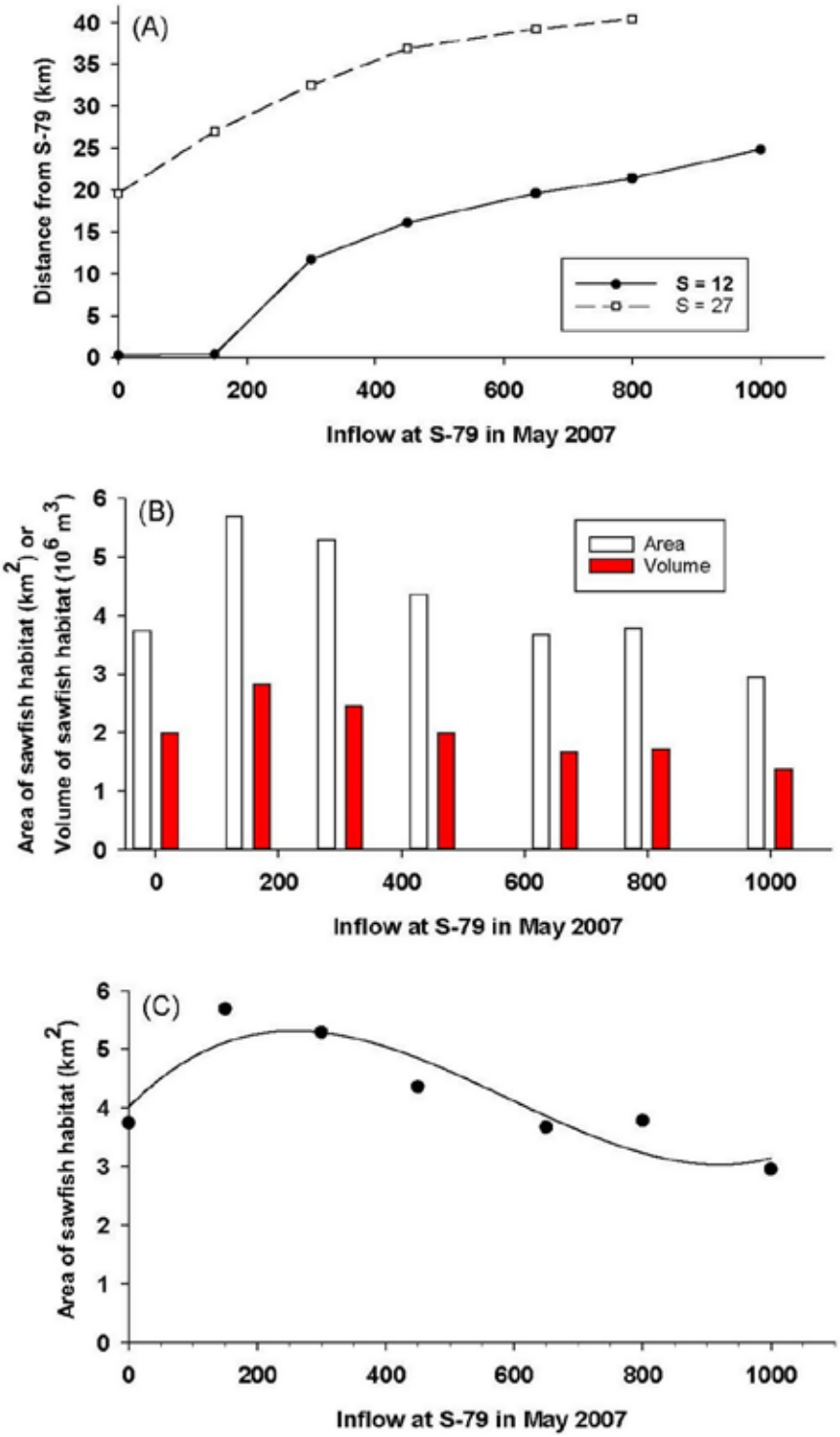

Figure 71. (**A**) The position of the S_{12} and S_{27} salinity isohalines as a function of dry season inflow. (**B**) The A_{saw} and V_{saw} as a function of dry season inflow. (**C**) Scatterplot and polynomial curve fit between inflow at S-79 and the A_{saw}.

Addendum to Component 11

Recalculation of Habitat Area with Respect to a Different Optimum Salinity Range for Sawfish

Poulakis (personal communication, 2016) suggests a different optimum salinity range from 18 to 30 to be used for juvenile sawfish in the CRE. Habitat area was recalculated based on the same hydrodynamic modeling results (**Figure 70**) and bathymetric data. As discharge increases habitat area and volume (**Figure 72B** and **72C**) decreases. This is because as discharge increases, both isohalines of the 18 and 30 are pushed downstream, but the retreat of the 30 isohaline cannot make up the loss of area due to the retreat of 18 isohaline (**Figure 72A**). It appears, that for this range of salinity, there would not be an optimum flow that maximizes the habitat area or volume for the sawfish.

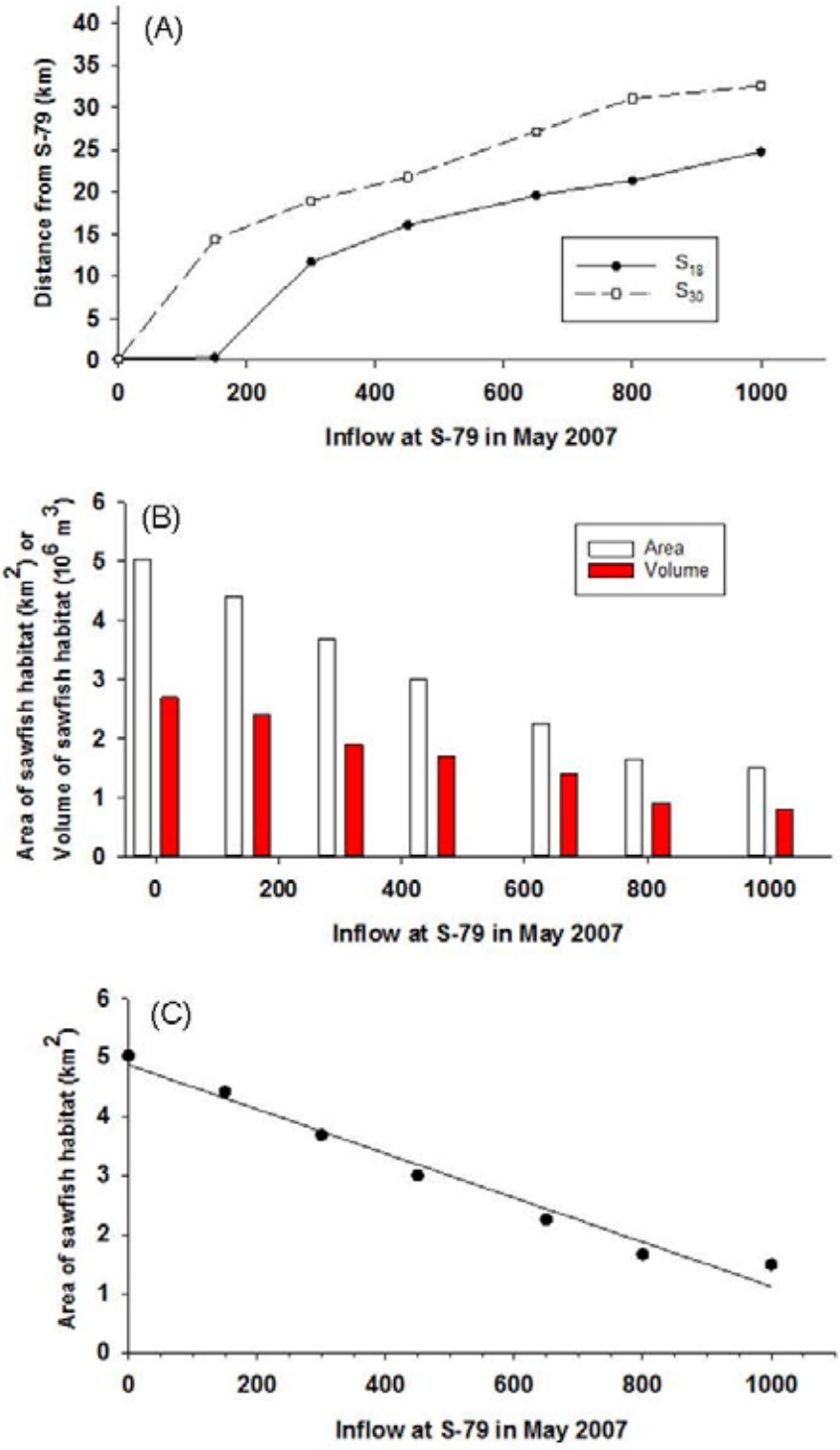

Figure 72. (**A**) The position of the S_{18} and S_{30} isohalines as a function of dry season inflow. (**B**) The A_{saw} and V_{saw} as a function of dry season inflow. (**C**) Scatterplot and polynomial curve fit between inflow at S-79 and the A_{saw}.

REFERENCES

Able, K.W. 2005. A re-examination of fish estuarine dependence: Evidence for connectivity between estuarine and ocean habitats. *Estuarine, Coastal, and Shelf Science* 64:5-17.

Adams, J.B., G.C. Bate, T.D. Harrison, P. Huizinga, S. Taljaard, L. van Niekerk, E.E. Plumstead, A.K. Whitfield and T.H. Wooldridge. 2002. A method to assess the freshwater inflow requirements of estuaries and application to the Mtata Estuary, South Africa. *Estuaries* 25(6B):1382-1393.

Ahn, H. and R.T. James. 2001. Variability, uncertainty, and sensitivity of phosphorus deposition load estimates in South Florida. *Water, Air, and Soil Pollution* 126:37-51.

Alber, M. 2002. A conceptual model of estuarine freshwater inflow management. *Estuaries* 25:1246-1261.

Aleem, A.A. 1972. Effect of river outflow management on marine life. *Marine Biology* 15:200-208.

Andrews, J.D., D. Haven and D.B. Quayle. 1959. Freshwater kill of oysters (*Crassostrea virginica*) in James River, Virginia, 1958. *Proceedings of the National Shellfish Association* 49:29-49.

Anon. 1958. The Venice system for the classification of marine waters according to salinity. *Limnology and Oceanography* 3:346-347.

Antonini, G.A., D.A. Fann and P. Roat. 2002. *A Historical Geography of Southwest Florida Waterways, Volume Two: Placida Harbor to Marco Island*. National Seagrant College Program, Silver Spring, MD.

Austin, J.A. 2004. Estimating effective longitudinal dispersion in the Chesapeake Bay. *Estuarine, Coastal, and Shelf Science* 60:359-368.

Azevedo, I.C., A.A. Bordalo and P. Duarte. 2014. Influence of freshwater inflow variability on the Douro estuary primary productivity: A modeling study. *Ecological Modelling* 272:1-15.

Baisre, J.A. and Z. Arboleya. 2006. Going against the flow: Effects of river damming in Cuban fisheries. *Fisheries Research* 81:283-292.

Balci, P. and L. Bertolotti. 2012. Appendix 10-2: Caloosahatchee River Watershed Protection Plan 2012 Update. *South Florida Environmental Report – Volume I*, South Florida Water Management District, West Palm Beach, FL. Available online at http://apps.sfwmd.gov/sfwmd/SFER/2012_SFER/v1/appendices/v1_app10-2.pdf.

Baldwin, L. and M.J. Hunt. 2014. Daily Water Temperature Time Series for the Upper Caloosahatchee Estuary. Publication WR-2014-003, South Florida Water Management District, West Palm Beach, FL.

Barnes, T.K. 2005. Caloosahatchee Estuary Conceptual Ecological Model. *Wetlands* 25(4):884-897.

Barnes, T.K., A.K. Volety, K. Chartier, F.J. Mazzotti and L. Pearlstine. 2007. A habitat suitability index model for the eastern oyster (*Crassostrea virginica*), a tool for

restoration of the Caloosahatchee Estuary, Florida. *Journal of Shellfish Research* 26(4):949-959.

Barras, J., S. Beville, D. Britsch, S. Hartley, S. Hawes, J. Johnston, P. Kemp, Q. Kinler, A. Martucci, J. Porthouse, D. Reed, K. Roy, S. Sapktoa and J. Suhayda. 2004. *Historical and Projected Coastal Louisiana Land Changes: 1978–2050*. Open File Report 03-334, United States Geologic Survey, Washington, DC.

Bartleson, R.D., M.J. Hunt and P.H. Doering. 2014. Effects of temperature on growth of *Vallisneria americana* in a sub-tropical estuarine environment. *Wetlands Ecology and Management* DOI 10.1007/s1 1273-014-9354-6.

Bataller, E.E., A.D. Boghen and M.D.B. Burt. 1999. Comparative growth of the eastern oyster *Crassostrea virginica* (Gmelin) reared at low and high salinities in New Brunswick, Canada. *Journal of Shellfish Research* 18:107-114.

Beck, M.W., R.D. Brumbaugh, L. Airoldi, A. Carranza, L.D. Coen, C. Crawford, O. Defeo, G.J. Edgar, B. Hancock, M.C. Kay, H.S. Lenihan, M.W. Luckenback, C.L. Toropova, G. Zhang and X. Guo. 2011. Oyster reefs at risk and recommendations for conservation, restoration, and management. *Bioscience* 61:107-116.

Beckage, B., L. Joseph, P. Belisle, D.B. Wolfson and W.J. Platt. 2007. Bayesian change-point analyses in ecology. *New Phytologist* 174:456-467.

Black, W.M. 1887. *Condition of Caloosahatchee Basin*. Letter to Chief of Engineers, File Copy 1155(2). Federal Records Center, Southeast Region, United States Army, Washington, DC. Pages 126–129 and 214–217.

Blanch, S.J., G.G. Ganf and K.F. Walker. 1998. Growth and recruitment in *Vallisneria americana* as related to average irradiance in the water column. *Aquatic Botany* 61:181-205.

Bortone, S.A. and R.K. Turpin. 2000. Tapegrass life history metrics associated with environmental variables in a controlled estuary. Pages 65-79 in: Bortone S.A. (ed.), *Seagrass Monitoring, Ecology, Physiology, and Management*, CRC Press, Boca Raton, FL.

Bourn, W.S. 1932. Ecological and physiological studies on certain aquatic angiosperms. *Contributions from Boyce Thompson Institute* 4:425-496.

Bourn, W.S. 1943. Seawater tolerance of *Vallisneria spiralis* L. and *Potamogeton foliosus* Raf. *Contributions from Boyce Thompson Institute* 6:303-308.

Boustany, R.G., T.C. Michot and R.F. Moss. 2010. Effects of salinity and light on biomass and growth of *Vallisneria americana* from lower St. Johns River, FL, USA. *Wetlands Ecology and Management* 18:203-217.

Bowers, D.G. and H.L. Brett. 2008. The relationship between CDOM and salinity in estuaries: An analytical and graphical solution. *Journal of Marine Systems* 73:1-7.

Breitburg, D. 2002. Effects of hypoxia, and the balance between hypoxia and enrichment, on coastal fishes and fisheries. *Estuaries* 25(4B):767-781.

Browder, J. 1985. Relationship between pink shrimp production in the Tortugas and water flow patterns in the Florida Everglades. *Bulletin of Marine Science* 37: 839-856.

Brown, J.R. and E.B. Hartwick. 1988. Influences of temperature, salinity and available food upon suspended culture of the Pacific oyster, *Crassostrea gigas*. 1. Absolute and allometric growth. *Aquaculture* 70:231-251.

Butler, J.P. 1954. The southern oyster drill. Proceedings of the National Shellfisheries Association 44:67-75.

Bulger, A.J., B.P. Hayden, M.E. Monaco, D.M. Nelson and M.G. McCormick-Ray. 1993. Biologically-based estuarine salinity zones derived from a multivariate analysis. *Estuaries* 16:311-322.

Burnett, W.C., P.K. Aggarwal, A. Aureli, H. Bokuniewicz, J.E. Cable, M.A. Charette, E. Kontar, S. Krupa, K.M. Kulkarmi, A. Loveless, W.S. Moore, J.A. Oberdorfer, J. Oliveira, N. Ozyurt, P. Povinec, A.M.G. Privitera, R. Rajar, R.T. Ramessur, J.Scholten, T. Stieglitz, M. Taniguchi and J.V. Turner. 2006. Quantifying submarine groundwater discharge in a coastal zone via multiple methods. *Science of the Total Environment* 367:498-543.

Buzan, D., W. Lee, J. Culbertson, N. Kuhn and L. Robinson. 2009. Positive relationship between freshwater inflow and oyster abundance in Galveston Bay, Texas. *Estuaries & Coasts* 32:206-212.

Buzzelli, C. 2011. Ecosystem modeling in small sub-tropical estuaries and embayments. Pages 331–353 in: Wolanski, E. and D.S. McLusky (eds.), *Treatise on Estuarine and Coastal Science, Volume 9,* Academic Press, Waltham, MA.

Buzzelli, C., R. Robbins, P. Doering, Z. Chen, D. Sun, Y. Wan, B. Welch and A. Schwarzchild. 2012. Monitoring and modeling of *Syringodium filiforme* (manatee grass) in the southern Indian River Lagoon. *Estuaries and Coasts* 35:1401-1415.

Buzzelli, C., P. Doering, Y. Wan, P. Gorman and A. Volety. 2013a. Simulation of potential oyster density with variable freshwater inflow (1965–2000) to the Caloosahatchee River Estuary, Southwest Florida, USA. *Environmental Management* 52(4):981-994.

Buzzelli, C., Z. Chen, T. Coley, P. Doering, R. Samimy, D. Schlezinger and B. Howes. 2013b. Dry season sediment-water exchanges of nutrients and oxygen in two Florida estuaries: Patterns, comparisons, and internal loading. *Florida Scientist* 76(1):54-79.

Buzzelli, C., Y. Wan, P. Doering and J.N. Boyer. 2013c. Seasonal dissolved inorganic nitrogen and phosphorus budgets for two sub-tropical estuaries in South Florida, USA. *Biogeosciences* 10:6721-6736.

Buzzelli, C, M. Parker, S. Geiger, Y. Wan, P. Doering and D. Haunert. 2013d. Predicting system-scale impacts of oyster clearance on phytoplankton productivity in a small sub-tropical estuary. *Environmental Modeling & Assessment* 18(2):185-198.

Buzzelli, C., B. Boutin, M. Ashton, B. Welch, P. Gorman, Y. Wan and P. Doering. 2014a. Fine-scale detection of estuarine water quality with managed freshwater releases. *Estuaries and Coasts* 37:1134-1144.

Buzzelli, C., P. Doering, Y. Wan, D. Sun and D. Fugate. 2014b. Modeling ecosystem processes with variable freshwater inflow to the Caloosahatchee River Estuary, Southwest Florida. I. Model development. *Estuarine, Coastal, and Shelf Science* 151:256-271.

Buzzelli, C., P. Doering, Y. Wan, D. Sun and D. Fugate. 2014c. Modeling ecosystem processes with variable freshwater inflow to the Caloosahatchee River Estuary, Southwest Florida. II. Nutrient loading, submarine light, and seagrass. *Estuarine, Coastal, and Shelf Science* 151:272-284.

Buzzelli, C., K. Carter, L. Bertolotti and P. Doering. 2015. Chapter 10: St. Lucie and Caloosahatchee River Watershed Protection Plan Annual and Three-Year Updates. *South Florida Environmental Report – Volume I*, West Palm Beach, FL. Available online at http://apps.sfwmd.gov/sfwmd/SFER/2015_sfer_final/v1/chapters/v1_ch10.pdf.

Buzzelli, C., P. Gorman, P.H. Doering, Z. Chen and Y. Wan. 2015b. The application of oyster and seagrass models to evaluate alternative inflow scenarios related to Everglades restoration. *Ecological Modelling* 297:154-170.

Carlson, J.K., S.J.B. Gulak, C.A. Simpfendorfer, R.D. Grubbs, J.G. Romine and G.H. Burgess. 2014. Movement patterns and habitat use of smalltooth sawfish, *Pristis pectinata*, determined using pop-up satellite archival tags. *Aquatic Conservation: Marine and Freshwater Ecosystems* 24:104-117.

Chamberlain, R.H. and P.H. Doering. 1998a. Freshwater inflow to the Caloosahatchee Estuary and the resource-based method for evaluation. In: S.F. Treat (ed.), *Proceedings of the Charlotte Harbor Public Conference and Technical Symposium*, South Florida Water Management District, Punta Gorda, Florida.

Chamberlain, R.H. and P.H. Doering. 1998b. Preliminary estimate of optimum freshwater inflow to the Caloosahatchee Estuary: A resource based approach. In: S.F. Treat (ed.), *Proceedings of the Charlotte Harbor Public Conference and Technical Symposium*, South Florida Water Management District, Punta Gorda, Florida.

Chamberlain, R.H., P.H. Doering, K.M. Haunert and D. Crean. 2003. Appendix C: Impacts of Freshwater Inflows on the Distribution of Zooplankton and Ichthyoplankton in the Caloosahatchee Estuary, Florida. In: SFWMD, *Technical Documentation to Support Development of Minimum Flows and Levels for the Caloosahatchee River and Estuary*, South Florida Water Management District, West Palm Beach, FL.

Chatfield, C. 1989. *The Analysis of Time Series: An Introduction, Fourth Edition*. Chapman and Hall, New York, NY.

Chen, Z., P.H. Doering, M. Ashton and B.A. Orlando. 2015. Mixing behavior of colored dissolved organic matter and its potential ecological implication in the Caloosahatchee River Estuary, Florida. *Estuaries and Coasts* DOI 10.1007/s/12237-014-9916-0.

Childers, D.L., J.N. Boyer, S.E. Davis, C.J. Madden, D.T. Rudnick and F. Sklar. 2006. Relating precipitation and water management to nutrient concentrations in the oligotrophic "upside-down" estuaries of the Florida Everglades. *Limnology and Oceanography* 51:602-616.

Childress, M.J. 2010. Modeling the impact of drought on South Carolina blue crabs using a spatially explicit individual-based population model. *Proceedings of the 2010 South Carolina Water Resources Conference*, Institute of Computational Ecology, Clemson University, Clemson, SC.

Christian, D. and Y.P. Sheng. 2003. Relative influence of various water quality parameters on light attenuation in Indian River Lagoon. *Estuarine, Coastal, and Shelf Science* 57:961-971.

Clark, A.E. 1935. Effects of temperature and salinity on early development of the oyster. 16:10, *Progress Report of the Atlantic Biological Station*, St. Andrews, New Brunswick.

Clarke K.R. 1993. Non-parametric multivariate analyses of changes in community structure. *Australian Journal of Ecology* 18:117-143.

Clarke, K.R. and R.N. Gorley. 2006. *PRIMER v6: User Manual/Tutorial*. PRIMER-E, Plymouth, United Kingdom.

Clarke, K.R. and R.M Warwick. 2001. *Change in Marine Communities: An Approach to Statistical Analysis and Interpretation, 2nd Edition*. PRIMER-E, Plymouth, United Kingdom.

Cloern, J.E. and A.D. Jassby. 2009. Patterns and scales of phytoplankton variability in estuarine-coastal ecosystems. *Estuaries and Coasts* 33:230-241.

Cloern, J.E. and A.D. Jassby. 2012. Drivers of change in estuarine-coastal ecosystems: Discoveries from four decades of study in San Francisco Bay. *Review of Geophysics* 50(RG4001):1-33.

Cloern, J.E., S.Q. Foster and A.E. Kleckner. 2014. Phytoplankton primary production in the world's estuarine-coastal ecosystems. *Biogeosciences* 11:2477-2501.

Coen, L.D., R.D. Brumbaugh, D. Bushek, R.E. Grizzle, M.W. Luckenbach, M.H. Posey, S.P. Powers and S.G. Tolley. 2007. Ecosystem services related to oyster restoration. *Marine Ecology Progress Series* 341:303-307.

Collins A.B., M.R. Heupel and C.A. Simpfendorfer. 2008. Spatial distribution and long-term movement patterns of cownose rays *Rhinoptera bonasus* within an estuarine river. *Estuaries and Coasts* 31:1174–1183.

Committee on Environment and Natural Resources. 2010. *Scientific Assessment of Hypoxia in U.S. Coastal Waters*. Interagency Working Group on Harmful Algal Blooms, Hypoxia, and Human Health of the Joint Subcommittee on Ocean Science and Technology, Washington, DC.

Condie, S.A., D. Hayes, E.A. Fulton and M. Savina. 2012. Modelling ecological change over a half a century in a subtropical estuary: Impacts of climate change, land-use, urbanization, and freshwater extraction. *Marine Ecology Progress Series* 457:43-66.

Copeland, B.J. 1966. Effects of decreased river flow on estuarine ecology. *Journal of the Water Pollution Control Federation* 38:1831-1839.

Copp, G.H. 1992. Comparative microhabitat use of cyprinid larvae and juveniles in a lotic floodplain channel. *Environmental Biology of Fishes* 33:181-193.

Costanza, R. and M. Ruth. 1998. Using dynamic modeling to scope environmental problems and build consensus. *Environmental Management* 22(2):183-195.

Cowardin, L.M., V. Carter, F.C. Golet and E.T. LaRoe. 1979. *Classification of Wetlands and Deepwater Habitats of the United States*. Fish and Wildlife Service, United States Department of the Interior, Jamestown, ND. December 4, 1998.

Crowder, L.B. 1986. Ecological and morphological shifts in Lake Michigan fishes: Glimpses of the ghost of competition past. *Environmental Biology of Fishes* 16:147-157.

Dale, V.H. and S.C. Beyeler. 2001. Challenges in the development and use of ecological indicators. *Ecological Indicators* 1:3-10.

Davis, H.C. 1958. Survival and growth of clam and oyster larvae at different salinities. *Biological Bulletin* 114:296-307

Dawes, C.J. and J.M. Lawrence. 1989. Allocation of energy resources in the freshwater angiosperms *Vallisneria americana* Michx. and *Potomogeton pectinatus* L. in Florida. *Florida Scientist* 52:59-63.

Day, J.W., C.A.S. Hall, W.M. Kemp and A. Yanez-Arancibia. 1989. Estuarine Ecology. John Wiley & Sons, Inc., New York, NY.

Day, J.W, J. Barras, E. Clarain, J. Johnston, D. Justic, G.P. Kemp, J.-Y. Ko, R. Lane, W.J. Mitsch, G. Steyer, P. Templet and A. Yanez-Arancibia. 2005. Implications of global climate change and energy cost and availability for the restoration of the Mississippi delta. *Ecological Engineering* 24:253-265.

Deegan, L., H. Kennedy and C. Neil. 1984. Natural factors and human modifications contributing to marsh loss in Louisiana's Mississippi River deltaic plain. *Environmental Management* 3:133-144.

Dekshenieks, M.M., E.E. Hofmann and E.N. Powell. 1993. Environmental effects on the growth and development of eastern oyster, *Crassostrea virginica* (Gmelin, 1791), larvae: a modeling study. *Journal of Shellfish Research* 12:241-254.

Dekshenieks, M.M., E.E. Hofmann, J.M. Klinck and E.N. Powell. 1996. Modeling the vertical distribution of oyster larvae in response to environmental conditions. *Marine Ecology Progress Series* 136:97-110.

Dekshenieks, M.M., E.E. Hofmann, J.M. Klinck and E.N. Powell. 2000. Quantifying the effects of environmental change on an oyster population: A modeling study. *Estuaries* 23:593-610.

Diaz, R.J. and R. Rosenberg. 2008. Spreading dead zones and consequences for marine ecosystems. *Science* 321:926-929.

Dobberfuhl, D.R. 2007. Light limiting thresholds for submerged aquatic vegetation in a blackwater river. *Aquatic Botany* 86:346-352.

Doering, P.H. and R.H. Chamberlain 1998. Water Quality in the Caloosahatchee Estuary, San Carlos Bay and Pine Island Sound. In: *Proceedings of the Charlotte Harbor Public Conference and Technical Symposium; 1997 March 15-16; Punta Gorda, FL*. Technical Report Number 98-02, Charlotte Harbor National Estuary Program, Punta Gorda, FL.

Doering, P.H., R.H. Chamberlain, K.M. Donohue and A.D. Steinman. 1999. Effect of salinity on the growth of *Vallisneria americana* Michx. from the Caloosahatchee Estuary, Florida. *Florida Scientist* 62(2):89-105.

Doering, P.H., R.H. Chamberlain and J.M. McMunigal. 2001. Effects of simulated saltwater intrusions on the growth and survival of wild celery, *Vallisneria americana*, from the Caloosahatchee Estuary (South Florida). *Estuaries* 24(6A):894-903.

Doering, P.H., R.H. Chamberlain, and D. Haunert. 2002. Using submersed aquatic vegetation to establish minimum and maximum freshwater inflows to the Caloosahatchee Estuary, Florida. *Estuaries* 25:1343-1354.

Doering, P.H., R.H. Chamberlain and K.M. Haunert. 2006. Chlorophyll *a* and its use as an indicator of eutrophication in the Caloosahatchee Estuary, Florida. *Florida Scientist* 69:51-72.

Dolbeth, M., F. Martinho, I. Viegas, H. Cabral and M.A. Pardal. 2008. Estuarine production of resident and nursery fish species: Conditioning by drought events? *Estuarine and Coastal Shelf Science* 78:51-60.

Drinkwater, K.F. and K.T. Frank. 1994. Effects of river regulation and diversion on marine fish and invertebrates. *Aquatic Conservation: Freshwater and Marine Ecosystems* 4:135-151.

Dyer, K.R. and R.J. Orth (eds.). 1994. *Changes in Fluxes in Estuaries*. Olsen & Olsen, Fredensborg, Denmark.

Eby, L.A. and L.B. Crowder. 2002. Hypoxia-based habitat compression in the Neuse River Estuary: Context-dependent shifts in behavioral avoidance thresholds. *Canadian Journal of Fisheries and Aquatic Sciences* 59:952-963.

Erdman, C. and J. Emerson. 2007. An R package for performing a Bayesian analysis of change point problems. *Journal of Statistical Software* (23):1-13.

FDEP. 2009. *Final TMDL Report – Nutrient TMDL for the Caloosahatchee Estuary (WBIDs 3240A, 3240B, and 3240C)*. Florida Department of Environmental Protection, Tallahassee, FL. September 2009. Available online at http://www.dep.state.fl.us/water/tmdl/final_tmdl.htm.

Fernandez-Carvalho, J., J.L. Imhoff, V.F. Faria, J.K. Carlson and G.H. Burgess. 2014. Status and the potential for extinction of the largetooth sawfish *Pristis* in the Atlantic Ocean. *Aquatic Conservation: Marine and Freshwater Ecosystems* 24:478-497.

Fisher W.S., J.T. Winstead, L.M. Oliver, H.L. Edminston and G.O. Bailey. 1996. Physiological variability of eastern oysters from Apalachicola Bay, Florida. *Journal of Shellfish Research* 15:543-555.

Flaig, E.G. and J. Capece. 1998. Water use and runoff in the Caloosahatchee Watershed. Pages 73–80 in: *Proceedings of the Charlotte Harbor Public Conference and Technical Symposium, March 15–16, 1997, Punta Gorda, FL*. Technical Report No. 98-02, Charlotte Harbor National Estuary Program, Punta Gorda, FL.

Flannery, M.S., E.B. Peebles and R.T. Montgomery. 2002. A percent-of-flow approach for managing reductions of freshwater inflows from unimpounded rivers to southwest Florida estuaries. *Estuaries* 25:1318-1332.

Frazier, T.K., S.K. Notestein, C.A. Jacoby, C.J. Littles, S.R. Keller and R.A. Swett. 2006. Effects of storm-induced salinity changes on submersed aquatic vegetation in Kings Bay, Florida. *Estuaries and Coasts* 29(6A):943-953.

French, GT and K.A. Moore. 2003. Interactive effects of light and salinity stress on the growth, reproduction, and photosynthetic capabilities of *Vallisneria americana* (wild celery). *Estuaries* 26(5):1255-1268.

Funahashi, T., A. Kasai, M. Ueno and Y. Yamashita. 2013. Effects of short time variation in the river discharge on the salt wedge intrusion in the Yura Estuary, a micro-tidal estuary, Japan. *Journal of Water Resource and Protection* 5:343-348.

FWRI. 2003. *Florida Fish and Wildlife Conservation Commission Marine Fisheries Information System 2002-2003 License/Permit Summary*. Florida Fish and Wildlife Research Institute, Florida Fish and Wildlife Conservation Commission, Tallahassee, FL.

Galtsoff, P. 1964. The American oyster, *Crassostrea virginica* Gmelin. *United States Fish and Wildlife Service Fishery Bulletin* 64:1-480.

Georgiou, I.Y. 1999. *Three-Dimensional Hydrodynamic Modeling of Saltwater Intrusion and Circulation in Lake Pontchartrain*. Dissertation, Department of Civil and Environmental Engineering, University of New Orleans, New Orleans, LA.

Geyer, W.R., R. Chant and R. Houghton. 2008. Tidal and spring-neap variations in horizontal dispersion in a partially mixed estuary. *Journal of Geophysical Research* 113:1-16.

Gillanders, B.M and M.J. Kingsford. 2002. Impact of changes in flow of freshwater on estuarine and open coastal habitats and the associated organisms. *Oceanography and Marine Biology: An Annual Review* 40:233-309.

Gillson, J. 2011. Freshwater flow and fisheries production in estuarine and coastal systems: Where a drop of rain is not lost. *Reviews in Fisheries Science* 19(3):168-186.

Gonzalez-Ortegon, E. and P. Drake. 2012. Effects of freshwater inputs on the lower trophic levels of a temperate estuary: Physical, physiological, or trophic forcing? *Aquatic Sciences* 74:455-469.

Guillian, M. and L. Aguirre-Macedo. 2009. Seasonal variation of physiological parameters in the eastern oyster *Crassostrea virginica* from a tropical region of the Gulf of Mexico. *Journal of Shellfish Research* 28(3):439-446.

Guillory, V. 2000. Relationship of blue crab abundance to river discharge and salinity. *Proceedings Annual Conference Southeastern Association of Fish and Wildlife Agencies* 54:213-220.

Gunter, G. and G.E. Hall. 1962. *Biological Investigation of the Caloosahatchee Estuary in Connection with Lake Okeechobee Discharges through the Caloosahatchee River*. Submitted to the United States Army Corps of Engineers, Jacksonville, FL. Serial Number 25.

Haller, W.T., D.L. Sutton and W.C. Barlowe. 1974. Effects of salinity on growth of several aquatic macrophytes. *Ecology* 55:891-894.

Halpern, B.S., H.M. Regan, H.P. Possingham and M.A. McCarthy. 2006. Accounting for uncertainty in marine reserve design. *Ecology Letters* 9:2-11.

Hauxwell, J., T.K. Frazer and C.W. Osenberg. 2004. Grazing by manatees excludes both new and established wild celery transplants: Implications for restoration in Kings Bay, FL, USA. *Journal of Aquatic Plant Management* 42:49-53.

Hauxwell, J, T.K. Frazer and C.W. Osenberg. 2007. An annual cycle of biomass and productivity of *Vallisneria americana* in a subtropical spring fed estuary. *Aquatic Botany* 87:61-68.

Heupel, M.R. and C.A. Simpfendorfer. 2008. Movement and distribution of young bull sharks *Carcharhinus leucas* in a variable estuarine environment. *Marine Ecology Progress Series* 1:277-289.

Heupel, M.R., B.G. Yeiser, A.B. Collins, L. Ortega and C.A. Simpfendorfer. 2010. Long-term presence and movement patterns of juvenile bull sharks, *Carcharhinus leuca*, in an estuarine river system. *Marine and Freshwater Research* 61:1-10.

Heupel, M.R., J.K. Carlson and C.A. Simpfendorfer. 2007. Shark nursery areas: Concepts, definitions, characterization and assumptions. *Marine Ecology Progress Series* 337:287-297.

Hill, M.O. 1973. Diversity and evenness: A unifying notation and its consequences. *Ecology* 54:427-432.

Hoffacker, A. 1994. 1993 *Caloosahatchee River Submerged Aquatic Vegetation Observations*. Letter Report from W. Dexter Bender and Associates, Fort Myers, FL, to the South Florida Water Management District, West Palm Beach, FL. March 2, 1994.

Hopkinson, C.S. and J.J. Vallino. 1995. The relationship among man's activities in watershed and estuaries: A model of runoff effects on estuarine community metabolism. *Estuaries* 18:598-621.

Hofstetter, R.P. 1977. *Trends in population levels of the American oyster,* Crassostrea virginica *Gmelin on Public Reefs in Galveston Bay, Texas*. Texas Parks and Wildlife Department, Austin, TX.

Hubbs, C.L. 1943. Terminology of early stages of fishes. *Copeia* 1943(4):260.

Hunt, M.J. and P.H. Doering. 2013. *Salinity Preferences and Nursery Habitat Considerations for Blue Crab (*Callinectes sapidus*), Bull Shark (*Carcharhinus leucas*), and Smalltooth Sawfish (*Pristis pectinata*) in the Caloosahatchee Estuary*. Technical publication WR-2013-001, South Florida Water Management District, West Palm Beach, FL.

Ippen A.T. 1966. Salt Intrusion in Estuaries. In: A.T. Ippen (ed.), *Estuaries and Coastal Hydrodynamics*, McGraw-Hill, New York, NY.

Ippen, A.T and D.R.F. Harleman. 1961. *One-Dimensional Analysis of Salinity Intrusion in Estuaries*. Technical Bulletin Number 5, United States Army Corps of Engineers, Vicksburg, MS.

Jarvis, J.C. and K.A. Moore. 2008. Influence of environmental factors on *Vallisneria* americana seed germination. *Aquatic Botany* 88:283-294.

Jassby, A.D., W.J. Kimmerer, S.G. Monismith, C. Armor, J.E. Cloern, T.M. Powell, J.R. Schubel and T.J. Vendlinski. 1995. Isohaline position as a habitat indicator for estuarine populations. *Ecological Applications* 5:272-289.

Jay, D.A., W.R. Grey, R.J. Uncles, J. Vallino, J. Largier and W.R. Boynton. 1997. A review of recent developments in estuarine scalar flux estimation. *Estuaries* 20(2):262-280.

Kemp, W.M., W.R. Boynton, J.E. Adolf, D.F. Boesch, W.C. Boicourt, G. Brush, J.C. Cornwell, T.R. Fisher, P.M. Glibert, J.D. Hagy, L.W. Harding, E.D. Houde, D.G. Kimmel, W.D. Miller, R.I.E. Newell, M.R. Roman, E.M. Smith and J.C. Stevenson. 2005. Eutrophication of Chesapeake Bay: Historical trends and ecological interactions. *Marine Ecology Progress Series* 303:1-29.

Kemp, W.M., J.M. Testa, D.J. Conley, D. Gilbert and J.D. Hagy. 2009. Temporal responses of coastal hypoxia to nutrient loading and physical controls. *Biogeosciences* 6:2985-3008.

Kennedy, V.S. 1991. American Oyster, *Crassostrea virginica*. Pages 3-1 to 3-20 in: S.L. Funderburk, S.J. Jordan, J.A. Mihursky and D. Riley (eds.), *Habitat Requirements for Chesapeake Bay Living Resources, Second Edition*, Chesapeake Research Consortium, Inc., Solomons, MD.

Kimes, C.A. and L.C. Crocker. 1999. A historical overview of the Caloosahatchee and its watershed. *Harbor Happenings, Spring Newsletter of the Charlotte Harbor National Estuary Program* 3(1):8-13.

Kimura, R., D.H. Secor, E.D. Houde and P.M Piccoli. 2000. Up-estuary dispersal of young-of-the-year bay anchovy *Anchoa mitchilli* in the Chesapeake Bay: Inferences from microprobe analysis of strontium in otoliths. *Marine Ecology Progress Series* 208:217-227.

Konyha, K. and Y. Wan. 2011. *Calibration and Refinement of the Tidal Caloosahatchee Basin Linear Reservoir Model*. Technical report to support the Caloosahatchee Estuary Water Reservation Project, South Florida Water Management District, West Palm Beach, FL.

Kraemer, G.P., R.H. Chamberlain, P.H. Doering, A.D. Steinman and M.D. Hanisak. 1999. Physiological responses of transplants of the freshwater angiosperm *Vallisneria americana* along a salinity gradient in the Caloosahatchee Estuary (southwest Florida). *Estuaries* 22(1):138-148.

Kuijper, K and L.C. Van Rijn. 2011. Analytical and numerical analysis of tides and salinities in estuaries, Part II: Salinity distribution in prismatic and convergent tidal channels. *Ocean Dynamics* 61:1743-1765.

La Peyre, M.K., A.D. Nickens, A.K. Volety, G.S. Tolley and J.F. La Peyre. 2003. Environmental significance of freshets in reducing *Perkinsus marinus* infection in eastern oysters *Crassostrea virginica*: Potential management applications. *Marine Ecology Progress Series* 248:165-176.

La Peyre, M.K., B. Gossman and J.F. La Peyre. 2009. Defining optimal freshwater flow for oyster production: Effects of freshet rate and magnitude of change and duration on eastern oysters and *Perkinsus marinus* infection. *Estuaries and Coasts* 32:522-534.

Lamon, E.C., K.H. Reckhow and K.E. Havens. 1996. Using generalized additive models for prediction of chlorophyll *a* in Lake Okeechobee, Florida. *Lakes & Reservoirs: Research and Management* 2:37-46.

Lancelot, C. and K. Muylaert. 2011. Trends in estuarine phytoplankton ecology. Pages 5–15 in: E. Wolanski and D.S. McLusky (eds.), *Treatise on Estuarine and Coastal Science, Volume 7*, Academic Press, Waltham, MA.

Lane, R.R., J.W. Day, B.D. Marx, E. Reyes, E. Hyfield and J.N. Day. 2007. The effects of riverine discharge on temperature, salinity, suspended sediment and chlorophyll *a* in a Mississippi delta estuary measured using a flow-through system. *Estuarine, Coastal, and Shelf Science* 74:145-154.

Langevin, C.D. 2003. Simulation of submarine groundwater discharge to a marine estuary: Biscayne Bay, Florida. *Ground Water* 41(6):758-771.

Lauer, N., M. Yeager, A.E. Kahn, D.R. Dobberfuhl and C. Rossa. 2011. The effects of short term salinity exposure on the sublethal stress response of *Vallisneria americana* Michx. (Hydrocharitaceae). *Aquatic Botany* 95:207-213.

Lehrter, J.C. and J. Cebrian. 2010. Uncertainty propagation in an ecosystem nutrient budget. *Ecological Applications* 20(2):508-524.

Livingston, R.J. 2007. Phytoplankton bloom effects on a gulf estuary: Water quality changes and biological response. *Ecological Applications* 17(5):S110-S128.

Livingston, R.J., X. Niu, F.G. Lewis and G.C. Woodsum. 1997. Freshwater input to a gulf estuary: Long term control of trophic organization. *Ecological Applications* 7:277-299.

Livingston, R.J., F.G. Lewis, G.C. Woodsum, X-F. Niu, B. Galperin, W. Huang, J.D. Christensen, M.E. Monaco, T.A. Battista, C.J. Klein, R.L. Howell and G.L. Ray. 2000. Modelling oyster population response to variation in freshwater input. *Estuarine, Coastal, & Shelf Science* 50:655-672.

Liu, W-C., M-H. Hsu, A.Y. Kuo and M-S Li. 2001. Influence of bathymetric changes on hydrodynamics and salt intrusion in estuarine system. *Journal of the American Water Resources Association* 37:1405-1416.

Loneragan, N.R. and S.E. Bunn 1999. River flow and estuarine ecosystems: Implications for coastal fisheries from a review and a case study of the Logan River, southeast Queensland. *Australian Journal of Ecology* 24:431-440.

Longley, W.L., G.L. Powell and A.W. Green. 1994. Freshwater inflows to Texas bays and estuaries: Ecological relationships and methods for determination of needs. Texas Water Development Board and Texas Parks and Wildlife Department, Austin, TX.

Loosanoff, V.L. 1953. Behavior of oysters in water of low salinities. *Proceedings of the National Shellfish Association* 43:135-151.

Loosanoff, V.L. 1965. Gonad development and discharge of spawn in oysters of Long Island Sound. *Biological Bulletin* (Woods Hole) 129:546-561.

Lovett-Doust, J. and G. Laporte. 1991. Population sex ratios, population mixtures and fecundity in a clonal dioecious macrophyte, *Vallisneria americana*. *Journal of Ecology* 79:477-489.

Mackin, J.G. and S.H. Hopkins. 1962. Studies on oyster mortality in relation to natural environments and to oil fields in Louisiana. *Publications of the Institute of Marine Science, University of Texas* 7:1-131.

MacWilliams, M.L., F.G. Salcedo and E.S. Gross. 2009. *San Francisco Bay-Delta UnTRIM Model Calibration Report, Sacramento and Stockton Deep Water Ship Channel 3-D Hydrodynamic and Salinity Modeling Study*. Prepared for United States Army Corps of Engineers, San Francisco, CA.

Madden, C.J. and J.W. Day. 1992. An instrument system for high-speed mapping of chlorophyll *a* and physico-chemical variables in surface waters. *Estuaries* 15:421-427.

Mattson, R.A., K.W. Cummins, R.W. Merritt, P.A. Montagna, T. Palmer, J. Mace, J. Slater, and C. Jacoby. 2012. Benthic Macroinvertebrates. In: E.F. Lowe, L.E. Battoe, H. Wilkening, M. Cullum and T. Bartol (eds.), *The St. Johns River Water Supply Impact Study Final Report*. St. Johns River Water Management District, Palatka, FL.

Mazzotti, F.J., L.G. Pearlstine, T. Barnes, A. Volety, A. Chartier, A. Weinstein and D. DeAngleis. 2006. *Stressor Response Models for the Blue Crab,* Callinectes sapidus. Department of Wildlife Ecology and Conservation, Florida Cooperative Extension Service, Institute of Food and Agricultural Sciences, University of Florida, Gainesville, FL.

McFarland, D.G. 2006. *Reproductive Ecology of* Vallisneria americana Michaux. Report ERDC/TN SAV-06-4, United States Army Engineer Research and Development Center, Vicksburg, MS.

McPherson, B.F. and R.L. Miller. 1994. Causes of light attenuation in Tampa Bay and Charlotte Harbor, southwestern Florida. *Water Resources Bulletin* 30(1):43-53.

Meeter, D.A., R.J. Livingston and G.C. Woodsum. 1979. Long-term climatological cycles and population changes in a river-dominated estuarine system. Pages 315-338 in: R.J. Livingston (ed.), *Ecological Processes in Coastal and Marine Systems, Marine Science Volume 10,* Springer, New York, NY.

Millero, F. 2010. History of the equation of state of seawater. *Oceanography* 23(3):18-33.

Montagna, P.A. and T. Palmer. 2014. *Minimum Flow and Level Analysis of Benthic Macrofauna in the Caloosahatchee Estuary*. Draft report to the South Florida Water Management District, West Palm Beach, FL.

Montagna, P.A., M. Alber, P.H. Doering and M.S. Connor. 2002a. Freshwater inflow: Science, policy, management. *Estuaries* 25:1243-1245.

Montagna, P.A., R.D. Kalke and C. Ritter. 2002b. Effect of restored freshwater inflow on macrofauna and meiofauna in upper Rincon Bayou, Texas, USA. *Estuaries* 25:1436-1447.

Montagna, P.A., E.D. Estevez, T.A. Palmer and M.S. Flannery. 2008. Meta-analysis of the relationship between salinity and molluscs in tidal river estuaries of Southwest Florida, U.S.A. *American Malacological Bulletin* 24:101-115.

Montagna, P.A., T.A. Palmer and J.B. Pollack. 2013. Hydrological changes and estuarine dynamics. *Springer Briefs in Environmental Science*, New York, NY.

Moore, KA, E.C. Shields and J.C. Jarvis. 2010. The role of habitat and herbivory on the restoration of tidal freshwater submerged aquatic vegetation populations. *Restoration Ecology* 18(4):596-604.

Moses, C.S., W.T. Anderson, C. Saunders and F. Sklar. 2013. Regional climate gradients in precipitation and temperature in response to climate teleconnections in the greater Everglades ecosystem of South Florida. *Journal of Paleolimnology* 49:5-14.

Murphy, M.D., A.L. McMillen-Jackson and B. Mahoudi. 2007. *A Stock Assessment of the Blue Crab,* Callinectes sapidus*, in Florida Waters*. In-House Report 2007-006, Florida Fish and Wildlife Commission, Florida Wildlife Research Institute, St. Petersburg, FL.

Murrell, M., J.D. Hagy, E.M. Lores and R.M. Greene. 2007. Phytoplankton production and nutrient distributions in a subtropical estuary: Importance of freshwater flow. *Estuaries and Coasts* 30:390-402.

Nelson, D.M. (ed.). 1992. *Distribution and Abundance of Fishes and Invertebrates in Gulf of Mexico Estuaries, Volume I: Data Summaries*. Estuarine Living Marine Resources Report Number 10, National Ocean Service, National Oceanic and Atmospheric Administration, Rockville, MD.

Nixon, S.W. 1981. Freshwater inputs and estuarine productivity. Pages 31–57 in: R. Cross and D. Williams (eds.), *Proceedings of the Nation Symposium on Freshwater Inflow to Estuaries, Volume I and II*, FWS/OBS-81/04, United States Fish and Wildlife Service Washington, DC.

Nixon, S.W., S.B. Olsen, E. Buckley and R. Fulweiler. 2004. *Lost to the Tide: The Importance of Freshwater Flow to Estuaries*. Final Report submitted by the Graduate School of Oceanography, University of Rhode Island, Kingston, RI, to the Coastal Resources Center, Narragansett, RI.

Nixon, S.W., C.A. Oviatt, J. Frithsen and B. Sullivan. 1986. Nutrients and the productivity of estuarine and coastal marine ecosystems. *Journal of the Limnological Society of South Africa* 12(1/2):43-71.

NOAA. 2009. *Critical Habitat for the Endangered Distinct Population Segment of Smalltooth Sawfish*. National Oceanic and Atmospheric Administration, Federal Register, Rules and Regulations 74(169):45353-45378.

Norton, S.L., T.R. Wiley, J.K. Carlson, A.L. Frick, G.R. Poulakis and C.A. Simpfendorfer. 2012. Designating critical habitat for juvenile endangered smalltooth sawfish in the United States. *Marine and Coastal Fisheries: Dynamics, Management, and Ecosystem Science* 4(1):473-480.

Nosach, C. 2007. *Influence of environmental factors on the germination of South Florida* Vallisneria americana. Senior Thesis, Eckerd College, St. Petersburg, FL.

Obeysekera, J., P. Trimble, C. Neidrauer and L. Cadavid. 2007. Consideration of Climate Variability in Water Resources Planning and Operations – South Florida's Experience. In: K.C. Kabbes (ed.), *World Environmental and Water Resource Congress 2007: Restoring Our Natural Habitat*, American Society of Civil Engineers, Baltimore, MD.

Obeysekera, J., L. Kuebler, S. Ahmed, M.-L. Chang, V. Engel, C. Langevin, E. Swain and Y. Wan. 2011. Use of hydrologic and hydrodynamic modeling for ecosystem

restoration. *Critical Reviews in Environmental Science and Technology* 41(S1):447-488.

Ogden, J.C., S.M. Davis, K.J. Jacobs, T. Barnes and H.E. Fling. 2005. The use of conceptual ecological models to guide ecosystem restoration in South Florida. *Wetlands* 25(4):795-809.

Ortega, L.A., M.R. Heupel, P. Van Beynen and P.J. Motta. 2009. Movement patterns and water quality preferences of juvenile bull sharks (*Carcharhinus leucas*) in a Florida estuary. *Environmental Biology of Fishes* 84:361-373.

Paerl, H.W., L.M. Valdes, B.L. Peierls, J.E. Adolf and L.W. Harding. 2006. Anthropogenic and climatic influences on the eutrophication of large estuarine ecosystems. *Limnology and Oceanography* 51(1/2):448-462.

Palmer, T.A., P.A. Montagna, J.B. Pollack, R.D. Kalke and H.R. DeYoe. 2011. The role of freshwater inflow in lagoons, rivers, and bays. *Hydrobiologia* 667:49-67.

Palmer, T.A., P.A. Montagna, R.H. Chamberlain, P.H. Doering, Y. Wan, K.M. Haunert and D.J. Crean. 2015. Determining the effects of freshwater inflow on benthic macrofauna in the Caloosahatchee Estuary, Florida. *Integrated Environmental Assessment and Management* 12(3):529-39, doi:10.1002/ieam.1688.

Peebles, E.B., S.E. Burghart and D.J. Hollander. 2007. Causes of inter-estuarine variation in bay anchovy (*Anchoa mitchilli*) salinity at capture. *Estuaries and Coasts* 30:1060-1074.

Peebles, E.B. and M.F.D. Greenwood. 2009. Spatial abundance quantiles as a tool for assessing habitat compression in motile estuarine organisms. *Florida Scientist* 72:277-288.

Perry, H.M. 1984. *A Profile of the Blue Crab Fishery of the Gulf of Mexico*. Gulf State Marine Fisheries Commission, Ocean Springs, MS.

Perry, H.M. and T.D. McIlwain. 1986. *Species Profiles: Life Histories and Environmental Requirements of Coastal Fishes and Invertebrates (Gulf of Mexico): Blue Crab*. Biological Report 82(11.55), United States Fish and Wildlife Service, Washington, DC and TR EL-82-4, United States Army Corps of Engineers, Washington, DC.

Peterson, M.S. 2003. A conceptual view of environment-habitat-production linkages in tidal river estuaries. *Reviews in Fisheries Science* 11(4):291-313.

Petes, L.E., A.J. Brown and C.R. Knight. 2012. Impacts of upstream drought and water withdrawals on the health and survival of downstream estuarine oyster populations. *Ecology and Evolution* 2(7):1712-1724.

Petrie M.D. and N.A. Brunsell. 2011. The role of precipitation variability on the ecohydrology of grasslands. *Ecohydrology* doi:12.1002/eco.224.

Phillips, R. C. and V.G. Springer 1960. *A Report on the Hydrography, Marine Plants and Fishes of the Caloosahatchee River Area, Lee County, Florida*. Special Report Number 5, Florida State Board of Conservation Marine Lab, Tallahassee, Florida.

Pollack, J.B., H-C. Kim, E.K. Morgan and P.A. Montagna. 2011. Role of flood disturbance in natural oyster (*Crassostrea virginica*) population maintenance in an estuary in South Texas, USA. *Estuaries and Coasts* 34:187-197.

Posey, M.H., T.D. Alphin, H. Harwell and B. Allen. 2005. Importance of low salinity areas for juvenile blue crabs, *Callinectes sapidus* Rathbun, in river-dominated estuaries of southeastern United States. *Journal of Experimental Marine Biology and Ecology* 319:81-100.

Poulakis, G.R., P.W. Stevens, A.A. Timmers, T.R. Wiley and C.A. Simpfendorfer. 2011. Abiotic affinities and spatiotemporal distribution of the endangered smalltooth sawfish, *Pristis pectinata*, in a southwestern Florida estuary. *Marine and Freshwater Research* 62:1165-1177.

Poulakis, G.R., P.W. Stevens, A.A. Timmers, C.J. Stafford and C.A. Simpfendorfer. 2013. Movements of juvenile endangered smalltooth sawfish, *Pristis pectinata*, in an estuarine river system: Use of non-main-stem river habitats and lagged responses to freshwater inflow related changes. *Environmental Biology of Fishes* 96:763-778.

Poulakis, G.R., P.W. Stevens, R.D. Grubbs, D.D. Chapman, J. Gelsleichter, G.H. Burgess, T.R. Wiley, J.A. Olin, L.S. Hollensead, A.T. Fisk, D.A. Blewett, R.M. Scharer, H.J. Grier, J.A. DeAngelo, J.M. Darrow, Y. Papstamatiou and M.D. Bakenhaster. 2014. *Smalltooth Sawfish (*Pristis Pectinata*) Research and Outreach: An Interdisciplinary Collaborative Program*. Report to Fisheries Species Recovery Grant NA10NMF4720032, National Oceanic and Atmospheric Administration, Washington, DC.

Powell, E.N., J.M. Klinck, E.E. Hofmann and M.A. McManus. 2003. Influence of water allocation and freshwater inflow on oyster production: A hydrodynamic-oyster population model for Galveston Bay, Texas, USA. *Environmental Management* 31:100-121.

Powers, S.P., C.H. Peterson, R.R. Christian, E. Sullivan, M.J. Powers, M.J. Bishop and C. Buzzelli. 2005. Effects of eutrophication on bottom habitat and prey resources of demersal fishes. *Marine Ecology Progress Series* 302:233-243.

Prandle, D. 1985. On salinity regimes and the vertical structure of residual flows in narrow tidal estuaries. *Estuarine, Coastal Shelf Science* 20:615-635.

Prandle, D. 2004. Salinity intrusion in partially mixed estuaries. *Estuarine, Coastal Shelf Science* 54:385-397.

Prandle D. 2009. *Estuaries, Dynamics, Mixing, Sedimentation and Morphology*. Cambridge University Press, Cambridge, United Kingdom.

Punt, A.E. 2003. Evaluating the efficacy of managing West Coast groundfish resources through simulations. *Fisheries Bulletin* 101:860–873.

Qian, S.S., Y. Pan and R.S. King. 2004. Soil total phosphorus threshold in the Everglades: A Bayesian changepoint analysis for multinomial response data. *Ecological Indicators* 4:29-37.

Qiu, C. 2002. *Hydrodynamic and Salinity Modeling, Technical Supporting Document for Caloosahatchee River Minimum Flow and Levels Update*. South Florida Water Management District, West Palm Beach, FL.

Qiu, C. 2006. *Addendum to CH3D Calibration Report in Estero Bay and Caloosahatchee Estuary*. South Florida Water Management District, West Palm Beach, FL.

Qiu, C., Y. Sheng and Y. Zhang, 2007. Development of a hydrodynamic and salinity model in the Caloosahatchee and Estero Bay, Florida, P 106-123, *Estuarine and Coastal Modeling*, Proceeding of the Tenth International Conference edited by M. L. Spaulding, ASCE

Qiu, C. and Y. Wan. 2013. Time series modeling and prediction of salinity in the Caloosahatchee River Estuary. *Water Resources Research* 49:1-13.

Rabalais, N.N., R.J. Diaz, L.A. Levin, R.E. Turner, D. Gilbert and J. Zhang. 2010. Dynamics and distribution of natural and human-caused hypoxia. *Biogeosciences* 7:585-619.

Radabaugh, K.R. and E.B. Peebles. 2012. Detection and classification of phytoplankton deposits along an estuarine gradient. *Estuaries and Coasts* 35:1361-1375.

Reckhow, K.H. 1994. Water quality simulation modeling and uncertainty analysis for risk assessment and decision making. *Ecological Modelling* 72:1-20.

RECOVER. 2012. *2012 System Status Report Interim Update*. Restoration Coordination and Verification, c/o United States Army Corps of Engineers, Jacksonville, FL, and South Florida Water Management District, West Palm Beach, FL. Available online at http://141.232.10.32/pm/ssr_2012/ssr_main_2012.aspx.

RECOVER. 2014. *2014 System Status Report*. Restoration Coordination and Verification, c/o United States Army Corps of Engineers, Jacksonville, FL, and South Florida Water Management District, West Palm Beach, FL. Available online at http://141.232.10.32/pm/ssr_2014/ssr_main_2014.aspx.

Regan, H.M., M. Colyvan and M.A. Burgman. 2002. A taxonomy and treatment of uncertainty for ecology and conservation biology. *Ecological Applications* 12(2):618-628.

Restrepo, V.R., J.M. Hoenig, J.E. Powers, J.W. Baird and S.C. Turner. 1992. Monte Carlo simulation applied to *Xiphias gladius* and *Gadus morhua*. *Fishery Bulletin* 90:736-748.

Ricker, W.E. 1973. Linear regressions in fishery research. *Journal of the Fisheries Research Board of Canada* 30:409-434.

Ricker, W.E. 1975. A note concerning Professor Jolicoeur's comments. *Journal of the Fisheries Research Board of Canada* 32:1494-1498.

Robins, J.B., I.A. Halliday, J. Staunton-Smith, D.G. Mayer and M.J. Sellin. 2005. Freshwater-flow requirements of estuarine fisheries in tropical Australia: A review of the state of knowledge and application of a suggested approach. *Marine and Freshwater Research* 56:343-360.

Rogers, S.G., J.D. Arredondo and S.N. Latham. 1990. *Assessment of the Effects of the Environment on the Georgia Blue Crab Stock*. S-K Project Number NA90AA-H-SK018, Georgia Department of Natural Resources, Brunswick, GA.

Rozas, L.P. and T.J. Minello. 2006. Nekton use of *Vallisneria americana* Michx. (wild celery) beds and adjacent habitats in coastal Louisiana. *Estuaries and Coasts* 29(2):297-310.

Ruggieri, E. 2012. A Baysian approach to detecting c hang points in climatic records. *International Journal of Climatology* doi:10.1002/JOC.3447.

Sackett, J.W. 1888. *Survey of the Caloosahatchee River, Florida*. Report to the Captain of the United States Engineering Office, St. Augustine, FL.

Sandoz, M.D. and R. Rogers. 1944. The effect of environmental factors on hatching, molting, and survival of zoea larvae of the blue crab, *Callinectes sapidus*, Rathbun. *Ecology* 25(2) 216-228.

Saundry, P. and C. Cleveland (eds.). 2011. *Wadden Sea, Encyclopedia of Earth*. National Council for Science and the Environment, Washington, DC.

Savenije, H.H.G. 1992. *Rapid Assessment Technique for Salt Intrusion in Alluvial Estuaries*. Ph.D. Dissertation, IHE report series, Number 27, Delft, the Netherlands.

Savenije, H.H.G. 2005. *Salinity and Tides in Alluvial Estuaries*. Elsevier, Amsterdam

Scavia, D., D. Justic and V.J. Bierman. 2004. Reducing hypoxia in the Gulf of Mexico: Advice from three models. *Estuaries* 27(3):419-425.

Schlacher, T.A., A.J. Skillington, R.M. Connolly, W. Robinson and T.F. Gaston. 2008. Coupling between marine plankton and freshwater flow in the plumes off a small estuary. *International Review of Hydrobiology* 93(6):641-658.

Schwarz, C.J. 2013. Chapter 8: Regression – Hockey Sticks, Broken Sticks, Piecewise, Change Points. In: C.J. Schwarz (ed.), *Sampling, Regression, Experimental Design and Analysis for Environmental Scientist, Biologists and Resource Managers*. Simon Fraser University, Burnaby, British Columbia.

Seaman, W. (ed.). 1988. *Florida Aquatic Habitat and Fishery Resources*. Florida Chapter, American Fisheries Society, Eustis, FL.

SFWMD. 2000. *Draft Technical Documentation to Support Development of Minimum Flows and Levels for the Caloosahatchee River and Estuary*. South Florida Water Management District, West Palm Beach, FL. September 6, 2000. Available online at https://www.sfwmd.gov/sites/default/files/documents/mfl_caloos_092000.pdf.

SFWMD. 2003. *Draft Caloosahatchee Minimum Flows and Levels Status Update Report*. South Florida Water Management District, West Palm Beach, FL. February 3, 2003. Available online at https://www.sfwmd.gov/sites/default/files/documents/caloo2003doc.pdf.

SFWMD. 2010. *Final Adaptive Protocols for Lake Okeechobee Operations*. South Florida Water Management District, West Palm Beach, FL. September 16, 2010.

SFWMD. 2014. *Document to Support a Water Reservation Rule for the CERP Caloosahatchee River (C-43) West Basin Storage Reservoir Project*. South Florida Water Management District, West Palm Beach, FL.

SFWMD. 2012. *2012 Lower West Coast Water Supply Plan Update*. South Florida Water Management District, West Palm Beach, FL.

Sheaves, M., R. Baker, I. Nagelkerten and R.M. Connolly. 2015. True value of estuarine and coastal nurseries for fish: Incorporating complexity and dynamics. *Estuaries and Coasts* 38:401-414.

Sheldon, J. and M. Alber. 2006. The calculation of estuarine turnover times using freshwater fraction and tidal prism models: A critical evaluation. *Estuaries and Coasts* 29(1):133-146.

Sheng, Y.P. 1986. A Three-dimensional Mathematical Model of Coastal, Estuarine and Lake Currents Using Boundary-fitted Grid. Technical Report No. 585, Aeronautical Research Associates, Princeton, N.J.

Sheng, Y.P. 1987. On Modeling Three-Dimensional Estuarine and Marine Hydrodynamics. Pages 35–54 in: J.C.J. Nihoul and B.M. Jamart (eds.), *Three-Dimensional Models of Marine and Estuarine Dynamics.* Elsevier Oceanography Series, Waltham, MA.

Sheng, Y.P. 2002. *Impact of Caloosahatchee Flow on Circulation and Salinity in Charlotte Harbor, Technical Report*. Civil & Coastal Engineering Department, University of Florida, Gainesville, FL.

Sheng, Y.P and C. Villaret, 1989. Modeling the effect of suspended sediment stratification on bottom exchange processes. Journal of Geophysical Research, 94(10):14429-14444.

Sheng, Y.P and Y. Zhang. 2006. *Estero Bay and Caloosahatchee Salinity Modeling, Final Report*. Submitted to South Florida Water Management District, West Palm Beach, FL.

Shumway, S.E. 1996. Natural Environmental Factors. Pages 467–503 in: V.S. Kennedy, R.I.E. Newell and A. Eble (eds.), *The Eastern Oyster (*Crassostrea virginica*)*. Maryland Sea Grant College, College Park, MD.

Simpfendorfer, C.A., B.G. Yeiser, T.R. Wiley, G.R. Poulakis, P.W. Stevens and M.R. Heupel. 2011. Environmental influences on the spatial ecology of juvenile smalltooth sawfish (*Pristis pectinata*): Results from acoustic monitoring. *Plos One* 6(2):1-12.

Sklar, F.H. and J.A. Browder. 1998. Coastal environmental impacts brought about by alterations to freshwater flow in the Gulf of Mexico. *Environmental Management* 22(4):547-562.

Spencer, D., C.J. Lemckert, Y. Yu, J. Gustafson, S.Y. Lee and H. Zhang. 2014. Quantifying dispersion in an estuary. *Journal of Coastal Research* Special Issue 70:29-34.

Stanley, J.G. and M.A. Sellers. 1986. American Oyster. In: *Species Profiles: Life Histories and Environmental Requirements of Coastal Fishes and Invertebrates (Gulf of Mexico).* United States Fish and Wildlife Service, Washington, DC.

Stevens, P.W., M.F.D. Greenwood, T.C. MacDonald, C.F. Idelberger and R.H. Michael, Jr. 2008. *Relationships between Freshwater Inflows and Fish Populations in the Caloosahatchee River Estuary, Florida*. File Code: F2706-07-F1, Fish and Wildlife Research Institute, Florida Fish and Wildlife Conservation Commission, Tallahassee, FL.

Stevens, P.W., M.F.D. Greenwood, C.F. Idleberger and D.A. Blewitt. 2010. Mainstem and backwater fish assemblages in the tidal Caloosahatchee River: Implications for freshwater inflow studies. *Estuaries and Coasts* 33:1216-1224.

Stevens, P.W., M.F.D. Greenwood and D.A. Blewett. 2013. Fish assemblages in the oligohaline stretch of a southwest Florida river during periods of extreme freshwater inflow variation. *Transactions of the American Fisheries Society* 142:1644-1658.

Sun, D. 2004. Preliminary Feasibility Study of Saltwater Barrier in the Loxahatchee River Estuary. Coastal Tech, Vero Beach, FL.

Sun. D. 2009. *Development of the CH3D Hydrodynamic Model for the St. Lucie Estuary, Technical Document to Support a Water Reservation Rule for the North Fork of the St. Lucie Estuary*. South Florida Water Management District, West Palm Beach, FL.

Sutcliffe, W.H., 1972. Some relations of land drainage, nutrients, particulate material, and fish catch in two eastern Canadian bays. *Journal of the Fisheries Research Board of Canada* 29:357-362.

Sutcliffe, W.H. 1973. Correlations between seasonal river discharge and local landings of American lobster (*Homarus americanus*) and Atlantic halibut (*Hippolossus hippoglossus*) in the Gulf of St. Lawrence. *Journal of the Fisheries Research Board of Canada* 30:856-859.

Sutherland, K., N.A. Strydom and T.H. Woolridge. 2012. Composition, abundance, distribution, and seasonality of larval fishes in the Sundays Estuary, South Africa. *African Zoology* 47(2):229-244.

Titus, J.E. and D.T. Hoover. 1991. Toward predicting reproductive success in submersed freshwater angiosperms. *Aquatic Botany* 41:111-136.

Tolley, S.G. A.K. Volety and M. Savarese. 2005. Influence of salinity on the habitat use of oyster reefs in three Southwest Florida estuaries. *Journal of Shellfish Research* 24:127-137.

Tolley, S.G. A.K. Volety, M. Savarese, L.D. Walls, C. Linardich and E.M. Everham III. 2006. Impacts of salinity and freshwater inflow on oyster-reef communities in Southwest Florida. *Aquatic Living Resources* 19:371-387.

Tolley, S.G., D. Fugate, M.L. Parsons, S.E. Burghart and E.B. Peebles. 2010. *The Responses of Turbidity, CDOM, Benthic Microalgae, Phytoplankton, and Zooplankton to Variation in Seasonal Freshwater Inflow to the Caloosahatchee Estuary*. Final Project Report to the South Florida Water Management District, West Palm Beach, FL, and the United States Department of Education, Washington, DC.

Tolley, S.G., B.M. Brosious, J.T. Evans, J.L. Nelson, L.H. Haynes, L.K. Smith, S.E. Burghart and E.B. Peebles. 2012. Freshwater inflow effects of larval fish and crab settlement onto oyster reefs. *Journal of Shellfish Research* 31(3):895-908.

Turner, R.E. 2006. Will lowering estuarine salinity increase Gulf of Mexico oyster landings? *Estuaries & Coasts* 29:345-352.

Twilley, R.R. and J.W. Barko. 1990. The growth of submersed macrophytes under experimental salinity and light conditions. *Estuaries* 12:311-321.

Urban, D.L. 2006. A modeling framework for restoration ecology. In D.A. Falk, M.A. Palmer and R.J. Hobbs (eds.), *Foundations of Restoration Ecology*, Island Press, Boca Raton, FL.

USACE, 1957. *General Design Memorandum, Caloosahatchee River and Control Structures (Canal 43 Lock and Spillway Structures 77, 78, and 79), Part IV: Central and Southern Florida Project*. Serial Number 36, Jacksonville District, United States Army Corps of Engineers, Jacksonville, FL.

USACE 2008. *St. John's River Circulation and Salinity for the Jacksonville Harbor Navigation Study*. United States Army Corps of Engineers, Jacksonville, FL.

USACE and SFWMD. 2010. *Central and Southern Florida Project Caloosahatchee River (C-43) West Basin Storage Reservoir Integrated Project Implementation Report and Environmental Impact Statement*. United States Army Corps of Engineers, Jacksonville, FL, and South Florida Water Management District, West Palm Beach, FL.

Van der Burgh, P. 1972. *Ontwikkeling van een methode voor het voorspellen van zoutverdelingen in estuaria, kanalen en zeeën*. Rijkswterstaat, Deltadienst.

Van Engel, W. 1958. The blue crab fishery in Chesapeake Bay. *Commercial Fisheries Review* 20:6-17.

Volety, A.K., M. Savarese, S.G. Tolley, W.S. Arnold, P. Sime, P. Goodman, R.H. Chamberlain and P.H. Doering. 2009. Eastern oysters (*Crassotrea virginica*) as an indicator for restoration of Everglades ecosystems. *Ecological Indicators* 9:S120-S136.

Wan, Y. and K. Konyha. 2015. A simple hydrologic model for rapid prediction of runoff from ungauged coastal catchments. *Journal of Hydrology* 528:571-583

Wan, Y., Z-G. Ji, J. Shen, G.Hu and D. Sun. 2012. Three dimensional water quality modeling of a shallow sub-tropical estuary. *Marine Environmental Research* 82:76-86.

Wan, Y., C. Qiu, P.H. Doering, M. Ashton, D. Sun and T. Coley. 2013. Modelling residence time with a three-dimensional hydrodynamic model: Linkage with chlorophyll *a* in a sub-tropical estuary. *Ecological Modelling* 268:93-102.

Wang, H., W. Huang, M.A. Harwell, L. Edmiston, E. Johnson, P. Hseih, K. Milla, J.D. Christensen, J. Stewart and X. Liu. 2008. Modeling oyster growth rate by coupling oyster population and hydrodynamic models for Apalachicola Bay. *Ecological Modelling* 211:77-89.

Wells, H.W. 1961. The fauna of oyster beds, with special reference to the salinity factor. *Ecological Monographs* 31:239-266.

Wetz, M.S., E.A. Hutchinson, R.S. Lunetta, H.W. Paerl and J.C. Taylor 2011. Severe droughts reduce estuarine primary productivity with cascading effects on higher trophic levels. *Limnology and Oceanography* 56:627-638.

Whitfield, A.K., M. Elliot, A. Basset, S.J.M. Blaber and R.J. West. 2012. Paradigms in estuarine ecology – A review of the Remane diagram with a suggested revised model for estuaries. *Estuarine, Coastal, and Shelf Science* 97:78-90.

Wigand, C., R. Wehr, K. Limburg, B. Gorham, S. Longergan and S. Findlay. 2000. Effect of *Vallisneria americana* (L.) on community structure and ecosystem function in lake mesocosms. *Hydrobiologia* 418:137-146.

Wilbur, D. 1992. Associations between freshwater inflows and oyster productivity in Apalachicola Bay, Florida. *Estuarine, Coastal, and Shelf Science* 35:179-190.

Wilbur, D. 1994. The influence of Apalachicola River flows on blue crab, *Callinectes sapidus*, in north Florida. *Fishery Bulletin* 92:180-188.

Wolanski, R., L.A. Boorman, L. Chicharo, E. Langlois-Saliou, R. Lara, A.J. Plater, R.J. Uncles and M. Zalewski. 2004. Ecohydrology as a new tool for sustainable management of estuaries and coastal waters. *Wetland Ecology & Management* 12:235-276.

Woodward-Clyde. 1999. *Distribution of Oysters and Submerged Aquatic Vegetation in the St. Lucie Estuary*. Submitted to the South Florida Water Management District, West Palm Beach, FL.

Zachary, A. and D.S. Haven. 1973. Survival and activity of the oyster drill *Urosalpinx cinerea* under conditions of fluctuating salinity. *Marine Biology* 22:45-52.

Zheng, L. and R.H. Weisberg. 2004. Tide, buoyancy, and wind-driven circulation of the Charlotte Harbor Estuary: A model study. *Journal of Geophysical Research* 109:C0611, doi:10.1029/2003JC001996.

Zhu, J., R.H. Weisberg, L. Zheng and S. Han. 2015. Influences of channel deepening and widening on the tidal and non-tidal circulations of Tampa Bay. *Estuaries and Coasts* 38:132-150.

This page left blank intentionally.

APPENDIX A: PUBLIC COMMENTS AND RESPONSES TO *ASSESSMENT OF THE RESPONSES OF THE CALOOSAHATCHEE RIVER ESTUARY TO LOW FRESHWATER INFLOW IN THE DRY SEASON*, AUGUST 2016 DRAFT

This appendix provides the reader with a summary of public comments received during and after the two-day public Caloosahatchee Science Symposium held in Fort Myers on September 14-15, 2016 (agenda provided). The symposium was held to present a scientific assessment conducted by SFWMD that was summarized in the August 2016 draft science document titled *Assessment of the Responses of the Caloosahatchee River Estuary to Low Freshwater Inflow in the Dry Season.* This version of the draft science document was made available to the public for review and comment 30 days prior to the symposium, and an additional 30-day comment period followed the symposium. All verbal and written comments received before, during, and after the symposium were reviewed by SFWMD, and where appropriate, they were addressed in the final science document.

Many of the public comments contained in this appendix refer to page and line numbers only included in the August 2016 draft science document. For reference, the August 2016 version of the science document can be obtained online at https://www.sfwmd.gov/our-work/mfl or by request to Don Medellin at dmedelli@sfwmd.gov. The final version of the science document does not include line numbers.

Agenda

Caloosahatchee Science Symposium

September 14 – 15, 2016

South Florida Water Management District/Lower West Coast Service Center
2301 McGregor Boulevard, Fort Myers, FL 33901

Study	Description	Presenter	Time
Day 1 (Wednesday, September 14, 2016)			
Morning Session – Physical Studies:			
	Introduction and Objectives	Don Medellin	10:00 – 10:30
	Overview of the Caloosahatchee Estuary	Peter Doering, Ph.D.	10:30 – 11:00
Hydrodynamics	Influence of alterations on hydrodynamics	Detong Sun, Ph.D.	11:00 – 11:30
Inflows vs. Salinity	Monthly freshwater-salinity relationships at Ft. Myers	Chris Buzzelli, Ph.D.	11:30 – 12:00
	Lunch – On Your Own	**All**	12:00 – 1:30
Afternoon Session – Water Column Studies:			
Water Quality	Fine scale relationships between water quality and inflow	Chris Buzzelli, Ph.D.	1:30 – 2:00
Zooplankton	Inflow, zooplankton and habitat compression	Peter Doering, Ph.D.	2:00 – 2:30
	Break	**All**	2:30 – 2:45
Ichthyoplankton	Relationships between ichthyoplankton and inflow	Cassondra Thomas, Ph.D.	2:45 – 3:15
	Question/Answer Session	**All**	3:15 – 5:00
Day 2 (Thursday, September 15, 2016)			
Morning Session – Fauna Studies:			
	Introduction and Objectives	Don Medellin	9:00 – 9:15
Benthic Fauna	Macrofauna-salinity patterns relative to inflow	Chris Buzzelli, Ph.D.	9:15 – 9:45
Oyster Habitat	Assess conditions for oyster survival and growth in lower CRE	Chris Buzzelli, Ph.D.	9:45 – 10:15
	Break	**All**	10:15 – 10:30
Sawfish	Area and volume of sawfish habitat with variable dry season inflow	Detong Sun, Ph.D.	10:30 – 11:00
Blue Crabs	Relationships between blue crab landings, rainfall, and inflow	Peter Doering, Ph.D.	11:00 – 11:30
	Lunch – On Your Own	**All**	11:30 – 1:00
Afternoon Session – Flora Studies:			
Vallisneria data	Empirical relationships between tape grass, salinity, and inflow	Peter Doering, Ph.D.	1:00 – 1:30
Vallisneria model	Model exploration of tape grass, salinity, light, and inflow	Chris Buzzelli, Ph.D.	1:30 – 2:00
	Break	**All**	2:00 – 2:15
	Question/Answer Session	**All**	2:15 – 3:45
	Next Steps & Wrap-up	Don Medellin	3:45 – 4:00

THIS SYMPOSIUM IS OPEN TO THE PUBLIC. THE DRAFT SCIENCE SUMMARY IS AVAILABLE AT http://www.sfwmd.gov/mfl. COMMENTS ON THE DRAFT SCIENCE SUMMARY ARE REQUESTED TO BE SUBMITTED BY OCTOBER 14, 2016 TO: Don Medellin, Principal Scientist, South Florida Water Management District, P.O. Box 24680, West Palm Beach, FL 33406; (800) 432-2045, ext. 6340; (561) 682-6340; dmedelli@sfwmd.gov.

Comments from Caloosahatchee Science Symposium (September 14–15, 2016)

Date	Entity	Comment	Response
9/14/16	Florida Gulf Coast University	Component 1. Why didn't the modeling for Component 1 include the changes that occurred in the watershed with the physical alterations in the estuary?	The modeling exercise that was done was designed to look at systematic physical or structural changes or alterations (5 total) to the Caloosahatchee Estuary using a model that simulates estuarine circulation and salinity based on bathymetry, freshwater inflow, wind and ocean tides. The purpose was to isolate the effects of each alteration on salinity in the estuary. Modeling alterations or pre-development conditions within the watershed was (a) not possible with the model we used and (b) beyond the scope of this analysis.
9/14/16	Sanibel Captiva Conservation Foundation (SCCF) – Rae Ann Wessel	Component 2. There is a concern that the flow estimates from S-79 (used in Component 2) to produce a salinity of 10 at Ft. Myers was too low and that documented higher flows were required.	Additional technical analysis was performed. A daily statistical analysis was performed using the average daily values. Results were compared to data received from SCCF staff and to the results presented in Component 2. See additional technical analysis in **Attachment 1** below.
9/14/16	Eric Milbrandt	Component 2. There seems to be an increasing trend over the 20 year period. Should consider a trend analysis of all years for Q_{calcs}.	The magnitude of the inflow associated with S10 at FtM is inversely correlated to rainfall the previous dry season. No trend.
9/14/16	City of Sanibel – James Evans	Component 4. Suggested that staff evaluate the effects of gelatinous predators and the potential for prey when habitat compression or impingement occur.	See Addendum to Study Component 4.
9/14/16	City of Sanibel – James Evans	What months are within the wet and dry seasons that was evaluated?	Wet Season = –November - April Dry Season = May - October
9/14/16	SCCF – Rae Ann Wessel	There are two different studies that indicate the flows at S-79 should be much higher than 300 cfs – Tolley study indicated the flows should be 1200 cfs. How do you reconcile these flow differences?	The Tolley et al (2010) study made several estimates of critical inflows for zooplankton ranging from 800 to 1200 cfs. These estimates were based on relationships between flow and center of abundance, total abundance, and position of the 90th percentile of population distribution. The estimates of critical flow are based largely on visual inspection of graphical plots. While there is nothing wrong with this approach, when the data are variable, what one investigator sees may not agree with what another sees. Since our analysis has to pass peer review, we used a statistical approach to avoid the potential of conflicting visual interpretations. The discrepancies between our analysis and the Tolley report arise from two sources. First, we used pre-determined

Date	Entity	Comment	Response
			periods over which to average the flow data, rather than picking the lag with the highest correlation coefficient. Averaging periods were limited to those over which flows might be managed. This will affect flow estimates. Secondly, there are some statistical considerations. The impingement analysis will serve as an example. Taking into account the associated error, any one of the statistical estimates for individual taxa overlaps the 1000 cfs estimated by Tolley. However, the central tendency of results for the 7 taxa is about 400 cfs. Our approach along with results and attendant errors were presented in the report and at the workshop.
9/15/16	Florida Fish and Wildlife Conservation Commission – Gregg Poulakis	Component 11. Based on data from the Caloosahatchee, the preferred salinity range of the smalltoothed sawfish is 18-30 psu. Mr. Poulakis Suggested revising the analysis.	See Addendum to Study Component 11.
9/15/16	SCCF – Rae Ann Wessel	General Comment. The monitoring data is flawed because we are paying to restore/replant tape grass in the estuary which may skew the monitoring data (Vallisneria Data-Component 7).	Since monitoring began in 1998, investigators were careful to locate restorative plantings away from monitoring sites so there is no direct effect on monitoring results. Restorative planting may influence monitoring sites by supplying seeds. This may enhance the rate of recovery when salinity and light conditions are favorable. Identifying stressful conditions is relevant to the MFL. There is no evidence that restorative plantings have served as a seed source to monitoring sites in the estuary. No restorative planting has established a permanent tape grass bed. Like native populations, transplants have died when conditions become stressful.

Written Public Comments (Letters) Received by SFWMD

Date	Entity	Comment	Response
10/21/2016	Sanibel Captiva Conservation Foundation (SCCF) – Letter	General Comment-Page 1 of SCCF Letter. There has been a permanent loss of approximately 1,000 acres of tape grass.	There is no supporting documentation of a permanent loss of 1,000 acres of tape grass. The only relatively accurate assessment of Tape grass in the Caloosahatchee Estuary was done by Hoffacker in 1993, a year that in Hoffacker's opinion exhibited unusually lush and wide spread growth of SAV, including Tape Grass. There may be 1000 fewer acres of tape grass today then there were in 1993, but 1993 was atypical. Claiming a 1000 acre loss based on an atypically dense and widespread distribution is technically flawed.
10/21/2016	SCCF – Letter	General Comment-Page 1 of SCCF Letter. The MFL target is based on the original field research was done under a different regulation schedule held several feet higher than the current LORS 08 schedule and during a wet climate cycle (1990s). The current schedule holds water levels lower within Lake Okeechobee and coincides with several consecutive years of drought.	The response of organisms to changes in salinity and flow which forms the basis of the current MFL target will be the same no matter how climate has fluctuated or regulation schedules have changed over the past 20 years. What does change on an annual basis is the amount of water required at S-79 to achieve 10 psu at Ft. Myers. See Component 2.
10/21/2016	SCCF – Letter	Component 1-Page 1 of SCCF Letter. SCCF agrees that alterations during from the 1880s-1960s have caused impacted resources before these alterations occurred. SCCF is concerned that these alterations are a prominent reference point in the District analysis.	See Section 373.0421, Florida Statutes
10/21/2016	SCCF – Letter	Component 2-Page 2 of SCCF Letter. Dr. Bartleson's analysis of an exponential curve fit for salinity data from the Ft. Myers Yacht Basin and the 30-day avg. flow from S-79 showed a regression equation that calculates 10 psu at 620 cfs.	SFWMD requested the raw data that SCCF used to generate this exponential curve. It was not provided. From the information we did get from SCCF, we could not reproduce the curve, despite best efforts. The District analyzed the relationship between flow at S-79 and salinity at Ft. Myers and compared its results to Dr. Bartleson's. See Component 2 and additional technical analysis in Attachment 1 below.
10/21/2016	SCCF – Letter	General Comment-p.iii Line 41 in Draft Science Document (August Draft). The Caloosahatchee estuary should include San Carlos Bay to determine the MFL. Truncating the boundary of the estuary does not allow for a complete analysis of the effects of dry season inflow to determine the MFL	The science re-evaluates the MFL based on the boundary of the adopted MFL and all available science data was taken into consideration. San Carlos Bay is the downstream limit of the adopted MFL Rule 40E-8.021(2), Florida Administrative Code. From a technical perspective, it is evident that the response of salinity to low flows at Shell Point and beyond is relatively sluggish. The

Date	Entity	Comment	Response
			same change in flow at S-79, causes a proportionally smaller change in salinity as distance from S-79 increases. According to Qiu and Wan 2013, an increase in flow from 0 cfs to 1000 cfs would change salinity at the I-75 Bridge from 31.86 to 0 or by 100%. The same change in flow 0-1000 cfs at Cape Coral would reduce salinity from 21.42 to 15.86 (25%). At Shell Point, salinity would change from 30.58 psu to 26.32 (14%). It is the upper estuary that is most responsive and sensitive to low flows. Setting the boundary of the estuary at Shell Point rather than San Carlos Bay does not materially affect our analysis.
10/21/2016	SCCF – Letter	Executive Summary-p.iii Line 41 in Draft Science Document (August Draft). To account for the variability around the mean a conservative approach could take the average flow for each indicator and add the positive range of variability to prevent significant harm (545+ 774 = 1319 cfs for tape grass). This method will take into account the inter-annual variability in rainfall and acceptable range of flows for setting the MFL.	It is not statistically valid to only consider the positive portion of the standard deviation around a mean. The entire range of flows should be considered. Additionally, the mean and range of flows for multiple ecological indicators must be carefully considered when determining an appropriate minimum flow and minimum water level (MFL), otherwise, the flow for one ecological indicator could be detrimental to other indicators.
10/21/2016	SCCF – Letter	Science Summary-p.11 Line 1059. Q1 estimates should also consider the range of flows caused by high interannual variability	Inter-annual variability is explicitly or implicitly included in estimates of QI. For Component 2, “Analysis of the relationship between freshwater in flow at S-79 and salinity in the Caloosahatchee River Estuary 1993-2013”, a separate analysis is done for each year and results are then averaged. Inter-annual variation is therefore explicitly included. For other analyses, such as Component 9 (Oyster habitat), the days upon which a given salinity criterion was exceeded where identified over a period of record spanning many years (in this case WY2005-2014). Flows at S-79 on those days were averaged. Again, since a multiyear period of record was analyzed, inter-annual variability is included. Since averaging was on a daily time scale, rather than an annual one, the differences between years are represented implicitly.
10/21/2016	SCCF – Letter	Component 4 (p.11 Line 1137). Based on a study done by S.G.Tolley, it appears that freshwater flows on the order of 800-1000 cfs would be sufficient to release these organisms from impingement caused by the S-79 lock and dam. How can the re-analysis results presented and	The Tolley et al (2010) estimated that flows in the range of 800-1000 cfs would alleviate impingement on S-79. These estimates were based on relationships between flow and the position of the 90th percentile of population distribution. The estimates themselves are largely based on visual inspection of graphical plots. While there is nothing wrong with this

Date	Entity	Comment	Response
		conclusions be so different, especially since it's the same data?	approach, when the data are variable, what one investigator sees may not agree with what another sees. Since our analysis has to pass peer review, we used a statistical approach to avoid the potential of conflicting visual interpretations. The discrepancies between our analysis and the Tolley report arise from two sources. First, we used pre-determined periods over which to average the flow data, rather than picking the lag with the highest correlation coefficient. Averaging periods were limited to those over which flows might be managed. This difference will affect flow estimates. Secondly, there are some statistical considerations. Taking into account the associated error, any one of the statistical estimates for individual taxa overlaps the 800-1000 cfs estimated by Tolley. However, the central tendency of results for the 7 taxa is about 400 cfs. Our approach along with results and attendant errors were presented in the report and at the workshop.
10/21/2016	SCCF – Letter	Components 7 and 8 (p.13; Lines 1204-1208) are inconsistent in the salinity targets for Ft. Myers. Component 7 set Q1 targets to achieve salinities of 9-10 at FTM while Component 8 used annual-inflow-salinity relationships to hold salinities at 12 which led to shoot mortality in the model. Flow estimates are too low to support the previous studies or model runs.	The empirical analysis of salinity and Vallisneria (Component 7) targeted a salinity of 9-10 as the upper limit for limited growth. The simulations (Component 8) were conducted to determine the salinity where Vallisneria suffered net mortality. Thus, a salinity of 12 resulted from the model study.
10/21/2016	SCCF – Letter	Component 9: p13 Line 1219. Why were salinities at Cape Coral targeted for salinities ranging from 20-25? Flows necessary to keep salinities above 25 at Shell Point should have been used for calculating minimum flows, not Cape Coral. This approach used upstream sites for calculating flow/salinity relationships appears to favor a lower minimum flows. Why not use real-time data and adaptive management to hit the salinity targets?	As detailed in Component 9, the premise is that the upper boundary for oyster habitat (e.g., Cape Coral) was the location to assess for potential effects of elevated salinity. Oyster habitat is not a good indicator for the CRE. A majority of the habitat is downstream near Shell Point where salinity is >20-25 ~85% of the time. Powell (2017) examines Gulf of Mexico oysters and probable mechanisms of Dermo. Salinity is not a controlling variable. Reference: (Powell, E.N., 2017. What Is Going on with Perkinsus marinus in the Gulf of Mexico? Estuaries and Coasts 40:105-120.
10/21/2016	SCCF – Letter	Component 10 (p.13; Line 1224). Higher flow (>1000 cfs) may be important in the short-term recovery of the blue crab fishery.	For our analysis, we assumed that recovery occurred under conditions of average rainfall. The focus of our analysis was not to identify

Date	Entity	Comment	Response
			flows that promote recovery, rather to identify those that cause significant harm.
10/21/2016	SCCF – Letter	Component 11 (p.14; Line 1240). Why weren't 30 day average flows used for the 30 day average salinities at the Yacht Basin used in the re-analysis?	The hydrodynamic model application was a test case for WY2007. Discharge at S-79 was held constant in the last 3 months of simulation. In this sense, the flow can be considered 30 day average and salinity is the equilibrium for the flow.
10/21/2016	SCCF – Letter	Science Summary-p.14; Line 1253. The 10 component studies used different flow and salinity for Q1. The same selection criteria were not used and each had different study periods, different locations and larger inter and intra annual variability and, therefore, cannot be lumped together and a median selected out of thin air. The report is a nice review but the "same selection criteria" were not used and differ greatly from the conclusions of the original report 800-1000 cfs (Tolley) versus 237+255 for icthyoplankton even though the same data were used. It appears that the S-79 flow estimates are purposefully analyzed to show low flows, in some cases. How will the target to minimize harm be chosen from such different approaches?	The data used to generate the 237 + 255 cfs were based on a study conducted by R. Chamberlain (1986-1989). Not at all the same data as Tolley et al 2010. 2) How the various estimates of flow magnitude from the 10 studies are combined into a final estimate is important and critical. The approach that we use to choose the flow target will be detailed in the technical document that supports rulemaking. 3) The MFL will be peer reviewed by a panel of impartial experts.
10/21/2016	SCCF – Letter	Science Summary-p.15; Table 2 and p.17; Line 1292. The months for the dry season should be expanded to include May and October to reduce inter-annual variability in flow and salinity. The most significant problem with this table is that not all of the components used the same 30-day average 10 psu criteria at FTM which is the basis for the rule. The flow numbers can't be compared in a table because the criteria are for each differed. One median flow based on all of these components is not valid. If this approach is used then each component should be reanalyzed and include the 30-day average salinity not to exceed 10 at FTM.	We have used a standard definition for wet and dry seasons that is used for reporting under the Northern Everglades and Estuaries Protection Program (Chapter 10 of the South Florida Environmental Report). The analyses presented in the document were intended to elucidate the response of a series of estuarine indicators to low fresh water inflows during the dry season. These analyses were not intended to test the efficacy of the 30-day average, 10 psu criterion that is part of the current rule.
10/21/2016	SCCF – Letter	Science Summary (Component 4)-p.16; Table 3. The original zooplankton study concluded 800-1000 cfs. The Val model is too low because they used salinities of 12 at FTM to determine S-79 flows. These ranges	It was not the intention of this analysis to evaluate the current MFL criteria (i.e., 30-day average salinity of 10 at Ft. Myers or daily average of 20). Rather it was to analyze as much data as possible from as many sources

Date	Entity	Comment	Response
		are not comparable because different selection criteria for flow were used.	as possible and to let the results of these analyses form the basis of MFL criteria.
10/21/2016	SCCF – Letter	Science Summary (Component 9)-p.19; Line 1380. Oyster habitat at Cape Coral should not be used the salinity target location. The analysis should not use the upper freshwater limit of distribution but the center of abundance similar to the other studies (ichthyoplankton, zooplankton and Vallisneria)	As detailed in Component 9, the premise is that the upper boundary for oyster habitat (e.g., Cape Coral) was the location to assess for potential effects of elevated salinity. Oyster habitat is not a good indicator for the CRE. A majority of the habitat is downstream near Shell Point where salinity is >20-25 ~85% of the time. Powell (2017) examines Gulf of Mexico oysters and probable mechanisms of Dermo. Salinity is not a controlling variable. Reference: (Powell, E.N., 2017. What Is Going on with Perkinsus marinus in the Gulf of Mexico? Estuaries and Coasts 40:105-120.
10/21/2016	SCCF – Letter	Science Summary-p.19 Line 1388. Acknowledgement of re-analysis results from widely different approaches but then conclusions from Table 2 using the "same selection criteria." Why does the estuary boundary end at Glover's bight and not Sanibel Lighthouse?	The boundary of the adopted MFL for the Caloosahatchee River is defined in Rule 40E-8.021 (2), Florida Administrative Code. San Carlos Bay is the downstream boundary of the adopted MFL. See response to similar comment above.
10/16/16	Hidetoshi Urakawa, Associate Professor, Florida Gulf Coast University (FGCU – Letter)	Science Summary. Uncertainty itself is not important but how to address is important. Therefore, I think "Interpretation of Uncertainty", "Understanding of Uncertainty" or some similar heading is better. [refers to Importance of Uncertainty section near the front of the Science Summary]	Edits made.
10/16/16	FGCU – Letter	Component 2-Methods. Please add a brief explanation of WY.	Edits made.
10/16/16	FGCU – Letter	Component 2- Discussion. The statement is inscrutable. To explain the observed great variability, it says the amount of ungauged freshwater input from the Tidal Basin is a key component to the total freshwater budget. According to this statement, the Tidal Basin flow is likely not measured yet. But the last sentence says these inputs have been incorporated into a published model. It is hard to understand the interaction between presented data and the current discussion. P.S. The Tidal	The amount of water required to make 10 psu is also dependent on previous year's rainfall, not just tidal basin inflow.

Date	Entity	Comment	Response
		Basin flow is 21% according to line 3900 in Component 10.	
10/16/16	FGCU – Letter	Component 2-Results [Figure 14]. "Monitoring station" is missing from this part of the caption [it is included in the caption for the figure above this one]. Is it on purpose?	No edits made.
10/16/16	FGCU – Letter	Component 3. I think it is good if the authors mention that hypoxia events of CRE are not a critical issue for the overall ecology of the estuary in this point and limited to an upstream deep channel.	No edits made.
10/16/16	FGCU – Letter	Component 3. It is fine, but no historical events are discussed. Are there any past ecological disasters associated with hypoxia? If not, it should be stated here for better understanding of the level of hypoxia problem in the CRE.	There are no past ecological disasters associated with hypoxia.
10/16/16	FGCU – Letter	Component 3. Figure 20 was not printed out correctly as a PDF file. It should be corrected.	No edits made.
10/16/16	FGCU – Letter	Component 3. I think the authors should add a statement that the most part of CRE maintains a healthy condition in terms of DO level as a part of previous studies.	No edits made.
10/16/16	FGCU-Letter	Component 3-Discussion (4th paragraph) "The model (269 cfs) and field results (469 cfs) indicated that freshwater…" is better than the current writing. The current writing is a bit confusing.	Edits made.
10/16/16	FGCU-Letter	Component 5. Please delete "just downstream of Station 2". Abstract should be independent and should not cite sampling stations at which the authors do not know.	Edits made.
10/16/16	FGCU-Letter	Component 5. Do ichthyoplankton really include decapods? What is the meaning of "ichthyo-"? Ichthyoplankton should include fish eggs.	Edits made.
10/16/16	FGCU-Letter	Component 5 Line 2667. Please delete "from a study conducted".	Edits made.
10/16/16	FGCU-Letter	Component 5 line 2705. COA. If this is the first time, please spell it out.	Edits made.
10/16/16	FGCU-Letter	Component 5 line 2734. "Juvenile bay anchovy" is better than "juvenile fish", if my understanding is correct.	Anchovy may not be the only species that seeks low salinity during the juvenile stage. No edits made.
10/16/16	FGCU-Letter	Component 5 line 2736. Not "are" but "were".	Edits made.
10/16/16	FGCU-Letter	Component 5 line 2744. Could you rephrase the sentence? I am not sure	Edits made.

Date	Entity	Comment	Response
		[of] the meaning that juvenile fish abundance could serve as an indicator for freshwater inflow. Can we accurately estimate the flow rate based on ichthyoplankton data?	
10/16/16	FGCU-Letter	Component 5 line 2674-2677. Month zero should be corrected. I am not sure if crabs and shrimps were included in ichthyoplankton or zooplankton in this figure. Lines 2678-2681. Please make the statement clear if decapods are included in ichthyoplankton in this report.	Edits made.
10/16/16	FGCU-Letter	Component 5 line 2757. This statement is redundant (see line 2735). [refers to the statement "Juvenile fish were most frequently found in salinities ranging from 4 to 6 with frequency of occurrence declining at salinities that were >10."]	No edits made.
10/16/16	FGCU-Letter	Component 5-Results and Discussion. Is this a standard deviation? It is quite large. A geometric mean might be better than an arithmetic mean. [refers to 255.5 cfs in the statement "The 30-day average inflows associated with these salinity values ranged from 12.3 to 1,357 cfs and averaged 237.5 ± 255.5 cfs" in Results and Discussion in Component Study 5].	This is an arithmetic mean and standard deviation as was done for all other flow ranges. It demonstrates the variability of the system. No edits made.
10/16/16	FGCU-Letter	Component 9. Please delete "mortality". Survival and mortality are similar meaning here.	No edits made.
10/16/16	FGCU-Letter	Component 9. I like this figure but it is a bit unclear. The sizes of oysters in each box are different: small shell in a low salinity box while a large shell in a high salinity box. What do these differences stand for? Does y-axis mean survival or growth rate? What is a possible unit? [refers to Figure 56]	This figure is a conceptual cartoon. The oysters are deliberately shown as different sizes to illustrate the effects of salinity on growth.
10/16/16	FGCU-Letter	Component 9-Table 29. It is understandable but Cape Coral (CC) and Shell Point (SP) is better.	Edits made.
10/16/16	FGCU-Letter	Component 10-Abstract. CPUE and CRE should be spelled out when used first time.	No edits made.
10/16/16	FGCU-Letter	Component 10-Methods. It is nice if the authors can define water year (WY) when it comes first time.	No edits made.

Date	Entity	Comment	Response
10/16/16	FGCU-Letter	Component 10. It should be Table 33. [refers to a needed correction to the Table 33 reference shown in the text of Component Study 10]	Edits made.
10/16/16	FGCU-Letter	Component 11. I believe these two paragraphs are not necessary in this component. It is simply redundant. Start from line 4230 is a good idea.	No edits made.
10/16/16	FGCU-Letter	Component 11. Please add “their” in front of “pathogens”.	No edits made.
10/16/16	FGCU-Letter	Component 11. Is it correct? [refers to figure referenced in the Methods/Bathymetric Analyses section Component Study 11 as Fig. A11-2]	Edits made.
10/16/16	FGCU-Letter	Component 11. The “-“ looks like a “minus” sign. [refers to the Note with Figure 66]	Edits made.
10/16/16	FGCU-Letter	Component 11. Same as last comment. The “-“ looks like a “minus” sign. [refers to the caption with Figure 67]	Edits made.
10/16/16	FGCU-Letter	Component 11. Labels of Figures A, B, and C are missing. [refers to Figures 71A, 71B, and 71B]	Edits made.
10/16/16	Conservancy of Southwest Florida – Jennifer Hecker (CSWF-Letter)	Component 1. Other factors outside of the physical alteration of the river, such as the loss of headwaters at Lake Hicpochee, over-drainage of the watershed (with resulting loss of base flow) which could increase salinity, and water management practices such as cutting off freshwater flows from Lake Okeechobee to the river also need to be assessed to determine the comparative influence they have on salinity.	The modeling exercise were experiments to look at systematic physical or structural changes within the estuary with an emphasis on bathymetry. Modeling alterations or pre-development conditions within the watershed was beyond the scope of this analysis.
10/14/16	CSWF-Letter	Component 1. The Conservancy suggests running other [salinity] scenarios that take into account the Lake connection as well as a natural conditions scenario.	See our response above. The numerical experiments were designed to look at bathymetry changes and structural changes within the estuary and to isolate their effects. Applying S-79 flow explicitly includes the lake connection.
10/14/16	CSWF-Letter	Component 1. Using the existing flows with predevelopment hydrology, not predevelopment flows, seems questionable in our view and we would caution making any conclusions based on these results. It is not replicating predevelopment nor current day conditions, but is instead an artificial hybrid scenario that has never existed nor exist presently.	Again, the model analysis was designed to examine the impacts from physical and structural changes and was able to isolate the effects from different alterations and identify that bathymetry changes especially deepening of the channel had significant impact on salinity. This would be true regardless of whether predevelopment flow or current condition flow was used.

Date	Entity	Comment	Response
10/14/16	CSWF-Letter	Component 2. We are concerned that the analysis [of the amount of inflow needed at S-79 to achieve a desired salinity level] did not involve a trend analysis and [we] think that even at a monthly scale, it would be good to do a time lag of one to two weeks.	See previous answer. The amount of inflow associated with S10 at FtM is inversely correlated to rainfall the previous dry season. There is no trend.
10/14/16	CSWF-Letter	Component 2. The modeling used seems to significantly underestimate the flow needed at S-79 based on real world monitoring of the system. We recommend a reanalysis to incorporate the real world data on what flows have achieved the target salinity.	See previous answer. Component 2 was based on approximately 20 years of observed data.
10/14/16	CSWF-Letter	Component 2. The conclusion that flow needs are not anticipated to increase over time does not seem logical in our view given the continued reduction in base flow and the continued sea level rise that will undoubtedly occur, causing further saltwater intrusion into the system.	This is not a conclusion of this document.
10/14/16	CSWF-Letter	Component 4. We support the suggestion made by the City of Sanibel staff to include an analysis of increased predation in this effort to study zooplankton response to flows from S-79.	See Addendum to Component 4.
10/14/16	CSWF-Letter	Component 11. The preferred salinity range used in the study presented for sawfish is 12-27 pus, extrapolated apparently from the Peace River. We support the more appropriate salinity range for the Caloosahatchee that FWC provided at the meeting, 18-30 psu, to be used for rerunning or future analysis.	See Addendum to Component 11.
10/14/16	CSWF-Letter	Component 11. The SFWMD's resource-based approach involving seven indicators does not address the needs of all endangered species using the Caloosahatchee. The Conservancy recommends adding endangered species as an indicator to specifically look at both the direct and indirect effects of flows on all endangered species using the Caloosahatchee and their habitat in the river and estuary (ex. nutrients and stagnation contributing to toxic algae blooms or flows triggering tape grass die offs, both which impact manatees).	The resource-based approach utilizes all available data available for ecological indicators and listed species (threatened or endangered) within the CRE. Many of the other listed species either have insufficient or minimal data available and a scientific analysis is not possible because the species are too mobile in order to have any statistical significance/relevance, or may not serve as a good ecological indicator for re-evaluating the MFL. A number of listed species are believed to, or are known to, utilize the open waters and wetlands of the CRE watershed. Of those species listed, only fish were considered suitable indicators of flow in our resource-based approach. Three listed fish species

Date	Entity	Comment	Response
			occur in the CRE; smalltooth sawfish (*Pristis pectinate*), gulf sturgeon (*Acipenser oxyrinchus desotoi*), and mangrove rivulus (*Kryptolebias marmoratus*). The smalltooth sawfish was included as an indicator species in the District's resource-based approach, as discussed in Component Study 11. While the gulf sturgeon is listed as threatened by both the Florida Fish and Wildlife Conservation Commission (FWC) and the U.S. Fish and Wildlife Service (FWS), there is some disagreement between the two agencies as to the species' range in Florida. The FWS includes the species in Lee County and specifically in the Caloosahatchee National Wildlife Refuge, while the FWC indicates the species only occurs in North Florida, from the Suwanee River Basin north. The mangrove rivulus is listed as a species of special concern by the FWC. It is not listed by the FWS. According to the FWC, the mangrove rivulus inhabits mangrove forests and it is an amphibious/fossorial species (it is capable of living on land and water, and it burrowers on land). Most of its time is spent on land where it can be found hidden in rotten wet logs or under moist leaf litter (*Taylor, D. S., Turner, B. J., Davis, W. P., and Chapman, B. B. 2008. A novel terrestrial fish habitat inside emergent logs. American Naturalist 171(2):263-266*). Therefore, this species was not considered a suitable indicator of flow.
10/14/16	CSWF-Letter	Component 7. The point made by the Sanibel-Captiva Conservation Foundation (SCCF) that tape grass coverage can be increasing due to aggressive replanting efforts rather than by improved salinity conditions alone is valid and should be addressed to determine how much it could have influenced the results of the study.	Since monitoring began in 1998, investigators were careful to locate restorative plantings away from monitoring sites so there is no direct effect on monitoring results. Restorative planting may influence monitoring sites by supplying seeds. This may enhance the rate of recovery when salinity and light conditions are favorable. Identifying stressful conditions is relevant to the MFL. In addition, there is no evidence that restorative plantings have served as a seed source to monitoring sites in the estuary. No restorative planting has established a permanent tape grass bed. Like native populations, transplants have died when conditions become stressful.
10/14/16	CSWF-Letter	Components 7 and 8. We support SCCF's recommendation that the SFWMD analyze the 30 year moving averages instead of the annual averages because real world data shows that 650 cfs flow is often insufficient to attain and maintain the 10 psu target.	See previous comments and Attachment to this document.

Date	Entity	Comment	Response
10/14/16	CSWF-Letter	Components 7 and 8. Since significant harm has already occurred, it would be appropriate to set the MFL at conditions that promote restoration and the recovery of these resources, rather than to just prevent further significant harm.	Section 373.042, F.S., sets the standard for setting MFLs.

Attachment 1: Doering, Peter H. and F. Zheng 2016. Salinity at the Ft. Myers Continuous Monitoring Station and Freshwater Inflow to the Caloosahatchee Estuary

Introduction

The current Minimum Flow and Level for the Caloosahatchee River and estuary was adopted in 2001. The rule has two salinity thresholds. The first is a 30-day moving average salinity of 10, measured at the surface sensor of the monitoring station located in the Ft. Myers Yacht Basin. The second is a daily average salinity of 20 measured at the same location. The salinity value of 10 is based on the salinity tolerance of tape grass (Vallisneria americana). It is generally agreed in the literature that a salinity of 10 or below is required for a sustainable population (French and Moore 2003). The District's work supports this conclusion (Doering et al 2002). Calculating the amount of freshwater inflow required to produce a surface salinity of 10 at Ft. Myers is an important step in evaluating the current MFL.

Surface water inflow to the Caloosahatchee Estuary is primarily delivered at the Franklin Lock and Dam (82% of total). Additional flows enter the estuary from the Calooshatchee Tidal Basin (18 % of total) downstream of S-79.

There are various ways to estimate the amount of freshwater inflow required to produce a salinity of 10 at Ft. Myers. Buzzelli (2016) regressed mean monthly flow at S-79 (x) on mean monthly salinity (y) at Ft. Myers for the water years 1993 through 2012. The relationship between discharge at S-79 and salinity at Ft. Myers could be described by a negative exponential relationship. Considering all months (n=256) the regression explained 82% of the variability and suggested that a mean monthly flow of 485 cfs at S-79 would produce a mean monthly salinity of 10 at Ft. Myers. Examination of individual water years indicated that this value was not constant but varied on an annual basis from 70 – 773 cfs and averaged ($\pm$ standard deviation) 445 $\pm$ 218 cfs. Bartleson (personal communication) regressed the 30-day moving average salinity at Ft. Myers (y) on the 30-day moving average flow at S-79 (x) using a negative exponential model. The regression explained 81 % of the variability in salinity and estimated that 620 cfs were necessary to produce a salinity of 10 at Ft. Myers. Considering the 95% confidence bounds on the regression coefficients the range was 597 cfs to 649 cfs.

Here we examine the relationship between daily average inflow and daily average salinity at Ft. Myers.

Methods

Flow at S-79 and salinity at the Ft. Myers monitoring station were downloaded from the District's data base DBHYDRO. The period of record covered the period 5/1/96 through 4/30/16. The data set was the same used in Chapter 8C of the 2017 South Florida Environmental Report. Rainfall for the tidal basin was also available from DBHYRO. These data were used to predict tidal basin inflow (5/1/96 – 5/31/14) using a linear reservoir model Wan and Konyha (2015).

Daily flow and salinity data were sorted by date and further classified according to season (wet season = May-October, dry season = April – November). A negative

exponential model was fit to the data using the SAS version 9.3 procedure Proc NLIN. The model was:

$$\text{Surface Salinity} = \text{beta0} * e^{(-\text{beta1}*\text{Flow})}$$

Salinity was average daily salinity for a given day

Flow was average daily flow on that day in cubic feet per second (cfs)

Separate regressions were computed for flow at S-79 and for total flow (S-79 + Tidal Basin). Overall and seasonal regressions (wet and dry) were also computed. To determine the flow that produces a salinity of 10 at Ft. Myers, the above equation was solved for flow assuming a salinity of 10. Proc NLIN provides the approximate upper and lower limits of the 95% confidence bands for beta0 and beta1. Again by solving the above equation for flow assuming a salinity of 10, these limits were used to estimate a potential range of flows that could result in a salinity of 10. It is important to note that if beta0 is less than 10, a negative value for inflow results if the equation is re-arranged and solved for a salinity of 10.

Results and Discussion

Over the period of record, daily surface salinity at Ft Myers averaged 6.8 $\pm$ 6.9. Flow at S-79 (1971 $\pm$ 2713 cfs) was nearly four times the tidal basin inflow. In estuaries, patterns of salinity and flow are generally inverse. When flow is low salinity is high. Flow in the wet season was higher than in the dry season and, as expected, salinity was lower in the wet season and higher in the dry season.

Using all the data, flows at S-79 associated with a salinity of 10 at Ft. Myers averaged 405.8 cfs (**Table 2**, **Figure 1**). Based on the 95% confidence limits for the two parameters of the exponential decay equation (1), flows could range from 373.2 cfs to 446.9 cfs. Dry season flows averaged 495 cfs, with a range of 446.3 to 557.8 cfs. Wet season flow at S-79 estimated to produce a salinity of 10 at Ft. Myers were considerably lower (range: 243.7 – 349.4 cfs).

Estimates of Total flows (S-79 + Tidal Basin) associated with a salinity of 10 at Ft. Myers were remarkably similar. Average estimates for the wet season, dry season, and all the data were within 20 cfs of each other (Table 3). This result contrasts with the large wet season/dry season difference for flows at S-79 (Table 2). It suggests: 1) that the total inflow required to produce a salinity of 10 at Ft Myers varies far less than the flow required from S-79; and 2) much of the seasonal variation in required flow at S-79 is due to seasonal differences in tidal basin inflow.

The magnitude of the daily flows at S-79 required to produce a salinity of 10 at Ft. Myers (373.2 – 446.9 cfs) are within the same range of mean monthly flows calculated by Buzzelli (2016, 70-773 cfs) and the mean estimates (405.7 cfs for average daily and 445 cfs for mean monthly) are quite close differing by only 9.6 % relative to the daily average.

The period of record chosen for analysis also appears to influence estimates of the flow required to produce a salinity of 10 at Ft. Myers. The analyses above were repeated for a POR of 6/29/2000 – 10/19/2014 and corresponding to that employed by Bartleson (personal communication). Comparison of Tables 1 and 4 and **Figures 1 and 2** reveals

that estimates based on the 6/29/2000 – 10/19/2014 POR are generally higher than those based on the longer POR (5/1/96 – 5/31/14). This difference may at least in part be due to inter-annual variation in the salinity/flow relationship similar to that observed by Buzzelli (2016). An example of such variation is given in **Figure 3** which compares the daily average salinity/flow relationships for water years 2000 and 2009. Note that in 2009, the estimated flow required to produce a salinity of 10 at Ft. Myers was over twice that estimated in 2000.

Comparison of the results in Table 4 (All Data category) with those of Bartleson indicates that the way both salinity and flow are averaged influences results. The flows producing 10 at Ft. Myers estimated by Bartleson using 30-day moving averages of both variables ranged from 597 cfs to 649 cfs. Estimates based on daily averages used in this report were lower ranging from 460 cfs to 551 cfs.

We repeated Bartleson's analysis, regressing the 30-day average surface salinity at Ft. Myers on the 30-day average flow at S-79. In order for our estimates of flows resulting in a salinity of 10 to come close to Bartleson's, we had to eliminate flows greater than 4000 cfs from the analysis (Table 6). Even then, our results were substantially lower than his.

Lastly, rather than rearranging the equation relating flow (x) to salinity (y) to estimate a flow associated with a salinity of 10, a regression of salinity (x) on flow (y) may be derived and the flow calculated directly. Palmer et al (2015) used a 2- parameter exponential decrease model:

$$Ln(Q+1)=ae^{-bS}$$

Q is flow at S-79

S is salinity

When such an approach was employed in the present case, estimates of the flow producing a salinity of 10 at Ft. Myers appeared low (e.g. 87 cfs for all the data) and unreasonable.

Conclusion

The relationship between flow (x) and salinity (y) was modeled using a two parameter negative exponential equation. Estimates of the flow required to produce a salinity of 10 at Ft. Myers depended on the period of record selected for analysis and methods used to pre-process the data (averaging periods) prior to regression. Results presented here corroborate the observations of Buzzelli (2016) who found considerable inter-annual variation in the relationship between flow at S-79 (x) and salinity at Ft. Myers (y). Two points relevant to establishing a minimum flow at S-79 may be made. First, using a regression approach to estimate a minimum flow based on salinity will not produce consistent results unless the POR is consistent and the data are consistent (e.g. daily average or monthly average). Secondly, because of inter-annual variation in the flow-salinity relationship, a flow at S-79 estimated from data spanning multiple years will not consistently produce a salinity of 10 at Ft. Myers.

Table 1. Mean surface salinity at Ft. Myers, discharge at S-79 (cfs) and Tidal basin inflow (cfs) calculated seasonally (dry, wet) and using all the data (overall). Mean, standard deviation (stdev) and number of observations (n) are given.

		All				Dry				Wet	
	Mean	**Stdev**	**n**		**Mean**	**Stdev**	**n**		**Mean**	**Stdev**	**n**
Surface Salinity	6.8	6.9	6618		8.8	6.8	3323		4.8	6.5	3295
S-79 Flow	1971	2713	7305		1321	2141	3625		2611	3045	3680
Tidal Basin Flow	510	626	6605		241	336	3262		774	724	3343

Table 2. Relationship of Salinity at Ft. Myers to discharge at S-79. Estimates of the exponential decay coefficients, Beta0 and Beta1, from non-linear regression. Also given are the approximate 95% confidence limits for these estimates, and the calculated flows at S-79 resulting in a Salinity of 10 at Ft. Myers. Period of Record = 5/1/96 – 4/30/16

S-79			**95% L**	**Estimate**	**95%U**	**R^2**	**n**
All Data	Beta0		13.8	14.0	14.2	0.526	6618
	Beta1		-0.00086	-0.00083	-0.00079		
	CFS for S-10		373.2	405.8	446.9		
Dry Season	Beta0		14.2	14.4	14.7	0.521	3323
	Beta1		-0.00078	-0.00089	-0.00083		
	CFS for S-10		446.3	495.0	557.8		
Wet Season	Beta0		12.6	13.0	13.4	0.457	3295
	Beta1		-0.00094	-0.00089	-0.00083		
	CFS for S-10		243.7	292.6	349.4		

Table 3. Relationship of Salinity at Ft. Myers to total inflow (S-79 + Tidal Basin). Estimates of the exponential decay coefficients, Beta0 and Beta1, from non-linear regression. Also given are the approximate 95% confidence limits for these estimates, and the calculated flows at S-79 resulting in a Salinity of 10 at Ft. Myers. Period of Record= 5/1/96 – 5/31/14

Total Inflow			**95% L**	**Estimate**	**95%U**	**R^2**	**n**
All Data	Beta0		15.8	16.0	16.3	0.576	5917
	Beta1		-0.00072	-0.00069	-0.00067		
	CFS for S-10		632.7	685.0	730.6		
Dry Season	Beta0		15.5	15.8	16.2	0.505	2960
	Beta1		-0.0007	-0.00066	-0.00062		
	CFS for S-10		625.9	696.5	775.4		
Wet Season	Beta0		15.9	16.4	16.919	0.555	2958
	Beta1		-0.00077	-0.00073	-0.00069		
	CFS for S-10		604.1	679.1	761.5		

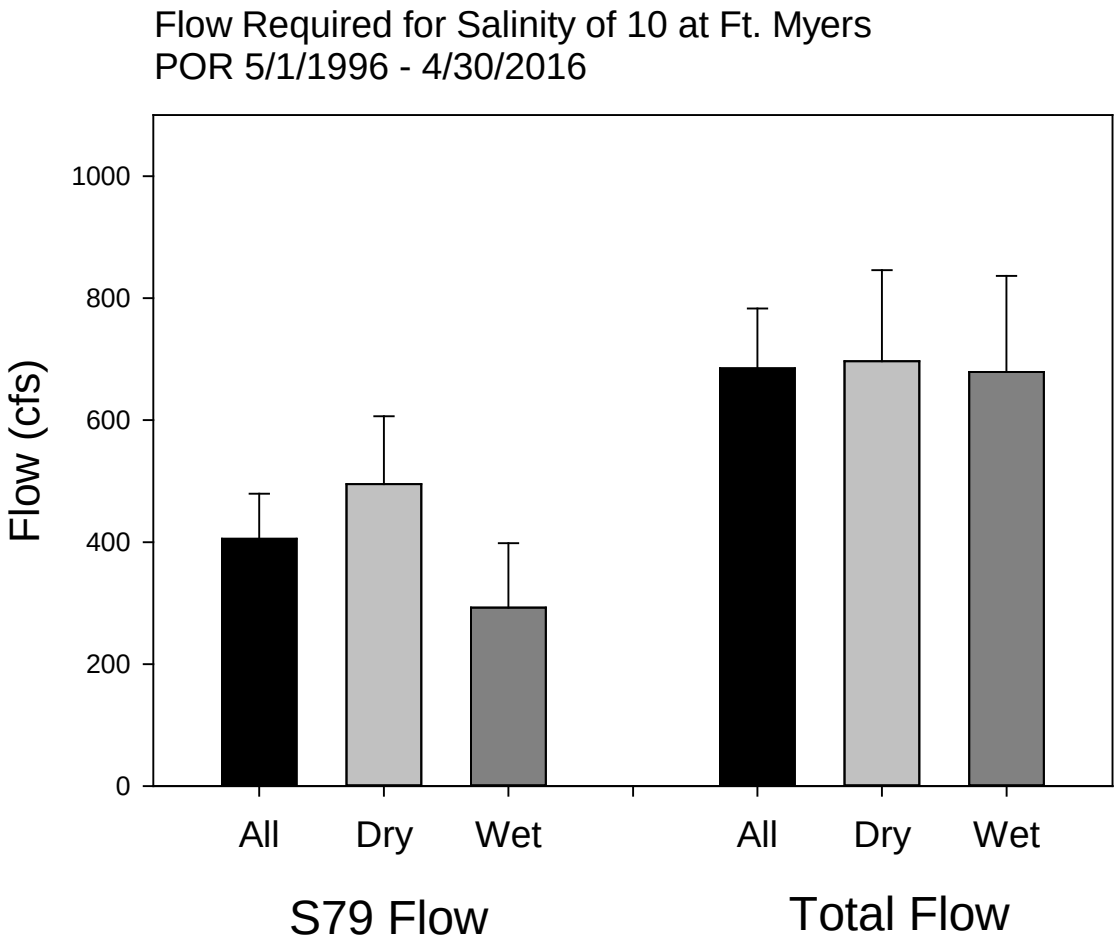

Figure 1. Daily average flow required to produce a daily average surface salinity of 10 at the SFWMD Ft. Myers Salinity Monitoring Station for the period of record 5/1/1996 – 4/30/2016. Calculations (± 95% Confidence Range) are given for entire time period, wet and dry seasons and for flow at S-79 and Total Flow (S-79 + Tidal Basin).

Table 4. Relationship of Salinity at Ft. Myers to discharge at S-79. Estimates of the exponential decay coefficients, Beta0 and Beta1, from non-linear regression. Also given are the approximate 95% confidence limits for these estimates, and the calculated flows at S-79 resulting in a Salinity of 10 at Ft. Myers. Period of Record = 6/29/2000 – 10/19/2014

S-79			95% L	Estimate	95%U	R^2	n
All Data	Beta0		15.00	15.27	15.55	0.556	4359
	Beta1		-0.00088	-0.00084	-0.0008		
	CFS for S-10		460.28	503.44	551.33		
Dry Season	Beta0		14.66	15.00	15.33	0.455	2235
	Beta1		-0.0008	-0.00075	-0.00069		
	CFS for S-10		477.65	540.07	618.57		
Wet Season	Beta0		15.34	15.83	16.32	0.557	2304
	Beta1		-0.00103	-0.00097	-0.0009		
	CFS for S-10		415.01	473.10	543.77		

Table 5. Relationship of Salinity at Ft. Myers to total inflow (S-79 + Tidal Basin). Estimates of the exponential decay coefficients, Beta0 and Beta1, from non-linear regression. Also given are the approximate 95% confidence limits for these estimates, and the calculated flows at S-79 resulting in a Salinity of 10 at Ft. Myers. Period of Record=6/29/2000– 10/19/2014

Total Inflow			95% L	Estimate	95%U	R^2	n
All Data	Beta0		16.92	17.25	17.58	0.601	4398
	Beta1		-0.00077	-0.00073	-0.0007		
	CFS for S-10		682.46	746.32	805.37		
Dry Season	Beta0		16.07	16.48	16.89	0.474	2235
	Beta1		-0.00076	-0.00071	-0.00066		
	CFS for S-10		623.62	703.02	793.52		
Wet Season	Beta0		18.99	19.57	20.15	0.654	2163
	Beta1		-0.00085	-0.00081	-0.00076		
	CFS for S-10		754.01	828.39	921.32		

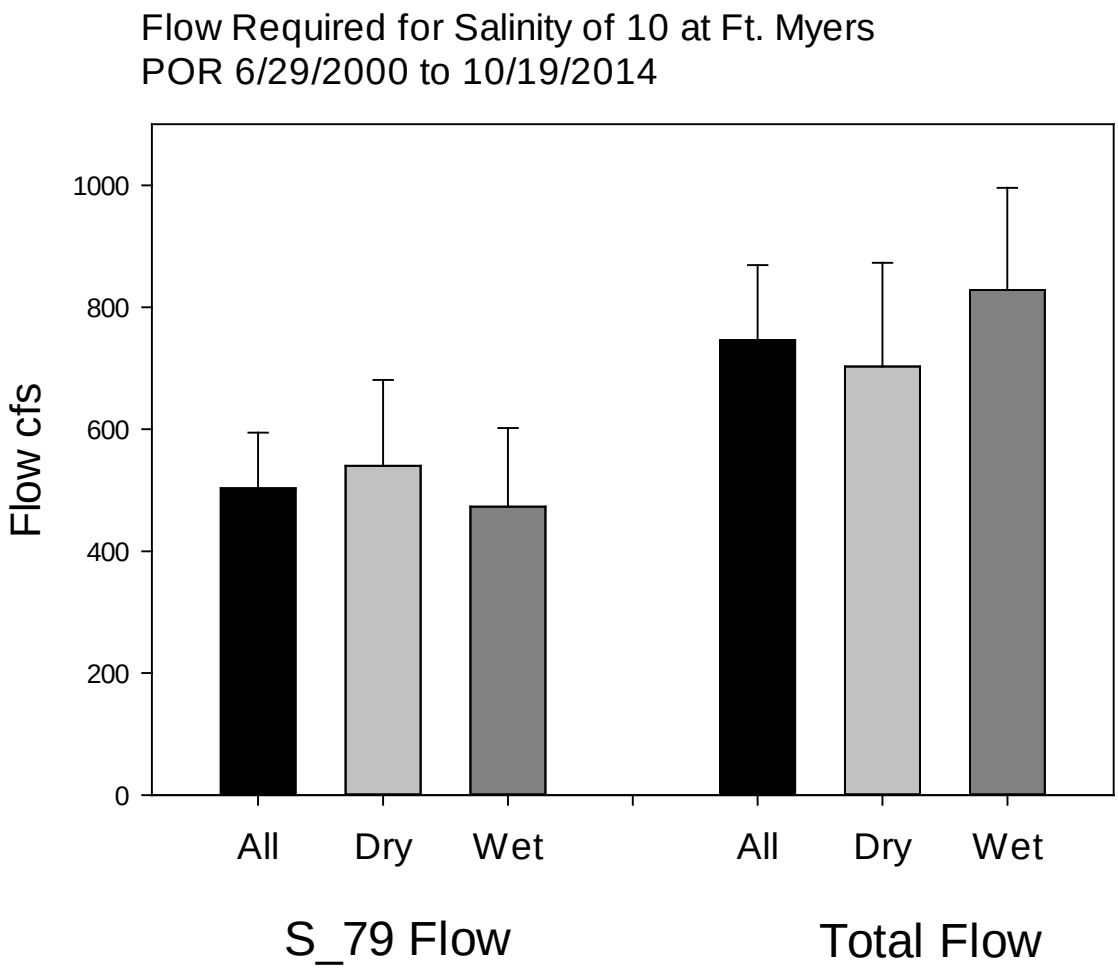

Figure 2. Daily average flow required to produce a daily average surface salinity of 10 at the SFWMD Ft. Myers Salinity Monitoring Station for the period of record 6/29/2000 – 10/19/2014. Calculations (+ 95% Confidence Range) are given for entire time period, we and dry seasons and fro flow at S-79 and Total Flow (S-79 + Tidal Basin).

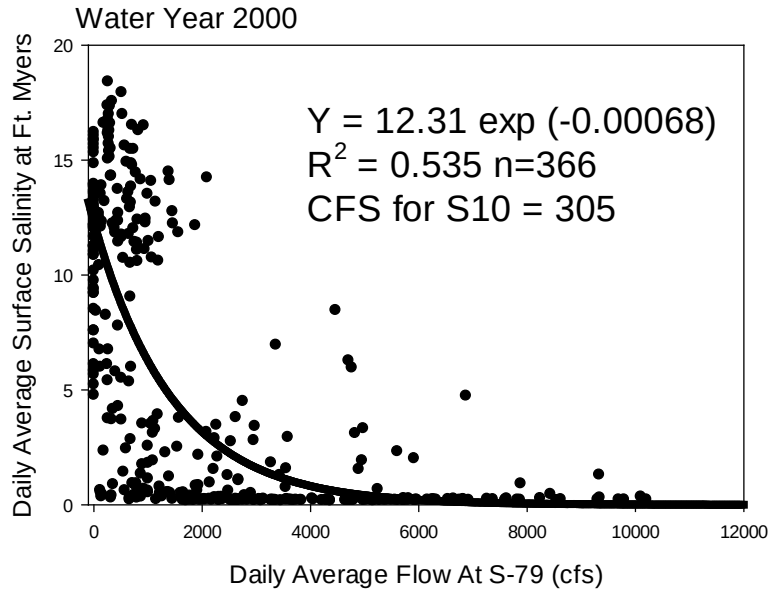

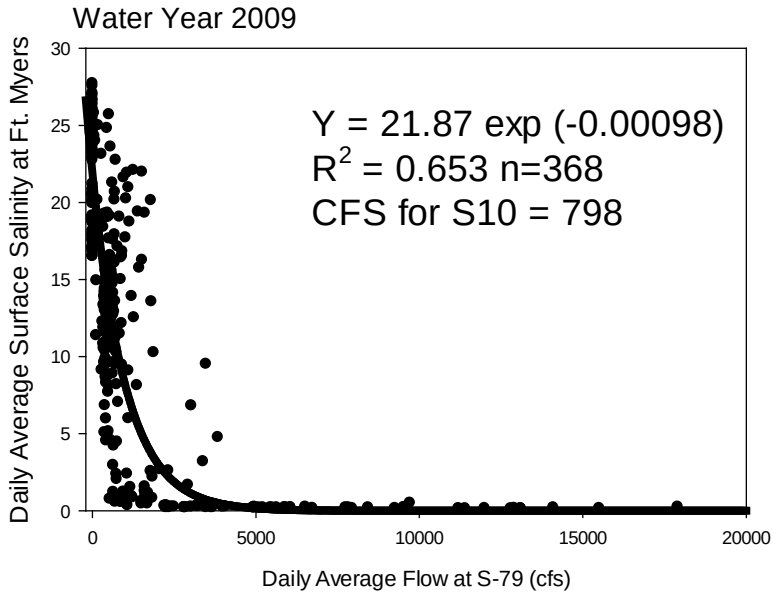

Figure 3. Daily average flow at S-79 and daily average surface salinity at Ft. Myers in water year 2000 (5/1/1999 – 4/30/2000) and water year 2009 (5/1/2008-4/30/2009). Also given is the flow at S-79 required to produce a salinity of 10 at Ft. Myers.

Table 6. Negative exponential relationships between 30-day moving average salinity at Ft. Myers and 30-day moving average discharge at S-79. Calculations were made for 2 different time periods using all data or just dry season data. Also the case where very high flows (>4000 cfs) were eliminated from the analysis was investigated.

	All-season flow				**All-season flow <4000 cfs**		
POR	R^2	Equation	Q for Salinity=10	Figure #	R^2	Equation	Q for Salinity=10
5/1/1996 ~ 4/30/2016	0.649	$y=9.244e^{-0.000561x}$	~ 0 *	Fig. 1	0.703	$y=17.184e^{-0.00113x}$	479
6/29/2000 ~ 10/29/2014	0.726	$y=10.475e^{-0.000565x}$	82	Fig. 3	0.703	$y=17.597e^{-0.00112x}$	505

* Too much high flows prevent from obtaining a reasonable Q in this case.

	Dry season flow				**Dry season flow <4000 cfs**		
POR	R^2	Equation	Q for Salinity=10	Figure #	R^2	Equation	Q for Salinity=10
5/1/1996 ~ 4/30/2016	0.757	$y=11.246e^{-0.000596x}$	197	Fig. 5	0.836	$y=17.184e^{-0.00113x}$	479
6/29/2000 ~ 10/29/2014	0.73	$y=12.441e^{-0.000674x}$	324	Fig. 7	0.861	$y=18.119e^{-0.00118x}$	504

Literature Cited

Buzzelli, C. 2016. Component Study 2: Analysis of the relationship between freshwater inflow at S-79 and salinity in the Caloosahatchee River Estuary 1993-2013. In: Buzzelli et al 2016. Assessment of the responses of the Calooshatchee River Estuary to low freshwater in flow in the dry season. South Florida Water Management District.

Doering, P.H., R.H. Chamberlain, and D. Haunert. 2002. Using submersed aquatic vegetation to establish minimum and maximum freshwater inflows to the Caloosahatchee Estuary, Florida. *Estuaries* 25:1343-1354.

French, GT and K.A. Moore. 2003. Interactive effects of light and salinity stress on the growth, reproduction, and photosynthetic capabilities of *Vallisneria americana* (wild celery). *Estuaries* 26(5):1255-1268.

Palmer, T.A., P.A. Montagna, J.B. Pollack, R.D. Kalke, and H.R. DeYoe. 2011. The role of freshwater inflow in lagoons, rivers, and bays. *Hydrobiologia* 667:49-67.

Wan, Y. and K. Konyha. 2015. A simple hydrologic model for rapid prediction of runoff from ungauged coastal catchments. *Journal of Hydrology* 528:571-583.

Bartleson, R. 2016 Personal communication.

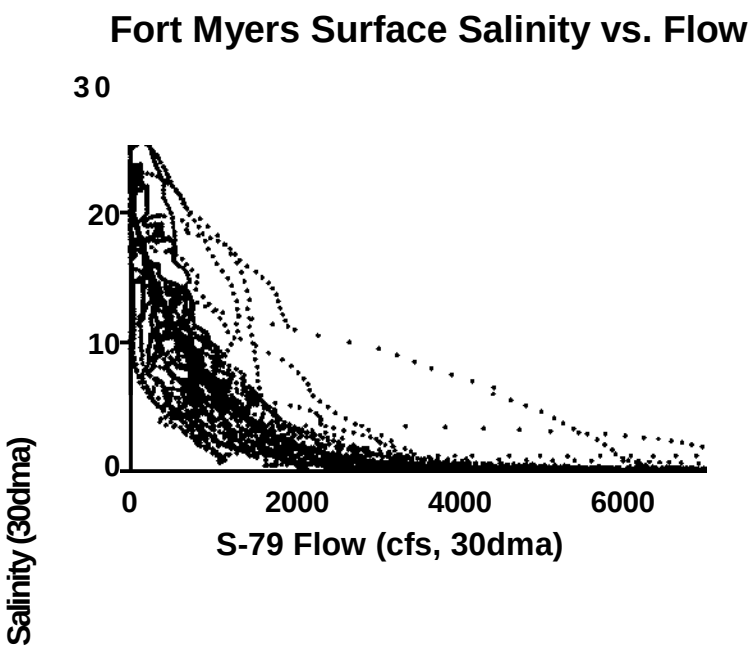

This is an exponential curve-fit of SFWMD Fort Myers Yacht Basin 30 day average surface salinity and the 30 day average flows at S-79 from 6/29/2000 to 10/19/2014 (periods when data were available). Salinity= 20.7 $\exp_{(-0.0011x\ Flow)}$. The R^2 is 0.81. The regression equation calculates 10 psu at 620 cfs. (Source of raw data: DBHYDRO, FortmyersM daily average conductivity25 and temperature, UNESCO calculation of salinity from conductivity (corrected from $_{C25)}$ and temperature and S-79 Flow. 95% confidence intervals: y(Salinity)=20.41to 20.94, K=0.001137 to 0.001194.

From: Eric Milbrandt [mailto:emilbran@sccf.org]
Sent: Monday, September 19, 2016 12:54 PM
To: Doering, Peter <pdoering@sfwmd.gov>
Subject: Re: Flows at S-79 and Salinity at Ft. Myers

Hi Peter,

We will send you the details about flow and salinity, Rick and I talked about it this morning. It's SFWMD salinity data lagged 3-days for 2012-2014. Also was done for 2000-2014. A summary was provided to Steve Shumer on Friday and you were cc'd I think.

Can you send the document or map showing the side-scan sonar oyster reefs from RECOVER? I did a quick search and could not find it.

On Mon, Sep 19, 2016 at 7:46 AM, Doering, Peter <pdoering@sfwmd.gov> wrote:

Hi Rae Ann,

As always it was nice to see you and to talk with you at the Caloosahatchee MFL Science Symposium last week.

During discussions, it became apparent that there was not general agreement on estimates of the discharge at S-79 that produces a surface salinity of 10 at the District's monitoring station at the Ft. Myers yacht basin. It seems estimates that SCCF is making may not agree with those that we presented during the symposium. During the question and answer period we asked that SCCF send us an analysis describing how estimates of the relationship between flow and salinity are being made and how the calculation of the discharge at S-79 required to produce a salinity 10 at Ft Myers is conducted. We would very much like to work with SCCF to understand the technical basis for any differences.

Please send us the details of the SCCF analysis, including the raw data and source of the data that were used. We would be happy to provide you more details of the analysis we presented at the symposium if you would like.

Best,

Peter Doering
Coastal Ecosystems Administrator
Applied Sciences Bureau
South Florida Water Management District
3301 Gun Club Road
West Palm Beach, FL 33406
561-682-2772
pdoering@sfwmd